

Analyses of Engineered Nanoparticles and Colloids at Sediment Water Interfaces

Analyse artifiziereller Nanopartikel und Kolloide an Wasser-Sediment-Grenzschichten

Von Dipl. Biol. Anne-Lena Fabricius

Geboren am 25.01.1982 in Hannover

Angenommene Dissertation

Zur Erlangung des akademischen Grades eines Doktors der Naturwissenschaften

Fachbereich 3: Mathematik/Naturwissenschaften

Universität Koblenz-Landau (Campus Koblenz)

Gutachterinnen und Gutachter:

Prof. Dr. Thomas A. Ternes

Prof. Dr. Joachim Scholz

Prof. Dr. Torsten C. Schmidt

Prüfungskommission:

Prof. Dr. Werner Manz

Prof. Dr. Thomas A. Ternes

Prof. Dr. Joachim Scholz

Prof. Dr. Torsten C. Schmidt

Vorgelegt am 30.08.2017

Tag der mündlichen Prüfung: 21.12.2017

Summary

Within aquatic environments sediment water interfaces (SWIs) are the most important areas concerning exchange processes between the water body and the sediment. These spatially restricted regions are characterized by steep biogeochemical gradients that determine the speciation and fate of natural or artificial substances. Apart from biological mediated processes (e.g., burrowing organisms, photosynthesis) the determining exchange processes are diffusion or a colloid-mediated transport. Hence, methods are required enabling to capture the fine scale structures at the boundary layer and to distinguish between the different transport pathways. Regarding emerging substances that will probably reach the aquatic environment engineered nanomaterials (ENMs) are of great concern due to their increased use in many products and applications. Since they are determined based on their size (<100 nm) they include a variety of different materials behaving differently in the environment. Once released, they will inevitably mix with naturally present colloids (< 1 μm) including natural nanomaterials.

With regard to existing methodological gaps concerning the characterization of ENMs (as emerging substances) and the investigation of SWIs (as receiving environmental compartments), the aim of this thesis was to develop, validate and apply suitable analytical tools. The challenges were to i) develop methods that enable a high resolution and low-invasive sampling of sediment pore water. To ii) develop routine-suitable methods for the characterization of metal-based engineered nanoparticles and iii) to adopt and optimize size-fractionation approaches for pore water samples of sediment depth profiles to obtain size-related information on element distributions at SWIs.

Within the first part, an available microprofiling system was combined with a novel micro sampling system equipped with newly developed sample filtration-probes. The system was thoroughly validated and applied to a freshwater sediment proving the applicability for an automatic sampling of sediment pore waters in parallel to microsensor measurements. Thereby, for the first time multi-element information for sediment depth profiles were obtained at a millimeter scale that could directly be related to simultaneously measured sediment parameters.

Due to the expected release of ENMs to the environment the aim was to develop methods that enable the investigation of fate and transport of ENMs at sediment water interfaces. Since standardized approaches are still lacking, methods were developed for the determination of the total mass concentration and the determination of the dissolved fraction of (nano)particle suspensions. Thereby, validated, routine suitable methods were provided enabling for the first time a routine-suitable determination of these two, among the most important properties regarding the analyses of

colloidal systems, also urgently needed as a basis for the development of appropriate (future) risk assessments and regulatory frameworks.

Based on this methodological basis, approaches were developed enabling to distinguish between dissolved and colloidal fractions of sediment pore waters. This made it possible for the first time to obtain fraction related element information for sediment depth profiles at a millimeter scale, capturing the fine scale structures and distinguishing between diffusion and colloid-mediated transport.

In addition to the research oriented parts of this thesis, questions concerning the regulation of ENPs in the case of a release into aquatic systems were addressed in a separate publication (included in the Appendix) discussing the topic against the background of the currently valid German water legislation and the actual state of the research.

Zusammenfassung

In der aquatischen Umwelt stellen Wasser-Sediment-Grenzschichten (WSG) die wichtigsten Bereiche bezüglich der Austauschprozesse zwischen dem Wasserkörper und dem Sediment dar. Diese räumlich begrenzten Regionen sind durch starke biogeochemische Gradienten charakterisiert, die die Spezierung und den Verbleib natürlicher und artifizieller Substanzen maßgeblich bestimmen. Abgesehen von biologischen Prozessen (z.B. grabende Organismen oder Photosynthese) ist der Austausch zwischen Wasser und Sediment von Diffusion oder Kolloid-gesteuerten Transport bestimmt. Dies erfordert Methoden, die es ermöglichen, die feinen Strukturen der Grenzschichten abzubilden und zwischen den unterschiedlichen Prozessen zu unterscheiden.

Hinsichtlich neu entwickelter Substanzen, die voraussichtlich in die aquatische Umwelt gelangen werden, sind artifizielle Nanomaterialien (engineered nanomaterials; ENMs) aufgrund ihrer zunehmenden Nutzung in Produkten und Anwendungen von großer Relevanz. Da sie auf der Grundlage ihrer Größe definiert werden (<100 nm), umfassen sie eine Vielzahl verschiedenster Materialien mit unterschiedlichem Verhalten in der Umwelt. Erreichen sie aquatische Systeme, mischen sie sich mit natürlich vorkommenden Kolloiden (<1 μm), die nanoskalige Partikel beinhalten.

Ausgehend von existierenden methodischen Lücken bezüglich der Charakterisierung von ENMs (als neu aufgekommene Substanzen) und WSG (als betroffene Umweltkompartimente) war das Ziel der vorliegenden Dissertation, die Entwicklung, Validierung und Anwendung einer geeigneten analytischen Basis, um ENMs an WSG untersuchen zu können. Die Herausforderungen lagen dabei in i) der Entwicklung von Methoden, die eine räumlich hochaufgelöste Beprobung von Sedimentporenwasser erlauben. ii) Der Bereitstellung routinetauglicher Methoden zur Charakterisierung metallbasierter ENMs und iii) der Entwicklung von Methoden zur Größenfraktionierung von Porenwässern, um größenbezogene Elementverteilungsmustern an WSG erhalten zu können.

Im ersten Teil erfolgte die Entwicklung von Filter-Probenahmesonden, die in ein neuartiges Probenahmesystem integriert wurden, welches mit einem kommerziell verfügbaren Microprofiling-system kombiniert wurde (microprofiling micro sampling system; *missy*). Nach umfangreicher Validierung konnte in Experimenten die Tauglichkeit des *missy* für eine minimal-invasive und automatisierte Beprobung von Sedimentporenwasser bei parallelen Messungen mittels Mikrosensoren gezeigt werden. Es wurde somit erstmal möglich, im Millimetermaßstab Multielementinformationen für Sedimenttiefenprofile zu erhalten und diese in einen direkten Zusammenhang mit verschiedenen Sedimentparametern zu setzen.

Aufgrund der zu erwartenden Freisetzung von ENMs in die Umwelt, war es das Ziel, Methoden bereitzustellen, die eine Untersuchung von Transportprozessen und dem Verbleib von ENMs an WSG ermöglichen. Da standardisierte Methoden noch immer fehlen, erfolgte die Entwicklung routinetauglicher Ansätze zur Bestimmung der Massenkonzentration sowie der gelösten Fraktion von ENM-Suspensionen. Somit konnten erstmals Methoden bereitgestellt werden, die eine routinetaugliche Bestimmung von zwei der wichtigsten Eigenschaften kolloidaler Systeme ermöglichen, die ebenfalls für die Entwicklung geeigneter Risikoabschätzungen und Regularien benötigt werden.

Basierend auf dieser methodischen Grundlage erfolgte die Entwicklung geeigneter Verfahren zur Bestimmung der gelösten und kolloidalen Fraktionen in Sedimentporenwässern. Dies ermöglichte es erstmalig, fraktionsbezogene Elementinformationen für Sedimenttiefenprofile in millimetergenauer Auflösung zu erhalten, was eine Unterscheidung zwischen Diffusion und kolloid-gesteuerten Transportprozessen gestattet.

Zusätzlich zu den forschungsorientierten Teilen der vorgelegten Dissertation wurden in einer weiteren, als Anhang beigefügten Publikation (Appendix III) Fragen zu einem möglichen Eintrag nanoskaliger Stoffe in Oberflächengewässer vor dem Hintergrund des aktuell gültigen Deutschen Wasserrechtes adressiert.

Table of Content

| | |
|---|-----|
| Summary | I |
| Zusammenfassung..... | III |
| 1 General Introduction | 1 |
| 1.1 Sediment water interfaces | 1 |
| 1.2 High resolution measurement and sampling techniques for SWIs..... | 5 |
| 1.2.1 Microsensors | 5 |
| 1.2.2 Sediment pore water sampling and size fractionation strategies..... | 7 |
| 1.3 Analyses of engineered nanoparticle suspensions | 10 |
| 1.4 Objectives | 12 |
| 1.5 Thesis outline | 13 |
| 1.6 References..... | 14 |
| 2 New Microprofiling and Micro Sampling System for Water Saturated Environmental Boundary Layers..... | 19 |
| 2.1 Abstract | 20 |
| 2.2 Introduction..... | 21 |
| 2.3 Experimental Section..... | 23 |
| 2.3.1 Terms and Definitions | 23 |
| 2.3.2 Chemicals and Materials | 23 |
| 2.3.3 Sample Probes..... | 24 |
| 2.3.4 Missy Setups..... | 25 |
| 2.3.5 Microprofiling System | 26 |
| 2.3.6 Characterization: Background Concentrations and Recoveries..... | 26 |
| 2.3.7 Micro Sampling System | 26 |
| 2.3.8 Profiling Experiments | 27 |
| 2.3.9 ICP-QMS-Analyses..... | 28 |
| 2.3.10 Data Analyses | 28 |
| 2.4 Results and Discussion | 29 |
| 2.4.1 Characterization: Background Concentrations and Recoveries..... | 29 |
| 2.4.2 Sediment Pore Water Profiles..... | 30 |
| Oxygen Profiles..... | 32 |
| pH Profiles | 33 |
| Redox Profiles..... | 33 |
| Metal(loid) Profiles..... | 34 |
| 2.4.3 General Evaluation of the Missy Setups..... | 35 |
| 2.4.4 Future applications..... | 36 |
| 2.5 References..... | 38 |

| | | |
|-------|---|----|
| 3 | ICP-MS Based Characterization of Inorganic Nanoparticles – Sample Preparation and Off-line Fractionation Strategies | 41 |
| 3.1 | Abstract | 42 |
| 3.2 | Introduction..... | 43 |
| 3.3 | Experimental section..... | 46 |
| 3.3.1 | Chemicals and materials..... | 46 |
| 3.3.2 | Nanoparticle suspensions | 46 |
| 3.3.3 | General characterization of the ENP suspensions | 46 |
| | Particle size distribution and zeta potential..... | 46 |
| 3.3.4 | Total concentration | 47 |
| | Sample preparation procedures..... | 47 |
| | Comparison of ICP-MS and gravimetry | 48 |
| | Precision of ICP-MS measurements | 49 |
| 3.3.5 | Dissolved fraction determination..... | 49 |
| | Comparison of different off-line fractionation approaches..... | 49 |
| | Dissolved fraction determination of different ENP suspensions | 51 |
| 3.4 | Results and discussion..... | 52 |
| 3.4.1 | General characterization of the ENP suspensions | 52 |
| | Particle size distribution and zeta potential..... | 52 |
| 3.4.2 | Total concentration | 53 |
| | Sample preparation procedures..... | 53 |
| | Comparison of ICP-MS analysis and gravimetry..... | 55 |
| | Precision of ICP-MS measurements | 56 |
| 3.4.3 | Determination of the dissolved fraction | 58 |
| | Comparison of different off-line fractionation approaches..... | 58 |
| | Dissolved fraction determination of different ENP suspensions | 61 |
| 3.5 | Summary and Conclusions | 63 |
| 3.6 | References..... | 64 |
| 4 | Metal and Metalloid Size Fractionation Strategies in Spatial High Resolution Sediment Pore Water Profiles..... | 68 |
| 4.1 | Abstract | 69 |
| 4.2 | Introduction..... | 70 |
| 4.3 | Experimental Section..... | 72 |
| 4.3.1 | Chemicals and materials..... | 72 |
| 4.3.2 | Microprofiling and microsampling | 72 |
| 4.3.3 | Sample preparation and ICP-QMS analyses | 74 |
| 4.3.4 | Data-analyses | 76 |
| 4.4 | Results and Discussion | 77 |

| | | |
|------------|--|-----|
| 4.4.1 | Sediment pore water profiles..... | 77 |
| | Depth profiles of oxygen concentration | 78 |
| | Depth profiles of the redox potential | 79 |
| | Fractionation of sediment pore water | 79 |
| 4.4.2 | Method evaluation, future improvements and applications | 82 |
| 4.5 | References..... | 85 |
| 5 | Final Conclusions | 88 |
| | Danksagung | 90 |
| | Appendix I Supporting Information Chapter 2: A New Microprofiling and Micro Sampling System for Water Saturated Environmental Boundary Layers..... | 91 |
| AI.I | Experimental | 92 |
| AI.I.I | Characterization of the sediment..... | 92 |
| AI.I.II | System characterization | 93 |
| AI.I.III | Software settings..... | 95 |
| AI.I.IV | Porewater Samples..... | 96 |
| AI.I.V | ICP-MS analyses..... | 97 |
| AI.I.VI | Calculation of the dead volume and shift of the sampling depth | 98 |
| AI.II | Results and Discussion | 99 |
| AI.II.I | Metal(loid) concentrations in pore water samples | 99 |
| AI.II.II | Single profiles of oxygen, redox potential and pH value..... | 104 |
| AI.II.III | Result of the micro annular gear pump..... | 105 |
| AI.II.IV | Carryover | 106 |
| AI.III | References..... | 107 |
| | Appendix II: Supporting Information Chapter 3: ICP-MS based characterization of inorganic nanoparticles – Sample preparation and off-line fractionation strategies | 108 |
| AII.I | Experimental | 109 |
| AII.I.I | ENP suspensions..... | 109 |
| AII.I.II | Microwave assisted digestion | 110 |
| AII.I.III | ICP-QMS analyses..... | 111 |
| AII.II | Results and Discussion | 112 |
| AII.II.I | TEM-images of nanoparticle suspensions | 112 |
| AII.II.II | Centrifugation: calculation of the run time..... | 113 |
| AII.II.III | Time dependent dissolution during dialysis..... | 115 |
| AII.II.IV | Calibration and results of the standard addition in ion selective electrode measurements..... | 116 |
| AII.III | References..... | 117 |
| | Appendix III Nanotechnology and Water Legislation..... | 118 |
| AIII.I | Summary | 119 |

| | | |
|--|--|-----|
| AIII.II | Nanotechnologie und Wasserrecht (Deutsche Originalversion)..... | 121 |
| AIII.II.I | Begriffliche Klärung | 121 |
| AIII.II.II | Stand der (umwelt)wissenschaftlichen Forschung..... | 122 |
| AIII.II.III | Die Einleitung nanoskaliger Stoffe in Grund-und Oberflächenwasser..... | 124 |
| AIII.II.IV | Umgang mit wassergefährdenden Stoffen | 125 |
| AIII.II.V | Der Rückgriff auf die REACH-Verordnung | 126 |
| AIII.II.VI | Ausblick..... | 127 |
| AIII.II.VII | Literatur | 130 |
| Appendix IV Supporting Information Chapter 4: Metal and Metalloid Size Fractionation Strategies in Spatial High Resolution Sediment Pore Water Profiles..... | | 132 |
| AIV.I | Sediment Characteristics..... | 133 |
| AIV.II | Microprofiling and micro sampling | 135 |
| AIV.III | ICP-QMS analyses | 137 |
| AIV.IV | Preliminary experiments for CPE method adjustment | 138 |
| AIV.V | Calculation of the dead volume and shift of the sampling depth..... | 140 |
| AIV.VI | Concentrations of As and Sb in pore water samples..... | 142 |
| AIV.VII | Metal(loid) concentrations in SPW samples of the reference profiles | 145 |
| AIV.VIII | Metal(loid) concentrations in fractions of pore water samples after UF..... | 147 |
| AIV.IX | Metal(loid) concentrations in fractions of pore water samples after CPE..... | 153 |
| AIV.X | References..... | 160 |

1

General Introduction

The aim to investigate metals and metalloids (metal(loid)s) in different size-fractions in aquatic systems requires the availability of appropriate and validated methods for the sampling and sample preparation as well as for the measurement procedures sensitive enough with respect to complex matrices. Focusing on sediment water interfaces (SWIs) and size fraction related fate and transport of metal(loid)s necessitate on the one hand systems that enable minimal invasive sampling procedures that do not (or to an as possible low extent) influence the conditions at the sampling site and the characteristics of the samples taken. On the other hand, the sample preparation, in this case with a special focus on size fractionation, should capture the (colloidal) status of the sample without modifying it.

The challenging methodological tasks in studying SWIs are the fine scale heterogeneity of the boundary layers demanding spatial high resolution investigations. Moreover, the potential impacts of the procedures applied on the characteristics of the sampling site and the samples need to be considered. Since the mobility of metal(loid)s at the SWI is governed by biogeochemical gradients, it is important to determine different sediment parameters (like, e.g., the oxygen concentration, the redox potential of the pH value) in parallel to the analyses of the compounds of interest.

With regard to the protection of aquatic environments, methods are required that enable to investigate fate, transformation and impacts of substances released into the systems. ENMs are a group of increasingly used materials that are known to reach the aquatic environment to a certain extend.¹ In contrast to many other chemicals ENMs are not dissolved but suspended in liquid phases and, hence, demand for other sample preparation and measurement methods.

In the following paragraphs SWIs as receiving environmental systems and the available methodological basis for sampling and measurement are described in more detail. Equally, questions concerning the increased use of ENMs and the related risk assessment and regulation are discussed together with the analytical challenges.

1.1 Sediment water interfaces

Within aquatic environments the SWIs are the regions where the exchange processes between the water, sediment, and the sediment pore water take place. Since they are often spatially restricted, the different conditions between the water and the sediment lead to the development of steep biogeochemical gradients of different parameters like the oxygen concentration, the redox

potential, or the pH value. In turn, this governs the fluxes of compounds across the SWI, including dissolved and colloidal mediated exchange processes. However, the actual conditions at a given site are moreover influenced by a variety of different other factors including the chemical characteristics of the sediment and the overlying water body, the content and composition of the organic material and the activities of microbes or other sediment organisms present, but also natural or anthropogenic disturbances, like floods, dredging or the discharge of substances.

One of the key factors determining the conditions at the SWI is the availability of oxygen important as electron acceptor in redox-reactions, especially with regard to the (microbial) degradation of organic material.^{2,3} The O₂ concentration and the gradients that develop at the SWI are, in absence of mechanical disturbances (by, e.g., burrowing organisms or high flow velocities), mainly driven by diffusive fluxes of O₂ from the overlying water into the sediment and the oxygen consumption either caused by chemical or biologically mediated reactions. Beside oxidation of inorganic compounds like, e.g., NH₃, Mn²⁺, Fe²⁺, H₂S or CH₄, the uptake by (micro)organisms during degradation processes is the main factor in establishing the gradient that can lead to a O₂ depletion within the first millimeters of the sediment.^{2,3} If dwelling, filtrating or photosynthetic active organisms are present that introduce O₂ into the upper sediment layers or produce O₂ at the sediment surface, respectively, the gradients are less pronounced and more heterogeneous.²⁻⁴

In close relation to the oxygen concentration is the redox potential, reflecting the electron availability or the oxidizing/reducing capacity of a system^{5,6} and gives an indication for the reactions taking place. As mentioned, the redox potential depends strongly, but not exclusively, on the availability of oxygen. It can also be influenced by the activities of different bacteria (involved in the reduction of oxygen, nitrate, manganese, iron or sulfate or in methanogenesis) and depends on the content and forms of carbon, nitrogen, sulfur, iron and manganese.^{2,4,6,7} If other electron acceptors (e.g., nitrate, Mn(IV), Fe(III) or sulfate) are available, oxygen can become depleted also in deeper sediment layers, while the redox potential remain positive, reflecting oxidizing conditions.^{4,6,7} Beside this, the pH value of the solution as another determining factor, can bias the redox potential: low pH values (high activity of protons) lead to higher redox potentials, while high pH values (>7) lead to reduced values^{6,8,9} But, also vice versa the redox potential, or rather the conditions reflected by it, can affect the pH of the system. Under oxidizing conditions (indicated by a high redox potential) the oxidation of sulfides to sulfate and the related release of protons and/or the precipitation of Fe (hydr)oxides may cause an acidification.^{10,11} Moreover, the pH conditions depend strongly on the characteristics of the sediment (minerals phase, buffering capacity, degradable organic substance content, grain sizes) and the microorganisms present.^{12,13} Hence, pH and the redox potential can, but does not necessarily be (negatively) correlated to each other^{5,14-17}

Regarding the mobility of (trace) metal(loid)s at the SWI, both, the redox potential as well as the pH value, are important factors. Their influence on the dissolution behavior of different elements depends on the chemistry, speciation and binding characteristics of the metal(loid)s, but also on the activity of microorganisms population,^{18, 19} the presence and quality of organic matter (as binding, adsorbing, complexing or chelating compounds)^{5, 13} and on the presence of sorption sites.^{5, 20}

Concerning the element cycling at SWIs, Fe and Mn are main components influencing the distribution of other (trace) elements.²¹ The two elements often show a comparable but not totally similar behavior in dependence of the sediment parameters. Both become dissolved at low redox- / reducing conditions. This is due to the depletion of oxygen and the transfer of electrons to other acceptors like Mn- or Fe-(oxyhydr)oxides during microbial degradation processes. This reduction reactions lead to a release of dissolved Mn²⁺ and Fe²⁺ that can then be detected in the sediment pore water.^{20, 21} In comparison, Mn shows a higher mobility than Fe due to a reduction at higher redox potentials and a slower re-oxidation in presence of oxygen. Nevertheless, the mobility of Mn can be strongly reduced by microbes governing the oxidation of Mn²⁺. In presence of HS⁻, which is produced during (microbial mediated) sulfate reduction at low redox potentials, insoluble Fe-sulfides can be formed causing the precipitation and remove of dissolved Fe from the water phase under reducing conditions.^{5, 21, 22} However, the availability of HS⁻ depends not only on the redox conditions, but also on the concentration of sulfates (app. >30 μmol/L⁴), the presence of sulfate reducing bacteria and on the availability of organic matter.⁵ In contrast to Fe, Mn-sulfides dissolve easily, but Mn can (equally to Fe) precipitate as carbonate.^{21, 22} In addition to the redox conditions, the solubility of Fe and Mn is impacted by the pH conditions. A pH decrease cause the dissolution of Mn- and Fe-(oxyhydr)oxides even under oxic conditions.^{5, 21, 22} The pH, and thereby the dissolution behavior of Fe and Mn, can in turn be influenced and enhanced by the oxidation of H₂S/sulfides and the production of sulfuric acid.¹⁵ The chemical compounds and the speciation of Fe and Mn¹⁵ in a given environment and the reactions taking place depend, as described, on a variety of different factors that need to be taken into account in this context.^{5, 21, 22} As mentioned, the fate and behavior of Fe and Mn at the SWI is also important due to their impact on other trace elements (like, e.g., Co, As, Cd, Cr or Zn) associated with their (oxyhydr)oxides, showing a co-release or co-precipitation/adsorption with the dissolution/precipitation of Fe- and Mn-compounds.^{2, 5, 20, 22, 23} This can result in a apparently redox-dependent distribution of elements (like., e.g., Zn or Mo) that normally do not show a sensitivity to the redox conditions.¹⁴

In addition to, as well as in dependence on the reactions and processes described above, the colloidal-mediated transport plays a major role in the fate and behavior of (trace) metal(loid)s in aquatic systems and at SWIs.^{2, 24} Due to their small size (1 nm - 1 μm^{25, 26}) and related huge relative

surface area, substances (including metal(loid)s or radionuclides) can strongly attach to and being transported with them.^{24, 27} Colloids can consist either of inorganic materials such as Fe, Al, Mn, or Si (hydr)oxides, carbonates, phosphates or organic substances, like, e.g., humic and fulvic acids, polysaccharides or extracellular polymeric substances, but also viruses or small bacteria.^{24, 26, 28} The mobility of colloidal (inorganic) substances is governed by different factors including the flow velocities, the particle densities and sizes, the surface chemistry, the pH and the ionic strength.²⁶ It is thereby related to the characteristics and processes of the environmental system described above. The colloidal fractions can be seen as another mobile phase between the mobile aqueous one and the immobile solid phase.²⁶ As a result of the gradients between the water and the sediment or of changing environmental conditions, including physicochemical parameters (e.g., of the redox conditions, the pH value or ionic strength) or flow velocities, processes like dissolution, precipitation, suspension or sedimentation can lead to different fluxes between the phases.^{22, 26} Hence, the mobility of different metal(loid)s at the SWI depends not only on the chemical speciation and the reactions they are involved in, but also on the size fractions. Regarding the size distribution of different metal(loid)s some general characteristics can be found, even though the partitioning depends on the environmental conditions and processes at a given site. Mn, Sb and V are known to be mainly present in the dissolved phase, whereas Fe, Pb and Al are predominantly be found in the colloidal and particulate fractions.²⁹⁻³¹ However, the co-cycling of trace elements with major components, like Fe, Mn (as described) or S, or the association with dissolved organic material (DOM) can also determine the particle size distribution of trace elements.^{31, 32} Beside the determining physicochemical conditions and processes (e.g., aggregation and sedimentation or dissolution and precipitation³³) influencing the particle size distribution, the classification of the dissolved, colloidal and particulate fractions vary among different studies in dependence of the methods applied and the per convention defined limits for the different size classes.^{29, 34-37}

Taken together, to understand the behavior of trace metal(loid)s at SWIs and the processes that govern their transport and distribution, requires not only the investigation of the total concentrations of the analytes of interest, but also of different size fractions and species as well as of the characteristics of the given environment and the distribution of the major compounds present. Therefore, suitable and validated measurement techniques and sampling procedures as well as appropriate sample preparation strategies and analytical methods are required. Since the boundary layers between water and sediment are often narrow and characterized by fast changing conditions and heterogenic structures, the methods applied should be suitable to capture the fine scale patterns.

1.2 High resolution measurement and sampling techniques for SWIs

As described in the previous paragraph, the mobility of metal(loid)s at sediment water interfaces depends on a variety of different factors and processes that need to be investigated in parallel to the different chemical species. Due to the development of a variety of different kinds of microsensors during the last decades, the measurement of several sediment parameters and analytes, including (among others) the oxygen concentration, the redox potential and the pH value, became possible at spatial resolutions in the mm to μm range.^{4, 15, 38, 39} This enabled for these parameters a direct and non-destructive analyses of the sediment pore water *in situ* capturing the fine scale structures and fast changing conditions at SWIs without any further extraction procedures.³⁸ However, aside from the data that can be obtained by microsensors, analytes have to be determined in the pore water. Similar to the variety of different microsensors, numerous sampling and extraction strategies are available for sediments and sediment pore waters.^{40, 41} In order to obtain a holistic understanding of the processes at the SWI, measurement and sampling techniques need to be combined and synchronized, in simultaneously considering the capacities and limitations of the methods, including potential sources of error possibly biasing the results.

1.2.1 Microsensors

The huge number of different microsensors (commercially) available nowadays enable the measurement of numerous parameters (O_2 , redox potential, pH value, temperature, diffusivity, flow, irradiance) and analytes (CH_4 , H_2S , CO_2 , N_2O , H_2O_2 , DOC, total S, Glucose), including ions (NO_3^- , NH_4^+ , Ca_2^+ , S_2^- , Mn_2^+ , Fe_2^+ , I^-). Even though different terms are used for sensors enabling high resolution measurements and for the term “microsensor,” it can in general be understood as sensors usable for measurements with a resolution $<1\text{ mm}$ ^{38, 39} Beside investigations of the boundary layers of SWIs, the sensors are also applied to study biofilms, tissues or symbiotic associations, including related processes like oxygen consumption, photosynthesis or (de)nitrification.^{39, 42, 43} Depending on the measurement principles, based on different electrochemical, optical and microbiological reactions and processes, the sensors display diverse designs with different advantages and drawbacks. However, a comprehensive description of all existing sensor types and the respective measurement principles is beyond the scope of this work, but can be found in several (review) publications^{38, 39, 42}. At this point only some of the most and widely used sensors in sediment studies will be briefly described:

In general, signals of electrochemical measurements can either be currents generated in relation to the analyte concentration (amperometric microsensors, mostly Clark-Type) or a voltage that is

created as a reaction to the analyte (potentiometric microsensors). In case of the latter, a reference electrode immersed in the same solution, is necessary to measure the potential. Examples of potentiometric microsensors are redox- and pH-electrodes. In the case of the redox potential, the measurement is based on the voltage generated by the electron flow of redox reactions taking place at the surface of the electrode tip made of an inert metal (mostly platinum, sometimes gold) in relation to a reference electrode. Since the potential is caused by the sum of all reactions of different redox couples, it is less a precise value, but rather gives an indication of the reducing or oxidizing capacity of the system and its general tendency to spend or consume electrodes.^{6, 39, 43} Because of the direct contact of the electrode surface to the environmental matrix, the measurements can be hampered by dissolved components adsorbed to the electrode surface or oxides build in presence of molecular oxygen that inhibit the electron transfer.^{44, 45} Moreover, in environmental systems the reactions taking place are typically not in a chemical and fast establishing equilibrium that would be required for a precise and stable measurement.⁴⁵ Nevertheless, the redox potential (or the potential determined by means of a Pt- and connected reference electrode) is an often determined parameter enabling a good, even though not absolute, estimation of the conditions of a given system and the reactions possible.

In contrast to redox electrodes, pH electrodes are ion selective sensors, reflecting the potential of a specific reaction instead of mixed reactions⁸. The electrode is placed in an electrolyte solution behind a (glass) membrane selectively permeable for hydrogen ions.^{8, 39, 43} The micro pH-sensors, already applied for several decades, are miniaturized versions of larger commercial ones showing comparable characteristics with regard to accuracy and low interferences, but a higher fragility.^{4, 39, 42} The reference electrode can either be an external or an internal one.^{4, 43} Beside sensors for hydrogen ions, some are available for several other species like NO_3^- , NO_2^- , NH_4^+ , Ca_2^+ , S_2^- .^{39, 42}

For many analytes, including O_2 , H_2S , H_2 , N_2O and CO_2 , miniaturized (amperometric) Clark-type gas sensors are available where the electrode is placed in an electrolyte solution behind an ion-impermeable membrane and, hence, do not get in contact with the surrounding medium.^{38, 39, 42} The concentration is determined on the basis of the partial pressure of the gas in the sample medium that diffuse along the gradient through the membrane, react with the electrode and thereby generate a current, measured in (milli)ampere.³⁹ The signal can be induced either by an oxidation or reduction or a pH change in the internal electrolyte³⁹ The best known and often applied Clark-type sensor is the oxygen microsensor that displays good and stable performances, with a fast response time (90% in 0.1 s), low detection limits (<1 μM) and an a good robustness against interferences from chemical species, stirring or diffusivity.^{38, 39, 42} The materials used for the cathodes/anodes and the electrolyte solution vary in dependence of the chemical species of interest.³⁹

Beside electrochemical sensors, phosphorescence based optodes are available for oxygen, pH and CO₂ measurements. The sensors contain fluorescing dyes which fluorescence is dynamically diminished in presence of the analyte. Optodes are not disturbed by electromagnetic fields, pH variations or high concentration of sulfide, CO₂, salts or metals.³⁸ However, the measurements strongly depend on temperature and pressure and the response times (5-30 s) are lower in comparison to the electrochemical sensors.

1.2.2 Sediment pore water sampling and size fractionation strategies

To determine components that cannot be directly measured by means of sensors, the sediment pore water has to be sampled prior to the analyses. The sampling can be performed either *ex situ* or *in situ* by application of different active or passive methods. In the case of *ex situ*, or indirect methods, the pore water is sampled together with the sediment and separated from the solid phase outside the examined environment.^{40, 41} The main drawback of these methods is the risk of an oxidation of the anoxic sediment samples when they get in contact with air which necessitate to perform the sampling and sample preparation under an inert atmosphere.^{40, 41} However, since the sediment is sampled together with the pore water, it can be analyzed in parallel and related to the results.⁴⁰ The *ex situ* methods include centrifugation and squeezing. The former is a relatively simple and fast method also applicable to huge sample volumes, but risks a bias of the results by artifacts due to, e.g., pressure, speed or duration of the procedure or changes of the conditions (e.g., temperature or O₂ concentration) that potentially affect the speciation and fractionation of the compounds of interest.^{40, 41} Since the parameters (speed, duration, volume, separation of supernatant from the sediment) of the centrifugation applied can vary, a comparability of the results (inter-laboratory and inter-operator) is not necessarily given, even though some approaches combine the centrifugation with a simultaneous filtration or separation by an inert solvent^{40, 41, 46}. Sediment squeezing is performed using different devices (available are core section squeezers and whole-core squeezers) that allow forcing the pore water through an outlet to separate it from the sediment.^{40, 41} This force can either be realized by a piston, the introduction of gas or the application of a vacuum (applied to the exit). Beside the risk of an oxidation of the samples, the pressure may lead to a CO₂ degassing or a destruction of different compounds present in the sediment (e.g., organic materials, microorganisms) and, thereby, affect the forms and distribution of analytes.⁴⁰

In contrast to the *ex situ* methods, in the case of the *in situ* methods the sediment pore water is sampled directly from the matrix, minimizing the sources of errors of the *ex situ* approaches related to the sediment sampling (e.g., contamination from the sampling devices, mixing of anoxic and oxic layers), temperature and pressure changes and oxidation.⁴¹ The *in situ* methods subsume different

suction based filtration techniques (including commercial products like rhizon samplers) as well as dialyses approaches (like diffusive gradients in thin films (DGT)). Comparable to the squeezers, a huge variety of different suction filtration apparatuses as well as diffusion-based methods were developed since the early 1970s and improved with regard to the sampling from different and distinct depth and higher spatial resolutions.^{40, 41, 47 48} The filtration devices include simple designs like perforated volumetric pipettes or air stones, and more sophisticated ones, like e.g., rhizon samplers⁴⁷ spring-,^{49, 50} syringe-^{51, 52}, or (vacuum)pump⁵²-driven samplers. They are either made for single- or multilevel-sampling with spatial resolutions at the cm range (1-0.5 cm)^{47, 53} and depth down to depth of 5 m.⁴⁸ The basic principle of the dialyses devices is the establishment of a diffusion driven equilibrium of dissolved compounds between the sediment pore water and a medium (deionized water or gel), placed behind a membrane. One of the most widely used devices are so called “peepers” containing several chambers between two plastic shields that are separated from the environment by a membrane and filled with deionized water^{40, 41}. The peepers are placed in the sediment for several days or weeks to allow the formation of the equilibrium of the dissolved substances. Afterwards, the peepers are removed from the sediment and rinsed prior to the recovery of the samples by pipetting the water from the chambers as fast as possible to avoid oxidation if no inert gas environment is available.^{40, 41} Methods called “diffusive equilibration in thin films” (DET) use a thin layer of a gel instead of the compartments filled with deionized water, enabling equilibration times of < 1 hour and a higher spatial resolutions at the millimeter (or even sub-millimeter) scale.^{41, 54, 55} After sampling, the chemical species dissolved in the gel need to be rapidly fixed to prevent the samples to be oxidized.^{40, 56} A further development includes an ion exchange resin placed behind the diffusive gel that accumulates the dissolved species. In contrast to the DET techniques based on the establishment of an diffusive equilibrium, a constant diffusive gradient is used for the sampling (DGT).⁵⁷ The mass transport is determined by the diffusion through the gel and the metal bound to the resin increases with the time of exposure and decreased thickness of the gel and the resin (as long as the resin is not saturated).^{40, 57} After sampling, the gel is removed from the resin and the metals accumulated can be extracted using nitric acid and analyzed via AAS or ICP-MS.^{40, 57} Beside peepers, DGT is a an established and widely used technique in different scientific fields, but attention must be paid to several aspects including, e.g., the geometry, possible charge effects, binding of compounds to the gel or filter as well as reaction rates with the binding layer.⁵⁸

All sampling methods described exhibit different advantages and drawbacks that need to be taken into account for the decision which technique should be applied. Moreover, the risk of contact with air and related oxidation of the samples during sampling or sample preparation, the possible impacts of the sampling procedure (in the case of *ex situ* methods) or the installation of the sampling device

at the sampling site (in the case of *in situ* methods) and the potential effects on the sample characteristics and the results need to be taken into account. Besides, a spatial high resolution in the (sub-)mm range that is as approximately comparable with the measurements of the microsensors described above can only be obtained by some DET^{54, 56}/DGT^{55, 59} and peepers⁶⁰ approaches. These, however, still require the installation of the devices at the sampling site as well as an extensive preparation of the devices (prior to the sampling) and samples (after sampling) and well trained operators.

1.3 Analyses of engineered nanoparticle suspensions

As mentioned in the first paragraph, ENPs are increasingly used in numerous products and applications, leading thereby to an increased probability of an exposure of workers and consumers as well as of a release into the environment⁶¹. To generally ensure a safe usage and to avoid (negative) impacts on humans and the environment, the implementation of an appropriate risk assessment and adequate regulatory frameworks are required. With regard to aquatic environments, questions concerning transport, transformations, potential sinks as well as effects on organisms and ecosystems are of great concern. All this demands the availability of an analytical basis including suitable and easily implementable sampling and sample preparation strategies as well as validated measurement methods.

With the growth of the sector of nanotechnologies and the related increase of the economic and thereby also political important aspects concerning the assurance of a safe production and usage of nanomaterials became essential questions. Beside the governmental interest in innovative and promising technologies including their funding, adequate risk assessments and regulations became relevant issues on the national and international level.⁶²⁻⁶⁴ Even though the existing legal rules for other chemicals were in general found to be suitable for ENMs, the nano-specific characteristics are not captured and require additional and specific parts considering the unique properties.⁶⁵⁻⁶⁸ While provisions of the frameworks regarding e.g., the precautionary principle, consequences and restrictions for hazardous materials or labelling and packaging are equally applicable to ENMs, the standard analytical measurements and (eco)toxicological tests are not necessarily appropriate for nanoforms of a substance differing from the bulk material.^{66, 67, 69, 70} Nevertheless, some regulations are already implemented like, e.g. obligatory registration for ENMs in some countries (e.g., France, Denmark, Belgium, Norway and the USA)⁷¹ or nano-specific provisions included in legal rules concerning the declaration or risk assessment measures (e.g., EU-regulations on cosmetic and biocidal products and food).⁷²⁻⁷⁴ However, the implementation of any legal rule requires an analytical basis of routine suitable techniques and validated methods for control and monitoring measurements. Thereby, the increased production of nanomaterials and the demand for regulatory frameworks and risk assessments lead to the development of new techniques or the adaptation of existing methods^{75, 76}. This includes techniques like different (Flow) Field Flow-Fractionation devices, light scattering based techniques extended to particle sizes in the nano range, zeta-potential measurements or single particle ICP-MS. Moreover classical approaches like electron microscopy (transmission or scanning; TEM or SEM), BET-surface measurement or different filtration methods were adapted to ENMs and considerably improved during the last decade.^{75, 77} Nevertheless, even though the possibilities of the investigation of ENMs were significantly extended, the methods

available are often laborious, expensive and/or demand well trained operators and are still far from being routine suitable.^{64, 75} Beside the diversity of the materials themselves (different metals or oxides, like Ag, Au, Fe, SiO₂, TiO₂, CeO₂, ZnO, CuO, quantum dots like CdSe, ZnS, core-shell systems or fullerenes), the different forms in different matrices throughout the life cycle have equally to be taken into account. Moreover, the development and validation of the sampling, sample preparation and measurement methods is additionally impeded because only few certified reference materials are available.⁷⁵ Hence, the detection, characterization and quantification of ENPs, especially in different environmental matrices, remain challenging tasks, especially for non-“nano”-specialized laboratories (e.g., in (eco)toxicological and environmental research or administrative services). Accordingly, the adequate analytical basis urgently needed for the implementation of any legal rule is still not yet available for many aspects.^{62, 64, 68, 75}

1.4 Objectives

The general objective was to develop a methodological basis enabling spatial high resolution investigations of dissolved and colloidal fractions at SWIs. With a special interest in ENMs as emerging substances, it was the aim to provide validated analytical tools for the characterization of ENMs and studying colloid-mediated transport processes at SWIs.

Therefore, as a first fundamental step, methods were required enabling to investigate the fine scale structures of sediment water interfaces. The objective of **chapter 2** was to provide methods that allow to measure different sediment parameters in parallel to the sampling of sediment pore water at a resolution in the millimeter range. Via the analysis of the pore water samples by means of ICP-MS, multi-element information should be obtained over sediment depth profiles and correlated to the parameters measured. Hence, the goal was to develop a sample probe and a microsampling system and to combine it with a (commercially available) microprofiling system to provide a basis for investigations of natural processes as well as the fate of anthropogenically released substances or the effects of other (mechanical) disturbances at SWIs.

Within **Chapter 3** the focus was set to the development of validated analytical methods for the characterization of colloidal systems to determine i) the total mass concentrations and ii) the dissolved fraction of nanoparticle suspensions. As a powerful and widely applicable technique ICP-MS is used in numerous studies to measure element concentrations of ENP suspensions. Based on this, the suitability of standard ICP-MS methods together with the required sample preparation procedures should be verified for different nanomaterials to define a best practice for total mass determinations. Comparably, different off-line fractionation approaches were compared to identify the most appropriate one for ENP suspensions. In this context, the goal was to provide routine-suitable and easily implementable validated methods to characterize ENP and colloid suspensions.

Aiming to distinguish between dissolved and colloid-mediated transport processes at SWIs, in **Chapter 4** the two size fractionation methods that were identified as the most promising ones in Chapter 3 should be combined with the microprofiling and micro sampling system developed in Chapter 2. Therefore, the methods should be adjusted to small volumes of 0.5 mL and conducted in a glove box under an inert atmosphere. In order to allow a direct analysis of undiluted SPW samples and fractions, an ICP-MS method had to be developed that enable the analysis of sample volumes <500 μ L. With regard to the increased use of ENMs, the methods developed aimed (among others) to enable the investigation of transport processes of ENMs at SWIs and their potential impacts on the natural element distribution.

1.5 Thesis outline

Development of a microprofiling and microsampling system enabling low invasive spatial high resolution investigations of sediment water interfaces.

Chapter 2 explains in detail the development and installation of the microprofiling and micro sampling system (*missy*) including the combination and synchronization of the different components as well as the manufacturing of the newly developed sample probes. Results are presented obtained by an application of the *missy* to a freshwater sediment. With the aim to enable other scientists to adopt the approach, the system and its applications were transparently described, including the advantages and drawbacks, other potential applications as well as potential sources of errors.

Determining the best practice advice for routine suitable nano-analytics.

Chapter 3 describes an approach how to develop, validate and implement routine-suitable analytical methods for the characterization of nanoparticle suspensions. With regard to two main issues related to regulatory frameworks and risk assessment, methods available to determine the total mass concentration and the dissolved fraction were comparably validated. In this context a focus was set on the development of universally applicable methods implementable as standard approaches required for, e.g., legislative rules or tests that is often neglected in nano analytics. Hence, based on the investigations best practice advices were defined suitable to be applied as routine analytical tools for ENP suspensions previously not available.

Development of size fractionation strategies for sediment depth profiles at a millimeter range.

Chapter 4 combines the outcomes of Chapter 2 and Chapter 4 to realize size fractionation analyses (< 450 nm) of pore water samples of sediment depth profiles. The combination of the *missy* with two fractionation approaches enabled for the first time to obtain size dependent information for element distributions at SWIs at a spatial high resolution. Due to the minimal invasive sampling, the sample preparation under an Argon atmosphere and the direct ICP-MS measurements of sample volumes of 300 μ L some of the most cumbersome potential sources of error were overcome.

Final conclusions

Chapter 5 summarizes critically the outcomes of the previous chapters with regard to the obtained analytical possibilities, potential future applications and further improvements.

1.6 References

1. Duester, L.; Kaegi, R.; Wimmer, A., et al. In ABSTRACT BOOK: Final conference of the COST Action ES1205 Engineered Nanomaterials from Wastewater Treatment & Stormwater to Rivers, Final conference of the COST Action ES1205, University of Aveiro, Portugal, 2017; University of Aveiro, Portugal, 2017; p 228.
2. Santschi, P.; Höhener, P.; Benoit, G., et al., Chemical processes at the sediment-water interface. *Marine Chemistry* 1990, 30, (0), 269-315.
3. Jorgensen, B. B.; Revsbech, N. P., Diffusive boundary-layers and the oxygen-uptake of sediments and detritus. *Limnology and Oceanography* 1985, 30, (1), 111-122.
4. Revsbech, N. P.; Jorgensen, B. B., Microelectrodes - their use in microbial ecology. *Advances in Microbial Ecology* 1986, 9, 293-352.
5. Du Laing, G.; Rinklebe, J.; Vandecasteele, B., et al., Trace metal behaviour in estuarine and riverine floodplain soils and sediments: A review. *Science of the Total Environment* 2009, 407, (13), 3972-3985.
6. Søndergaard, M., Redox Potential. In *Encyclopedia of Inland Waters*, Likens, G. E., Ed. Academic Press: Oxford, 2009; pp 852-859.
7. Canfield, D. E.; Thamdrup, B., Towards a consistent classification scheme for geochemical environments, or, why we wish the term 'suboxic' would go away. *Geobiology* 2009, 7, (4), 385-392.
8. Honold, F., Honold Brigitte Ionenselektive Elektroden: Grundlagen und Anwendungen in Biologie und Medizin. Birkhäuser Basel: 1991.
9. DeLaune, R. D.; Reddy, K. R., Redox Potential A2 - Hillel, Daniel. In *Encyclopedia of Soils in the Environment*, Elsevier: Oxford, 2005; pp 366-371.
10. Cappuyns, V.; Swennen, R., Kinetics of element release during combined oxidation and pH(stat) leaching of anoxic river sediments. *Applied Geochemistry* 2005, 20, (6), 1169-1179.
11. Cappuyns, V.; Swennen, R.; Devivier, A., Influence of ripening on pH(stat) leaching behaviour of heavy metals from dredged sediments. *Journal of Environmental Monitoring* 2004, 6, (9), 774-781.
12. Gäbler, H.-E., Mobility of heavy metals as a function of pH of samples from an overbank sediment profile contaminated by mining activities. *Journal of Geochemical Exploration* 1997, 58, (2-3), 185-194.
13. Cappuyns, V.; Swennen, R., The application of pH(stat) leaching tests to assess the pH-dependent release of trace metals from soils, sediments and waste materials. *Journal of Hazardous Materials* 2008, 158, (1), 185-195.
14. Ye, S. Y.; Laws, E. A.; Gambrell, R., Trace element remobilization following the resuspension of sediments under controlled redox conditions: City Park Lake, Baton Rouge, LA. *Applied Geochemistry* 2013, 28, 91-99.
15. Tankere, S. P. C.; Statham, P. J.; Price, N. B., Biogeochemical cycling of Mn and Fe in an area affected by eutrophication: The Adriatic Sea. *Estuarine Coastal and Shelf Science* 2000, 51, (4), 491-506.
16. Fabricius, A. L.; Duester, L.; Ecker, D., et al., New Microprofiling and Micro Sampling System for Water Saturated Environmental Boundary Layers. *Environmental Science & Technology* 2014, 48, (14), 8053-8061.
17. Frohne, T.; Rinklebe, J.; Diaz-Bone, R. A., Contamination of Floodplain Soils along the Wupper River, Germany, with As, Co, Cu, Ni, Sb, and Zn and the Impact of Pre-definite Redox Variations on the Mobility of These Elements. *Soil & Sediment Contamination* 2014, 23, (7), 779-799.
18. Chen, S. Y.; Lin, J. G., Bioleaching of heavy metals from sediment: significance of pH. *Chemosphere* 2001, 44, (5), 1093-1102.

19. Schaller, J.; Brackhage, C.; Mkandawire, M., et al., Metal/metalloid accumulation/remobilization during aquatic litter decomposition in freshwater: A review. *Science of the Total Environment* 2011, 409, (23), 4891-4898.
20. Balistrieri, L. S.; Murray, J. W.; Paul, B., The geochemical cycling of trace-elements in a biogenic meromictic lake. *Geochimica Et Cosmochimica Acta* 1994, 58, (19), 3993-4008.
21. Giblin, A. E., Iron and Manganese. In *Encyclopedia of Inland Waters*, Likens, G. E., Ed. Academic Press: Oxford, 2009; pp 35-44.
22. Rigaud, S.; Radakovitch, O.; Couture, R. M., et al., Mobility and fluxes of trace elements and nutrients at the sediment-water interface of a lagoon under contrasting water column oxygenation conditions. *Applied Geochemistry* 2013, 31, 35-51.
23. Huerta-Diaz, M. A.; Tessier, A.; Carignan, R., Geochemistry of trace metals associated with reduced sulfur in freshwater sediments. *Applied Geochemistry* 1998, 13, (2), 213-233.
24. Kretzschmar, R.; Schafer, T., Metal retention and transport on colloidal particles in the environment. *Elements* 2005, 1, (4), 205-210.
25. Guo, L.; Santschi, P. H., Ultrafiltration and its Applications to Sampling and Characterisation of Aquatic Colloids. In *Environmental Colloids and Particles*, John Wiley & Sons, Ltd: 2007; pp 159-221.
26. Sen, T. K.; Khilar, K. C., Review on subsurface colloids and colloid-associated contaminant transport in saturated porous media. *Advances in Colloid and Interface Science* 2006, 119, (2-3), 71-96.
27. Ran, Y.; Fu, J. M.; Sheng, G. Y., et al., Fractionation and composition of colloidal and suspended particulate materials in rivers. *Chemosphere* 2000, 41, (1-2), 33-43.
28. Spectrum Laboratories, I., SPECTRUMLABS:COM relative Size chart. In.
29. Itoh, A.; Nagasawa, T.; Zhu, Y. B., et al., Distributions of major-to-ultratrace elements among the particulate and dissolved fractions in natural water as studied by ICP-AES and ICP-MS after sequential fractionation. *Anal. Sci.* 2004, 20, (1), 29-36.
30. Dabrin, A.; Roulier, J. L.; Coquery, M., Colloidal and truly dissolved metal(oid) fractionation in sediment pore waters using tangential flow filtration. *Applied Geochemistry* 2013, 31, 25-34.
31. Macgregor, K.; MacKinnon, G.; Farmer, J. G., et al., Mobility of antimony, arsenic and lead at a former antimony mine, Glendinning, Scotland. *Science of The Total Environment* 2015, 529, 213-222.
32. Canavan, R. W.; Van Cappellen, P.; Zwolsman, J. J. G., et al., Geochemistry of trace metals in a fresh water sediment: Field results and diagenetic modeling. *Science of the Total Environment* 2007, 381, (1-3), 263-279.
33. Von der Kammer, F.; Baborowski, M.; Tadjiki, S., et al., Colloidal particles in sediment pore waters: Particle size distributions and associated element size distribution in anoxic and re-oxidized samples, obtained by FFF-ICP-MS coupling. *Acta Hydrochimica Et Hydrobiologica* 2004, 31, (4-5), 400-410.
34. Schijf, J.; Zoll, A. M., When dissolved is not truly dissolved-The importance of colloids in studies of metal sorption on organic matter. *Journal of Colloid and Interface Science* 2011, 361, (1), 137-147.
35. Gustafsson, O.; Gschwend, P. M., Aquatic colloids: Concepts, definitions, and current challenges. *Limnology and Oceanography* 1997, 42, (3), 519-528.
36. Kottelat, R.; Vignati, D. A. L.; Chanudet, V., et al., Comparison of small- and large-scale ultrafiltration systems for organic carbon and metals in freshwater at low concentration factor. *Water Air and Soil Pollution* 2008, 187, (1-4), 343-351.
37. Huerta-Diaz, M. A.; Rivera-Duarte, I.; Sanudo-Wilhelmy, S. A., et al., Comparative distributions of size fractionated metals in pore waters sampled by in situ dialysis and whole-core sediment squeezing: Implications for diffusive flux calculations. *Applied Geochemistry* 2007, 22, (11), 2509-2525.

38. Stockdale, A.; Davison, W.; Zhang, H., Micro-scale biogeochemical heterogeneity in sediments: A review of available technology and observed evidence. *Earth-Science Reviews* 2009, 92, (1-2), 81-97.
39. Köhl, M.; Revsbech, N. P., Biogeochemical Microsensors for Boundary Layer Studies. In *The Benthic Boundary Layer: Transport processes and Biogeochemistry.*, Jørgensen, B. P. B. B., Ed. Oxford University Press: Oxford, 2001; pp p. 180-210.
40. Mudroch, A. A., Jose M. , *Manual of Aquatic Sediment Sampling*. CRC Press, Inc. : 1995.
41. Bufflap, S. E.; Allen, H. E., Sediment Pore-Water Collection Methods for Trace-Metal Analysis - A Review. *Water Research* 1995, 29, (1), 165-177.
42. Revsbech, N. P., Analysis of microbial communities with electrochemical microsensors and microscale biosensors. In *Environmental Microbiology*, Leadbetter, J. R., Ed. 2005; Vol. 397, pp 147-166.
43. Lee, W. H.; Lee, J.-H.; Choi, W.-H., et al., Needle-type environmental microsensors: design, construction and uses of microelectrodes and multi-analyte MEMS sensor arrays. *Measurement Science & Technology* 2011, 22, (4).
44. Peiffer, S., Characterisation of the Redox State of Aqueous Systems: Towards a Problem-Oriented Approach. In *Redox: Fundamentals, Processes and Applications*, Schüring, J., et al., Eds. Springer Berlin Heidelberg: Berlin, Heidelberg, 2000; pp 24-41.
45. Galster, H., Technique of Measurement, Electrode Processes and Electrode Treatment. In *Redox: Fundamentals, Processes and Applications*, Schüring, J., et al., Eds. Springer Berlin Heidelberg: Berlin, Heidelberg, 2000; pp 13-23.
46. Saager, P. M.; Sweerts, J.-P.; Ellermeijer, H. J., A simple pore-water sampler for coarse, sandy sediments of low porosity. *Limnology and Oceanography* 1990, 35, (3), 747-751.
47. Seeberg-Elverfeldt, J.; Schluter, M.; Feseker, T., et al., Rhizon sampling of porewaters near the sediment-water interface of aquatic systems. *Limnology and Oceanography-Methods* 2005, 3, 361-371.
48. Beck, M.; Dellwig, O.; Kolditz, K., et al., In situ pore water sampling in deep intertidal flat sediments. *Limnology and Oceanography-Methods* 2007, 5, 136-144.
49. Sayles, F. L.; Mangelsdorf, P. C.; Wilson, T. R. S., et al., A sampler for the in situ collection of marine sedimentary pore waters. *Deep Sea Research and Oceanographic Abstracts* 1976, 23, (3), 259-264.
50. Barnes, R. O., An in situ interstitial water sampler for use in unconsolidated sediments. *Deep Sea Research and Oceanographic Abstracts* 1973, 20, (12), 1125-1128.
51. Goodman, K. S., An apparatus for sampling interstitial water throughout tidal cycles. *Hydrobiological Bulletin* 1979, 13, (1), 30-33.
52. Howes, B. L.; Dacey, J. W. H.; Wakeham, S. G., Effects of sampling technique on measurements of porewater constituents in salt marsh sediments¹. *Limnology and Oceanography* 1985, 30, (1), 221-227.
53. Torres, N. T.; Hauser, P. C.; Furrer, G., et al., Sediment porewater extraction and analysis combining filter tube samplers and capillary electrophoresis. *Environmental Science: Processes & Impacts* 2013, 15, (4), 715-720.
54. Davison, W.; Grime, G. W.; Morgan, J. A. W., et al., Distribution of dissolved iron in sediment pore waters at submillimetre resolution. *Nature* 1991, 352, (6333), 323-325.
55. Davison, W.; Fones, G. R.; Grime, G. W., Dissolved metals in surface sediment and a microbial mat at 100- μ m resolution. *Nature* 1997, 387, (6636), 885-888.
56. Davison, W.; Zhang, H.; Grime, G. W., Performance Characteristics of Gel Probes Used For Measuring the Chemistry of Pore Waters. *Environmental Science & Technology* 1994, 28, (9), 1623-1632.
57. Davison, W.; Zhang, H., In situ speciation measurements of trace components in natural waters using thin-film gels. *Nature* 1994, 367, (6463), 546-548.

58. Davison, W.; Zhang, H., Progress in understanding the use of diffusive gradients in thin films (DGT) - back to basics. *Environmental Chemistry* 2012, 9, (1), 1-13.
59. Ding, S. M.; Wang, Y.; Xu, D., et al., Gel-Based Coloration Technique for the Submillimeter-Scale Imaging of Labile Phosphorus in Sediments and Soils with Diffusive Gradients in Thin Films. *Environmental Science & Technology* 2013, 47, (14), 7821-7829.
60. Xu, D.; Wu, W.; Ding, S. M., et al., A high-resolution dialysis technique for rapid determination of dissolved reactive phosphate and ferrous iron in pore water of sediments. *Science of the Total Environment* 2012, 421, 245-252.
61. Nowack, B.; Mueller, N. C.; Krug, H. F., et al., How to consider engineered nanomaterials in major accident regulations? *Environmental Sciences Europe* 2014, 26, (1), 2.
62. Organisation for Economic Cooperation and Development (OECD) Testing Programme of Manufactured Nanomaterials. <http://www.oecd.org/chemicalsafety/nanosafety/testing-programme-manufactured-nanomaterials.htm> (03.05.2017),
63. European Commission (EC) Nanomaterials in REACH and CLP. http://ec.europa.eu/environment/chemicals/nanotech/reach-clp/index_en.htm (19.04.2017),
64. Federal Ministry for the Environment, N. C., Building and Nuclear Safety (BMUB), Der Nano-Dialog der Bundesregierung. <http://www.bmub.bund.de/themen/gesundheit-chemikalien/nanotechnologie/nanodialog/> (03.05.2017),
65. European Commission (EC), Communication from the Commission to the European Parliament, the Council and the European Economic and Social Committee; Second Regulatory Review on Nanomaterials. In EUROPEAN COMMISSION: Brussels, 2012; Vol. COM(2012) 572 final.
66. Environmental Protection Agency (EPA), Chemical Substances When Manufactured or Processed as Nanoscale Materials: TSCA Reporting and Recordkeeping Requirements - final rule. In EPA-HQ-OPPT-2010-0572, 2017; Vol. 2070-AJ54.
67. Aitken, R. A., Bassan, A., Friedrichs, S., Hankin, S.M., Hansen, S.F., Holmqvist, J., Peters, S.A.K., Poland, C.A., Tran, C.L. Specific Advice on Exposure Assessment and Hazard/Risk Characterisation for Nanomaterials under REACH (RIP-oN 3) - Final Project Report; 2011.
68. European Chemicals Agency (ECHA) Nanomaterials - ECHA. <https://echa.europa.eu/de/regulations/nanomaterials> (20.04.2017),
69. European Chemicals Agency (ECHA) Update of the Workplan on Nanomaterials - 39th Meeting of the Management Board 24-25 September 2015; Luxembourg, 25.9.2015, 2015; p 10.
70. European Commission (EC) Nanomaterials. http://ec.europa.eu/growth/sectors/chemicals/reach/nanomaterials_en (05.05.2017),
71. Little Pro Regulations on Nanomaterials in EU and Nano Register 2016. http://www.chemsafetypro.com/Topics/EU/Regulations_on_Nanomaterials_in_EU_and_Nano_Register.html (20.04.2017),
72. European Commission (EC), Regulation (EC) No 1223/2009 of the European Parliament and of the Council of 30 November 2009 on cosmetic products. In 2009; Vol. L 342/59.
73. European Commission (EC), Regulation (EU) No 528/2012 of the European Parliament and of the Council of 22 May 2012 concerning the making available on the market and use of biocidal products (1). In 2009; Vol. 528/2012.
74. European Commission (EC), Regulation (EU) No 1169/2011 of the European Parliament and of the Council of 25 October 2011 on the provision of food information to consumers, amending Regulations (EC) No 1924/2006 and (EC) No 1925/2006 of the European Parliament and of the Council, and repealing Commission Directive 87/250/EEC, Council Directive 90/496/EEC, Commission Directive 1999/10/EC, Directive 2000/13/EC of the European Parliament and of the Council, Commission Directives 2002/67/EC and 2008/5/EC and Commission Regulation (EC) No 608/2004. In 2009; Vol. L 304/18
75. Laborda, F.; Bolea, E.; Cepria, G., et al., Detection, characterization and quantification of inorganic engineered nanomaterials: A review of techniques and methodological approaches for the analysis of complex samples. *Analytica Chimica Acta* 2016, 904, 10-32.

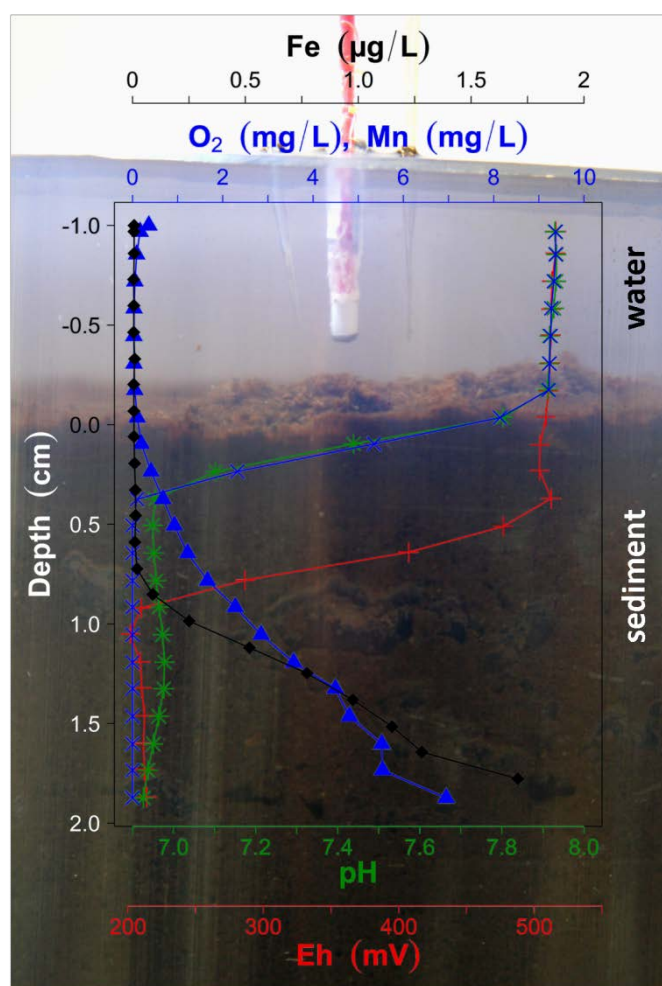
76. Majedi, S. M.; Lee, H. K., Recent advances in the separation and quantification of metallic nanoparticles and ions in the environment. *TrAC Trends in Analytical Chemistry* 2016, 75, 183-196.
77. Hassellöv, M.; Kaegi, R., Analysis and Characterization of Manufactured Nanoparticles in Aquatic Environments. In *Environmental and Human Health Impacts of Nanotechnology*, John Wiley & Sons, Ltd: 2009; pp 211-266.

2

New Microprofiling and Micro Sampling System for Water Saturated Environmental Boundary Layers

Anne-Lena Fabricius, Lars Duester, Dennis Ecker and Thomas A. Ternes

Environmental Science and Technology, 2014, 48 (14), pp 8053–8061



2.1 Abstract

The spatial high resolution of a microprofiling system was combined with the multi-element capability of ICP-MS to enable a better understanding of element distributions and related processes across environmental boundary layers. A combination of a microprofiling system with a new micro filtration probe head connected to a pump and a fraction collector (*microprofiling and micro sampling system, missy*) is presented. This enables for the first time a direct, dynamic, and high resolution automatic sampling of small water volumes (<500 μL) from depth profiles of water saturated matrices (e.g., sediments, soils, biofilms). Different membrane cut-offs are available and resolutions of a few (matrices with a high physical resistance) to a submillimeter scale (matrices with low physical resistance) can be achieved. In this Article (i) the modular setups of two *missys* are presented; (ii) it is demonstrated how the micro probe heads are manufactured; (iii) background concentrations and recoveries of the system as well as (iv) exemplary results of a sediment water interface are delivered. On this basis of this, potentials, possible sources of errors, and future applications of the new *missy* are discussed.

2.2 Introduction

Understanding biogeochemical processes at the boundary layer of sediment water interfaces (SWI) requires the investigation of physicochemical parameters (like the O₂ concentration, redox potential or, pH value) in parallel to the distribution of different analytes (e.g., trace metals, nutrients, or organic compounds) in the pore water at a spatial high resolution. Due to the development of different measurement and sampling techniques, the possibilities to study these heterogeneous and dynamic environments were improved considerably during the last decades.¹ In particular, the availability of numerous microsensors and -electrodes (e.g., O₂, redox potential, pH value, H₂S, N₂O) enables the analysis of several parameters/analytes at a high resolution and provides a better understanding of processes at boundary layers and micro niches of the SWI or biofilms.^{2, 3} Apart from that, the analysis of chemical species at the SWI is performed on the basis of pore water samples.¹ Commonly applied sampling techniques can be categorized^{4, 5} as either *ex situ* methods, like centrifugation or squeezing,^{6, 7} or *in situ* methods like dialysis^{8, 9} (including diffusive gradients/equilibration in thin film (DGT/DET) or peepers)^{3-5, 10} and suction based techniques.¹¹⁻¹³ Drawbacks of these approaches are, on the one hand, the requirement of either the installation of the sampling devices at the sampling site and/or elevated sample preparation procedures (e.g., slicing, centrifugation, or re-elution from/digestion of accumulation gels) that may influence the environmental conditions at the area studied and/or the characteristics of the samples. On the other hand, only few techniques allow for a spatial resolution at a millimeter or submillimeter scale and hence do not capture fine-scale differences of heterogeneous (micro)environments even though some DGT-based methods are reported that enable a high resolution sampling.^{1, 10, 14, 15}

The investigation of trace metal distributions at the SWI, particularly in relation to different physicochemical parameters, is important to gain a holistic understanding of biogeochemical processes determining the mobility and transformation of chemical species and to assess potential risks arising from contaminated sediments (of, e.g., industrial,⁸ urban,^{14, 16} or mining areas,⁶ deltas¹⁷ or fish farms¹⁸). One of the most common and powerful analytical techniques in environmental analytical chemistry of metals and metalloids (metal(loid)s) is inductively coupled plasma-mass spectrometry (ICP-MS). Multi-element capabilities combined with low detection limits led to a widespread dissemination of ICP-MS systems within the last decades.

To combine the analytical benefits of ICP-MS analyses with the spatial information on microprofiling, a *micro*profiling and *micro*sampling (filtration) *system* (*missy*) was developed. Two different setups of a *missy* were tested for background concentrations and recoveries and their applicability to investigate metal(loid) distributions at the SWI at a spatial high resolution. Therefore,

proof-of-principle experiments were conducted, studying the distributions of five exemplary chosen metal(loid)s along a transect of a sediment core in correlation to the redox potential, O₂ concentration, and pH value. With the aim to enable other scientists to create and install their own *missy* setup or to adapt the ones presented to their scientific questions/needs, detailed information on the system and on potential applications is delivered. On the basis of the results of the first applications, the potentials and possible sources of error and suggestions for improvements of the system are discussed.

2.3 Experimental Section

2.3.1 Terms and Definitions

Since some of the terms addressed in this Article are not sufficiently defined or have several meanings, a short overview of basic terms/concepts, focusing on environmental analytical sciences and sampling of liquids, is given.

The term micro sampling (also micro-sampling) is used either for samples <1 mg (e.g., in laser ablation¹⁹) or <1 mL or for sampling with low flow rates in the $\mu\text{L}/\text{min}$ range (e.g., for ICP-MS analyses²⁰). In this study, micro sampling addresses a volume <1 mL per sampling point as well as sampling with a flow rate of 5 $\mu\text{L}/\text{min}$.

Microprofiling (also micro-profiling or micro profiling) is most commonly used to describe studies performed with microsensors/-electrodes, e.g., redox potential, N_2O , oxygen or multi-analyte arrays.²¹ For high resolution depth profiling (on, e.g., sediments or biofilms), experiments are often conducted using laboratory stands equipped with micromanipulators enabling a precise operation of the microsensors.^{22, 23}

For filtration approaches different devices are applied like rhizon samplers^{11, 24} or comparable probes^{12, 13} with membranes made of, e.g., poly(ether sulfone) (PES), with different cut-offs (e.g., 0.1 or 0.45 μm). Beside this, micro dialysis can be applied to quantify metal(loid)s in liquids. However, most of the micro dialysis studies address in vivo metabolization²⁵ and only few with an environmental focus are available (e.g., Torto and Mogopodi²⁶). For the experiments conducted in this study, filtration was found to be more suitable than micro dialysis, because the latter can be hampered by, e.g., uncertainties in dialyzing efficiency with changing media compositions or by challenges in calibration.²⁵

2.3.2 Chemicals and Materials

Ultrapure water was produced using an USF ELGA Purelab Plus system (ELGA LabWater, Germany). ICP-element standards (1 g/L) and nitric acid (HNO_3 , 65% w/w, for analysis) were purchased from Merck GmbH (Germany). The acid was sub-boiled using a dst-1000 (Savillex, USA). Prior to use, all vessels and the 96-microwell plates (Riplate RW, 1 mL, PP, Ritter medical, Germany) were rinsed >24 h with HNO_3 (1.3%). All tubes and connectors used were made of fluorinated ethylene propylene (FEP) or from polyether ether ketone (PEEK). The sediment examined in the experiments was a mixture of 80% sieved (20 - 63 μm) and freeze-dried natural freshwater sediment (information on the general characteristics of the sediment is given in Table A1. 1–Appendix A1) and of 20% sand (Spielsand, Silex GmbH, Germany) to produce an idealized, homogeneous sediment

core. The freshwater sediment was sampled in 2012 at the river Lahn (stream km 136, water gate Lahnstein, Germany, 50°18'29.47"N 7°36'46.24"O). After homogenizing the mixture, the sediment was placed in an aquarium (glass tank, 20 × 15 × 20 cm) filled with demineralized water (electric conductivity ~0.5 µS/cm; demineralization system by Grünbeck Wasseraufbereitung GmbH, Germany) and left untreated for 9 weeks to allow the gradients at the SWI to develop. If required, evaporated water was refilled.

2.3.3 Sample Probes

The manufacturing of the probes used within the experiments is presented in Figure 2.1. They consisted of a PES porous hollow fiber (0.45 µm) head connected to a tube which was stabilized by pipet tips. However, also other materials and cut-offs are available and can be used for probe manufacturing. To manufacture a probe, the hollow fiber was cut in 3 mm pieces using a scalpel. A piece of ~25 cm of (FEP) tube (inner diameter 0.125 mm Upchurch, USA), with an outer diameter that fits tightly into the fiber, was inserted fully in the fiber piece (refer to Figure 2.1 a).

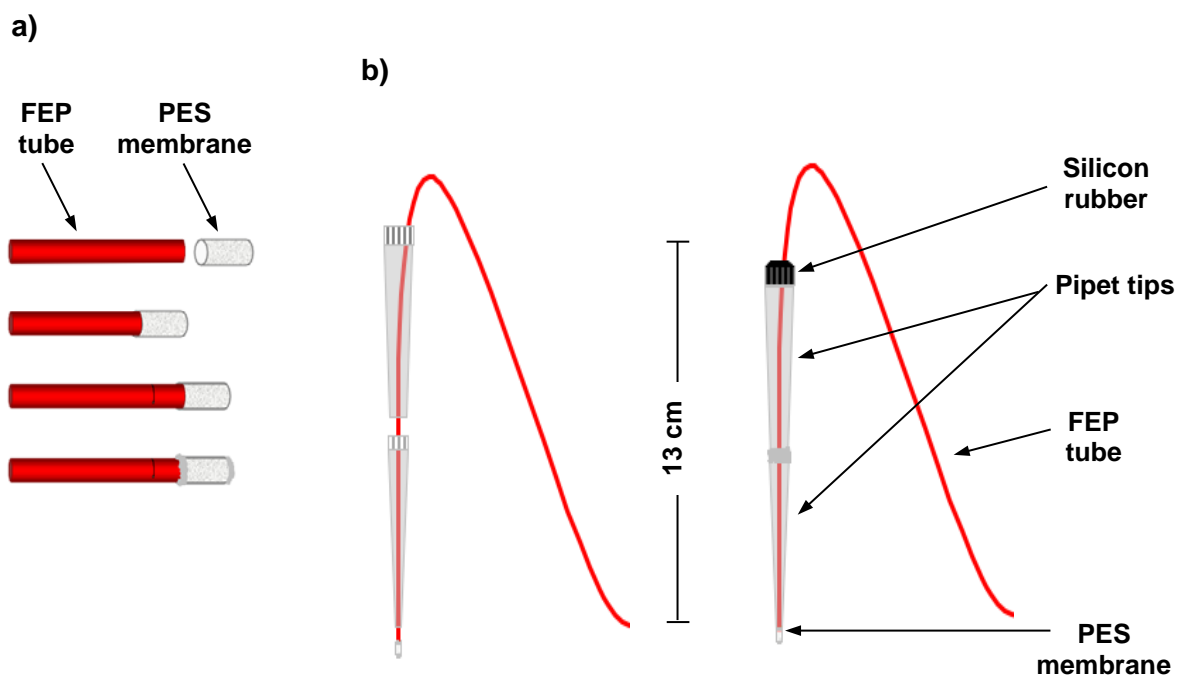


Figure 2.1: Schematic drawing of the manufacturing of a micro sampling probe. (a) Connecting the tube with the PES membrane and sealing of the membrane. (b) Connection of two pipet tips and fixing of the tube by silicon rubber (a detailed description is given in the text).

Using a binocular (SZB 300, VWR, Germany), the FEP tubing was marked at the end of the fiber piece by means of a scalpel. Subsequently, the tubing was removed 2 mm using the scalpel scratch as mark, resulting in an overlap of the tube and the fiber piece of ~1 mm. The distances were measured using an objective micrometer. The PES piece and the FEP tube were connected using molten (by

means of a lighter) polypropylene (PP) pipet tips (Finntip, Thermo Scientific, Germany). After sealing the open end of the piece of hollow fiber with molten PP, the probe head was tested for leak tightness of the connection between tube and fiber as well as of the end of the fiber. Therefore, a syringe (Hamilton, Switzerland, Gastight #1750) filled with water was connected to the tube via a Finger Tight Fitting (PEEK, F-120X) and a Luer adapter (PEEK, P-659, both Upchurch, USA) and water was pressed extremely carefully through the PES membrane to avoid ruptures. After the probe head was found to be leak proof (water penetrates only through the membrane, visible under the binocular), the tube was inserted into two connected pipet tips (Finntip 1000, Thermo Scientific, Germany; Figure 2.1b) and fixed with molten PP as described above. Finally, the FEP tube was fixed at the pipet tip using a self-setting silicone rubber (Sugru, FormFormForm Limited, United Kingdom) to stabilize the probe.

2.3.4 Missy Setups

Two different *missy* setups were tested; both combining a microprofiling with a micro sampling system. In the case of the first setup (*missy* setup 1, presented in Figure 2.2), the micro sampling system consists of a low pressure high precision syringe pump (neMESYS), a Rheodyne valve (Qmix EX), and a miniature positioning system (rotAXYS, all three Cetoni, Germany). In the alternative setup (*missy* setup 2), the syringe pump and the valve were replaced by a micro annular gear pump (mzr-2542) connected to a console drive module (mzr-S06, both HNP Microsystems, Germany). By synchronizing the software of the profiling (SensorTrace PRO, Unisense, Denmark) and the sampling system (QmixElements, Cetoni GmbH, Germany), it was possible to measure profiles of oxygen and redox potential or pH value in parallel to the sampling of water and pore water.

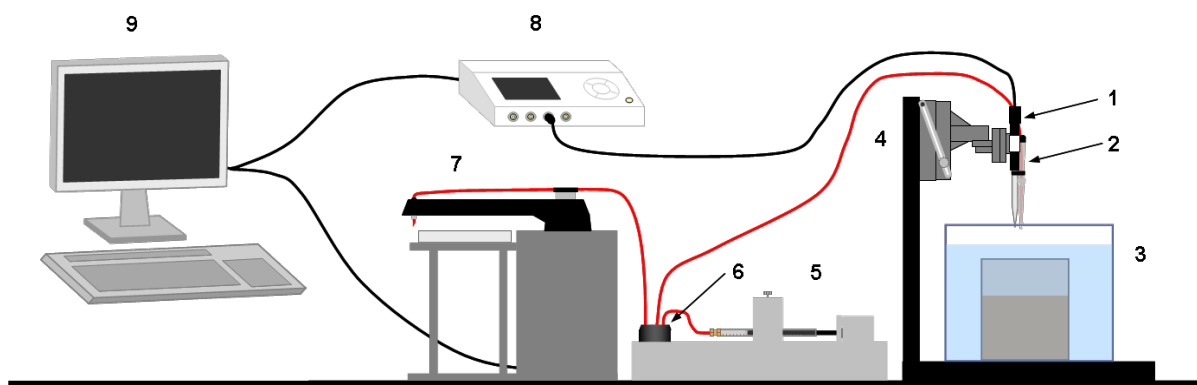


Figure 2.2: Schematic drawing of the *missy* setup 1. 1, microelectrode; 2, sample probe; 3, aquarium with sediment core; 4, laboratory stand with two profiling motors (X- and Z-axis); 5, syringe pump; 6, Rheodyne valve; 7, fraction collector: positioning system with a microwell plate; 8, microsensor multimeter; 9, PC.

2.3.5 Microprofiling System

Measurements of the oxygen concentration, the redox potential, and the pH value were conducted by means of a microprofiling system equipped with a computer controlled motorized micromanipulator (Unisense, Denmark). Oxygen was measured using a Clark-type O₂ microsensor (OX-100, Unisense Denmark), profiles of redox potential and pH value were obtained by application of microelectrodes (standard hydrogen potential; RD-100, pH-100 glass electrode, Unisense, Denmark) connected to an Ag/AgCl-reference electrode (REF321, Radiometer Analytical, Denmark). To facilitate the reading, the term “redox potential” is used for the potential measured by the platinum electrode even though this represents the operationally determined value and not the thermodynamic potential. Sensors/electrodes were connected to a microsensor multimeter that transferred the data to the microprofiling software (SensorTrace PRO). The pH/redox microelectrode and the O₂ microsensor were calibrated previous to the experiments in accordance to the instructions given in the manuals.

2.3.6 Characterization: Background Concentrations and Recoveries

Prior to the experiments, the metal(loid) background concentrations of the sampling system were determined for ultrapure water and the experiment matrix (aquarium water). The latter was taken as a reference for the profiling experiments and was additionally compared to samples filtered by syringe filters (Minisart NML Syringe Filters 16555 K, surfactant-free cellulose acetate, pore size 0.45 µm, Sartorius, Germany). Analyses of ultrapure water were conducted after cleaning the *missy* and after the profiling experiments. Moreover, the recoveries for the two systems were determined in ultrapure water and nitric acid (1.3%). A detailed description and discussion of the background and recovery experiments are given in the Appendix A1 (paragraph System Characterization). All values presented were determined on the basis of ten, in the case of the syringe filter approach five, replicates and were tested for outliers (see the section Data Analyses).

2.3.7 Micro Sampling System

The sediment profiles of pore water, exemplary presented, were obtained by application of the *missy* setup 1. Therefore, an intended volume of 500 µL was sampled with a flow rate of 5 µL/min and transferred (25 µL/min) to the well plate on the positioning system. To reduce evaporation of the samples, the well plate was covered by a self-adhesive foil (adhesive polyethylene film for ELISA incubation, nonsterile, VWR, Germany). In agreement with the general convention, the elemental concentrations of the samples, filtered by the PES membrane (cut-off <0.45 µm) of the probe, were defined as “dissolved”, even though also colloids can pass the pores. At the beginning of each experiment all parts of the sampling system were filled with aquarium water. The volume of each

sample (depending on the gas to water ratio at the sampling point ~50 – 450 μL) was determined by pipetting the sample from the well plate into centrifugal tubes (15 mL, PP, VWR, Germany). After diluting the samples to 3-4 mL using 1.3% HNO_3 , the metal(loid) concentrations were determined by means of ICP-MS. Setup 2 including the micro annular gear pump was only tested for general comparability.

2.3.8 Profiling Experiments

In total, a transect of five profiles was measured from 1 cm above the sediment surface to 2 cm within the sediment. The sediment surface (0 cm) of the first profile was identified by the help of the O_2 electrode (beginning of the O_2 decline) and verified by an USB microscope (DNT DigiMicro 2.0, Germany). To map the microstructures of the sediment surface and to provide the comparability between the profiles, the surface setting was also kept for the following profiles. The profiles were approximately 0.5 cm separated from each other (manually positioned with the micromanipulator). Per profile 480 data points were measured for O_2 concentration, pH and redox potential (step size of 63 μm) and 24 water samples were taken, each sampled over a distance of 1.1 mm. The time required per profile was 44 h (Table A1. 5, Appendix A1). To avoid influences of the sampling procedure on the sediment parameters measured, the electrodes/sensors and the sample probe were fixed in such a manner that the tips were at the same height. The difference between the measurements and sampling depths was considered in the depth correction after the experiments. To avoid biases of the results by a potential carryover from the last sample of a profile (2 cm in the sediment) to the first samples of the following profile (overlying water; see also below), two dummy samples were inserted (first two samples) in each profile. Further details on the measurement settings of the two systems are given in the Appendix (Table A1. 5 and Table A1. 6). In order to test the comparability of different sample probes, a new probe was used after three profiles (refer to Figure 2.3 c - g). Since for some elements a carryover from the last sample of a profile (e.g., very high concentrations of Mn) to the first samples of the following profile (e.g., very low Mn concentrations in the overlying water) was observed, an additional experiment was conducted to quantify the maximum amount of elements potentially carried over. Therefore, after a profiling experiment was finished, seven additional samples were taken from the water phase (1 cm above the sediment surface). Sample preparation and measurements were carried out as described (see the section on the Micro Sampling System). Since only a sensor for redox potential or pH measurements can be run, three profiles of the pH value were measured after the experiments described above. To avoid an unfavorable stratification of the water column, the overlying water was slightly disturbed by a soft air stream on the surface, generated by an aquarium pump (MARINA 50, Model 11110, Germany) connected to a pipet tip.

2.3.9 ICP-QMS-Analyses

The metal(loid) concentrations of the pore water samples were determined by means of ICP-MS (Agilent 7700 series), equipped with a PFA-ST Micro Flow nebulizer (ES – 2040) and a PFA inert sample introduction kit with a sapphire injector (inner diameter 2.5 mm, all Agilent Technologies, Germany). Measurements were conducted at a RF power of 1550 W and carrier and dilution gas flows of 0.95 and 0.1 L/min, respectively. Details on the isotopes analyzed, the measurement modes as well as the certified reference materials (CRMs) used are given in the Appendix (Table A1. 7). External calibration was conducted using multi-element standard solutions.

2.3.10 Data Analyses

Data analyses (calculations and statistical tests) and plotting of the profiles were performed using R (version 3.0.2; 2013-09-25),²⁷ for 2D-plots the R package “gplots”²⁸ was applied. The R-package “outliers”²⁹ was used to test for outliers within the replicates of the blank and recovery experiments. Values were excluded if identified as outliers (p-value of <0.01) by the results of two tests (Grubb’s and a Dixon-Test³⁰).

To correlate the element concentrations of the pore water samples with the microprofiling parameters (O₂, redox potential and pH), the dead volume of the sampling system was considered (Table A1. 8, Appendix A1) causing a shift of the element profiles upward in relation to the parameters measured by electrodes/sensors (0.3 and 0.2 mm for *missy* setup 1 and 2, respectively; Table A1. 9, Appendix A1).

2.4 Results and Discussion

2.4.1 Characterization: Background Concentrations and Recoveries

The background concentrations determined for the aquarium water by the different sampling approaches were comparable and were clearly above the values found for ultrapure water (Table 2.1 and Table 2.2). Hence, an influence of the backgrounds of the *missy* on the results of the profiling experiments can be excluded.

Table 2.1: Background Concentrations ($\mu\text{g/L}$) of the Microwell Plates and the Sampling Systems of the two *Missy* Setups (without the Microwell Plate) Determined for Aquarium Water.^a

| Aquarium water | Manganese | Iron | Cobalt | Zinc | Antimony |
|----------------------|-----------------|-----------------|-----------------|------------------|------------------|
| Direct sampling | 1.16 ± 0.01 | 1.97 ± 0.16 | 0.14 ± 0.01 | 67.67 ± 1.05 | 14.86 ± 0.13 |
| Well plate | 3.44 ± 0.29 | 5.87 ± 1.82 | 0.18 ± 0.01 | 60.89 ± 4.02 | 16.15 ± 0.20 |
| <i>Missy</i> setup 1 | 1.61 ± 0.26 | 6.37 ± 3.14 | 0.17 ± 0.01 | 70.71 ± 6.03 | 15.85 ± 0.43 |
| <i>Missy</i> setup 2 | 1.81 ± 0.23 | 5.44 ± 2.39 | 0.16 ± 0.01 | 61.19 ± 9.49 | 14.43 ± 0.24 |

^aValues given represent the mean concentrations of ten replicates and the corresponding confidence interval (CI; $\alpha = 0.05$) after testing for outliers.

Table 2.2: Background Concentrations ($\mu\text{g/L}$) of the Microwell Plates and the Sampling Systems of the Two *Missy* Setups (Without the Microwell Plate) Determined for Ultrapure Water.^a

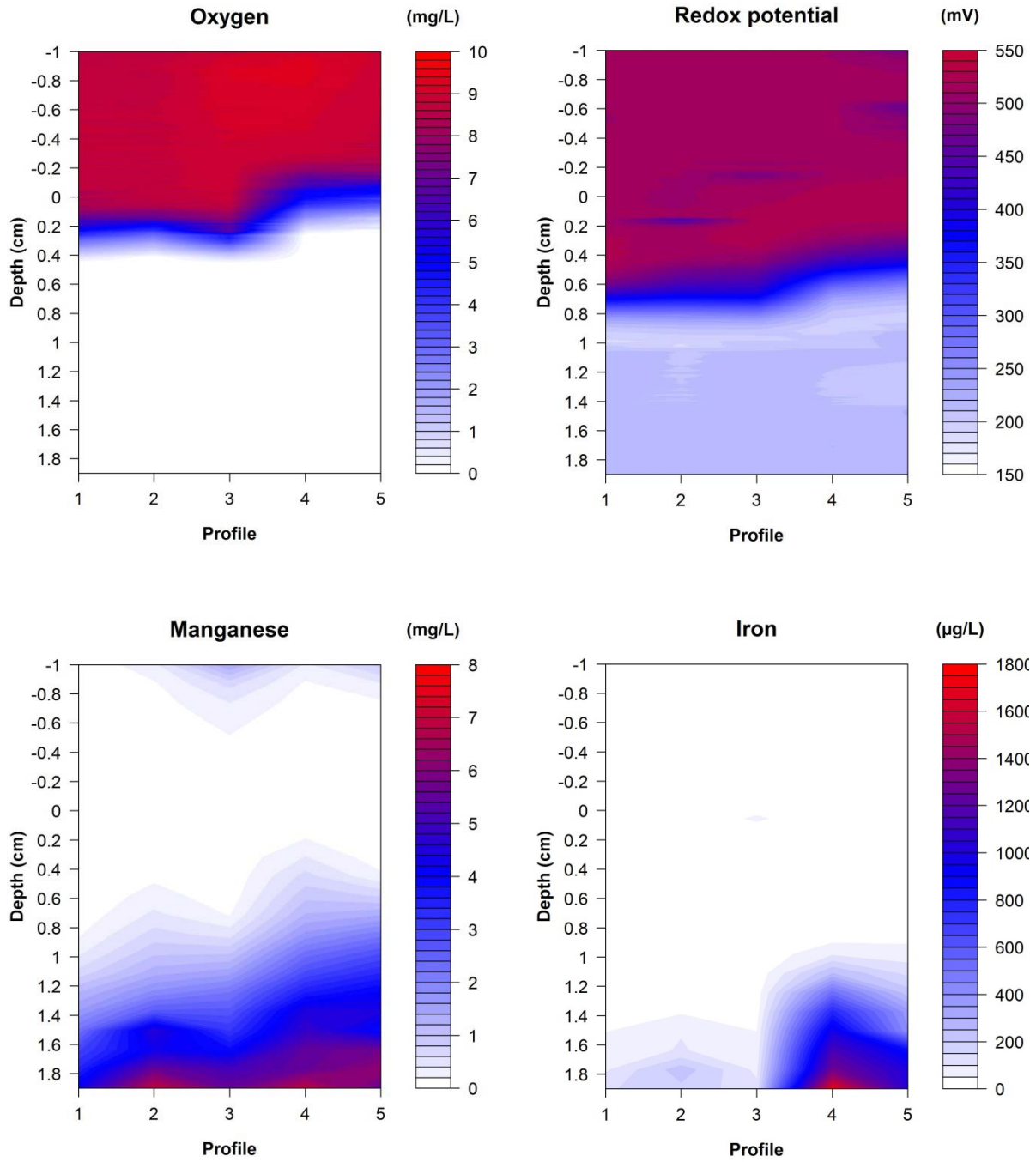
| Ultrapure water | Manganese | Iron | Cobalt | Zinc | Antimony |
|----------------------|------------------|------------------|-----------------|-------------------|----------|
| Well plate | 0.26 ± 0.03 | 1.85 ± 0.79 | <0.01 | 2.41 ± 0.50 | <0.17 |
| <i>Missy</i> setup 1 | | | | | |
| Before | 1.46 ± 0.88 | 0.87 ± 0.69 | <0.01 | 8.37 ± 2.35 | <0.17 |
| After | 17.90 ± 2.96 | 3.83 ± 1.08 | 0.12 ± 0.05 | 19.49 ± 2.86 | <0.17 |
| <i>Missy</i> setup 2 | | | | | |
| Before | 1.90 ± 0.38 | 13.28 ± 3.89 | 0.05 ± 0.01 | 16.07 ± 9.43 | <0.17 |
| After | 0.42 ± 0.08 | 3.29 ± 1.07 | <0.01 | 28.80 ± 27.03 | <0.17 |

^aIn case of the sampling systems, background concentrations were analyzed before and after the profiling experiments. Values given represent the mean concentrations of ten replicates and the corresponding confidence interval (CI; $\alpha = 0.05$) after testing for outliers.

Nevertheless, the comparison of the analyses of ultrapure water before and after the profiling experiments as well as the results of the recovery experiments (Table A1. 4, Appendix A1) indicate potential sources of error that may bias the results if trace metal analyses (ng/L to µg/L) are required: in case of *missy* setup 1, precipitation of metal(oid)s during sampling under atmospheric conditions caused elevated background concentrations in experiments with ultrapure water after the profiling experiments (Table 2.2). Due to the small dimensions of the *missy* compounds, this known challenge of reoxidation during sampling^{4, 5} can be overcome by placing the devices in a glovebag or glovebox containing an inert, oxygen free atmosphere. Since the pore water has only to be acidified prior the ICP-MS measurements, the sample preparation can be conducted in a glovebox or bag. A detailed discussion of potential sources of error that should be considered if trace analyses are required is given in the Appendix A1 (paragraph “System Characterization”).

2.4.2 Sediment Pore Water Profiles

The results of the oxygen concentration and redox potential as well as the concentrations of Mn, Fe, Co, Zn, and Sb determined along a transect of the sediment core are given in Figure 2.3. Measurements (O₂ and redox potential) were conducted in parallel to the sampling from 1 cm above to 2 cm below the sediment surface. Since the settings for the vertical position of the micromanipulator were not changed, the SWI varies along the transect displaying the surface micro relief. For a better orientation, the depth scale is given at the y-axis ignoring the micro relief of the sediment surface. In addition to the 2D-plots, single profiles of the three parameters (O₂, redox, and pH) are presented in comparison to the concentrations of the major redox-sensitive elements Mn and Fe in Figure 2.4. The element concentrations of all pore water samples are given in the Appendix A1 (Table A1. 10 – Table A1. 14). Individual profiles of the five replicates of the O₂ concentration and redox potential as well as the three replicates of the pH value are given in Figure A1. 1. For exemplary results obtained by the second *missy* setup refer to Figure A1. 2 of Appendix 1.



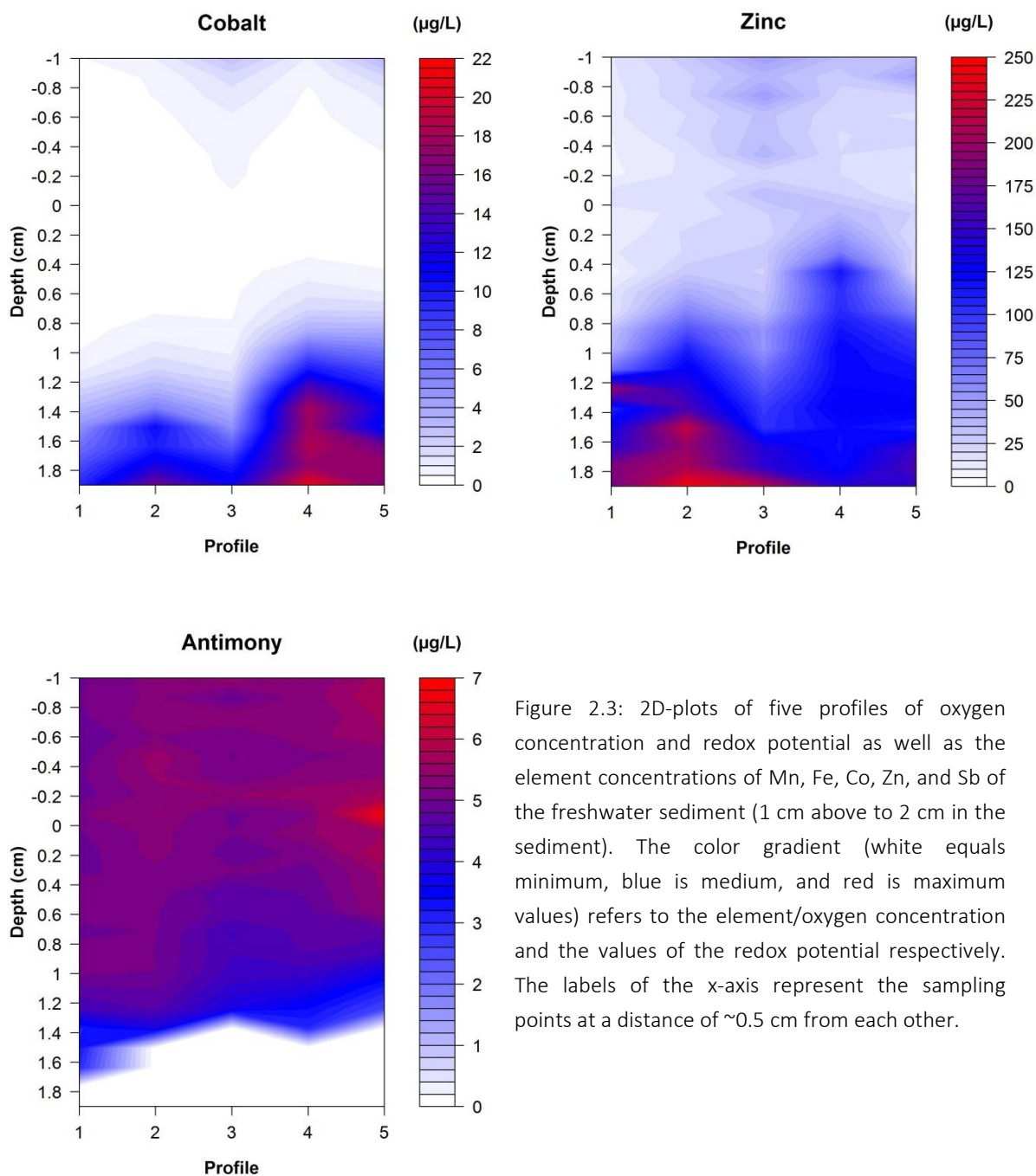


Figure 2.3: 2D-plots of five profiles of oxygen concentration and redox potential as well as the element concentrations of Mn, Fe, Co, Zn, and Sb of the freshwater sediment (1 cm above to 2 cm in the sediment). The color gradient (white equals minimum, blue is medium, and red is maximum values) refers to the element/oxygen concentration and the values of the redox potential respectively. The labels of the x-axis represent the sampling points at a distance of ~ 0.5 cm from each other.

Oxygen Profiles

The O_2 concentration of the overlaying water was $8.7 - 9.3 \text{ mg O}_2/\text{L}$ and decreased rapidly below the limit of detection ($0.01 \text{ mg O}_2/\text{L}$) within the first millimeter of the sediment. The shape of the single O_2 profiles (Figure A1. 1, Appendix A1), with high concentration in the water phase and a rapid depletion within the upper $\sim 2 - 4$ mm of the sediment, is characteristic for shallow, stirred waters, where the introduction of oxygen is only driven by diffusion processes.² Thicker oxic zones can only be found in the presence of photosynthetic bacteria, intense water movement (e.g., currents, waves)

or bioturbation.² Moreover, the depletion is enhanced by microbial O₂ consumption during aerobic degradation of organic material and a limited O₂ flux into the sediment.² The latter, caused by the diffusive boundary layer above the sediment surface, acts as a barrier for dissolved molecules.^{31, 32} The results of the third profile indicate a small hole/step in the sediment where oxygen could penetrate deeper into the sediment.

pH Profiles

The decline of the pH value (Figure 2.4) can be related to (aerobic) respiration processes leading to a release of CO₂ and an increase of the proton concentration.^{2, 3, 33} A slight minimum of the pH was observed at the beginning of the anoxic region probably indicating the O₂/H₂S-interface where H₂S, diffusing from deeper sediment layers, was oxidized to sulfuric acid.^{2, 3} Beside this, the pH can also be influenced by different processes at the surfaces present (of, e.g., oxides, carbonates, silicates, sulfides or phosphates).^{2, 34}

Redox Profiles

In good agreement to the O₂ and pH profiles, a decrease of the redox potential from the water phase (~450 mV) to the lower regions of the sediment (~200 mV) was detected, that was located approximately 1 mm deeper in the sediment (refer to Figure 2.3 and Figure 2.4). This decline can be related to the reduced availability of oxygen as electron acceptor in the anoxic layers of the sediment.^{2, 33} However, the redox potential can also be influenced by other components and processes (e.g., oxidizing capacities of Fe and Mn (oxyhydr)oxides, sulfides, nitrate, or microbial activities)^{2, 33, 34} not further addressed in this study.

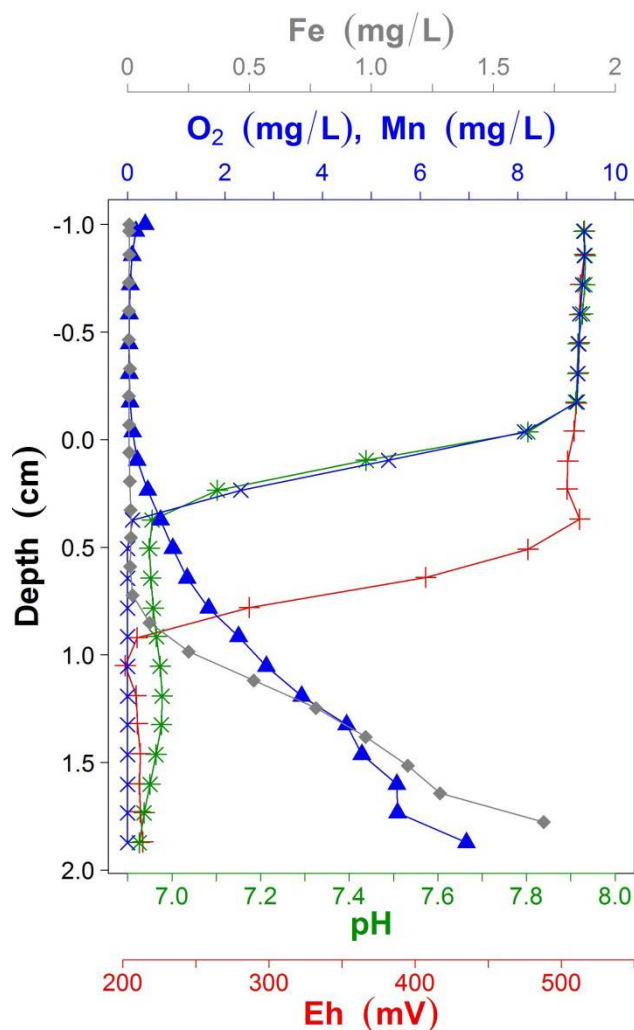


Figure 2.4: Profiles of oxygen (×), redox potential (+) and pH value (*) in comparison to the concentrations of dissolved Mn (▲) and Fe (◆). Measurements of the pH value and the O₂ concentration were conducted in parallel. Profiles of the redox potential and the element concentrations represent the results of the fourth profile. The distance between the data points represents the mean values for the sampling depth (movement of the micro manipulation system during sampling, 1.1 mm) of the respective sample (refer to Table A1. 5).

Metal(loid) Profiles

For the distributions of dissolved Mn, Fe, Co, and Zn in the pore water, an increase within the deeper, anoxic regions of the sediment with a low redox potential was visible. In contrast to this, dissolved Sb was detected in the overlaying water and the pore water samples of the upper sediment layers but not in the deeper areas. The results of Mn, Fe, Co, and Zn are in agreement with the theory on redox-dependent processes of sediment-water systems and can be explained by the reduction of Mn and Fe (oxyhydr)oxides and a resulting release of Mn²⁺ and Fe²⁺ as well as associated trace metals (like Co and Zn).³⁴⁻³⁶ Comparing the pore water concentrations of Mn and Fe, a thicker layer of dissolved Mn was detected, explicable by its reduction at higher redox potentials and a slower (re-)oxidation in comparison to Fe.^{16, 35, 36} Thereby, in contrast to Fe²⁺ only released in deeper layers of the sediment, Mn²⁺ can diffuse to regions near the sediment surface (Figure 2.4). The similarity of the distribution of Co and Mn confirms results of other studies that have shown a preferential association of Co with Mn-oxides, rather than with Fe-oxides.^{17, 35} In the case of dissolved

Zn, the results demonstrate that also nonredox sensitive elements^{16, 35} can be (indirectly) related to the redox gradient due to the sorption to Mn- or Fe-(oxyhydr)oxides.^{17, 35} However, the elevated concentrations of Mn, Co and Zn in the overlaying water of the third and fifth profile indicate a carryover from the previous experiments in the case of continuously used sample probes with only a short rinsing between two profiles (by excluding the two first samples). This is confirmed by the results of the additional experiment, carried out to quantify the amount of analytes that might (at a maximum) be transferred from the last sample of one profile to the first samples of the next (Table A1. 15, Appendix A1).

In comparison to the other elements, Sb was inversely distributed, with higher concentrations in the overlaying water and the oxic sediment layers and a rapid decrease below the limit of detection in the deeper anoxic areas. This confirms thermodynamic calculations, predicting the prevalent speciation of Sb as the soluble Sb(OH)_6^- at oxic conditions and a limited availability of dissolved species by Sb(OH)_3 formation under anoxic conditions.^{37, 38} Moreover, studies describing the distribution of Sb along depth profiles of water bodies found comparable results for the transition zone from oxic to anoxic regions.^{38, 39} Nevertheless, the distribution of dissolved Sb in freshwater systems can vary strongly in relation to the biophysicochemical conditions.^{37, 40} Hence, the total concentration in pore water samples may also show different or inverse distributions of dissolved Sb species to those presented in this study.^{41, 42}

Besides the different physicochemical parameters discussed, in the case of Sb and of Zn, the concentration gradient between the water used to (re)fill the aquarium and the sediment was an important factor. In comparison to the background concentrations of the aquarium water (~15 µg Sb/L and 60 to 70 µg Zn/L; Table 2.1), determined several weeks after the profiling experiments, the respective values found for Sb (~5 µg/L) and Zn (~10 to 20 µg/L) within the profiling experiments were clearly lower, indicating an ongoing flux of the two elements toward the overlying water. In the case of the redox sensitive elements (Mn, Fe and Co), diffusion toward the overlying water is limited due to the reoxidation of these elements in the oxic zone. However, the results of Sb and Zn demonstrate aging processes of the sediment and raise the need to address in the future also time dependent processes.

2.4.3 General Evaluation of the Missy Setups

Both *missy* setups equipped with the self-manufactured probes were found to be suitable for a direct micro sampling of sediment pore water. The distributions of Mn and Fe,³⁶ Co,⁴³ Zn,⁴⁴ and Sb⁴⁵ were generally congruent to those reported for freshwater systems demonstrating the direct applicability of the *missy* for analyses in standard concentration ranges of close to natural sediment

pore waters ($\mu\text{g/L}$ to mg/L). Nevertheless, for both setups some aspects were identified that have to be taken into account: in case of setup 1, the higher dead volume of $121 \mu\text{L}$ caused a stronger shift of the sampling depth in relation to the microprofiling measurements (Table A1. 8 and Table A1. 9, Appendix A1). Moreover, the time required to empty the syringe causes a small gap between two samples. The micro annular gear pump (setup 2) maintains a continuous sampling of pore water and a reduction of the dead volume to $82 \mu\text{L}$. One remarkable factor of uncertainty is caused by compartments (volume $18.8 \mu\text{L}$) included in the pump to compensate for pressure variations (information given by the manufacturer). This may lead under extreme conditions (very steep concentration gradients) to slight biases of the element concentrations in the water samples. Regarding the replicates analyzed for the backgrounds and recoveries, no remarkable differences were found between the two setups (e.g., for the metal(loid) distributions or outliers). On the contrary, the volumes sampled by the annular gear pump varied, with an average of 7.6%, slightly stronger than those sampled by the syringe pump (2.1%). Concerning the cleaning of the systems required to remove residues after the pore water sampling (see also the discussion in the paragraph “System Characterization” of Appendix A1), the Rheodyne valve (setup 1) can easily be disassembled and enables for a rinsing of all components. The annular gear pump can only be cleaned by pumping acid and/or ultrapure water (no disassembly possible). However, the results obtained by the two systems were in good agreement (Figure 2.3, Figure 2.4, and Figure A1. 2, Appendix A1), even though the slight differences found for the system backgrounds and recoveries (Table 2.1, Table 2.2, and Table A1. 9, Appendix A1) demonstrate the importance of a thorough characterization of all components of a system and a comprehensive validation of the methods applied, especially if trace metal analyses (ng/L - $\mu\text{g/L}$) are envisaged. Comparing the two setups, setup 1 seems, until now, to provide a more constant and reproducible sampling procedure but is more expansive than setup 2. Both *missy* setups combine the advantages of microprofiling experiments with a direct, high resolution filtration-based method that allows for a multi-element analysis via ICP-MS. Although other (static) systems like DGT^{14, 15} or peepers⁴⁶ can also be applied to a (sub-)millimeter scale, the dynamic sampling approach provides for the first time the possibility to apply a direct sampling of pore waters at a spatial high resolution.

2.4.4 Future applications

Beside the application demonstrated in this study, the *missy* may further be improved and adapted to the demands of other scientific questions by modifying the sample probe (e.g., further miniaturization, use of other materials or filtration cut-offs) or by changing the measurement/sampling settings (e.g., step size, measurement/sampling times). Beside natural processes, the dynamic profiling technique can be applied to investigate the effects of anthropogenic

disturbances (e.g., pollutants or mechanical disturbances) and may thus help to assess potential impacts of intended projects in hydraulic engineering or to study the fate of emerging substances at aquatic interfaces. Potential applications are the assessment of dredging activities on contaminated sediments of, e.g., mining sites,^{6, 47} industrial or urban areas.¹⁶ In addition to trace metal(loid) fractionation and speciation, the fate and behavior of organic compounds/pollutants (like nutrients or pesticides) or emerging substances (e.g., biocides, pharmaceuticals or nanomaterials) can be studied after an adaptation of the probe heads and the materials used. Since the microprofiling systems are suitable for *in situ* applications,⁴⁹ the *missy* approach can potentially be applied not only in laboratory experiments but also under field conditions.

2.5 References

1. Stockdale, A.; Davison, W.; Zhang, H., Micro-scale biogeochemical heterogeneity in sediments: A review of available technology and observed evidence. *Earth-Science Reviews* 2009, 92, (1-2), 81-97
2. Revsbech, N. P.; Jorgensen, B. B., Microelectrodes - their use in microbial ecology. *Advances in Microbial Ecology* 1986, 9, 293-352.
3. Tankere, S. P. C.; Bourne, D. G.; Muller, F. L. L.; Torsvik, V., Microenvironments and microbial community structure in sediments. *Environmental Microbiology* 2002, 4, (2), 97-105.
4. Bufflap, S. E.; Allen, H. E., Sediment pore-water collection methods for trace-metal analysis - a review. *Water Research* 1995, 29, (1), 165-177.
5. Mudroch, A. A., Jose M., Manual of Aquatic Sediment Sampling. CRC Press, Inc. : 1995.
6. Lourino-Cabana, B.; Lesven, L.; Billon, G.; Denis, L.; Ouddane, B.; Boughriet, A., Benthic exchange of sedimentary metals (Cd, Cu, Fe, Mn, Ni and Zn) in the Deule River (Northern France). *Environmental Chemistry* 2012, 9, (5), 485-494.
7. Scholz, F.; Hensen, C.; Noffke, A.; Rohde, A.; Liebetrau, V.; Wallmann, K., Early diagenesis of redox-sensitive trace metals in the Peru upwelling area - response to ENSO-related oxygen fluctuations in the water column. *Geochimica Et Cosmochimica Acta* 2011, 75, (22), 7257-7276.
8. Rigaud, S.; Radakovitch, O.; Couture, R. M.; Deflandre, B.; Cossa, D.; Garnier, C.; Garnier, J. M., Mobility and fluxes of trace elements and nutrients at the sediment-water interface of a lagoon under contrasting water column oxygenation conditions. *Appl. Geochem.* 2013, 31, 35-51.
9. Lewandowski, J.; Ruter, K.; Hupfer, M., Two-dimensional small-scale variability of pore water phosphate in freshwater lakes: Results from a novel dialysis sampler. *Environmental Science & Technology* 2002, 36, (9), 2039-2047.
10. Davison, W.; Fones, G. R.; Grime, G. W., Dissolved metals in surface sediment and a microbial mat at 100- μm resolution. *Nature* 1997, 387, (6636), 885-888.
11. Seeberg-Elverfeldt, J.; Schluter, M.; Feseker, T.; Kolling, M., Rhizon sampling of porewaters near the sediment-water interface of aquatic systems. *Limnology and Oceanography-Methods* 2005, 3, 361-371.
12. Duester, L.; Prasse, C.; Vogel, J. V.; Vink, J. P. M.; Schaumann, G. E., Translocation of Sb and Ti in an undisturbed floodplain soil after application of Sb(2)O(3) and TiO(2) nanoparticles to the surface. *Journal of Environmental Monitoring* 13, (5), 1204-1211.
13. Duester, L.; Vink, J. P. M.; Hirner, A. V., Methylantimony and -arsenic species in sediment pore water tested with the sediment or fauna incubation experiment. *Environmental Science & Technology* 2008, 42, (16), 5866-5871.
14. Ding, S. M.; Sun, Q.; Xu, D.; Jia, F.; He, X.; Zhang, C. S., High-Resolution Simultaneous Measurements of Dissolved Reactive Phosphorus and Dissolved Sulfide: The First Observation of Their Simultaneous Release in Sediments. *Environmental Science & Technology* 2012, 46, (15), 8297-8304.
15. Ding, S. M.; Wang, Y.; Xu, D.; Zhu, C. G.; Zhang, C. S., Gel-Based Coloration Technique for the Submillimeter-Scale Imaging of Labile Phosphorus in Sediments and Soils with Diffusive Gradients in Thin Films. *Environmental Science & Technology* 2013, 47, (14), 7821-7829.
16. Ye, S. Y.; Laws, E. A.; Gambrell, R., Trace element remobilization following the resuspension of sediments under controlled redox conditions: City Park Lake, Baton Rouge, LA. *Appl. Geochem.* 2013, 28, 91-99.
17. Canavan, R. W.; Van Cappellen, P.; Zwolsman, J. J. G.; van den Berg, G. A.; Slomp, C. P., Geochemistry of trace metals in a fresh water sediment: Field results and diagenetic modeling. *Science of the Total Environment* 2007, 381, (1-3), 263-279.

18. Morata, T.; Sospedra, J.; Falco, S.; Rodilla, M., Exchange of nutrients and oxygen across the sediment-water interface below a Sparus aurata marine fish farm in the north-western Mediterranean Sea. *Journal of Soils and Sediments* 2012, 12, (10), 1623-1632.
19. Bleiner, D.; Bogaerts, A., Multiplicity and contiguity of ablation mechanisms in laser-assisted analytical micro-sampling. *Spectrochimica Acta Part B-Atomic Spectroscopy* 2006, 61, (4), 421-432.
20. Kang, J. Z.; Duan, T. C.; Guo, P. R.; Wang, C.; Chen, H. T.; Zeng, X. J., Matrix effects of micro-sampling system for inductively coupled plasma mass spectrometry. *Chemical Journal of Chinese Universities-Chinese* 2004, 25, (2), 252-255.
21. Lee, W. H.; Lee, J.-H.; Choi, W.-H.; Hosni, A. A.; Papautsky, I.; Bishop, P. L., Needle-type environmental microsensors: design, construction and uses of microelectrodes and multi-analyte MEMS sensor arrays. *Measurement Science & Technology* 2011, 22, (4).
22. Krawczyk-Baersch, E.; Grossmann, K.; Arnold, T.; Hofmann, S.; Wobus, A., Influence of uranium (VI) on the metabolic activity of stable multispecies biofilms studied by oxygen microsensors and fluorescence microscopy. *Geochimica Et Cosmochimica Acta* 2008, 72, (21), 5251-5265.
23. Laverman, A. M.; Meile, C.; Van Cappellen, P.; Wieringa, E. B. A., Vertical distribution of denitrification in an estuarine sediment: Integrating sediment flowthrough reactor experiments and microprofiling via reactive transport modeling. *Applied and Environmental Microbiology* 2007, 73, (1), 40-47.
24. Meers, E.; Du Laing, G.; Unamuno, V. G.; Lesage, E.; Tack, F. M. G.; Verloo, M. G., Water extractability of trace metals from soils: Some pitfalls. *Water Air Soil Pollut.* 2006, 176, (1-4), 21-35.
25. Stenken, J. A., Methods and issues in microdialysis calibration. *Analytica Chimica Acta* 1999, 379, (3), 337-358.
26. Torto, N.; Mogopodi, D., Opportunities in microdialysis sampling of metal ions. *Trac-Trends in Analytical Chemistry* 2004, 23, (2), 109-115.
27. Team, R. C. R: A language and environment for statistical computing., R Foundation for Statistical Computing: Vienna, Austria., 2013.
28. G. R. Warnes, B. B., L. Bonebakker, R.Gentleman, W. H. A.Liaw, T. LumLey, M. Maechler, A. Magnusson, S. Moeller, M. Schwartz and B. Venables gplots: Various R programming tools for plotting data, R package version 2.11.3.; 2013.
29. Komsta, L. Tests for outliers, R Package 'outliers' version 0.14; 2013.
30. Kromidas, S., Handbuch Validierung in der Analytik: Wirtschaftlichkeit. Praktische Fallbeispiele. Alternativen. Checklisten. 1 ed.; Wiley-VCH Verlag GmbH & Co. KGaA: 2000.
31. Jorgensen, B. B.; Des Marais, D. J., The diffusive boundary layer of sediments: oxygen microgradients over a microbial mat. *Limnology and Oceanography* 1990, 35, (6), 1343-55.
32. Jorgensen, B. B.; Revsbech, N. P., Diffusive boundary-layers and the oxygen-uptake of sediments and detritus. *Limnology and Oceanography* 1985, 30, (1), 111-122.
33. Søndergaard, M., Redox Potential. In *Encyclopedia of Inland Waters*, Likens, G. E., Ed. Academic Press: Oxford, 2009; pp 852-859.
34. Stumm, W. M., J.J., Aquatic Chemistry: chemical equilibria and rates in natural waters. 3rd ed.; John Wiley and Sons 1995.
35. Balistrieri, L. S.; Murray, J. W.; Paul, B., The geochemical cycling of trace-elements in a biogenic meromictic lake. *Geochimica Et Cosmochimica Acta* 1994, 58, (19), 3993-4008.
36. Giblin, A. E., Iron and Manganese. In *Encyclopedia of Inland Waters*, Likens, G. E., Ed. Academic Press: Oxford, 2009; pp 35-44.
37. Filella, M.; Belzile, N.; Chen, Y. W., Antimony in the environment: a review focused on natural waters II. Relevant solution chemistry. *Earth-Science Reviews* 2002, 59, (1-4), 265-285.
38. Takayanagi, K.; Cossa, D., Vertical distributions of Sb(III) and Sb(V) in Pavin Lake, France. *Water Research* 1997, 31, (3), 671-674.

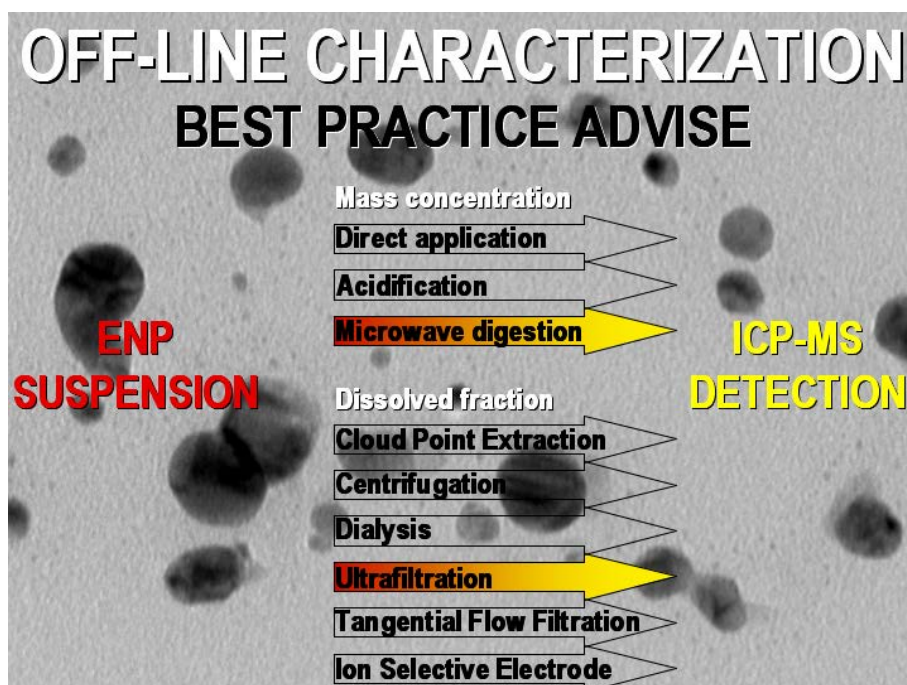
39. Cutter, G. A., Dissolved arsenic and antimony in the black sea. *Deep-Sea Research Part a-Oceanographic Research Papers* 1991, 38, S825-S843.
40. Filella, M.; Belzile, N.; Chen, Y. W.; Elleouet, C.; May, P. M.; Mavrocordatos, D.; Nirel, P.; Porquet, A.; Quentel, F.; Silver, S., Antimony in aquatic systems. *Journal De Physique Iv* 2003, 107, 475-478.
41. Chen, Y. W.; Deng, T. L.; Filella, M.; Belzile, N., Distribution and early diagenesis of antimony species in sediments and porewaters of freshwater lakes. *Environmental Science & Technology* 2003, 37, (6), 1163-1168.
42. Shieh, G.-M. Analytical Techniques for Arsenic and Antimony Speciation Studies in Interstitial Water of River Sediments, A dissertation, University of Idaho 1993.
43. Schrauzer, G. N., Cobalt. In *Elements and Their Compounds in the Environment*, Wiley-VCH Verlag GmbH: 2008; pp 825-839.
44. Peganova, S.; Eder, K., Zinc. In *Elements and Their Compounds in the Environment*, Wiley-VCH Verlag GmbH: 2008; pp 1203-1239.
45. Filella, M.; Belzile, N.; Chen, Y. W., Antimony in the environment: a review focused on natural waters I. Occurrence. *Earth-Science Reviews* 2002, 57, (1-2), 125-176.
46. Xu, D.; Wu, W.; Ding, S. M.; Sun, Q.; Zhang, C. S., A high-resolution dialysis technique for rapid determination of dissolved reactive phosphate and ferrous iron in pore water of sediments. *Science of the Total Environment* 2012, 421, 245-252.
47. Percival, J. B.; Outridge, P. M., A test of the stability of Cd, Cu, Hg, Pb and Zn profiles over two decades in lake sediments near the Flin Flon Smelter, Manitoba, Canada. *Science of the Total Environment* 2013, 454, 307-318.
48. Cathalot, C.; Lansard, B.; Hall, P. O. J.; Tengberg, A.; Almroth-Rosell, E.; Apler, A.; Calder, L.; Bell, E.; Rabouille, C., Spatial and Temporal Variability of Benthic Respiration in a Scottish Sea Loch Impacted by Fish Farming: A Combination of In Situ Techniques. *Aquatic Geochemistry* 2012, 18, (6), 515-541.
49. Pedersen, O.; Pulido, C.; Rich, S. M.; Colmer, T. D., In situ O₂ dynamics in submerged *Isoetes australis*: varied leaf gas permeability influences underwater photosynthesis and internal O-2. *Journal of Experimental Botany* 2011, 62, (13), 4691-4700.

3

ICP-MS Based Characterization of Inorganic Nanoparticles – Sample Preparation and Off-line Fractionation Strategies

Anne-Lena Fabricius, Lars Duester, Björn Meermann and Thomas A. Ternes

Analytical and Bioanalytical Chemistry, 2014, 406(2), pp 467-479



3.1 Abstract

Validated and easily applicable analytical tools are required to develop and implement regulatory frameworks and an appropriate risk assessment for engineered nanoparticles (ENPs). The challenge to develop routine suitable standardized methods enabling to obtain reliable results for ENPs was not addressed before. Concerning metal-based ENPs, two main aspects are the quantification of the absolute mass concentration and of the “dissolved” fraction in, e.g., (eco)toxicity and environmental studies. To provide information on preparative aspects and on potential uncertainties, several off-line methods were compared to determine (1) the total concentration of suspensions of five metal-based ENP materials (Ag, TiO₂, CeO₂, ZnO, and Au; two sizes), and (2) six methods to quantify the “dissolved” fraction of an Ag ENP suspension. Focusing on inductively coupled plasma-mass spectrometry, the total concentration of the ENP suspensions was determined by direct measurement, after acidification and after microwave-assisted digestion. Except for Au 10 nm, the total concentrations determined by direct measurements were clearly lower than those measured after digestion (between 61.1 % for Au 200 nm and 93.7 % for ZnO). In general, acidified suspensions delivered better recoveries from 89.3 % (ZnO) to 99.3 % (Ag). For the quantification of dissolved fractions two filtration methods (ultrafiltration and tangential flow filtration), centrifugation and ion selective electrode were mainly appropriate with certain limitations, while dialysis and cloud point extraction cannot be recommended. With respect to precision, time consumption, applicability, as well as to economic demands, ultrafiltration in combination with microwave digestion was identified as best practice. Thereby, for the first time, methods were provided that allow a standardized determination of the total mass concentration as well as the dissolved fraction of ENP suspensions.

3.2 Introduction

Due to an increased use of engineered nanoparticles (ENPs) in a variety of products and applications, the exposure of workers and consumers as well as the release into the environment has to be expected. To ensure the safety of the different ENPs and to reduce environmental and (eco)toxicological impacts, an appropriate risk assessment and the development of adequate regulatory frameworks are required. This demands not only for a comprehensive number of scientific studies but also for the availability of validated and easily applicable analytical methods.¹⁻³ These tools should also be implementable by non-“nano”-specialized laboratories (e.g., in (eco)toxicological and environmental research or administrative services). Until now, the detection, characterization, and quantification of ENPs, especially in different matrices, are still challenging tasks and the analytical methods required to provide sufficiently reliable data are most often laborious, expensive, and/or demand specialized and trained operators. Standardized protocols developed for the analysis of chemicals are mostly not directly applicable to ENP suspensions since they do not account for physicochemical parameters which are important for nanoparticle characterization (like size, shape, agglomeration/aggregation state, or surface area). Furthermore, many techniques are only suitable for specific samples or sample matrices or are limited to a certain range of, e.g., concentration or size⁴⁻⁶. Since only a few size-, but not mass- and number- concentration certified nanoparticle reference materials are available (e.g., NIST reference materials 8011-8013⁷, ERM-FD100 and ERM-FD304⁸, or BAM-N001⁹), the validation of analytical methods for ENPs is challenging and often multi-method approaches are required to provide reliable data as well as to assess and control the limitations of different techniques.^{6, 10, 11} Beside this, it has to be taken into account that the properties of ENPs can differ strongly among each other and from their (chemically identical) bulk material and may vary over time or in dependence on the surrounding matrix.¹²⁻¹⁴ Some of the most important questions regarding the analysis of nanomaterials are connected to fractionation, since the particle size and the percentage of the dissolved fractions may have a strong impact on toxicity¹⁵⁻¹⁸ and fate.^{13, 19, 20} It is hence crucial to distinguish between the particulate and the dissolved fraction to gain an understanding on the fate and transport characteristics of the particles and ionic forms and their possible (independent or synergistic) environmental and (eco)toxicological impacts.¹ Regarding the determination of the dissolved fraction of ENP suspensions, several aspects, including the properties of the particles (e.g., size, shape, aggregation state, surface characteristics, coatings) [²¹⁻²³] and of the surrounding matrix (pH value, temperature, ionic strength)^{22, 24, 25} as well as the concentration and the intensity/duration of the dissolution process, have to be taken into account.^{26, 27} Moreover, it has to be considered that the percentage of the dissolved fraction can, but does not

necessarily, reach a stable status^{28, 29} and that also a complete dissolution is possible^{22, 25, 28}. Commonly applied methods to separate the dissolved fraction from the particles are, e.g., centrifugal ultrafiltration,^{16, 21, 24, 25, 30} (ultra)centrifugation,^{5, 28} dialysis,^{16, 26} or the detection of silver ions by ion selective electrodes^{30–32}. Irrespective of the separation method applied, a precise quantification of the total mass concentrations of the different fractions is indispensable, not at least because the actual dose metric-based risk assessment demands for an exact determination to enable a comparison with the results of former exposure or (eco)toxicological studies.^{1–3} As a standard technique in elemental analysis, inductively coupled plasma-mass spectrometry (ICP-MS) has become one of the most commonly used tools for the determination of the total concentration of inorganic nanoparticle suspensions.^{32, 33} One increasingly applied technique to quantify directly the total concentration of the particulate and the dissolved fraction of ENP suspensions is single particle ICP-MS (SP-ICP-MS). Even though this method provides a powerful tool for the characterization of most metal-based nanoparticles, it is a rather sophisticated method that demands well-educated and trained operators since several special considerations regarding, e.g., the instrumental parameters (e.g., dwell time or detector dead time), the sample characteristics (e.g., preferably monodisperse suspensions and spherical and solid particles), and handling (e.g., volume and concentration of the sample introduced) or the interpretation of the data have to be taken into consideration^{34–36}. In terms of classical measurement approaches (based on steady state signals), it is still questionable if mass concentrations can be determined properly by a direct application of suspensions via the nebulizer and the spray chamber. Even though some publications point out that ENP suspensions require a digestion procedure prior to the measurements,^{4, 32} the actual biases for directly measured ENP suspensions were (to the best of the authors' knowledge) not addressed in detail yet. However, for daily routine analysis, fast and simple sample preparation protocols are needed, and in case of fractionation techniques coupled on-line to ICP-MS (e.g., field flow fractionation, hydrodynamic chromatography, or size exclusion chromatography), a digestion of the sample prior to quantification is impossible. This study aims to investigate (1) if and which sample preparation procedure is required prior to ICP-MS measurements to quantify precisely the total concentration of some of the most commonly used and discussed nanoparticle suspensions (Ag, TiO₂, CeO₂, ZnO, Au).^{37, 38} Therefore, three sample preparation approaches were compared, including microwave-assisted digestion, acidification of the suspensions, as well as direct measurement via ICP-MS without further preparation. In addition to the ICP-MS-based analysis, a gravimetric approach was carried out. Beside the determination of the total concentration, (2) the question how the dissolved fraction of an ENP suspension can be determined properly was addressed. Therefore, a quantitative multi-method approach was undertaken to elucidate the advantages and limitations of different, preferably easily

implementable approaches. Using a silver ENP suspension, five off-line fractionation methods (two filtration techniques, dialysis, ultracentrifugation, and cloud point extraction) were compared to determine the “dissolved” fraction, supplemented by measurements with an ion-selective electrode (ionic silver). Special attention was put on the uncertainties of the methodologies and their limitations. Focusing on the challenge to develop standardized and easily implementable analytical protocols for nanomaterials, the study presented delivers best practice advice. With this so far missing approach, the reliability of studies that include fractionation and total mass determination can be improved. The study supports the development of standard protocols for validated analyses of ENP suspensions suitable for everyday applications, which are requested in several directives. Hence, it supports the urgently needed process from “specialized nano analytics” to “customary nano analytics.”

3.3 Experimental section

3.3.1 Chemicals and materials

Acids; ICP-element standards of Ag, Ti, Ce, Zn, Au, and Ru (1 g/L); as well as hydrogen peroxide and sodium thiosulfate pentahydrate were purchased from Merck GmbH (Germany). Sodium nitrate (pro analysis grade) was obtained from Carl Roth (Germany). Hydrochloric (30 %) and sulfuric acid (96 %) as well as hydrogen peroxide (30 %) were at high purity grade (Suprapur); nitric acid (65 % w/w, for analysis) was sub-boiled (dst-1000, Savillex, USA). Ultrapure water (18.2M Ω ×cm) was produced using an Arium pro VF system (Sartorius AG, Germany). Prior to use, all vessels were rinsed >24 h with HNO₃ (1.3 %).

3.3.2 Nanoparticle suspensions

Eight different ENP suspensions were examined: The silver (Ag) nanoparticle suspension was obtained from RAS materials GmbH (Germany; AgPURE-W, suspended in 3–5 % ammonium nitrate solution), cerium dioxide (CeO₂) by Nyacol Nanotechnologies Inc. (USA, 20 wt %, 3 % acetic acid). Titanium dioxide (TiO₂, anatase) powder was kindly provided by Tronox (Germany). Stable, additive-free TiO₂-suspensions were produced by a high-power-density ball milling procedure (for detailed information refer to Duester et al. Zinc oxide (ZnO) was purchased from Particular GmbH (Germany; suspended in sodium citrate solution ~100 mg/L); gold (Au) ENP suspensions were obtained from Sigma-Aldrich Chemie GmbH (Germany, suspended in 100 mg/L sodium citrate solution, stabilized by proprietary surfactants not further described by the manufacturer). Further information provided by the manufacturer can be found in the Appendix A2 (Table A2. 1). For the two-method comparisons conducted (sample preparation procedures and determination of the dissolved fraction), the stock suspensions were diluted to working suspensions (WS) of a mass concentration of approximately 1 to 10 mg/L (refer to the Appendix A2, Table A2. 1).

3.3.3 General characterization of the ENP suspensions

Particle size distribution and zeta potential

Prior to the experiments, the particle size distribution of the ENP suspensions was determined by means of Dynamic Light Scattering (DLS; ZetaSizer NanoZS, Malvern Instruments GmbH, UK) and Nanoparticle Tracking Analysis (NTA; LM10, Nanosight Ltd., UK). In case of the ZnO suspension, aggregation was observed (~1,700 nm) and ultrasonication was applied to obtain reproducible particle size distributions. This was conducted using an ultrasonic homogenizer (GM 3100 HF-Generator, UW3100 ultrasonic converter, equipped with a micro-sonotrode MS 72; Bandelin electronic GmbH Co. KG, Germany) applying the following sonication program: 3×2 min, 40 W, in a

pulse mode of 20 s energy/5 s pause. The other suspensions were stable over the experimental period and re-dispersion by ultrasonication was not necessary. Transmission electron microscopy (TEM; Philips EM-420, Philips, Netherlands) measurements were carried out at an acceleration voltage of 120 kV, equipped with a LaB6-cathode and a slow-scan CCD camera. Twenty-five microliters of the suspension was placed onto graphite-coated copper grids and dried overnight prior to the measurements. Mean particle sizes were estimated on the basis of the TEM-images measuring at least 57 particles per sample. Zeta potential measurements were carried out using a ZetaSizer NanoZS (Malvern instruments GmbH, UK).

3.3.4 Total concentration

Sample preparation procedures

A comparison of different sample preparation procedures was conducted, including microwave assisted digestion, acidification, and dilution in ultrapure water. For microwave assisted digestion, 0.5 mL of the suspension was mixed with 1.4 mL of acid and 0.1 mL of an internal standard (Ru). Detailed information about the experimental setup (acids, concentrations, pH values of the WS, reference materials) is given in the Appendix (Table A2. 2). Using a microwave system (turboWave, MLS GmbH, Germany), suspensions were digested in a two-step program of a temperature ramp of 60 min to 240 °C (800 W), followed by an irradiation of 30 min at 240 °C (800 W). ZnO and Au ENPs were digested in a mixture of HNO₃ (1.1 mL ~65%) and HCl (0.3 mL ~30 %), for Ag ENPs HNO₃ (1.4 mL ~65 %), for CeO₂ a mixture of HNO₃ (1.2 mL ~65 %) and H₂O₂ (0.2 mL~30 %) was used. Digestion of TiO₂ ENPs was conducted in H₂SO₄ (1.4 mL ~96 %). The digested samples were diluted to 10 mL using ultrapure water. Previous to each experiment, blank values of the microwave vessels were determined, replacing the sample volume of the ENP suspensions (0.5 mL) by ultrapure water. At least six replicates of the ENP suspensions were investigated, whereat, for method validation purposes, in parallel to three replicates of the ENP suspension a blank sample (ultrapure water), a certified reference material (CRM) as well as an ICP-element standard (diluted to 1 mg/L) were analyzed. Experiments exhibiting that the expected values for CRM and/or ICP-element standard were biased >10 % were excluded from the evaluation. Equally, in cases where the IS added differed between the digested and the acidified samples >10 %, the results were waived. Digested suspensions were compared with acidified samples (same mixture but not digested) and directly measured nanoparticle suspensions, which were diluted in ultrapure water (instead of acid). Both sample preparations were performed at the same day of the measurements. The total elemental concentrations of the samples were determined by means of ICP-Quadrupole-MS (ICP-QMS; Agilent 7700 series, Agilent Technologies, Germany). The ICP-MS was equipped with a PEEK Mira Mist

nebulizer (Burgener research, Canada) and a PFA inert sample introduction kit with a sapphire injector (inner diameter 2.5 mm, for Agilent 7700 series, Agilent Technologies, Germany). Measurements were conducted at a RF power of 1,550 W, and a carrier gas flow of 1.17-1.18 L/min. Details about the isotopes analyzed, the measurement modi applied, as well as the reference materials used are given in the Appendix A2 (Table A2. 2 and Table A2. 3). Except for Au, the external calibration of ICP-QMS was matrixmatched. In case of Au, only a HCl matrix was used (to ensure the formation of stable gold-chloride complexes) since low concentrations (approx. <100 µg/L) of dissolved Au are instable. To verify the calibration procedure, CRMs were included in each measurement.

Comparison of ICP-MS and gravimetry

In addition to the ICP-MS-based analysis, a gravimetric approach was applied as an absolute and direct method. The results were compared to the concentrations determined upon microwave-assisted digestion of the stock suspensions ($n > 3$), applying the approach described above. Since in case of Au differences between the results of the two approaches were observed, concentrations were additionally determined by means of graphite furnace–atomic absorption spectrometry (GF-AAS, vario 6, Analytic Jena AG, Germany). The spectrometer was equipped with transversely heated graphite tube with an integrated platform and a gold hollow cathode lamp (absorption line set to $\lambda = 242.8$ nm; slit width, 0.8 nm). After addition of 5 µL of a Pd/Mg(NO₃) modifier, measurements were carried out at a pyrolysis temperature of 800 °C (10 s) and an atomization temperature of 1,950 °C (4 s). Instrument calibration was performed by external calibration via elemental standards; for quantification, signal-peak areas were determined upon integration (interval of 3.5 s).

For the gravimetric analysis, aluminum cups were annealed for at least 8 h at 450 °C by means of a muffle furnace (LE 6/11, B150, Nabertherm, Germany) until a constant weight was reached. Depending on the concentration expected (based on the producer information), a sample volume of 0.2 to 1.8 mL was pipetted into the cups and, again, repeatedly annealed to a constant weight. Weighing was conducted using a Sartorius M2P balance (Germany). To avoid biases by potential oxidation processes, combustion experiments were conducted in a nitrogen as well as atmospheric atmosphere. Only in case of silver the inert gas was required; for the other ENP suspensions, no differences were found between the results of the two treatments. To enable the comparison of the results measured by means of ICP-QMS and of those determined gravimetrically, the elemental concentrations were, in case of oxidic ENPs, converted into the concentrations of the oxides.

Precision of ICP-MS measurements

To investigate the influence of the particle size on the signal precision of the ICP-MS analysis, the relative standard deviations (RSD%; given by the ICP-MS software) of the measurements conducted were analyzed (five-fold measurements). Furthermore, a direct application approach was undertaken, comparing suspensions of Au ENP of different sizes (10 nm, 30 nm, 80 nm, 200 nm, diluted 1:1000) as well as an ICP-element standard solution (100 ng/L). Measurements were carried out using a sector field ICP-MS (ICP-SF-MS, Element 2, Thermo Scientific, Germany) equipped with a μ -flow PFA-ST ES-2040 nebulizer (both from Elemental Scientific Inc., USA) and a 1.8-mm sapphire injector (Elemental Scientific Inc., USA). RF power was set to 1,500 W, carrier gas flow to 1.205 L/min.

3.3.5 Dissolved fraction determination

Comparison of different off-line fractionation approaches

To investigate the suitability of different methods available for dissolved-fraction determination of ENP suspensions, five off-line fractionation experiments were conducted using a silver nanoparticle WS (AgPure, diluted 1:10,000), supplemented by measurements with an ion selective electrode (ISE; Ag/S 800, measurement range 10 μ g/L–108 g/L, WTW, Germany) in connection to a MultiLine P4 Universal Meter (WTW, Germany). Focusing on preferably fast and easily applicable approaches, the fractionation methods considered were dialysis, centrifugation, ultrafiltration (UF), and tangential flow filtration (TFF). Additionally, cloud point extraction (CPE) was included, even though this method was originally developed to extract and concentrate nanoparticles rather than to quantify the dissolved fraction.^{31, 40, 41} Parallel to the Ag ENP suspension, an ICP-MS single element standard (10 mg/L) and (for blank verification) ultrapure water were analyzed in triplicate. ENP suspensions were analyzed in (at least) six replicates. The ICP-silver standard was included to ensure the suitability of the methods for a quantitative analysis of the dissolved fraction and to estimate possible biases of the results caused by the procedure (e.g., losses due to interaction with the membranes). The percentage of “dissolved” silver (defined as <10 kDa molecular weight cut-off (MWCO) of the membranes) was calculated in relation to the total silver amount determined upon microwave-assisted digestion of the Ag ENP WS. Since the dissolution of silver in Ag ENP suspensions depends (among others) on the concentration of the suspension,^{25, 26} all experiments were carried out using a WS with an age of 2 to 5 weeks, after the equilibrium status was verified by ultrafiltration.

Cloud point extraction was carried out in accordance to Chao et al.³¹ In brief, 1 mL sample, 0.2 mL Triton-X 114 10 % w/v (diluted in ultrapure water; TR-X 114; Fisher Scientific GmbH, Germany, general purpose grade), and 0.1 mL Na₂S₂O₃·5H₂O (248.20 g/L) were diluted in 8.7 mL of acidified

water (~pH 2.9, adjusted by means of HNO₃ addition) and incubated for 30-40 min at 40 °C. To accelerate the phase separation, samples were centrifuged for 10 min at 5,000 rpm (Sigma Laboratory Centrifuge 3 K30, Sigma Laborzentrifugen GmbH, Germany). Eight milliliters of the upper aqueous phase was sampled to determine the dissolved fraction.

For the centrifugation experiments, a volume of 12 mL was centrifuged (ultracentrifuge, Sorvall WX90, Thermo Scientific, Germany, swinging bucket rotor; TH-641) for >48 h at 41,000 rpm and 4 °C. The centrifugation time at a speed of 41,000 rpm (maximum of the rotor) for sedimentation of silver particles of approximately 50 nm (determined by DLS; see “Results and discussion” section) was estimated on the basis of the procedure described in detail by Griffith⁴² and the information provided by the manufacturer of the centrifuge (further details are given in the Appendix A2, paragraph “Centrifugation: calculation of the run time”). To avoid redispersion of the nanoparticles, 1.1 mL of the supernatants was taken from the surface of the sample directly after centrifugation was finished. One milliliter was used to verify the efficiency of the method by NTA analysis by screening for particles remaining in the supernatant. To determine the total concentration of silver via ICP-QMS, 0.1 mL was used.

In case of the filtration methods (dialysis, UF and TFF), the “dissolved” fraction was defined by the MWCO of the membranes of 10 kDa, corresponding to approximately 1-2 nm. Dialysis was carried out on a multi-position magnetic stirrer (Variomag Telemodul 40S connected to a Variomag Electronicstirrer Telesystem, Thermo Scientific Germany) in 1 L bottles containing ultrapure water. Dialysis devices (Float-A-Lyzer G2, 8–10 kDa, Spectrum Laboratories Inc., USA) were filled with Ag ENP suspension or Ag solution (~9 mL) and dialyzed for 48 h. To investigate the time-dependent dissolution of Ag⁺ from Ag ENPs, additional samples were taken over a time period of 29 days (for time-dependent dissolution, refer to the Appendix A2, Figure A2. 2). To determine the dissolved fraction, the concentration of silver in the surrounding water was measured via ICP-QMS. Ultrafiltration (Amicon Ultra Centrifugal filter units, MWCO 10 kDa, Merck Millipore, Germany) and TFF (Microkros Hollow Fiber Filter Module, 10 kDa, Spectrum Laboratories Inc., Netherlands) were carried out in accordance to the operating instructions of the supplier. In case of UF and TFF, a possible clogging of the membranes by ENPs was tested after the experiments by filtering a dissolved elemental standard.

ISE was calibrated in a concentration range from 100 µg/L to 100 mg/L in accordance to the instructions given in the manual of the electrode. To provide a constant ionic strength required for optimal ISE measurement conditions, 2 % NaNO₃ solution (424.95 g/L) was added to each sample. The precision of the ISE was tested after calibration conducting a standard addition of a dissolved Ag

ICP standard to the WS (1–50 mg/L). The calibration as well as the results of the standard addition are given in the Appendix (Table A2. 4, Figure A2. 3 and, Table A2. 5).

Dissolved fraction determination of different ENP suspensions

Based on the results of the method comparison, the dissolved fraction of the other ENP suspensions included in this study was determined by means of ultrafiltration, as described above. Again, for method validation, ICP single-element standards of the respective elements as well as blank samples were included in the analyses. Except for ZnO, the dissolved fractions of the WS were stable over the experimental time of approximately 2 weeks. In case of ZnO, freshly diluted suspensions were compared to a WS diluted 24 h prior to the experiment.

3.4 Results and discussion

3.4.1 General characterization of the ENP suspensions

Particle size distribution and zeta potential

Particle size distributions of the ENP suspensions as well as the zeta potentials are summarized in Table 3.1. Beside the mean values of the hydrodynamic diameter and the zeta potential, the peak width (DLS, zeta potential) and the standard deviation (NTA) given by the software are shown. For DLS the z-averages of the measurements are given. For TEM analyses, the standard deviation of the particles measured is provided. Representative TEM images of the ENP suspensions can be found in the Appendix (Figure A2. 1).

Table 3.1: Particle size distribution and zeta potential of the ENP suspensions. Beside the mean values, the standard deviations (NTA, TEM) or the peak width (DLS, Zeta) are given respectively. Analyses of DLS, NTA, and zeta potentials were conducted in (at least) five replicates. If possible, the particle sizes were additionally estimated on the basis of TEM images ($n \geq 57$); due to aggregation, the size of TiO_2 and CeO_2 of individual particles were not measurable.

| | Ag | TiO_2 | CeO_2 | ZnO | Au 10 nm | Au 200 nm |
|----------------------------|-------------|----------------|----------------|----------------|-------------|--------------|
| DLS | 52 ± 20 | 108 ± 2 | 24 ± 9 | 429 ± 105 | 29 ± 12 | 181 ± 87 |
| NTA | 55 ± 19 | 197 ± 72 | 86 ± 4 | 285 ± 106 | (too small) | 247 ± 10 |
| TEM | 18 ± 4 | (<20 nm) | (<20 nm) | (13 ± 5) | 9 ± 2 | 279 ± 18 |
| Zeta-potential [mV] | -18 ± 7 | -30 ± 7 | 40 ± 10 | -32 ± 4 | -42 ± 1 | -46 ± 9 |

The difference of the particle sizes obtained by different methods is a well-known phenomenon since the properties of the suspensions (mainly particle shape, dispersity, agglomeration/aggregation state) can strongly influence the measurements.^{5, 10, 43} Moreover, the values determined on the basis of the TEM images represent the size of the core particles, whereas by application of DLS and NTA measurements the (larger) hydrodynamic diameter is obtained (e.g., Ag or ZnO). In case of bigger particles such as Au 200 nm, the influence of the electric dipole layer surrounding the particle on the size measured is less pronounced and, hence, the results are more similar. For TiO_2 and CeO_2 , the TEM images revealed that the particles are present as aggregates, leading to stable suspensions with much higher hydrodynamic diameters. Also in case of ZnO, agglomerates were observed. The instability was confirmed by a broad size distribution determined by DLS and NTA as well as by the time-dependent agglomeration observed (already mentioned in the experimental section). Nevertheless, for all three suspensions, the TEM images indicate that not exclusively aggregated but also single particles were present. Beside this, the particles of the TiO_2 , CeO_2 , and ZnO suspensions

were not spherical, which also biases the results determined by light scattering methods such as DLS and NTA.^{5, 10, 43} Regarding the zeta potentials, with the exception of Ag, all values measured were >28 mV, indicating repulsive forces between the particles that dominate the stability with increasing values of the zeta potential.⁴⁴⁻⁴⁶ With the exception of CeO₂, all samples showed negative values. The lower value of Ag may explain the polydispersity of the suspension because the more intense attractive forces between the particles can cause aggregate formation.

3.4.2 Total concentration

Sample preparation procedures

Figure 3.1 exhibits the relative total concentration obtained upon different sample preparation procedures (microwave digestion, acidification, as well as direct application). The values achieved after microwave digestion were set as 100 %. Error bars indicate the relative minimum and maximum offset values (acidification, direct application) in reference to the microwave digestion.

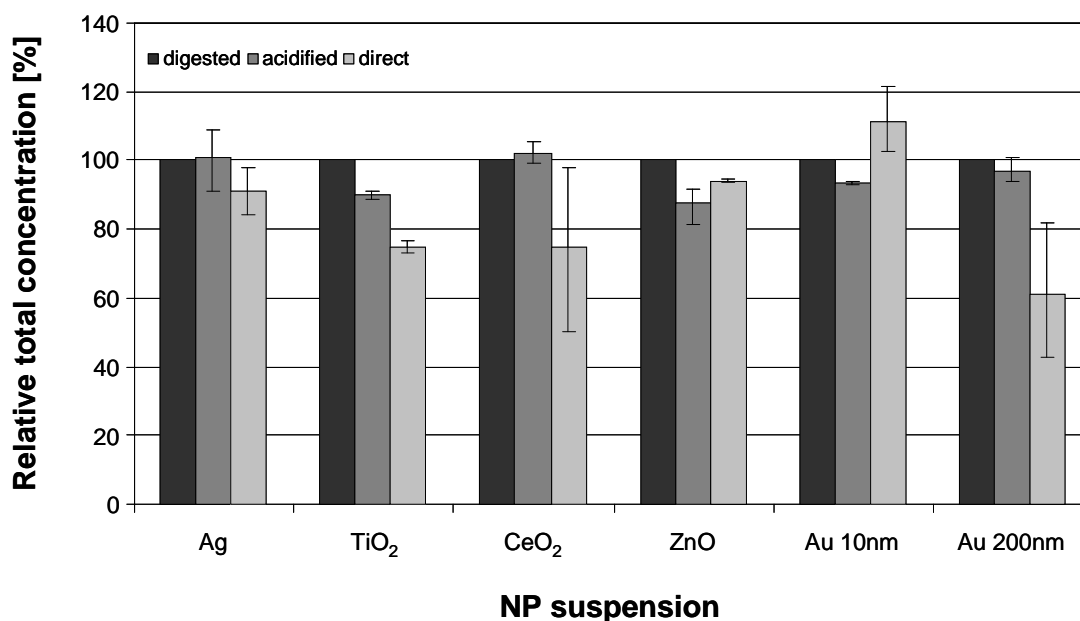


Figure 3.1: Relative concentration of ENPWS determined by means of ICP-QMS after microwave assisted digestion (anthracite), acidification (gray), and direct application (light gray). For each suspension, ≥ 6 replicates were analyzed. Results are presented as percentage of the results obtained upon microwave digestion (set as 100 %). Error bars represent the minimum and maximum values (acidification, direct application) in relation to the values of the digested samples.

Regarding the acidified samples, the relative concentrations of Ag (91.0–108.6 %, mean 100.6 %), CeO₂ (99.0% – 105.3 %, mean 102.2 %), and Au 200 nm (94.1–100.7 %, mean 96.5 %) were similar to those achieved upon microwave-assisted digestion (bias <5 %), even though for gold a slightly lower

mean value was determined. A reduction of relative concentrations by more than 5 % was found for TiO₂ (88.5–91.1 %, mean 89.8 %), ZnO (81.0–91.5 %, mean 87.4 %), and Au 10 nm (92.6–94.2 %, mean 93.6 %). The concentrations of the aqueous suspensions determined via direct ICP-QMS analysis without further sample pretreatment were, except for Au 10 nm (102.5–121.5 %, mean 111.2 %) and ZnO (93.3–94.2 %, mean 93.7 %), lower than those after acidification: Ag (84.0–97.7 %, mean 90.8 %), TiO₂ (73.3–76.5 %, mean 74.9 %), CeO₂ (50.3–98.2 %, mean 74.8 %), and Au 200 nm (42.6–82.1 %, mean 61.1 %). These findings indicate either losses during the transport of the particles into the plasma via tubings, nebulizer, and spray chamber or an incomplete atomization/ionization of the particles. The improved comparability of the acidified Ag, TiO₂, CeO₂, and Au 200 nm suspensions to the digested samples is possibly caused by a partial dissolution and/or reduction of the particle sizes, which, in turn, may have reduced the biases caused by insufficient transport or atomization/ionization processes. This effect is in accordance to several studies which indicate that the solubility of nanoparticles increases at low pH values^{16, 24, 27, 28} or that particles may dissolve completely after acidification.^{28, 47} However, for ZnO and Au 10 nm, inverse effects were observed which might be the result of agglomeration/aggregation and sedimentation processes induced by the reduced pH value. An acidification can cause a shift of the zeta potential towards zero (point of zero charge) where the electrostatic repulsion forces are reduced and the van-der-Waals forces became more dominant causing agglomeration and destabilization of the suspension.^{46, 48, 49} This may explain the results of the ZnO suspension, but probably not of the sterically (by surfactants) stabilized Au ENP suspensions, where a pH shift is expected to have lower impacts on the stability of the suspension.^{45, 46, 49, 50} Additionally, assuming an equal composition of the matrix of the two Au ENP suspensions, a destabilizing effect should have been observed in both cases. Nevertheless, regarding the much higher particle concentration of the Au 10 nm suspension in comparison to the Au 200 nm suspension (5.9×10¹² part/mL vs. 1.9×10⁹ part/mL; see Appendix A2, Table A2. 1), the probability of collision and adhesion of particles (particle-particle interaction) and, hence, also of agglomeration is increased. However, since the experiments were repeated three times by two different persons, each including three replicates of the Au ENP suspension, it is unlikely that the differences observed were caused by random errors (due to, e.g., incorrect handling, measurement settings, or contaminations). Since the concentrations of the digested samples were additionally verified by means of GF-AAS, only particle related effects might have biased the ICP-MS measurements. The results of the Au 200 nm ENP suspensions, analyzed in parallel, indicate that the effect is, as mentioned above, somehow related to the particle size, rather than to particle-effects in general. For a conclusive explanation of the phenomena, the effects of each step of the preparation procedure

should thus be further investigated, including important parameters like the zeta potential or the agglomeration status of the suspensions, which was not the focus of this study.

For most metal-based nanoparticle suspensions, a microwave-assisted digestion is advised prior to ICP-QMS measurements to ensure a correct quantification of the total metal concentration. Nevertheless, the results also demonstrate that an acidification of the suspensions provides an alternative if a digestion procedure is not feasible (e.g., due to time limitations in test protocols or with regard to coupled techniques). In cases where the differences between microwave-assisted digestion and an acidification are negligible, the latter is preferable due to reduced source of errors during extensive preparation procedures (e.g., potential analyte losses). The results of the Au 10 nm samples show that for some ENP suspensions also a direct application may be possible which emphasizes that an ENP/matrix matched preparation has to be thoroughly adapted.

Comparison of ICP-MS analysis and gravimetry

As an absolute method, a gravimetric approach was compared to the results of the ENP stock suspensions obtained by means of ICP-QMS after microwave-assisted digestion (Table 3.2).

Table 3.2: Comparison of concentrations and the respective confidence interval (CI; $\alpha = 0.05$) determined gravimetrically ($n \geq 5$) and by means of ICPQMS after microwave assisted digestion ($n \geq 3$) of the ENP stock suspension (SS).

| | Ag [g/L] | TiO ₂ [g/L] | CeO ₂ [g/L] | ZnO [mg/L] | Au 10 nm [mg/L] | Au 200 nm [mg/L] |
|---------------------|-------------|---------------------------|---------------------------|---------------|--------------------|---------------------|
| Gravimetric | 97.1 ± 1.2 | 5.3 ± 0.2 | 210 ± 13 | 684 ± 66 | 474 ± 143 | 545 ± 130 |
| Digestion SS | 101 ± 11 | 4.6 ± 0.2 | 266.8 ± 4.9 | 293 ± 21 | 56.4 ± 2.2 | 72.5 ± 3.6 |

According to the results of the two approaches, the ENP suspensions analyzed can be divided into two groups. For the highly concentrated and surfactant free suspensions, namely Ag, TiO₂, and CeO₂, the concentrations determined by means of the two approaches were comparable with each other, whereas in case of the less-concentrated ZnO and Au ENP suspensions, which are stabilized in sodium citrate solution, remarkable differences were found. Since the concentrations of the ICP-QMS analysis were similar to the results of the previously described experiments (characterization of the WS; data not shown), it was suspected that the gravimetric approach is, in case of the ZnO and Au ENP suspensions, biased by residues of the matrix (sodium citrate and surfactants) remaining in the aluminum cups after the combustion process. Equally, in some TEM images (see Au 200 nm; Appendix A2, Figure A2. 1), crystals were observed, presumably indicating remaining residues of the matrix. To further validate the results of the ICP-QMS measurements, the samples of the digested Au

stock suspensions were additionally analyzed by means of GF-AAS, leading to similar results as determined via ICP-QMS: Au 10 nm 52.3 ± 1.2 mg/L, Au 200 nm 68.5 ± 1.4 mg/L. It can be concluded that a gravimetric approach is only valid for suspensions in an exactly known matrix without interfering components (like surfactants or stabilizers). Beside this, the uncertainties of the methods increase with a decreasing concentration of the suspension, since the determination of low weights leads to elevated measurement uncertainties. In case of the highly concentrated suspensions and/or big particles (Au 200 nm), it has to be considered that pipetting errors (by, e.g., remaining suspension in the pipette tip) bias the results, which explains the differences found in case of Ag, TiO₂, and CeO₂. Hence, especially in case of such samples, a high number of replicates is recommended to limit the statistical uncertainty. For Ag, TiO₂, and CeO₂, similar results were found with regard to the concentrations provided by the manufacturer (Appendix A2, Table A2. 1 and Table A2. 2). In case of Au (especially Au 200 nm), the elemental concentrations determined were below those estimated on the basis of the concentrations given in particles/milliliter. This may be due to uncertainties caused by slight variations of the particle size distribution, which can lead to discrepancies to the calculated values (refer to the Appendix A2, Table A2. 1 and Table A2. 2). In contrast to that, the concentration of ZnO was approximately three times higher than expected from the producer information given.

Precision of ICP-MS measurements

The relative standard deviations (RSD%) of the ICP-QMS measurements of different sample preparation procedures were analyzed to test if particles, which are directly introduced into the ICP-MS system, cause signal instabilities in steady state measurements. The RSDs reflect the stability of the measurements and, thus, the precision of the ICP-QMS analyses (Table 3.3). To investigate, moreover, the size-dependence of the signal stability, gold-ENP suspensions containing particles of different sizes (10, 30, 80, 200 nm) as well as a dissolved gold ICP-MS single element standard were applied to ICP-QMS. Figure 3.2 illustrates the signals obtained.

Table 3.3: Precision of the ICP-QMS analysis represented by the mean values of the relative standard deviations (RSD%) of the samples measured (5 replicates) subsequent to different sample preparation procedures.

| | Ag | TiO ₂ | CeO ₂ | ZnO | Au 10 nm | Au 200 nm |
|---------------------|------|------------------|------------------|------|----------|-----------|
| Digested WS | 2.2% | 3.2% | 1.1% | 1.9% | 1.3% | 2.1% |
| Acidified WS | 2.2% | 5.0% | 1.4% | 1.8% | 0.9% | 1.6% |
| Direct WS | 2.7% | 13.3% | 4.4% | 3.0% | 3.8% | 32.6% |

Except for silver, all ENP suspensions, which were directly introduced into the ICP-MS system, showed elevated RSDs, compared to the samples digested and/or acidified. Even though in case of

CeO₂, ZnO, and Au 10 nm, only slight differences in signal stability were observed. The ICP-QMS signal stability of directly introduced TiO₂ and, especially, Au 200 nm suspensions were enhanced significantly (RSDs > 10 %). The results of the Au ENP suspensions of different particle size distributions illustrates that the stability of the signal decreased with increasing particle sizes

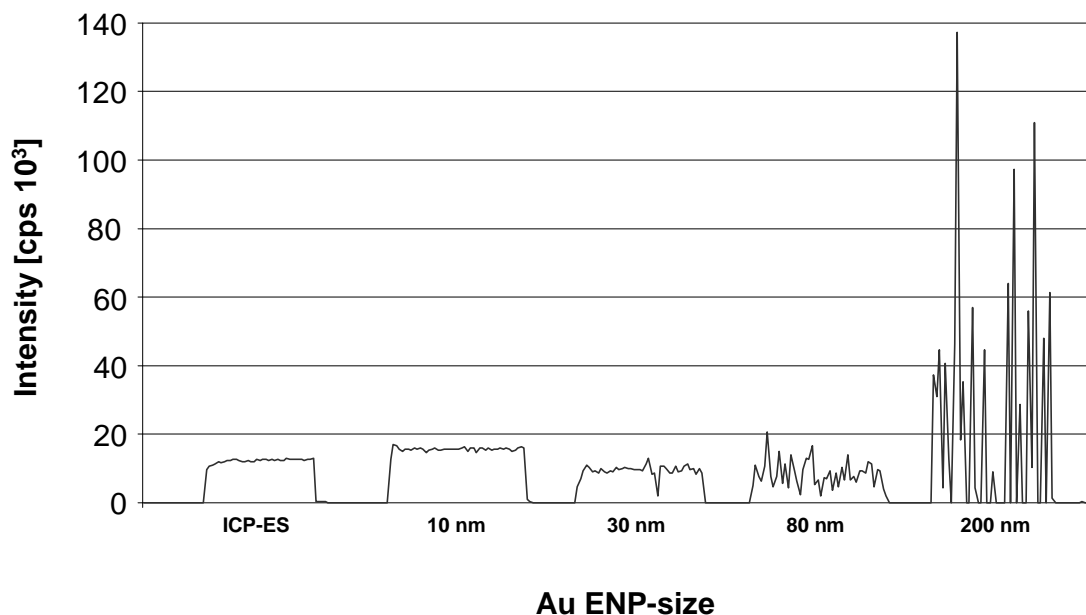


Figure 3.2: Direct application of Au ENP suspensions of different sizes (10, 30, 80, 200 nm) compared to a dissolved ICP single element standard (ES).

No differences were found between the dissolved ICP-element standard and the Au 10 nm particles. In addition to the size of the individual particles, the aggregation state (in case of TiO₂, CeO₂, and ZnO) of the suspensions as well as the solubility of the materials probably influenced the measurements, which might explain the constant RSDs of the Ag ENP suspension, known to dissolve fast.^{20, 25, 26, 28} In general, the effects observed are well known and used in SP-ICP-MS, where the concentrations and particle sizes of ENP suspensions are measured on the basis of signals of single particle events.^{34, 35} However, in comparison to SP-ICP-MS, in classical ICP-MS measurements higher concentrations and longer dwell times are applied causing an overlay of several, not defined single particle events and an instable steady state signal (illustrated in Figure 3.2). Moreover, the example of the Ag ENP suspension, which show only a marginally increased RSDs (refer to Table 3.3), demonstrates that this is (depending on the size, stability, and concentration of the suspension) not necessarily true for all kind of ENP suspensions.

Summing up, the results highlight that prior to any classical ICP-MS analysis of inorganic nanoparticle suspensions, it has to be investigated if and which kind of sample preparation

procedure is required to ensure a correct and valid quantification of the (metal) constituents. Mostly, a microwave-assisted digestion seems to be the favorable practice, but the results of the Ag, CeO₂, and Au 200 nm suspensions indicate that in some cases acidification is also suitable. Even though for small particles (like Au 10 nm) the results of a direct application are comparable to digested samples, this approach cannot be advised since instabilities of measurements are likely.

3.4.3 Determination of the dissolved fraction

Comparison of different off-line fractionation approaches

Testing different approaches to quantify the dissolved fraction of a Ag ENP suspension, five off-line fractionation methods as well as measurements with an ISE were compared; the results (mean value \pm CI; $\alpha = 0.05$) are presented in Figure 3.3. Only for dialysis, the results after 2 (gray bar) and after 12 days (light gray bar) are presented, since during dialysis a continuous dissolution of silver was observed (see Figure A2. 2 in the Appendix A2). In most cases, the results of the simultaneously analyzed dissolved ICP-element standard, included to test for the recoveries of the methods, were within a range of 100.0 ± 5.0 % (mean value \pm CI; $\alpha = 0.05$: centrifugation, 102.2 ± 11.1 %; dialysis, 99.7 ± 8.0 %; ultrafiltration, 95.8 ± 2.1 %; ion selective electrode, 102.1 ± 3.9 %). With the tangential flow filtration, recoveries of 87.5 ± 4.2 % were observed for the dissolved silver standard and 79.8 ± 42.2 % for the cloud point extraction. The silver concentrations of the blank samples, conducted with ultrapure water, were below the limit of detection (LoD, $0.26 \mu\text{g/L}$; refer to Table A2. 3, in the Appendix A2).

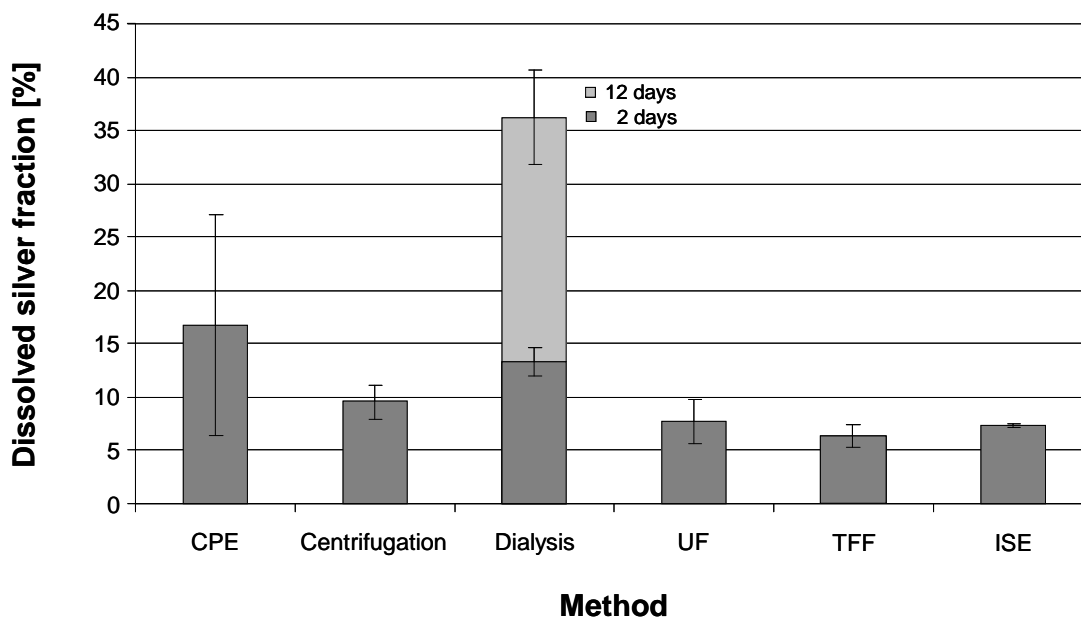


Figure 3.3: Dissolved fraction of silver ENPWS determined by means of six different methods applied ($n \geq 6$). Results are presented as percentage of the total Ag concentration of the WS determined after microwave assisted digestion. Error bars represent the CI ($\alpha = 0.05$). Except for ISE, concentrations were determined by means of ICP-QMS (for dilutions and measurement settings refer to the experimental section and Table A2. 2 in the Appendix A2). As a time-dependent method, for dialysis, the result obtained after 2 (gray) and 12 days (light gray) are shown. Filtration methods (UF, dialysis, TFF) were performed using membranes with a MWCO of 10 kDa.

The dissolved fractions determined via CPE ($16.7 \pm 6.5\%$) and dialysis after 2 days ($13.7 \pm 1.5\%$) were $>10\%$, whereas the results of the CPE showed the highest CIs of all methods applied. A slightly lower percentage for the dissolved fraction was determined by means of centrifugation ($9.5 \pm 1.6\%$). Similar results were found after application of UF ($7.7 \pm 1.3\%$), TFF ($6.3 \pm 1.2\%$), and ISE ($7.0 \pm 0.3\%$). In case of the CPE, the relatively high concentration of dissolved silver determined is most likely caused by particles remaining in the supernatant. As mentioned before, the method rather aims to extract and concentrate nanoparticles than to allow for quantitative extraction of dissolved silver.^{31, 40, 51} However, depending on the properties of the nanoparticle suspensions, the respective matrix, and the parameters of the procedure (e.g., ENP concentration, pH, salinity), the recoveries determined in different studies ranged, mostly, from $\sim 65\%$ up to $\sim 110\%$ of the initial ENP concentration.^{31, 40, 51} Hence, the variation found in these studies is comparable to the results presented here. This indicates that a certain amount of the particles is usually not incorporated in the TRX-114-phase and might bias the dissolved silver quantification. Apart from the low recoveries of the ICP-element standard, high CI values were obtained for both types of samples (ENP suspensions and element standard), indicating that the dissolved fraction was not precisely

quantified. Nevertheless, since the approach can in principle be applied to different ENPs (beside Ag, e.g., also Zn, Au or TiO₂) in different matrices,^{31, 40, 41, 52, 53} a further methodological adaptation of the parameters may potentially enable also an accurate and precise determination of the dissolved fraction. Especially with regard to low concentration of ENPs in complex matrices, this approach may provide a possibility to quantify the concentration of the nanoparticles and the dissolved fraction simultaneously. Regarding the centrifugation, the dissolved fraction determined was slightly enhanced in comparison to the results of UF, TFF, and ISE, probably indicating a bias by remaining, or rather redispersed, particles in the supernatant. Even though in some samples a few particles (approximately 25–50/mL supernatant) were detectable by means of NTA, the number was too small for precise particle number determination. However, the advantage of this approach is that, in contrast to the other methods, the sample matrix remains unchanged (contrary to CPE or ISE) and, furthermore, that interactions with membranes (possible during dialysis, TFF or UF) can be excluded. Nevertheless, to ensure a complete sedimentation especially of small particles of a low density, prolonged centrifugation times of (possibly) several days and/or higher speed are required which, in turn, demands an adequate equipment allowing for ultra high speeds (fixed angle rotor and respective tubes) which causes higher costs. Moreover, the sedimentation process also depends on shape and surface coatings of the particles as well as the heterogeneity of the sample.^{54, 55} In case of small particles (<20 nm), the influence of surface coating on the particle size and density becomes more dominant, which, in turn, influences the sedimentation coefficient and the centrifugation procedure.⁵⁴ Therefore, an adaptation of the method to the different characteristics of the respective ENP suspension (particle size, shape, polydispersity, matrix, etc.) is indispensable. Beside this, a thorough handling of the samples is crucial to avoid redispersion, which causes user dependence and may result in incorrect results. In case of dialysis, the ongoing release of silver (refer to Figure A2. 2 in the Appendix A2) demonstrates that the method cannot be applied to determine the dissolved fraction of a given Ag ENP suspension because the primary ratio between particles and water is remarkably changed. Since the release of silver ions depends, among others, on the concentration,^{25, 26} dialysis is suitable to investigate the time-dependent dissolution kinetics^{16, 26} but not to quantify the dissolved fraction of a given ENP suspension. In contrast to dialysis, centrifugal UF enables the determination of the dissolved fraction without matrix modifications. Possible interactions of silver ions with the membranes are, with regard to the recoveries of >95 % of the ICP-element standard, negligible, but have to be in general taken into account. Similar, clogging of the membranes by nanoparticles, tested by application of an ICP-element standard upon the filtration of ENP suspensions (recovery 108.1 % ± 3.0 %) can, in this case, be excluded. Moreover, UF is a fast and easily applicable method which is already commonly used to determine the dissolved fraction of ENP

suspensions.^{21, 22, 24, 25, 30, 56} In comparison to that, the results obtained by application of the tangential flow filtration are in good agreement with those obtained by the UF and ISE approach and show apparently good reproducibility. Nevertheless, several drawbacks became apparent during application: in some cases the liquid flow through the membranes was hindered, probably due to clogging of the pores, the approach is time-consuming and the recoveries of the ICP-element standard indicate losses during the procedure. Beside this, the hollow fibers were, at a price of 80 € per piece, the most expensive devices used during the study (compared to: Float-A-Lyzer for dialysis and Amicon ultra ultrafiltration units each ~11 € per piece). In contrast to the other methods applied, the ion selective electrode provides a possibility to determine the concentration of silver ions in a sample and, thus, to obtain results not biased by nanoparticles. This was verified by standard addition of dissolved Ag ICP-element standard to NP suspensions (101.5 % \pm 6.2 %) after calibration of the electrode. Hence, this approach can be taken as a control for the results of the other methods. However, although ISE facilitates the possibility for the fast and direct determination of the concentration of dissolved silver in different matrices,^{31, 40, 57} it is a tool only applicable to few ion-releasing ENPs (beside for Ag, ISEs are available for, e.g., Cd, Pb, and Cu) and, in comparison to ICP-MS measurements, to elevated dissolved silver concentrations ($\sim \geq 10$ $\mu\text{g/L}$; information given by the manufacturer).

Dissolved fraction determination of different ENP suspensions

Based on the results achieved upon the method comparison conducted using a Ag ENP suspension, ultrafiltration was identified as best practice for the determination of the dissolved fraction of the other ENP suspensions used within the comparison of the sample preparation procedures. The recoveries of the ICP-element standard were in the range of 100.0 ± 5.0 % (mean value \pm CI; $\alpha = 0.05$: Ag 95.8 ± 2.1 %, TiO_2 : 102.6 ± 4.6 %, CeO_2 : 99.3 ± 0.5 %, ZnO: 104.8 ± 6.4 %, Au 10 nm and Au 200 nm, 97.5 ± 0.01). Background concentrations for the elements analyzed (determined by filtration of ultrapure water) were, with the exception of Zn (0.4 ± 0.8 $\mu\text{g/L}$), below the respective limit of detection (refer to Table A2. 3 in the Appendix A2). The highest values for the dissolved fraction were determined for the suspensions of Ag (7.7 ± 1.3 %) and ZnO (4.4 ± 0.3 %). For ZnO, the dissolved fractions were determined for freshly diluted WS, whereas the results of silver are referred to the suspension used within the other experiments (described above). For ZnO, the dissolved fractions were additionally determined 24 h after the dilution. They showed increased values of 26.2 ± 8.0 % ($n = 3$). For CeO_2 , 0.4 ± 0.1 % was found; for TiO_2 and the two Au suspensions, the concentrations within the filtrates were below the respective limits of detection (refer to Table A2. 3). For these suspensions, no time dependent dissolution was observed. The release of ions from Ag and ZnO ENPs and the dependence of this process on several parameters (e.g., concentration, pH

value, particle size, aggregation state, additives)^{16, 21, 22, 25, 26, 28} is a well-known phenomenon, especially discussed in relation to the toxicological impacts of these nanoparticles.^{15, 16, 26, 30, 56, 58–61} In case of CeO₂ the solubility in aqueous matrices is expected to be low, even if at acidic pH values (pH <4) a certain dissolution is possible.^{24, 62} However, since the samples were not acidified and the TEM images (refer to Figure A2. 1 in the Appendix A2) of CeO₂ indicate the presence of very small individual particles, the results of the dissolved fraction were probably biased by particles that have passed the pores of the membranes. Similar, the solubility of TiO₂ ENPs can be slightly increased at low pH values but is generally expected to be very low in water.^{27, 29} Likewise, the release of soluble gold clusters from Au ENPs is, without the attachment of special ligands, improbable in water.^{63–65} Hence, the dissolved fractions determined are in good agreement with the results that can be expected from other studies.

Taken together, the results of the comparison of methods for (quantitative) off-line fractionation and ISE to determine the dissolved fraction of different ENP suspensions highlight that the suitability of the methods applied have to be thoroughly verified for each type of metal-based nanoparticle in a given matrix. Beside the advantages and limitations of different methods, the parameters influencing the properties of the nanoparticles (e.g., size aggregation state, solubility, zeta potential) and/or of the matrix (e.g., pH value, temperature, ionic strength) have to be considered carefully.^{22, 56, 66} Ultrafiltration is a fast and easily applicable method which is suitable to a variety of different ENP suspensions and it provides the possibility to obtain results comparable between different working groups from different scientific disciplines. Nevertheless, in case of more complex matrices (e.g., environmental samples or media used in (eco)toxicological test systems or food), the suitability of the method has to be verified to avoid biases (by e.g., interactions of ENPs or the matrix with the membranes).

3.5 Summary and Conclusions

Focused on daily routine and ICP-MS analysis of metal-based nanoparticles, different strategies for (1) the determination of the total metal concentration as well as (2) the dissolved metal fraction were compared. (1) It has been shown that a direct application of nanoparticle suspensions to an ICP-MS system does, applying steady state analyses, mostly not provide reliable data for total metal concentrations.

In fact, without any further sample preparation, it is very likely that imprecise results and/or instabilities of the measurements occur. Even though for some ENP suspensions (in this study Ag, CeO₂ or Au 200 nm) acidification was identified as an optimal practice, microwave-assisted digestion can be taken as a universally reliable method. In cases where an (extensive) sample preparation is not feasible (e.g., direct coupling of analytical devices to ICP-MS or due to time limitations in extensive test protocols), the uncertainties in the respective matrix should and can be easily addressed prior to an experiment. (2) Regarding the determination of the dissolved fraction, six methods were compared by application to an Ag ENP suspension to identify the most suitable approach. It has been shown that, in principle, several methods can be applied.

Nevertheless, problems like time-dependent dissolution (dialysis), methodological and handling difficulties (CPE, centrifugation, TFF), or elevated costs (TFF) have to be considered. As a method suitable for different ENP suspensions, centrifugal ultrafiltration provides an easy to handle and moderately expensive tool for the separation of the dissolved fraction from the particles. Moreover, by application of this approach to the ENP suspensions included in this study, the general suitability of the method for a variety of different nanomaterials was shown.

At the same time, the results also demonstrate that even for presumable simple analytical tasks concerning quantification and characterization of ENP suspensions, the analytical tools available are not necessarily suitable for all nanomaterials. It hence remains still necessary to verify the applicability of standard protocols for a given experimental approach and the ENP suspensions analyzed. Nevertheless, it has been shown that it is possible to identify and validate easily implementable standard procedures, which are crucial to ensure the comparability of the results of different laboratories and to provide a basis for the development and implementation of regulatory frameworks.

3.6 References

1. OECD (2012) Guidance on sample preparation and dosimetry for the safety testing of manufactured nanomaterials. OECD Environment, Health and Safety Publications, 2012 (No. 36)
2. European Commission (2012) Communication from the Commission to the European Parliament, the Council and the European Economic and Social Committee; Second Regulatory Review on Nanomaterials, 2012, EUROPEAN COMMISSION: Brussels
3. European Commission (2012) Commission staff working paper; types and uses of nanomaterials, including safety aspects. 2012. SWD (2012) 288 final (COM (2012) 572 final)
4. Ferreira da Silva B, Perez S, Gardinalli P, Singhal RK, Mozeto AA, Barcelo D (2011) Analytical chemistry of metallic nanoparticles in natural environments. *TrAC Trends Anal Chem* 30(3):528–540
5. Hassellöv M, Kaegi R (2009) Analysis and characterization of manufactured nanoparticles in aquatic environments. In: Lead J, Smith E (eds) *Environmental and human health impacts of nanotechnology*. Wiley, Hoboken, pp 211–266
6. Weinberg H, Galyean A, Leopold M (2011) Evaluating engineered nanoparticles in natural waters. *TrAC Trends Anal Chem* 30(1):72–83
7. National Institute of Standards & Technology (NIST) (2012) Reference Materials 8011, 8012, 8013, Gold Nanoparticles. <https://www-s.nist.gov/srmors/detail.cfm>. Last update 06.09.2013. Assessed 09 Sept 2013
8. Institute for Reference Materials and Measurements (2013) ERM®-FD100, Colloidal Silica in Water. http://irmm.jrc.ec.europa.eu/reference_materials_catalogue/Pages/index.aspx. Last update 12.08. 2013. Assessed 09 Sept 2013
9. Federal Institute for Materials Research and Testing (2013) B. Certification Report: Certified Reference Material BAM-N001; Particle Size Parameters of Nano Silver; http://www.bam.de/de/fachthemen/referenzmaterialien/rm_aktuell.htm. Last update 02.09.2013. Assessed 09 Sept 2013
10. Baalousha M, Ju-Nam Y, Cole PA, Gaiser B, Fernandes TF, Hriljac JA, Jepson MA, Stone V, Tyler CR, Lead JR (2012) Characterization of cerium oxide nanoparticles—part 1: size measurements. *Environ Toxicol Chem* 31(5):983–993
11. von der Kammer F, Ferguson PL, Holden PA, Masion A, Rogers KR, Klaine SJ, Koelmans AA, Horne N, Unrine JM (2012) Analysis of engineered nanomaterials in complex matrices (environment and biota): general considerations and conceptual case studies. *Environ Toxicol Chem* 31(1):32–49
12. Auffan M, Bottero JY, Chaneac C, Rose J (2010) Inorganic manufactured nanoparticles: how their physicochemical properties influence their biological effects in aqueous environments. *Nanomedicine* 5(6):999–1007
13. Stone V, Nowack B, Baun A, van den Brink N, von der Kammer F, Dusinska M, Handy R, Hankin S, Hassellöv M, Joner E, Fernandes TF (2010) Nanomaterials for environmental studies: classification, reference material issues, and strategies for physico-chemical characterisation. *Sci Total Environ* 408(7):1745–1754
14. Delay M, Frimmel FH (2012) Nanoparticles in aquatic systems. *Anal Bioanal Chem* 402(2):583–592
15. Kim S, Ryu DY (2013) Silver nanoparticle-induced oxidative stress, genotoxicity and apoptosis in cultured cells and animal tissues. *J Appl Toxicol* 33(2):78–89
16. Franklin NM, Rogers NJ, Apte SC, Batley GE, Gadd GE, Casey PS (2007) Comparative toxicity of nanoparticulate ZnO, bulk ZnO, and ZnCl₂ to a freshwater microalga (*Pseudokirchneriella subcapitata*): the importance of particle solubility. *Environ Sci Technol* 41(24): 8484–8490
17. Luyts K, Napierska D, Nemery B, Hoet PHM (2013) How physicochemical characteristics of nanoparticles cause their toxicity: complex and unresolved interrelations. *Environ Sci Process Impacts* 15(1):23–38
18. Prach M, Stone V, Proudfoot L (2013) Zinc oxide nanoparticles and monocytes: impact of size, charge and solubility on activation status. *Toxicol Appl Pharmacol* 266(1):19–26

19. Auffan M, Rose J, Wiesner MR, Bottero JY (2009) Chemical stability of metallic nanoparticles: a parameter controlling their potential cellular toxicity in vitro. *Environ Pollut* 157(4):1127–1133
20. Yu S-j, Yin Y-g, J-f L (2013) Silver nanoparticles in the environment. *Environ Sci Process Impacts* 15(1):78–92
21. Mudunkotuwa IA, Rupasinghe T, Wu CM, Grassian VH (2012) Dissolution of ZnO nanoparticles at circumneutral pH: a study of size effects in the presence and absence of citric acid. *Langmuir* 28(1):396–403
22. Reed RB, Ladner DA, Higgins CP, Westerhoff P, Ranville JF (2012) Solubility of nano-zinc oxide in environmentally and biologically important matrices. *Environ Toxicol Chem* 31(1):93–99
23. Vogelsberger W, Schmidt J, Roelofs F (2008) Dissolution kinetics of oxidic nanoparticles: the observation of an unusual behaviour. *Colloids Surf A Physicochem Eng Asp* 324(1–3):51–57
24. Cornelis G, Ryan B, McLaughlin MJ, Kirby JK, Beak D, Chittleborough D (2011) Solubility and batch retention of CeO₂ nanoparticles in soils. *Environ Sci Technol* 45(7):2777–2782
25. Liu JY, Hurt RH (2010) Ion release kinetics and particle persistence in aqueous nano-silver colloids. *Environ Sci Technol* 44(6): 2169–2175
26. Kittler S, Greulich C, Diendorf J, Koller M, Epple M (2010) Toxicity of silver nanoparticles increases during storage because of slow dissolution under release of silver ions. *Chem Mater* 22(16):4548–4554
27. Schmidt J, Vogelsberger W (2009) Aqueous long-term solubility of titania nanoparticles and titanium(IV) hydrolysis in a sodium chloride system studied by adsorptive stripping voltammetry. *J Solut Chem* 38(10):1267–1282
28. Elzey S, Grassian VH (2010) Agglomeration, isolation and dissolution of commercially manufactured silver nanoparticles in aqueous environments. *J Nanoparticle Res* 12(5):1945–1958
29. Schmidt J, Vogelsberger W (2006) Dissolution kinetics of titanium dioxide nanoparticles: the observation of an unusual kinetic size effect. *J Phys Chem B* 110(9):3955–3963
30. Navarro E, Piccapietra F, Wagner B, Marconi F, Kaegi R, Odzak N, Sigg L, Behra R (2008) Toxicity of silver nanoparticles to *Chlamydomonas reinhardtii*. *Environ Sci Technol* 42(23):8959–8964
31. Chao JB, Liu JF, Yu SJ, Feng YD, Tan ZQ, Liu R, Yin YG (2011) Speciation analysis of silver nanoparticles and silver ions in antibacterial products and environmental waters via cloud point extraction based separation. *Anal Chem* 83(17):6875–6882
32. Liu JF, Yu SJ, Yin YG, Chao JB (2012) Methods for separation, identification, characterization and quantification of silver nanoparticles. *TrAC Trends Anal Chem* 33:95–106
33. Fernandez B, Costa JM, Pereiro R, Sanz-Medel A (2010) Inorganic mass spectrometry as a tool for characterisation at the nanoscale. *Anal Bioanal Chem* 396(1):15–29
34. Evans EH, Horstwood M, Pisonero J, Smith CMM (2013) Atomic spectrometry update: review of advances in atomic spectrometry and related techniques. *J Anal At Spectrom* 28(6):779–800
35. Olesik JW, Gray PJ (2012) Considerations for measurement of individual nanoparticles or microparticles by ICP-MS: determination of the number of particles and the analyte mass in each particle. *J Anal At Spectrom* 27(7):1143–1155
36. Reed RB, Higgins CP, Westerhoff P, Tadjiki S, Ranville JF (2012) Overcoming challenges in analysis of polydisperse metal-containing nanoparticles by single particle inductively coupled plasma mass spectrometry. *J Anal At Spectrom* 27(7):1093–1100
37. Woodrow Wilson International Center for Scholars (2011) Nanotechnology. Health and environmental implications: an inventory of current research. Project on Emerging Nanotechnologies; <http://www.nanotechproject.org/>. Assessed 26 June 2013
38. Dekkers S, Prud'homme de Lodder L, de Winter R, Sips A, De Jong W (2007) Inventory of consumer products containing nanomaterials. RIVM letter report. 340120001/2007
39. Duyster L, Prasse C, Vogel JV, Vink JPM, Schaumann GE (2011) Translocation of Sb and Ti in an undisturbed floodplain soil after application of Sb₂O₃ and TiO₂ nanoparticles to the surface. *J Environ Monit* 13(5):1204–1211

40. Liu JF, Chao JB, Liu R, Tan ZQ, Yin YG, Wu Y, Jiang GB (2009) Cloud point extraction as an advantageous preconcentration approach for analysis of trace silver nanoparticles in environmental waters. *Anal Chem* 81(15):6496–6502
41. Liu JF, Liu R, Yin YG, Jiang GB (2009) Triton X-114 based cloud point extraction: a thermoreversible approach for separation/concentration and dispersion of nanomaterials in the aqueous phase. *Chem Commun* 12:1514–1516
42. Griffith OM (2010) Practical techniques for centrifugal separations. Thermo Fisher Scientific; application guide
43. Domingos RF, Baalousha MA, Ju-Nam Y, Reid MM, Tufenkji N, Lead JR, Leppard GG, Wilkinson KJ (2009) Characterizing manufactured nanoparticles in the environment: multimethod determination of particle sizes. *Environ Sci Technol* 43(19):7277–7284
44. Suttiponparnit K, Jiang J, Sahu M, Suvachittanont S, Charinpanitkul T, Biswas P (2011) Role of surface area, primary particle size, and crystal phase on titanium dioxide nanoparticle dispersion properties. *Nanoscale Res Lett* 6(1):27
45. Doane TL, Chuang CH, Hill RJ, Burda C (2012) Nanoparticle zetapotentials. *Acc Chem Res* 45(3):317–326
46. Malvern Instruments L (2001) Zeta potential—an introduction in 30 minutes (technical note MRK654-01). Zetasizer Nano series technical note
47. Dong XT, Hong GY, Yu DC, Yu DS (1997) Synthesis and properties of cerium oxide nanometer powders by pyrolysis of amorphous citrate. *J Mater Sci Technol* 13(2):113–116
48. Frimmel F, Delay M (2010) Introducing the “Nano-world”. In: Frimmel FH, Niessner R (eds) *Nanoparticles in the water cycle*. Springer, New York, pp 1–11
49. Jiang JK, Oberdorster G, Biswas P (2009) Characterization of size, surface charge, and agglomeration state of nanoparticle dispersions for toxicological studies. *J Nanoparticle Res* 11(1):77–89
50. Prathna TC, Chandrasekaran N, Mukherjee A (2011) Studies on aggregation behaviour of silver nanoparticles in aqueous matrices: effect of surface functionalization and matrix composition. *Colloids Surf A Physicochem Eng Asp* 390(1–3):216–224
51. Hartmann G, Hutterer C, Schuster M (2013) Ultra-trace determination of silver nanoparticles in water samples using cloud point extraction and ETAAS. *J Anal At Spectrom* 28(4):567–572
52. Hartmann G, Schuster M (2013) Species selective preconcentration and quantification of gold nanoparticles using cloud point extraction and electrothermal atomic absorption spectrometry. *Anal Chim Acta* 761:27–33
53. Majedi SM, Lee HK, Kelly BC (2012) Chemometric analytical approach for the cloud point extraction and inductively coupled plasma mass spectrometric determination of zinc oxide nanoparticles in water samples. *Anal Chem* 84(15):6546–6552
54. Jamison JA, Krueger KM, Yavuz CT, Mayo JT, LeCrone D, Redden JJ, Colvin VL (2008) Size-dependent sedimentation properties of nanocrystals. *ACS Nano* 2(2):311–319
55. Xiong B, Cheng J, Qiao YX, Zhou R, He Y, Yeung ES (2011) Separation of nanorods by density gradient centrifugation. *J Chromatogr A* 1218(25):3823–3829
56. El Badawy AM, Silva RG, Morris B, Scheckel KG, Suidan MT, Tolaymat TM (2011) Surface charge-dependent toxicity of silver nanoparticles. *Environ Sci Technol* 45(1):283–287
57. Benn TM, Westerhoff P (2008) Nanoparticle silver released into water from commercially available sock fabrics. *Environ Sci Technol* 42(11):4133–4139
58. Brunner TJ, Wick P, Manser P, Spohn P, Grass RN, Limbach LK, Bruinink A, Stark WJ (2006) In vitro cytotoxicity of oxide nanoparticles: comparison to asbestos, silica, and the effect of particle solubility. *Environ Sci Technol* 40(14):4374–4381
59. Kim JS, Kuk E, Yu KN, Kim JH, Park SJ, Lee HJ, Kim SH, Park YK, Park YH, Hwang CY, Kim YK, Lee YS, Jeong DH, Cho MH (2007) Antimicrobial effects of silver nanoparticles. *Nanomedicine Nanotechnol Biol Med* 3(1):95–101

60. Xia T, Kovochich M, Liong M, Madler L, Gilbert B, Shi HB, Yeh JI, Zink JI, Nel AE (2008) Comparison of the mechanism of toxicity of zinc oxide and cerium oxide nanoparticles based on dissolution and oxidative stress properties. *ACS Nano* 2(10):2121–2134
61. Zhang LL, Jiang YH, Ding YL, Daskalakis N, Jeuken L, Povey M, O'Neill AJ, York DW (2010) Mechanistic investigation into antibacterial behaviour of suspensions of ZnO nanoparticles against *E. coli*. *J Nanoparticle Res* 12(5):1625–1636
62. Van Hoecke K, Quik JTK, Mankiewicz-Boczek J, De Schampheleere KAC, Elsaesser A, Van der Meeren P, Barnes C, McKerr G, Howard CV, Van DeMeent D, Rydzynski K, Dawson KA, Salvati A, Lesniak A, Lynch I, Silversmit G, De Samber B, Vincze L, Janssen CR (2009) Fate and effects of CeO₂ nanoparticles in aquatic ecotoxicity tests. *Environ Sci Technol* 43(12):4537–4546
63. Khan Z, Singh T, Hussain JI, Hashmi AA (2013) Au(III)-CTAB reduction by ascorbic acid: preparation and characterization of gold nanoparticles. *Colloids Surf B Biointerfaces* 104:11–17
64. de Rivera FG, Angurell I, Rossell O, Seco M, Llorca J (2012) Organometallic surface functionalization of gold nanoparticles. *J Organomet Chem* 715:13–18
65. Saha K, Agasti SS, Kim C, Li XN, Rotello VM (2012) Gold nanoparticles in chemical and biological sensing. *Chem Rev* 112(5):2739–2779
66. Misra SK, Dybowska A, Berhanu D, Luoma SN, Valsami-Jones E (2012) The complexity of nanoparticle dissolution and its importance in nanotoxicological studies. *Sci Total Environ* 438:225–232

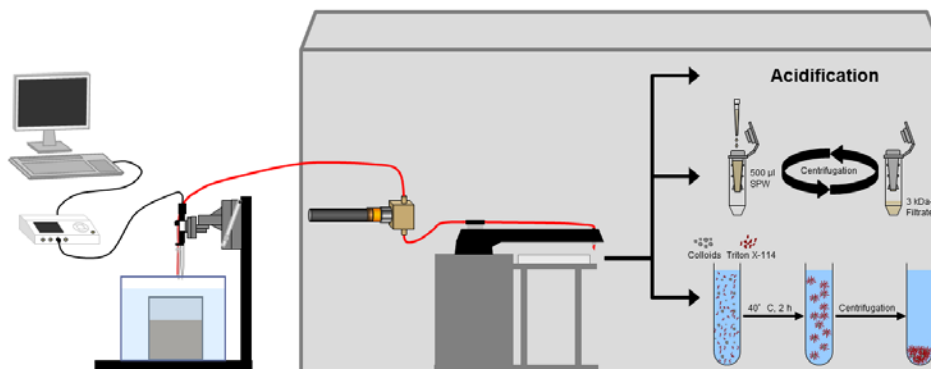
4

Metal and Metalloid Size Fractionation Strategies in Spatial High Resolution Sediment Pore Water Profiles

Anne-Lena Fabricius, Lars Duester, Dennis Ecker and Thomas A. Ternes

Environmental Science and Technology, 2016, 50 (17), pp 9506–9514

Sediment microprofiling and sampling → pore water fractionation → ICP-QMS



4.1 Abstract

Sediment water interfaces (SWIs) are often characterized by steep biogeochemical gradients determining the fate of inorganic and organic substances. Important transport processes at the SWI are sedimentation and resuspension of particulate matter and fluxes of dissolved materials. A *microprofiling* and micro sampling system (*missy*), enabling high resolution measurements of sediment parameters in parallel to a direct sampling of sediment pore waters (SPWs), was combined with two fractionation approaches (ultrafiltration (UF) and cloud point extraction (CPE)) to differentiate between colloidal and dissolved fractions at a millimeter scale. An inductively coupled plasma-quadrupole mass spectrometry method established for volumes of 300 μL enabled the combination of the high resolution fractionation with multi-element analyzes. UF and CPE comparably indicated that manganese is predominantly present in dissolved fractions of SPW profiles. Differences found for cobalt and iron showed that the results obtained by size-dependent UF and micelle-mediated CPE do not necessarily coincide, probably due to different fractionation mechanisms. Both methods were identified as suitable for investigating fraction-related element concentrations in SPW along sediment depth profiles at a millimeter scale. The two approaches are discussed with regard to their advantages, limitations, potential sources of errors, further improvements, and potential future applications.

4.2 Introduction

Sediment water interfaces (SWIs) are heterogeneous and often dynamic environments characterized by steep biogeochemical gradients impacting the turnover of substances between sediment, sediment pore water, and the overlaying water body.^{1,2} The conditions at these regions, spatially limited to a few centimeters, are determined by a variety of different processes including sedimentation, resuspension, diffusion, (micro)biological degradation of organic material, and bioturbation.^{1,2} In the absence of organisms, the dominant processes are mainly driven by the differences between the sediment and the water body of, e.g., the oxygen concentration, the pH value, the redox potential, and the related chemical reactions or concentrations of nutrients, metals, and metalloids (metal(loid)s) or other organic and inorganic substances.¹⁻³ The development of the gradients is related to the boundary layer at the SWI acting as a barrier for dissolved species.^{4,5} Comparably, the transport velocity of particles and associated substances also strongly decreases when they reach the sediment surface.² Beside this, the conditions are impacted by biological processes, either accelerating the stratification (due to the degradation of organic material or photosynthetic activities)^{2,4,5} or disturbing the gradients by introducing oxygen in deeper sediment layers (by, e.g., sediment-dwelling or filtering organisms).^{4,6,7} Studying the diffusional and particlerelated fluxes of substances at the SWI requires not only the determination of total concentrations but also the investigation of the element distribution between different size fractions (often and herein defined as dissolved, <1 nm; colloidal, 1 nm– 1 µm; and particulate, >1 µm⁸) in parallel to measurements of different physicochemical parameters. Additionally, the rapidly changing conditions and the microscale structures require methods that enable spatial high resolution investigations. Due to the availability of microsensors and -electrodes for several parameters (such as the oxygen concentration, the redox potential, or the pH value)^{5,9} and the development of different methods for pore water sampling,⁹⁻¹² options for fine-scale analyses at the SWI were considerably improved.^{9,10,13} However, many of the sampling and fractionation methods require the installation of the sampling device at the sampling site (e.g., diffusive equilibrium in thin film/diffusive gradient in thin film (DET/DGT) or dialysis devices), extensive sample preparation procedures (e.g., slicing and centrifugation of sediments or re-elution from accumulation materials), or both, possibly influencing the conditions at the sampling site and the characteristics of the samples. Hence, low invasive sampling strategies have to be combined with a storage and sample preparation under an inert, nonoxidizing atmosphere to avoid a bias of the results due to reoxidation processes, especially in the case of samples taken from anoxic sediments.^{14,15} To address size-fractionation-related processes along sediment depth profiles, methods are needed that are suitable for small sample volumes to allow spatial high resolution analyses.

To get a more holistic understanding of the geochemical cycling of elements at the SWI, also important with regard to contaminated sediments,¹⁶⁻¹⁸ the aim of this study is to provide methods enabling spatial high resolution analyses of fraction-related distributions of trace metal(loid)s in sediment pore waters (SPWs) along sediment depth profiles. By combining two fractionation methods with a microprofiling and micro sampling system (missy),¹² it was possible to investigate the distribution of different metal(loid)s between colloidal and dissolved fractions in SPW at a step size of ~2.4 mm in the vertical direction. The missy allows for a direct, automated, and minimally invasive suction-based sampling of pore water in parallel to measurements of different parameters (e.g., O₂ concentration, the redox potential, or the pH value). Fractionation of the SPW samples of ~500 µL was realized by ultrafiltration (UF) as a frequently used standardized filtration method⁸ and a (micelle-mediated) cloud point extraction (CPE), enabling the determination of dissolved and particulate fractions at the same time.¹⁹ To combine the high resolution sampling and the fractionation methods with the advantages of the multi-element capabilities of inductively coupled plasmaquadrupole mass spectrometry (ICP-QMS), an automated steady-state measurement approach was established for sample volumes of 300 µL. On the basis of the results of these laboratory experiments, it was demonstrated that both fractionation methods are capable to investigate fraction-related distribution of different metal(loid)s along sediment depth profiles. The methods are discussed comparatively, including potential sources of errors and further improvements as well as possible future applications.

4.3 Experimental Section

4.3.1 Chemicals and materials

Ultrapure water was produced using either an USF ELGA Purelab Plus (ELGA LabWater, Germany) or an Arium pro VF system (Sartorius AG, Germany). Nitric acid (HNO_3 , 65% w/w, for analysis) and ICP element standards (1 g/L) were purchased from Merck GmbH (Germany). The acid was sub-boiled using a DST-1000 (Savillex). Prior to use, all vessels as well as the 96 microwell plates (Riplate RW, 1 mL, PP; Ritter Medical) were rinsed for >24 h with HNO_3 (1.3%). Acetic acid and sodium acetate anhydrous (both Fluka and TraceSELECT for trace analysis), as well as ethylenediaminetetraacetic acid (EDTA, Aldrich, for trace analysis), were purchased from VWR. Triton X-114 (TRX 114 general purpose grade) was purchased from Fisher Scientific GmbH (Germany). To test for the applicability of the fractionation methods to sediment pore water samples, a homogenized sediment core was examined. Comparable to previous profiling experiments,¹² it contained 80% of a sieved (20–63 μm) and freeze-dried natural freshwater sediment from the river Lahn and 20% sand (Spielsand, Silex GmbH). Further information is given in the Appendix A3, paragraph “Sediment characteristics.” The core was placed in an aquarium (glass tank, 20 × 15 × 20 cm) filled with demineralized water (electric conductivity of $\sim 0.5 \mu\text{S}/\text{cm}$; system by Grünbeck Wasseraufbereitung GmbH, Germany) and left untreated for 9 weeks, which was found to be sufficient (refer to Fabricius et al. (2014))¹² to allow the gradients at the SWI to develop. If required, evaporated water was refilled.

4.3.2 Microprofiling and microsampling

The profiling experiments were conducted using a missy (refer to Figure 4.1 sections 1–6), enabling a spatial high resolution sampling of the sediment pore water in parallel to measurements of different sediment parameters. Because the development and validation of the missy was already published,¹² the profiling procedures will only be described briefly. Sediment pore water sampling was performed in parallel to measurement of the oxygen concentration and the redox potential. To avoid the reoxidation and precipitation of metal(loid)s, the sampling system was placed in a glovebox containing an argon atmosphere. Profiles of the oxygen concentration were measured using a Clark-type O_2 microsensor (OX-500), and the redox potential was determined by means of a platinum microelectrode (RD-500, both Unisense, Denmark) connected to an Ag/AgCl reference electrode (REF321, Radiometer Analytical, Denmark). The potential of the platinum electrode is referred as “redox potential” to facilitate the reading. Calibration of the sensor and the electrode (hereinafter referred as “sensors”) was carried out in accordance to the instruction given by the manufacturer. Profiles were run from 1 cm above the sediment surface to 2 cm within the sediment. The surface (0 cm) was determined visually and by the help of the O_2 sensor signal. The sensors and the sample

probe were fixed in such a manner that the tips were at the same height and at a distance of ~1–2 mm. Per profile, 490 data points were measured with a step size of 65 μm over a duration of 2.5 days (further information is given in paragraph “Microprofiling and microsampling” of the Appendix A3). Water samples (24 per profile) were continuously taken over a distance of 1.17 mm per sample (18 steps of 65 μm). This spatial resolution was defined by the movement of the motorized microprofiling system in the vertical direction, ignoring from which area around the probe the pore water was sampled. This uncertainty is based on the microspatial physical heterogeneity of the sediment investigated. In accordance to Fabricius et al. (2014),¹² samples of an intended volume of ~500 μL were collected over 2.5 h (sampling velocity of ~3.33 $\mu\text{L}/\text{min}$) in a 96 microwell plate covered by a self-adhesive foil (adhesive polyethylene film for ELISA incubation, nonsterile; VWR, Germany) to lower evaporation. The actual volume, depending on the gas-to water ratio at the sampling point, was estimated by help of a pipet used to transfer the samples from the well plate into other vessels. To get a sufficient volume for a size fractionation (see below) and a direct analysis of the pore water samples, two samples were pooled, leading to 12 samples of 1 mL (Table A3. 5). Smaller sample volumes were diluted to 1 mL using ultrapure water. Aiming to test and demonstrate the general suitability of the fractionation approaches for sediment depth profiles, several profiles were conducted for each of the three sample-preparation procedures (described below). Because the results of the total concentrations of these repeatedly taken profiles were very comparable to each other, the profiles of the reference experiments ($n = 3$), the UF ($n = 4$), and the CPE ($n = 5$) will hereinafter be treated as replicates, even though it is not feasible to conduct profiles in parallel and at the same position. These replicates were performed one after another at a distance of ~0.5 cm, which was found to be sufficient to avoid disturbances from the previous profiling procedure (refer to Fabricius et al.).¹² To achieve the best possible comparability between the profiles of one sample-preparation approach, the sensors and the sampling probe were kept fixed at the same position to each other in the microprofiling stand. To avoid a carryover from one profile to the next, sediment adhered to the surface of the membrane was carefully removed by help of a cotton bud, and the probe was rinsed by pumping aquarium water (>2 h). After the replicate experiments were finished, the probe head was rinsed by pumping HNO_3 (1.3%), followed by ultrapure water and aquarium water (each >2 h), and the microsensors were cleaned and recalibrated according to the instructions given by the manufacturer.

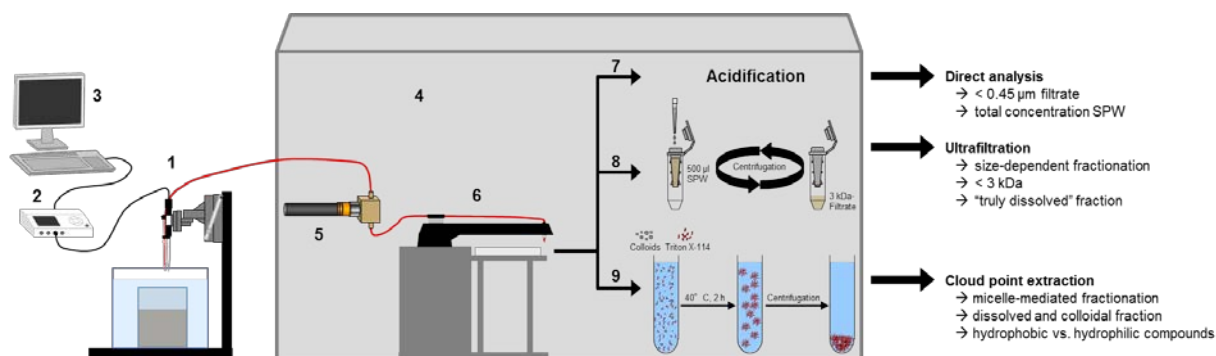


Figure 4.1: Schema of the experimental setup and sample-preparation strategies (not drawn to scale). Experiment with sample probe and microsensors (1) and microsensor multimeter (2) connected to PC (3). The sampling and sample preparation was conducted in a glovebox (4) containing an Ar atmosphere. The sampling system consisted of an annular gear pump (5) and a fraction collector (6). Samples were acidified (7) and directly measured and fractionated by ultrafiltration (8) or cloud point extraction (9).

4.3.3 Sample preparation and ICP-QMS analyses

A total of three different preparation procedures were applied to the sediment pore water samples obtained in the profiling experiments (Figure 4.1, steps 7–9): (i) in the case of the reference profiles, samples were diluted to 3 mL and directly measured without any further preparation step to ensure the comparability to a previously published and validated procedure.¹² In addition to this, (ii) a size-dependent centrifugal ultrafiltration and (iii) a micelle-mediated cloud point extraction were carried out to determine the fraction-related element distributions over sediment depth profiles. To confirm the comparability of the different experiments, the total element concentrations were determined for all pore water samples, regardless of the preparation procedure applied. Sampling and fractionation steps were conducted in a glovebox under an inert argon atmosphere. Element concentrations were measured by two ICP-QMS methods: samples of a volume ≥ 3 mL were analyzed by means of a routine method, whereas samples of 500 μL were measured via a newly established method for sample volumes of 300 μL (see below).

As described in Fabricius et al. (2014)¹² the sediment pore water samples of the three reference profiles were diluted in the glovebox to a volume of 3 mL using 1.3% HNO_3 and analyzed by means of ICP-QMS (Agilent 7700 series; Agilent Technologies, Germany). The device was equipped with a PFA-ST Micro Flow nebulizer (ES-2040) and a PFA inert sample introduction kit with a sapphire injector (inner diameter of 2.5 mm; Agilent Technologies, Germany). For sample introduction, an ASX-500 autosampler (CETAC Technologies) and the integrated sample introduction system (ISIS) of the ICP-QMS were used. In the following, this setup will be referred to as ICP-QMS setup 1.

If a fractionation was carried out, the 1 mL sample was split, with 500 μL used for the fractionation and 500 μL used to quantify the total element concentration in the SPW.

Centrifugal ultrafiltration was conducted using Amicon Ultra filter units (Ultracel-3, MWCO 3 kDa; Merck Millipore). A volume of 500 μL of the SPW was centrifuged for 25 min at 14000 g (Mikrocentrifuge MiniSpin Plus, Eppendorf, Germany). Afterward, the SPW sample and the 3 kDa filtrate were acidified adding 10 μL of concentrated HNO_3 (65%), transferred out of the glovebox, and frozen until measurements. To enable an analysis of the samples without any further dilution, the ICP-QMS measurements were adapted to a volume of 300 μL . Therefore, an ariMist nebulizer (Burgener Research) and a drainless spray chamber (Mini Spray Chamber CE; ESI Elemental Service and Instruments GmbH) were used, allowing for an introduction of the entire aerosol into the plasma. To ensure a nonpulsing low-flow transport of the carrier solution (~ 1 mL/min), a micro-annular gear pump (mzr-2542) connected to a console drive module (mzr-S06, HNP Microsystems, Germany) was used instead of the peristaltic pump of the ICP-QMS. Samples were introduced from a 96 deep-well plate using an ESI autosampler (SC-4 DX, ESI Elemental Service and Instruments GmbH) and the ISIS of the ICP-QMS. This setup will be referred to as ICP-QMS setup 2. Further details, including the certified reference materials and internal standards used, isotopes measured and detection limits, can be found in the ICP-QMS section of Appendix 3.

The CPE-fractionation approach was based on the protocol published by Hartman et al.²⁰ and adjusted for sample volumes of 500 μL . In contrast to the size-dependent UF, the separation of particles and dissolved components is obtained after the addition of a nonionic surfactant that, if a specific temperature is exceeded, forms micelles incorporating the hydrophobic and particulate compounds. After phase separation, the dissolved fraction can be determined in the aqueous phase, whereas the particles are extracted in the surfactant-rich phase.^{20,21} For size fractionation, a CPE mix containing 125 μL of Triton-X 114 (10 % w/v, diluted in ultrapure water), 125 μL of a saturated EDTA solution (~ 39 mM), 10 μL of sodium acetate solution (1 M), and 5 μL of acetic acid (1.25 M) was prepared fresh in 1.5 mL tubes (Eppendorf, Germany) that were transferred into the glovebox. After being mixed with 500 μL of the sediment pore water, samples were incubated for 2 h at 40 °C (Thermomixer equipped with a SmartBlock for 1.5 mL tubes; Eppendorf ThermoStat). Afterward, the samples were centrifuged (10 min, 10 000 rpm) and put back in the thermocycler, which was set to 4 °C to accelerate the phase separation. The phases were separated by pipetting the aqueous phase into another 1.5 mL tube. The unfractionated 500 μL portion of the SPW sample was acidified to a final concentration of 1.3 % HNO_3 . Samples were transferred outside the glovebox and frozen until further preparation and measurements. The two CPE phases were digested by means of a microwave system (turboWave; MLS GmbH, Germany). The TRX phase was suspended in 500 μL of HNO_3 ($\sim 65\%$) by help of a pipet and transferred to the digestion vessel. The tube was rinsed with 400 μL of ultrapure water. Samples of the aqueous phase were poured into the digestion vessels followed by

rinsing of the 1.5 mL tubes using 500 μL of HNO_3 (~65%). To estimate potential losses, 100 μL of internal standard (Ru, 100 mg/L) were added. Microwave assisted digestion was carried out by the application of a three-step program, including a ramp of 10 min to 180 °C, followed by a ramp of 4 min to 250 °C and an irradiation of 20 min at 250 °C. Afterward, the samples were poured into centrifugal tubes containing 3 mL of ultrapure water. To ensure a complete transfer of the sample, the digestion vessels were rinsed using the diluted samples. At least two blanks were included in each digestion run, replacing the sample by 500 μL of ultrapure water. Due to the small volumes, dilution factors were determined gravimetrically (AT 200, Mettler Toledo, Germany) by weighing the chemicals before fractionation and the upper and lower phase after fractionation as well as the digested samples. Analyses of the digested samples were performed using ICP-QMS setup 1, and those of the sediment pore water samples (0.45 μm) were performed by means of ICP-QMS setup 2.

To ensure the general suitability of the method for small sample volumes, CPE was applied to sediment water suspensions prior to the profiling experiments (for details, refer to paragraph 10.4, Appendix 3). The mass balances of the two phases were at 108 %, 106 %, and 107 % for Mn, Co, and Fe, respectively. For both UF and CPE, blanks were determined 10-fold using ultrapure water instead of sediment pore water (given with the results of the individual profiles in Table A3. 12 and Table A3. 18).

4.3.4 Data-analyses

Concentrations of the aqueous and TRX-phases of the CPE were calculated after subtraction of the digestion blanks by relating the results to the initial volume of the sediment pore water sample. Subsequently, results were corrected by the method background. Equally, concentrations of the 3 kDa fractions were calculated considering the dilution factors and the blanks of the method. For correlation of the element concentrations with the parameters measured by microsensors (O_2 and redox potential), the shift caused by the dead volume of the tubings was considered (Table A3. 8 and Table A3. 9).

4.4 Results and Discussion

4.4.1 Sediment pore water profiles

Sediment depth profiles of the oxygen concentration and the redox potential, as well as exemplary results for Mn, Fe, and Co determined in the sediment pore water samples, are provided in Figure 4.2 (reference profiles) and Figure 4.3 (fractionation studies). Additionally, profiles of As and Sb are given in the Appendix A3, Figure A3. 1 and Figure A3. 2. In the case of the oxygen concentration and the redox potential, the individual profiles measured at a step size of 65 μm are plotted to illustrate the fine-scale variances within and between the profiles. To easily correlate the parameters with the element concentrations, the mean values for the sampling distances were included as data points. For UF, only three profiles are available because the 500 μm glass tip of the O_2 sensor (profile 4) and the redox electrode (profile 1) were broken during profiling. Concerning the element concentrations, data points represent the middle of the sampling distance of 2.4 mm. To focus on the comparison of the different sample-preparation procedures, the mean values of the replicates are given instead of the individual profiles that are given in Table A3. 13–Table A3. 17 and Table A3. 19 – Table A3. 23. Thus, the arrow bars reflect the heterogeneity of the profile replicates together with the analytical uncertainty of the sample preparation and measurement. Because the microsensors and the sample probe were kept at the same position during the experiments of the different sample-preparation procedures (refer to the Experimental section), the sediment surface of the profiles presented in Figure 4.2 and Figure 4.3 varied slightly due to the microrelief.

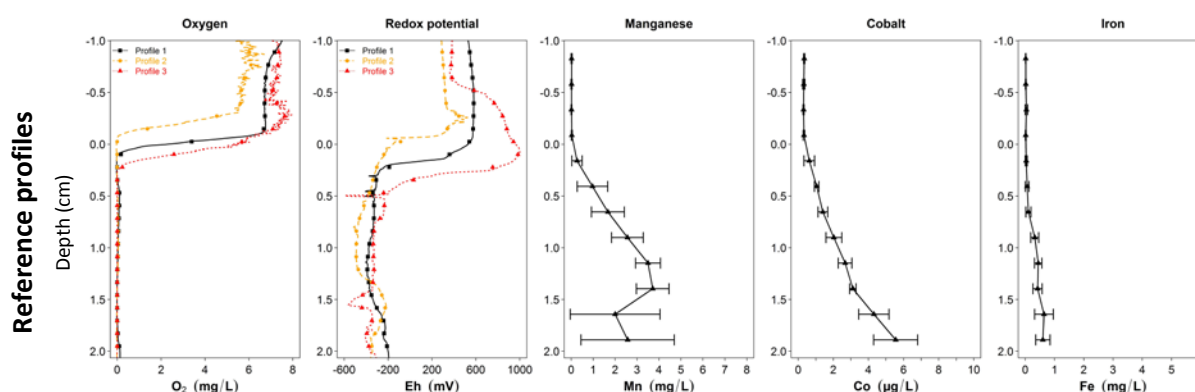


Figure 4.2: Sediment depth profiles of the O_2 concentration, the redox potential, and element concentrations in sediment pore water samples of the three reference profiles, taken from 1 cm above to 2 cm in the sediment. Data points are plotted at the middle of the sampling distance of 2.4 mm, representing the mean values of the O_2 concentration and the redox potential of the sampling distance. In the case of the element concentrations, data points represent the mean of the replicate profiles. Error bars showing the standard deviation of the replicate profiles, including the natural spatial heterogeneity as well as the uncertainty of the measurements.

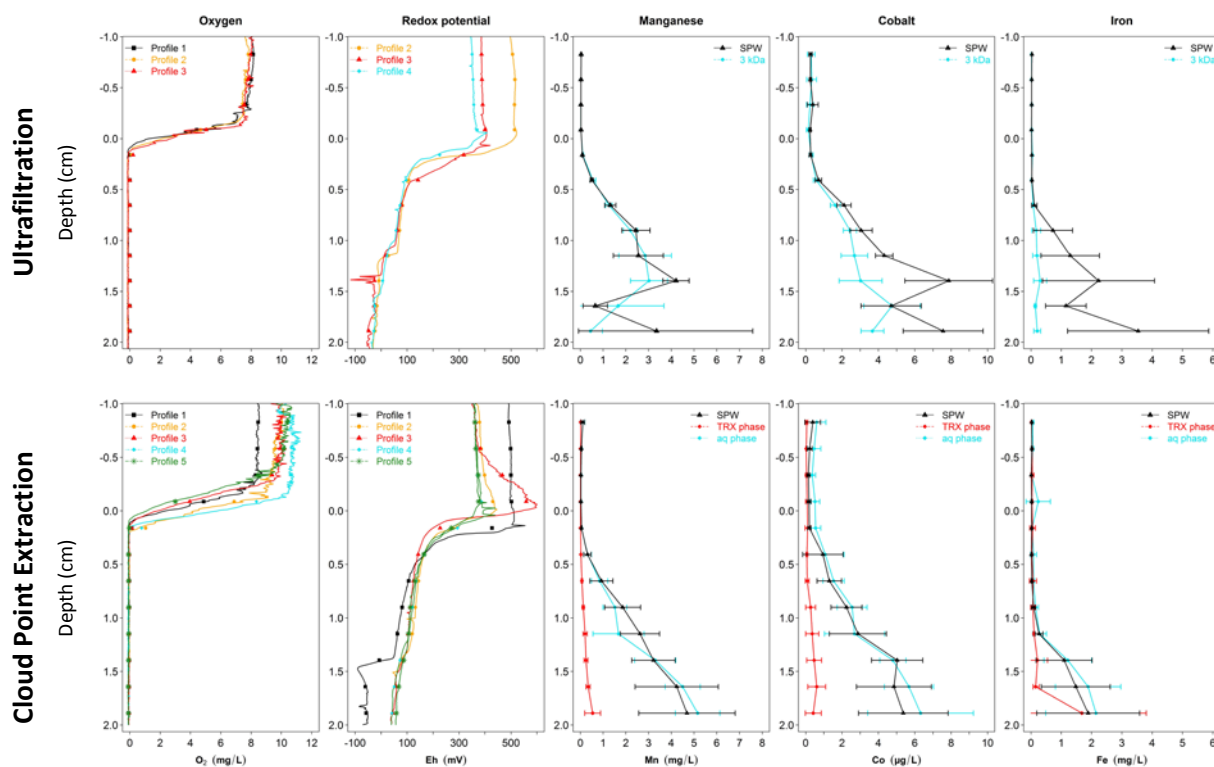


Figure 4.3: Sediment depth profiles of the O₂ concentration, the redox potential, and element concentrations in different fractions of sediment pore water samples, taken from 1 cm above to 2 cm in the sediment (SPW = sediment pore water; 3 kDa = dissolved fraction of UF; TRX = surfactant rich colloid containing the CPE phase; aq phase = aqueous CPE phase containing the dissolved fraction). Data points are plotted at the middle of the sampling distance of 2.4 mm, representing the mean values of the O₂ concentration and the redox potential for the sampling distance. In the case of the element concentrations, data points represent the mean of the replicate profiles. Error bars show the standard deviation of the replicate profiles, including the natural spatial heterogeneity as well as the uncertainty of the measurements. For UF, only three profiles for the O₂ concentration and the redox potential are given due to broken sensors.

Depth profiles of oxygen concentration

The mean oxygen concentrations in the water phase above the sediment were in a range between 5.8 and 10.3 mg O₂/L and decreased rapidly below the limit of detection (0.01 mg O₂/L) within the first 1–3 mm of the sediment (Figure 4.2 and Figure 4.3 and Table A3. 10). Such gradients are typical for shallow, slightly turbulent waters, where oxygen introduction in the sediment is mainly driven by diffusional processes.^{2,5} When the results of the profile replicates (reference, UF, and CPE) were compared, an increase of the O₂ concentrations in the water phase from 5.8– 7.3 mg O₂/L (Figure 4.2 and Table A3. 10) to 7.1–7.3 and 7.8– 10.3 mg O₂/L (CPE; Figure 4.3 and Table A3. 10) was detected. This might be related to a slight (seasonal) decrease of the water temperature from 19.0 °C in September (reference profiles) over 18.0 °C in late October (UF) to 17.9 °C in November (CPE). Nevertheless, because the temperature differences (especially between the UF and CPE profiles)

were low, slight O₂ variations were more probably caused by the fluctuations of the water level (due to evaporation and refilling of the aquarium), the amount of oxygen introduced by the air stream on the water surface, or both.

Depth profiles of the redox potential

The redox potential measured in the water phase was in a range between 300 and 500 mV for all profiles and declined in the deeper, anoxic layers of the sediment to values of approximately -40, -30, and 30 mV for the reference, the UF, and the CPE profiles, respectively (Figure 4.2 and Figure 4.3 and Table A3. 10). This decrease can mainly be related to the consumption of oxygen and other electron acceptors during the microbial decomposition of organic material.^{5,22} Beside this, the redox potential can also be influenced by a variety of other factors and processes (e.g., the pH value; type and amount of organic material; oxidizing capacities of Fe and Mn (oxyhydr)oxides; and the presence or absence of sulfides, nitrate, or phosphorus).^{5,22} The above-mentioned increase of the redox potential in the deeper sediment layers from the reference to the UF and CPE experiments (see also Table A3. 10) is probably caused by the elevated number of profiles conducted in the sediment core, causing the introduction of oxygen. However, the results of the profile replicates, taken at a distance of ~0.5 cm, were very comparable, and thus, it did not significantly disturb the proof of principle intended in this study. Nevertheless, this observation indicates that the total number of profiles taken in one core should be limited.

Fractionation of sediment pore water

Regarding the metal(loid) concentrations in the sediment pore water, two aspects have to be considered: (i) the total concentrations in relation to the sediment parameters measured and (ii) the partitioning of the analytes between the different fractions of UF and CPE among the depth profiles. When the results of the sediment pore water (SPW 0.45 µm) of the reference profiles and the UF and CPE experiments were compared, the concentrations found for Mn, Fe, and Co were generally found to be in a good agreement with each other and those found in a previous study conducted with a similar sediment core.¹² Thereby, the applicability of ICP-QMS setup 2 could also be confirmed as an alternative to commercially available devices with regard to small-volume measurements.²³ The increasing total concentrations of the elements in deeper anoxic layers of the sediment can be explained by the reduction of Mn and Fe (oxyhydr)oxides leading to a release of Mn²⁺ and Fe²⁺ and associated trace elements into the water phase.^{3,24,25}

In the case of iron, the comparison of the reference profiles with the fractionation experiments indicate ongoing reduction processes over the experimental period, leading to increased total concentrations in the later experiments. Regarding the results of the two fractionation methods

(Figure 4.3 and paragraphs 8.8 and 8.9 in the Appendix A3.), it should be kept in mind that the two approaches are based on different principles: the UF is a size-dependent separation of compounds that are bigger or smaller than the membrane cut-off of 3 kDa. By the application of the CPE, the particulate, hydrophobic compounds (extracted in the TRX phase) are separated from the dissolved, hydrophilic ones (found in the aqueous phase). In general, the analytes are concentrated and extracted in the TRX phase,^{26,27} and the aqueous phase is discarded or analyzed only for validation purposes^{19,28} but not to determine the dissolved fraction, as was done in this or previous studies run in our laboratory.²⁹ Hence, in contrast to a filtration routinely used as a size-fractionation method in numerous studies, the results of the CPE are only comparable to a limited extent to those of other CPE applications. However, one of the aims of the method comparison was to evaluate the capacity of the CPE method, originally developed for engineered nanoparticles, to separate natural colloids from the dissolved fraction in sediment pore water without further optimization. Regarding the Mn distributions upon fractionation, remarkably comparable results were found for the two fractionation approaches (Figure 4.3; individual profiles are given in Table A3. 13 and Table A3. 19), showing that the element is nearly exclusively present in the dissolved fractions (<3 kDa of the UF and in the aqueous phase of the CPE) of the SPW. The results are in agreement with other studies, detecting Mn only to a certain portion (up to ~20%) in colloidal fractions of sediment pore waters.³⁰⁻³⁴

In the case of Co (for individual profiles, see Table A3. 14 and Table A3. 20), slight differences between the UF and the CPE were detected; the results of the UF indicate that in the water body, the element is present in the dissolved fraction but generally at very low concentrations. In deeper anoxic regions of the sediment, the concentrations in the SPW and the 3 kDa fraction increases, but the portion of the dissolved fraction decreases. Other size-dependent fractionation studies comparably show that Co is predominantly present in the dissolved fraction of SPWs but can also be found up to ~20% in the colloidal fraction.^{18,32} Moreover, Huerta-Diaz et al. (2007)³⁰ demonstrated that the distribution between different fractions may vary along sediment depth profiles. In contrast to the UF, after CPE, the element was hardly (if at all) detectable in the TRX phase but present in the aqueous phase, with concentrations equal to the SPW 0.45 μm filtrate, indicating that the element is exclusively present as dissolved forms. The difference between the fractionation methods can be explained by soluble (hydrophilic) Co compounds that do not pass the 3 kDa membrane but remain dissolved in the aqueous phase of the CPE such as, e.g., soluble organic molecule-metal complexes.^{31,35,36} However, the EDTA used in the CPE to keep ionic species dissolved also potentially influences, as a strong complexing agent for cations, the partitioning of Co^{37,38} or other cations (equally found for Fe; see below). Even though stability constants are available for different element

species, the EDTA–metal complexes formed and the metal–metal–EDTA exchange reactions in the SPWs depends on the actual concentration and speciation of the elements and the EDTA present, as well as on the matrix characteristics that vary with the changing conditions over the depth profiles.^{39,40} Hence, the influence of the EDTA on the fractionation of the different elements should be elucidated empirically in future optimization experiments of the CPE procedure for colloidal systems.

Concerning Fe (for individual profiles, refer to Table A3. 15 and Table A3. 21), the size-fractionation methods show different results: after UF, the element was found in low concentrations of ~20 µg/L in the overlaying water body, mainly in the dissolved fraction. Within the sediment, a fast and strong increase of the total concentration in the SPW (0.45 µm) to the mg/L range was detected, whereas the concentration of the dissolved fraction increased only up to ~200 µg/L. In general, this is comparable to other studies confirming that high amounts of Fe can be found in colloidal fractions of surface water and SPW.^{17,31} The percentage of the dissolved fraction can vary over depth profiles and in relation to the characteristics of the sediment, redox reactions, and related dissolution and precipitation processes.^{24,25,30} In contrast to the UF, after CPE, Fe was (with the exception of the deepest sample) mostly found in the aqueous phase of the SPW. Comparable to Co, this can be related to the presence of soluble Fe compounds of >3 kDa remaining in the aqueous phase (e.g., organic metal complexes).^{31,35,36} Equally, an influence of the EDTA is possible (see the discussion above)^{37,39,41} but does not explain comprehensively that nearly all of the Fe is found in the aqueous phase. The last sampling point, showing high concentrations also in the TRX phase, indicates a higher quantity of colloidal, hydrophobic Fe species in the SPW of deeper sediment layers. Nevertheless, in the case of a ubiquitously present element such as Fe, this could be caused by contaminations due to the laboratory background that are particularly relevant in the case of small sample volumes. This was also indicated by varying results of the blank values of the two fractionation approaches (Table A3. 12 and Table A3. 18). Therefore, in addition to a general background correction, further precautionary measures (e.g., using a laminar flow box for the storage of chemicals and the experimental work and the acid cleaning of pipet tips) should be considered to avoid a contamination by ubiquitous metals. However, the concentrations of Fe in SPW fractions of different profiles also vary naturally in relation to the (micro)structures, parameters, and processes of the sediment.^{30,32} Even though the UF can be seen as a standard procedure, the novelty of the two approaches to investigate element concentrations in different size fractions of SPWs at a spatial high resolution over sediment depth profiles impedes a direct comparison to the results of other studies. To the best of the authors' knowledge, only one publication addressed the size fractionation of metal(loid)s in SPW among sediment profiles.³⁰ Nevertheless, as discussed, both size-

fractionation approaches gave reasonable results, proving the suitability of the application for such fractionation studies.

4.4.2 Method evaluation, future improvements and applications

In general, the two size-fractionation methods adapted to sample volumes of <500 μL were found to be suitable for investigating fraction-related element distributions in sediment pore water samples of depth profiles. Together with the capability of the missy (already demonstrated in a previous study)¹² to implement a direct SPW sampling at a spatial resolution at a millimeter range in the vertical direction and the ICP-QMS setup 2 developed for small sample volumes, size-fraction-related multi-element information along the sediment water interface can be obtained in parallel to parameters measured by the microsensors. Because sampling and fractionation was performed under an argon atmosphere, the risk of a reoxidation of reduced species¹⁴ and related shifts of the element distributions could be minimized. By comparing the two fractionation methods, the advantages and limitations were demonstrated: the UF approach using centrifugal filter units is more expensive but enables an almost-operator independent one-step fractionation that minimizes the risk of contaminations, losses, or other potential sources of systematic errors related to extensive sample-preparation procedures. However, because the size fractions are not separated, the UF does not allow for a quantitative analysis of both fractions. The fraction between 3 kDa and 0.45 μm has to be determined by subtraction from the concentration of the initial sample, impeding the calculation of mass balances and the assessment of potential losses. In the case of high amounts of suspended matter, problems of dead-end filtration (clogging of the membrane, reduction of the pore size, and increase of the required filtration force) may hamper the filtration. Moreover, the UF does not allow for a further adjustment or optimization. In contrast to the UF, the CPE approach enables the analysis of both phases but suffers from the drawbacks of a more-extensive preparation procedure (CPE and digestion) and the requirement of an experienced operator to ensure a reproducible phase separation. In addition, the results presented highlight that, with regard to small sample volumes, clean working conditions and a thorough handling of the samples is indispensable to minimizing the risk of contaminations. Because individual samples are often affected by contaminations (e.g., dust and improper pipet tips or vessels), a general background correction does not guarantee that the risk of a bias of the results is waived. Fortunately, in this study, only the results of Fe and (in one case) of Co indicated a random contamination. In general, the CPE can potentially be improved by a further adjustment and optimization (e.g., by the use of different complexing agents, buffers, surfactants, and procedures).

On the basis of the experiments conducted for the proof of principle of the two fractionation approaches for pore water samples of small volumes, the UF was actually identified as the easier

implementable, more-robust, and less-biased method. The CPE does suffer from several drawbacks described above but offers the possibility of an alternative, micelle-mediated, low-cost fractionation approach that allows separating hydrophilic and dissolved from hydrophobic and particulate compounds and, thus, provides additional information to size dependent (filtration) methods. Because, as mentioned, the CPE is typically applied for an extraction and preconcentration of substances but not for fractionation purposes, future investigations are necessary to further optimize (maybe simplify) and fundamentally validate the protocol, (in particular, with regard to the question which compounds and species are included in the two CPE fractions).⁴³

Overall, both methods enable for the first time the investigation of fraction-related element distributions along sediment depth profiles at a spatial resolution in the millimeter range. Within other publications, either only one depth (or the overlying water) or one fraction (e.g., separated by centrifugation, filtration of $<0.45 \mu\text{m}$, dialysis, or ionic species by the use of exchange resins)^{14,15,42,44} is addressed, the sampling or sample-preparation procedure risks affecting the conditions at the sampling site or the samples, or both.^{14,15} Moreover, in contrast to other fractionation methods (e.g., ultracentrifugation, field flow fractionation, or single-particle ICP-MS), the methods can be conducted within a glovebox or glovebag containing an inert atmosphere to avoid reoxidation processes. The methods are applicable to individual samples, allowing an immediate fractionation, which is necessary in, e.g., long-term experiments or field studies. However, the study presented was limited to some extent: because the hollow fibers used to fabricate the sampling probes are only available with cut-offs of $<0.45 \mu\text{m}$, bigger colloids ($0.45\text{--}1 \mu\text{m}$) and small particles ($>1 \mu\text{m}$) also present in SPWs were not considered. Moreover, the maximal depth of the profiles was set to 2 cm to avoid damage of the needle sensors. Hence, the aim of future experiments will be the combination of the fractionation strategies with other sampling systems, allowing for a deeper sampling (probably at a coarser resolution) and the consideration of the bigger-colloidal and small-particulate fractions. Additionally, the fraction-related distribution of other inorganic and organic substances (e.g., anionic species, nutrients, dissolved organic matter, pesticides, or pharmaceuticals), the sediments of different sampling sites, the potential effects of mechanical or chemical disturbances on the fractionation characteristics, or both can be investigated. In addition to laboratory experiments providing the advantages of controlled and stable conditions, the availability of field microprofiling systems (together with the automated sampling procedure and the easily applicable fractionation approaches) provide a potential for the further automatization of the methods for future in situ applications.

The ability to study fraction-related distributions at a high spatial resolution will help to gain a more-holistic understanding of the processes that govern the fate and behavior of different compounds in dependence of the fine-scale structures of the sediment water interface.

4.5 References

1. Lerman, A., Chemical Exchange Across Sediment-Water Interface. *Annual Review of Earth and Planetary Sciences* 1978, 6, 281-303.
2. Santschi, P.; Höhener, P.; Benoit, G.; Buchholtz-ten Brink, M., Chemical processes at the sediment-water interface. *Marine Chemistry* 1990, 30, (0), 269-315.
3. Rigaud, S.; Radakovitch, O.; Couture, R. M.; Deflandre, B.; Cossa, D.; Garnier, C.; Garnier, J. M., Mobility and fluxes of trace elements and nutrients at the sediment-water interface of a lagoon under contrasting water column oxygenation conditions. *Applied Geochemistry* 2013, 31, 35-51.
4. Jorgensen, B. B.; Revsbech, N. P., Diffusive boundary-layers and the oxygen-uptake of sediments and detritus. *Limnology and Oceanography* 1985, 30, (1), 111-122.
5. Revsbech, N. P.; Jorgensen, B. B., Microelectrodes - their use in microbial ecology. *Advances in Microbial Ecology* 1986, 9, 293-352.
6. Schaller, J.; Brackhage, C.; Mkandawire, M.; Dudel, E. G., Metal/metalloid accumulation/remobilization during aquatic litter decomposition in freshwater: A review. *Science of the Total Environment* 2011, 409, (23), 4891-4898.
7. Schaller, J.; Weiske, A.; Mkandawire, M.; Dudel, E. G., Invertebrates control metals and arsenic sequestration as ecosystem engineers. *Chemosphere* 2010, 79, (2), 169-173.
8. Guo, L.; Santschi, P. H., Ultrafiltration and its Applications to Sampling and Characterisation of Aquatic Colloids. In *Environmental Colloids and Particles*, John Wiley & Sons, Ltd: 2007; pp 159-221.
9. Stockdale, A.; Davison, W.; Zhang, H., Micro-scale biogeochemical heterogeneity in sediments: A review of available technology and observed evidence. *Earth-Science Reviews* 2009, 92, (1-2), 81-97.
10. Davison, W.; Fones, G. R.; Grime, G. W., Dissolved metals in surface sediment and a microbial mat at 100- μm resolution. *Nature* 1997, 387, (6636), 885-888.
11. Ding, S. M.; Wang, Y.; Xu, D.; Zhu, C. G.; Zhang, C. S., Gel-Based Coloration Technique for the Submillimeter-Scale Imaging of Labile Phosphorus in Sediments and Soils with Diffusive Gradients in Thin Films. *Environmental Science & Technology* 2013, 47, (14), 7821-7829.
12. Fabricius, A. L.; Duester, L.; Ecker, D.; Ternes, T. A., New Microprofiling and Micro Sampling System for Water Saturated Environmental Boundary Layers. *Environmental Science & Technology* 2014, 48, (14), 8053-8061.
13. Xu, D.; Wu, W.; Ding, S. M.; Sun, Q.; Zhang, C. S., A high-resolution dialysis technique for rapid determination of dissolved reactive phosphate and ferrous iron in pore water of sediments. *Science of the Total Environment* 2012, 421, 245-252.
14. Bufflap, S. E.; Allen, H. E., Sediment Pore-Water Collection Methods for Trace-Metal Analysis - A Review. *Water Research* 1995, 29, (1), 165-177.
15. Mudroch, A. A., Jose M. , *Manual of Aquatic Sediment Sampling*. CRC Press, Inc. : 1995.
16. Kretzschmar, R.; Schafer, T., Metal retention and transport on colloidal particles in the environment. *Elements* 2005, 1, (4), 205-210.
17. Macgregor, K.; MacKinnon, G.; Farmer, J. G.; Graham, M. C., Mobility of antimony, arsenic and lead at a former antimony mine, Glendinning, Scotland. *Science of The Total Environment* 2015, 529, 213-222.
18. Taylor, H. E.; Antweiler, R. C.; Roth, D. A.; Alpers, C. N.; Dileanis, P., Selected Trace Elements in the Sacramento River, California: Occurrence and Distribution. *Archives of Environmental Contamination and Toxicology* 2012, 62, (4), 557-569.
19. Liu, J. F.; Chao, J. B.; Liu, R.; Tan, Z. Q.; Yin, Y. G.; Wu, Y.; Jiang, G. B., Cloud Point Extraction as an Advantageous Preconcentration Approach for Analysis of Trace Silver Nanoparticles in Environmental Waters. *Analytical Chemistry* 2009, 81, (15), 6496-6502.

20. Hartmann, G.; Hutterer, C.; Schuster, M., Ultra-trace determination of silver nanoparticles in water samples using cloud point extraction and ETAAS. *J. Anal. At. Spectrom.* 2013, 28, (4), 567-572.
21. Melnyk, A.; Namiesnik, J.; Wolska, L., Theory and recent applications of coacervate-based extraction techniques. *Trac-Trends in Analytical Chemistry* 2015, 71, 282-292.
22. Søndergaard, M., Redox Potential. In *Encyclopedia of Inland Waters*, Likens, G. E., Ed. Academic Press: Oxford, 2009; pp 852-859.
23. Clarke, D. M., S; Winship, P.; Cook, B., Application Note: Micro-Volume Injection System for ICP-MS. In *Teledyne CETAC Technologies: Omaha, NE 68144-3334 USA*, 2015; p 2.
24. Balistrieri, L. S.; Murray, J. W.; Paul, B., The geochemical cycling of trace-elements in a biogenic meromictic lake. *Geochimica Et Cosmochimica Acta* 1994, 58, (19), 3993-4008.
25. Giblin, A. E., Iron and Manganese. In *Encyclopedia of Inland Waters*, Likens, G. E., Ed. Academic Press: Oxford, 2009; pp 35-44.
26. Ojeda, C. B.; Rojas, F. S., Separation and preconcentration by cloud point extraction procedures for determination of ions: recent trends and applications. *Microchimica Acta* 2012, 177, (1-2), 1-21.
27. Samaddar, P.; Sen, K., Cloud point extraction: A sustainable method of elemental preconcentration and speciation. *Journal of Industrial and Engineering Chemistry* 2014, 20, (4), 1209-1219.
28. De Jong, N.; Draye, M.; Favre-Réguillon, A.; LeBuzit, G.; Cote, G.; Foos, J., Lanthanum(III) and gadolinium(III) separation by cloud point extraction. *Journal of Colloid and Interface Science* 2005, 291, (1), 303-306.
29. Fabricius, A.-L.; Duester, L.; Meermann, B.; Ternes, T., ICP-MS-based characterization of inorganic nanoparticles—sample preparation and off-line fractionation strategies. *Analytical and Bioanalytical Chemistry* 2014, 406, (2), 467-479.
30. Huerta-Díaz, M. A.; Rivera-Duarte, I.; Sanudo-Wilhelmy, S. A.; Flegal, A. R., Comparative distributions of size fractionated metals in pore waters sampled by in situ dialysis and whole-core sediment squeezing: Implications for diffusive flux calculations. *Applied Geochemistry* 2007, 22, (11), 2509-2525.
31. Itoh, A.; Nagasawa, T.; Zhu, Y. B.; Lee, K. H.; Fujimori, E.; Haraguchi, H., Distributions of major-to-ultratrace elements among the particulate and dissolved fractions in natural water as studied by ICP-AES and ICP-MS after sequential fractionation. *Anal. Sci.* 2004, 20, (1), 29-36.
32. Dabrin, A.; Roulier, J. L.; Coquery, M., Colloidal and truly dissolved metal(oid) fractionation in sediment pore waters using tangential flow filtration. *Applied Geochemistry* 2013, 31, 25-34.
33. Kottelat, R.; Vignati, D. A. L.; Chanudet, V.; Dominik, J., Comparison of small- and large-scale ultrafiltration systems for organic carbon and metals in freshwater at low concentration factor. *Water Air and Soil Pollution* 2008, 187, (1-4), 343-351.
34. Durin, B.; Bechet, B.; Legret, M.; Le Cloirec, P., Role of colloids in heavy metal transfer through a retention-infiltration basin. *Water Sci. Technol.* 2007, 56, (11), 91-99.
35. Wu, F. C.; Evans, D.; Dillon, P.; Schiff, S., Molecular size distribution characteristics of the metal-DOM complexes in stream waters by high-performance size-exclusion chromatography (HPSEC) and high-resolution inductively coupled plasma mass spectrometry (ICP-MS). *J. Anal. At. Spectrom.* 2004, 19, (8), 979-983.
36. Itoh, A.; Kimata, C.; Miwa, H.; Sawatari, H.; Haraguchi, H., Speciation of trace metals in pond water as studied by liquid chromatography inductively coupled plasma mass spectrometry. *Bulletin of the Chemical Society of Japan* 1996, 69, (12), 3469-3473.
37. Repo, E.; Warchol, J. K.; Bhatnagar, A.; Mudhoo, A.; Sillanpaa, M., Aminopolycarboxylic acid functionalized adsorbents for heavy metals removal from water. *Water Research* 2013, 47, (14), 4812-4832.
38. Tanaka, T., Ion-chromatographic determination of divalent metal ions (Co, Ni, Cu, Zn, Cd) using EDTA as complexing agent. *Fresenius' Zeitschrift für analytische Chemie* 1985, 320, (2), 125-127.

39. Nowack, B.; Kari, F. G.; Kruger, H. G., The remobilization of metals from iron oxides and sediments by metal-EDTA complexes. *Water Air and Soil Pollution* 2001, 125, (1-4), 243-257.
40. Di Palma, L.; Mecozzi, R., Heavy metals mobilization from harbour sediments using EDTA and citric acid as chelating agents. *Journal of Hazardous Materials* 2007, 147, (3), 768-775.
41. Stumm, W. M., J.J., *Aquatic Chemistry: chemical equilibria and rates in natural waters*. 3rd ed.; Environmental Science and Technology: 1996.
42. Yang, Z.; Guo, W.; Fan, Y.; Lin, C.; He, M., High-resolution profiles of iron, manganese, cobalt, cadmium, copper and zinc in the pore water of estuarine sediment. *International Journal of Environmental Science and Technology* 2013, 10, (2), 275-282.
43. Duester, L.; Fabricius, A.-L.; Jakobtorweihen, S.; Philippe, A.; Weigl, F.; Wimmer, A.; Schuster, M. and Nazar, M. F., Can cloud point based enrichment, preservation and detection methods help to bridge gaps in aquatic nanometrology? *Analytical and Bioanalytical Chemistry* 2016, in publication.
44. Lewandowski, J.; Ruter, K.; Hupfer, M., Two-dimensional small-scale variability of pore water phosphate in freshwater lakes: Results from a novel dialysis sampler. *Environmental Science & Technology* 2002, 36, (9), 2039-2047.

5

Final Conclusions

The approaches developed in this thesis provide an analytical basis for the investigation of different aspects of (natural or artificial) colloidal systems as well as the conditions and processes at sediment water interfaces by means of direct and minimal-invasive procedures.

The development of the *missy* enables the investigation of numerous scientific questions concerning e.g., the comparison of different sediments, the fate and effects of substances (including elements, biocides, nutrients or pharmaceuticals) or mechanical disturbances (like, e.g., dredging, changing flow velocities or bioturbation). Potential impacts of disturbances can be studied in spiking experiments or simulated flow/dredging-scenarios. The high resolution provides the possibility to investigate these aspects in detail by capturing the heterogeneity of the thin boundary layers and the processes occurring at fine scale structures. By using other materials for the sample probes or other sensors, the applications can be extended to other analytes or to deeper (probably spatially less resolved) profiles. Even though the *missy* experiments were until now only conducted in the laboratory, the system and sample preparation methods can in principle also be adopted to field studies.

With a special regard to engineered nanomaterials as emerging substances reaching aquatic systems, methods were developed that allow on the one hand the characterization of ENP suspensions and, on the other hand the investigation of the fate, behavior and effects of ENMs at SWIs. Since the analytical approaches provided are routine suitable, they can also be adopted for standard applications required for, e.g., (ecotoxicological) tests or monitoring campaigns. As also discussed in the additional article (refer to Appendix III), this is needed as a basis for the development and implementation of regulatory frameworks and risk assessments. However, due to the variety of different materials with different properties used in nano-applications and -products, the development of universally applicable methods is difficult. It was shown that it is possible to define a best practice, but that the suitability for a given material should probably be verified prior to the application.

By the adaptation and further optimization of the fractionation methods to the *missy* samples an immediate sample preparation could be realized and combined to the high-resolution sampling. This enabled for the first time the high resolution investigation of fraction related element distribution in parallel to sediment parameters for sediment depth profiles. By conducting the fractionation procedures under an inert Argon atmosphere, some of the most important sources of error related

to sediment pore water sampling and preparation could be overcome. Due to the development of an ICP-MS methods enabling to analyze sample volumes of <500 μ l it was possible to measure the samples directly and without any further dilution. Nevertheless, analyzing small sample volumes, resulting from the high resolution is challenging due to potential sources of errors and uncertainties. A further development or adaptation to other analytes and applications is nonetheless possible and will help to distinguish between dissolved and colloid-mediated transport processes of ENPs as well as other substances or pollutants.

The *missy* applications in combination with the fractionation approaches will help to obtain a deeper and more holistic understanding of the processes and determining factors at the thin boundary layers between the water body and the sediment and will thereby also enable to estimate potential (harmful) effects of released substances in aquatic ecosystems.

Danksagung

Mein besonderer Dank gilt Lars Düster, der nicht nur meine Doktorarbeit betreut und mich in vielen Dingen ausgebildet hat, sondern dem es gelungen ist, mich für die Fragen der Umweltchemie zu begeistern. Dein stets offenes Ohr, deine ehrliche Meinung und konstruktive Kritik haben mir dabei bei allen wissenschaftlichen und unwissenschaftlichen Belangen ebenso geholfen wie die (wenn nötig) aufmunternden und motivierenden Worte. Durch deine unglaubliche Fähigkeit, mich im richtigen Moment ins kalte Wasser zu werfen und mir den Freiraum zu geben, mich auszuprobieren und Fehler zu machen, konnte ich vieles verwirklichen, wobei ich mich stets auf deine Unterstützung verlassen konnte.

Ich danke Thomas A. Ternes, der als mein Erstgutachter mit einem stets kritischen Blick maßgeblich dazu beigetragen hat, diese Arbeit an zahlreichen Punkten zu verbessern. Herrn Prof. Scholz und Herrn Prof. Dr. Torsten Schmidt danke ich für die Übernahme des Zweit- bzw. Drittgutachtens.

Insbesondere Dennis Ecker, aber auch Manfred Sturm, Björn Meermann und Harald Schmid danke ich für die gute Zusammenarbeit, die Unterstützung und den Spaß im Labor.

Ich danke meinen Freunden, die mich durch ihr Zuhören und ihre ehrliche Meinung auch in schwierigen Momenten unterstützt und immer wieder aufgebaut haben.

Nicht zuletzt gilt ein besonderer Dank meinen Eltern, Margarete Fabricius-Brand und Dirk Fabricius sowie meiner Großmutter Gisela Fabricius, die nicht nur all meine Ausflüge in neue Welten unterstützt haben, sondern die durch ihr unglaubliches Vertrauen in mich und meine Fähigkeiten mir den Mut gegeben haben, mich auch unsicheren und schwierigen Aufgaben zu stellen. Durch euren Rückhalt konnte ich vieles wagen und ausprobieren mit der Sicherheit, (wenn nötig) aufgefangen zu werden.

Appendix I
Supporting Information Chapter 2:

**A New Microprofiling and Micro Sampling System
for Water Saturated Environmental Boundary
Layers**

Anne-Lena Fabricius, Lars Duester, Dennis Ecker and Thomas A. Ternes

AI.I Experimental

AI.I.I Characterization of the sediment

Element contents of the sediment were determined after microwave assisted digestion using a MLS μ Prep-A (Ethos plus, MLS, Germany). Therefore, 10 mL of HNO₃ (65%) were added to 1 g of the sediment and digested as described below (Table A1. 1). After dilution with ultrapure water to a volume of 100 mL, ICP-MS measurements were performed as described in the experimental section.

Table A1. 1: Microwave program

| Time (min) | Energy (W) | Temperature (°C) |
|------------|------------|------------------|
| 9:30 | 500 | 100.0 |
| 2:41 | 750 | 125.0 |
| 7:32 | 1,000 | 210.0 |
| 5:00 | 1,000 | 205.0 |
| 15:00 | 500 | 205.0 |

Table A1. 2: Element content and standard deviations of the sediment used for the experiments. Element concentrations were measured by ICP-MS

| Element | Manganese | Iron | Cobalt | Zinc | Antimony |
|-----------------------|---------------|---------------|---------------|---------------|---------------|
| Concentration (mg/kg) | 222.5 ± 0.033 | 5,949 ± 99.36 | 2.991 ± 0.058 | 52.08 ± 1.141 | 0.011 ± 0.001 |

To determine the total organic carbon (TOC) 150-200 mg of the freeze dried sediment were mixed with 1 ml 1M HCl and incubated for 3-4 h at room temperature. Subsequently, the pre-digested samples were heated to 55°C for ~12 h. Measurements were conducted using an Eltra Helios (Eltra GmbH, Germany). Calibration was undertaken by threefold analysis of calcium carbonate (12%, pro analysis, Merck, Germany) and graphite (100% C, Eltra, Germany) and validated measuring (for channel 1, low carbon content) 100 mg CaCO₃ (12%), 200 mg graphite (100%, covered with sea sand) and ~150 mg of certified standard reference materials (1941a and 1941b; organics in marine sediment, TC 4.8% and 3.3% respectively). Validation for samples with high carbon content (channel 2) was done by measurements of 130 mg EDTA (42.1%, pro analysi, AppliChem, Germany), and 200 mg graphite (100%, covered with sea sand). Samples and reference materials were analyzed in triplicates.

Analyses of total carbon, nitrogen and sulfur content (CNS) were conducted by means of a Vario Macro CNS analyzer (Elementar, Germany). Calibration was carried out in 5 replicates using 25 mg sulfanilamide ($\geq 99\%$, Sigma Aldrich, Germany) mixed with 30 mg tungsten(VI)oxide (WO_3 , Elementar, Germany) and verified by measurements of acetanilide (pro analysi, Merck, Germany; 25 mg mixed with 30 mg WO_3) and the reference material Leco 308 (soil set-up standard, 502-308, Leco, Germany; 90 mg mixed with 110 mg WO_3). Samples (80 mg mixed with 96 mg WO_3) were analyzed in triplicates. To test the measurement stability sulfanilamide analyzes were repeated (triplicates) at the end of the measurements. The results for CNS and total (organic) carbon content of the sediment are given in Table A1. 3.

Table A1. 3: Results of CNS and TOC analyses of the sediment used for the experiments

| TC (%) | TOC (%) | N (%) | S (%) | C/N | C/S |
|--------|---------|-------|-------|------|-------|
| 5.03 | 4.82 | 0.76 | 0.20 | 6.59 | 25.55 |

AI.I.II System characterization

Background concentrations were determined with ultrapure water and aquarium water for the two missy setups. For these experiments the backgrounds of the microwell plates used for sample collection were quantified separately to determine the laboratory background and potential influences on the samples stored in the plates during the experiments. For background analyses of the microwell plates a volume of 500 μL was pipetted into the wells and left for two days, comparable to the duration of the sampling procedure of one profile. In case of the missy setups, new sample probes as well as new tubings were used. In case of setup 1, the syringe was rinsed >24 h using HNO_3 (1.3%) followed by flushing with ultrapure water. The Rheodyne valve was disassembled and the single components were incubated for several days in HNO_3 (1.3%) followed by ultrasonication and rinsing with ultrapure water. The micro annular gear pump was rinsed by pumping HNO_3 (6.5%) and, subsequently, diluted HNO_3 (1.3%) and ultrapure water for several hours. To test if and to which extent analytes remain in the system and to identify potential drawbacks and sources of errors (due to, e.g., oxidation processes within the system or adsorption of analytes to surfaces), the background concentrations for ultrapure water were additionally analysed after the profiling experiments without previous rinsing of the system. Beside the background concentrations, the recoveries of the system were determined using an ICP-MS multi-element standard (50 $\mu\text{g/L}$), diluted either in ultrapure water or HNO_3 (1.3%).

The blank values for ultrapure water (presented in Table 2.1), determined for the two missy setups and the well plate are in good agreement for Co and Sb, but differ for Mn, Zn and Fe, especially in case of setup 2. For both systems the differences to the well plate, representing the laboratory background, can be explained by Fe or Mn oxides and adsorbed metals (like Zn) precipitated in the system during previously conducted experiments when anaerobic samples became in contact to O₂ traces. In case of the second missy setup the elevated background concentrations of Mn, Fe and Co before the experiments are probably caused by a leaching of elements from the material of the rotors of the micro annular gear pump, made of ZrO₂-ceramics.¹ Since the background concentrations for setup 2 in ultrapure water determined in previous experiments were ~0.2 for Mn and ~4 µg/L for Fe and Zn (results not shown), it can be assumed that elements mobilised by the rinsing procedure with 6.5% nitric acid were still remaining in the pump. Hence, a prolonged flushing procedure after acid rinsing is essential to remove remaining analytes, and has to be especially considered if a high accuracy at low concentrations is required. However, since the background concentrations of the aquarium water (refer to Table 2.2), obtained by application of four different sampling methods, were generally in very good agreement, an influence of the rotor material on the results of the experiments with environmental matrices are unlikely. The slight differences between the directly sampled aquarium water and the values determined for the microwell plates, sampled without filtration, are most probably due to colloids that were removed in the filtration step of the other methods. As mentioned above, the increased concentrations of Fe found for the two missy setups in comparison to the direct sampling are explainable by Fe and Mn oxides precipitated in the system. Even though the error caused by Fe or Mn oxides is low compared to the pore water concentrations, the results display that the best practice is to place the sampling system in an anaerobic chamber, if a high precision at low elemental concentrations is required or if speciation studies should be undertaken. Additionally, it underlines the relevance of rinsing steps between two profiles. Nevertheless, with regard to the concentrations determined in the profiling experiments (refer to Table A1. 10 – Table A1. 14), a bias of the results caused by elevated background concentrations can be neglected in the experiments presented.

The recoveries for the two missy setups, presented in Table A1. 4, were determined using ICP-MS element standards (50 µg/L), either diluted in ultrapure water or HNO₃ (1.3%).

Table A1. 4: Recoveries and respective relative standard deviations (RSD) of the *missys* for ultrapure water and nitric acid (1.3%), determined on the basis of ten replicates. After testing for outliers, the mean values were related to the concentrations of the element solutions used, measured by means of ICP-MS.

| Ultrapure water | Manganese | Iron | Cobalt | Zinc | Antimony |
|------------------------|------------------|-------------|---------------|-------------|-----------------|
| Syringe pump | 102% ± 2% | 116% ± 6% | 102% ± 3% | 120% ± 8% | 102% ± 6% |
| Annular gear pump | 107% ± 4% | 123% ± 10% | 104% ± 1% | 128% ± 12% | 91% ± 5% |
| Nitric acid | | | | | |
| Syringe pump | 108% ± 3% | 144% ± 9% | 103% ± 2% | 139% ± 17% | 95% ± 2% |
| Annular gear pump | 100% ± 3% | 116% ± 10% | 99% ± 2% | 116% ± 8% | 85% ± 4% |

Independent of the matrix and the setup, the recoveries for Mn and Co were in a range of 100% ± 10%. Similar to the background concentration experiments, the values found for Fe and Zn were slightly elevated, due to remaining Fe oxides in the system (see discussion above). The low recoveries of Sb found for the annular gear pump, especially in the acid matrix, can be explained by adsorption processes to the ZrO₂-ceramic surfaces of the pump rotor. This is possible because Sb is present as Sb(OH)₆⁻ anion,⁴ and in neutral to low pH solutions, ZrO₂ may act as an anion-exchanger.^{5, 6} However, since the experiments were conducted at the given pH of the aquarium water and the pore water (pH ~7.8 – 6.8; refer to Figure A3.2) of the sediment, no losses under environmental conditions have to be expected. However, the data emphasise the need to adapt the sampling system to the experimental conditions and the analytical requirements of the scientific needs (analyte and environmental system dependent).

AI.I.III Software settings

Table A1. 5: Measurement settings of the microprofiling and the micro sampling system for *missy* setup 1

| Unisense (profiling) | | | Cetoni (sampling) | | |
|--|----------|---------|-------------------------------|----------|-------|
| Unisense start | (µm) | -10,000 | Sampling velocity | (µl/min) | 5 |
| Unisense end | (µm) | 20,000 | Emptying velocity | (µl/min) | 25 |
| Length profile | (µm) | 30,000 | Sample volume | (µL) | 500 |
| Wait before measure | (sec) | 340.0 | Number of samples per profile | | 24 |
| Measure period | (sec) | 10.0 | Sampling time | (sec) | 6000 |
| Step size µm | (µm) | 63 | Emptying time | (sec) | 1200 |
| Measurement points | | 480 | Time per sample | (sec) | 7200 |
| Averaged speed of the probe/electrodes | (µm/min) | 11.4 | Time per profile | (h) | 44.00 |

AI.I.IV Porewater Samples

For each profile 24 samples were taken, each over a distance of 1.1 mm. The first two samples (marked in grey, Table A1. 6) were excluded from further analyses, to minimize the potential biases caused by a carryover from previous profiles.

Table A1. 6: Sampling distances and mean values for pore water samples. The mean values were applied to correlate the microprofiling measurements (O_2 , redox potential, pH) to the element concentrations (see Figure 2.4). Samples marked in grey are dummy/rinsing samples between two profiles not considered in the results. Negative values indicate samples above the sediment (overlying water)

| Sample | Start (cm) | End (cm) | Mean (cm) | Sample | Start (cm) | End (cm) | Mean (cm) |
|--------|------------|----------|-----------|--------|------------|----------|-----------|
| 1 | -1.30 | -1.19 | -1.24 | 13 | 0.34 | 0.45 | 0.39 |
| 2 | -1.16 | -1.05 | -1.11 | 14 | 0.47 | 0.59 | 0.53 |
| 3 | -1.03 | -0.91 | -0.97 | 15 | 0.61 | 0.72 | 0.67 |
| 4 | -0.89 | -0.78 | -0.83 | 16 | 0.75 | 0.86 | 0.80 |
| 5 | -0.75 | -0.64 | -0.70 | 17 | 0.88 | 1.00 | 0.94 |
| 6 | -0.62 | -0.50 | -0.56 | 18 | 1.02 | 1.13 | 1.08 |
| 7 | -0.48 | -0.37 | -0.43 | 19 | 1.15 | 1.27 | 1.21 |
| 8 | -0.35 | -0.23 | -0.29 | 20 | 1.29 | 1.40 | 1.35 |
| 9 | -0.21 | -0.10 | -0.15 | 21 | 1.43 | 1.54 | 1.48 |
| 10 | -0.07 | 0.04 | -0.02 | 22 | 1.56 | 1.68 | 1.62 |
| 11 | 0.06 | 0.18 | 0.12 | 23 | 1.70 | 1.81 | 1.76 |
| 12 | 0.20 | 0.31 | 0.26 | 24 | 1.84 | 1.95 | 1.89 |

AI.I.V ICP-MS analyses

Table A1. 7: Information on ICP-MS analyses including isotopes measured, measurement mode (no gas = standard, He = collision cell; He gas flow of 5.5 mL/min), limits of detection (LoD, blank + 3 sigma) and limits of quantification (LoQ, blank + 10 sigma) as well as certified and information values (given in parentheses) of the certified reference materials (CRM) used. All analyses were <10% difference from the certified values at any time of a measurement series

| | Manganese | Iron | Cobalt | Zinc | Antimony |
|---------------------------|-----------------------------|------------------|------------------|------------------|-------------------|
| Isotope | ⁵⁵ Mn | ⁵⁶ Fe | ⁵⁹ Co | ⁶⁶ Zn | ¹²¹ Sb |
| Measurement modus | He | He | He | He | no gas |
| LoD (µg/L) | 0.09 | 0.23 | 0.01 | 0.10 | 0.15 |
| LoQ (µg/L) | 0.27 | 0.41 | 0.04 | 0.21 | 0.47 |
| Reference material | Concentration (µg/L) | | | | |
| SPS-SW 1* | 10.0 ± 0.1 | 20.0 ± 1 | 2.00 ± 0.02 | (20.0) | - |
| TM 27.3 ** | 2.25 ± 0.31 | 10.9 ± 3.5 | 2.05 ± 0.17 | 16.2 ± 2.6 | 1.49 ± 0.17 |
| SLRS-5 ** | 4.33 ± 0.18 | 91.2 ± 5.8 | (0.05) | 0.845 ± 0.095 | (0.3) |

* Surface water – trace metals, LGC standards GmbH

** Certified Reference Waters for Trace Elements, Environment Canada

AI.I.VI Calculation of the dead volume and shift of the sampling depth

The dead volume of the two *missys* were calculated on the basis of the dead volumes of the single components. In case of setup 1 the tubings and the PES membrane, the Rheodyne valve and the Luer adapter were considered. The dead volume of setup 2 included those of the tubings, the PES membrane and the useable volume of the micro annular gear pump, given by the manufacturer. The volumes of the tubing as well as of the PES membrane were calculated on the basis of equation 1 (Eq. 1). In case of the Luer adapter, the volume was measured by filling the adapter with water using a 250 μL syringe (Hamilton, Switzerland, Gastight® #1725) and reading the difference from the scale. The dead volume of the valve was given by the manufacturer. Since 1 mm^3 equals $1 \mu\text{L}$, the results were not further corrected.

$$V = r^2 \cdot \pi \cdot l \quad \text{Eq.1}$$

Table A1. 8: Calculation of the dead volume of the sampling systems

| Component | Symbol | | Setup 1 | Setup 2 |
|----------------------------------|---------------------|---|-------------------|------------------|
| Inner radius tubing | r_{tube} | = | 0.13 mm | 0.13 mm |
| Length tubing | l_{tubing} | = | 2,00 mm | 1,00 mm |
| Inner radius PES membrane | r_{PES} | = | 1.59 mm | 1.59 mm |
| Length PES membrane | l_{PES} | = | 2.00 mm | 2.00 mm |
| Volume tubing | V_{tubing} | = | 98 μL | 49 μL |
| Volume PES membrane | V_{PES} | = | 16 μL | 16 μL |
| Dead volume Rheodyne valve | V_{valve} | = | 2 μL | |
| Dead volume Luer adapter | V_{Luer} | = | 5 μL | |
| Useable volume annular gear pump | V_{AGP} | = | | 17 μL |
| Dead volume sampling system | V_{dead} | = | 121 μL | 82 μL |

Table A1. 9: Calculations of the shift of the sampling depth caused by the dead volume of the *missy*

| Component | Symbol | | Setup 1 | Setup 2 |
|-----------------------------------|-------------------|---|-------------------|-------------------|
| Distance for one sample | d_s | = | 1.320 mm | 1.197 mm |
| Sample volume | V_s | = | 500 μL | 500 μL |
| Dead volume | V_{dead} | = | 121 μL | 82 μL |
| Distance shift due to dead volume | d_{dead} | = | 0.319 mm | 0.196 mm |

$$d_{\text{dead}} = \frac{d_s \cdot V_{\text{dead}}}{V_s}$$

AI.II Results and Discussion

AI.II.I Metal(loid) concentrations in pore water samples

Table A1. 10: Concentrations (>LoQ) of Mn ($\mu\text{g/L}$) in the samples of profile 1 – profile 5

| Depth (cm) | Profile 1 | Profile 2 | Profile 3 | Profile 4 | Profile 5 |
|------------|-----------|-----------|-----------|-----------|-----------|
| -1.00 | 28.25 | 344.13 | 1418.13 | 360.24 | 869.07 |
| -0.97 | 10.78 | 172.54 | 663.38 | 168.23 | 381.66 |
| -0.86 | 5.92 | 105.25 | 396.84 | 91.98 | 164.24 |
| -0.72 | 4.14 | 71.28 | 252.19 | 52.31 | 91.35 |
| -0.58 | 3.26 | 55.03 | 172.28 | 35.08 | 42.92 |
| -0.45 | 2.96 | 43.91 | 116.69 | 31.05 | 28.37 |
| -0.31 | 3.07 | 34.01 | 79.91 | 32.75 | 23.60 |
| -0.17 | 3.92 | 30.41 | 67.09 | 49.83 | 21.52 |
| -0.04 | 5.24 | 29.46 | 56.85 | 104.27 | 23.25 |
| 0.10 | 5.20 | 37.58 | 39.87 | 196.03 | 33.88 |
| 0.23 | 6.09 | 73.64 | 40.13 | 411.19 | 86.03 |
| 0.37 | 7.05 | 158.17 | 44.36 | 675.34 | 246.08 |
| 0.51 | 26.03 | 286.42 | 75.30 | 927.42 | 771.28 |
| 0.64 | 66.51 | 447.99 | 189.90 | 1221.96 | 1388.03 |
| 0.78 | 175.83 | 676.66 | 513.55 | 1661.43 | 2116.68 |
| 0.92 | 363.19 | 964.13 | 985.26 | 2276.76 | 2797.06 |
| 1.05 | 677.78 | 1312.64 | 1522.95 | 2846.95 | 3400.93 |
| 1.19 | 1199.84 | 1857.04 | 2190.76 | 3568.25 | 4040.91 |
| 1.32 | 1622.58 | 2653.39 | 2678.90 | 4493.23 | 4436.05 |
| 1.46 | 2260.23 | 4601.07 | 3172.71 | 4803.49 | 3880.06 |
| 1.60 | 2950.49 | 4238.68 | 3869.93 | 5521.94 | 5725.56 |
| 1.73 | 3458.93 | 5580.64 | 5053.45 | 5536.26 | 6196.56 |
| 1.87 | 4244.12 | 7031.30 | 5591.11 | 6948.93 | 5593.46 |

Table A1. 11: Concentrations (>LoQ) of Fe ($\mu\text{g/L}$) in the samples of profile 1 – profile 5

| Depth (cm) | Profile 1 | Profile 2 | Profile 3 | Profile 4 | Profile 5 |
|------------|-----------|-----------|-----------|-----------|-----------|
| -1.00 | 29.70 | 9.40 | 11.38 | 7.09 | 23.72 |
| -0.97 | 17.47 | 11.01 | 8.93 | 6.57 | 15.49 |
| -0.86 | 14.03 | 11.32 | 12.40 | 7.29 | 13.28 |
| -0.72 | 8.82 | 8.17 | 10.41 | 5.19 | 10.81 |
| -0.58 | 8.04 | 8.05 | 12.04 | 5.95 | 13.41 |
| -0.45 | 8.14 | 8.47 | 10.74 | 5.18 | 19.96 |
| -0.31 | 7.87 | 7.02 | 8.74 | 9.96 | 9.11 |
| -0.17 | 9.71 | 7.09 | 10.49 | 5.39 | 11.38 |
| -0.04 | 11.08 | 7.34 | 58.64 | 6.24 | 12.73 |
| 0.10 | 7.32 | 6.88 | 8.17 | 6.74 | 11.25 |
| 0.23 | 8.47 | 6.93 | 8.74 | 9.21 | 15.80 |
| 0.37 | 7.28 | 8.19 | 14.50 | 12.53 | 9.75 |
| 0.51 | 8.68 | 8.09 | 12.47 | 13.71 | 14.30 |
| 0.64 | 9.06 | 9.06 | 11.44 | 10.61 | 18.28 |
| 0.78 | 9.77 | 10.44 | 11.80 | 20.27 | 30.52 |
| 0.92 | 10.24 | 26.37 | 12.98 | 90.15 | 70.57 |
| 1.05 | 12.26 | 15.29 | 14.75 | 250.81 | 134.84 |
| 1.19 | 22.79 | 23.75 | 20.68 | 517.84 | 221.50 |
| 1.32 | 32.06 | 43.41 | 27.53 | 772.47 | 370.89 |
| 1.46 | 47.55 | 97.56 | 49.42 | 976.45 | 406.48 |
| 1.60 | 72.85 | 103.78 | 66.49 | 1149.89 | 870.32 |
| 1.73 | 93.18 | 228.82 | 87.56 | 1281.64 | 1009.42 |
| 1.87 | 142.60 | 187.47 | 115.04 | 1707.33 | 1043.60 |

Table A1. 12: Concentrations (>LoQ) of Co ($\mu\text{g/L}$) in the samples of profile 1 – profile 5

| Depth (cm) | Profile 1 | Profile 2 | Profile 3 | Profile 4 | Profile 5 |
|-------------------|------------------|------------------|------------------|------------------|------------------|
| -1.00 | 0.47 | 1.02 | 2.85 | 0.93 | 3.30 |
| -0.97 | 0.28 | 0.55 | 1.72 | 0.57 | 1.87 |
| -0.86 | 0.23 | 0.52 | 1.27 | 0.40 | 1.15 |
| -0.72 | 0.25 | 0.37 | 0.93 | 0.35 | 0.89 |
| -0.58 | 0.25 | 0.35 | 0.68 | 0.30 | 0.61 |
| -0.45 | 0.23 | 0.31 | 0.58 | 0.25 | 0.48 |
| -0.31 | 0.22 | 0.28 | 0.56 | 0.27 | 0.47 |
| -0.17 | 0.23 | 0.28 | 0.49 | 0.26 | 0.40 |
| -0.04 | 0.22 | 0.29 | 0.48 | 0.29 | 0.40 |
| 0.10 | 0.25 | 0.27 | 0.36 | 0.31 | 0.39 |
| 0.23 | 0.26 | 0.31 | 0.36 | 0.41 | 0.39 |
| 0.37 | 0.23 | 0.31 | 0.34 | 0.76 | 0.52 |
| 0.51 | 0.25 | 0.33 | 0.40 | 1.28 | 0.96 |
| 0.64 | 0.25 | 0.46 | 0.42 | 2.04 | 1.95 |
| 0.78 | 0.35 | 0.72 | 0.59 | 3.63 | 3.63 |
| 0.92 | 0.49 | 1.21 | 0.85 | 6.70 | 5.66 |
| 1.05 | 0.88 | 1.97 | 1.36 | 10.05 | 7.79 |
| 1.19 | 1.92 | 3.53 | 2.29 | 14.51 | 9.65 |
| 1.32 | 3.27 | 5.60 | 3.51 | 17.97 | 11.46 |
| 1.46 | 4.74 | 10.61 | 4.83 | 17.64 | 10.21 |
| 1.60 | 6.27 | 9.83 | 7.20 | 18.42 | 15.82 |
| 1.73 | 7.80 | 12.24 | 9.78 | 17.38 | 17.36 |
| 1.87 | 9.36 | 15.81 | 11.54 | 21.08 | 16.49 |

Table A1. 13: Concentrations (>LoQ) of Zn ($\mu\text{g/L}$) in the samples of profile 1 – profile 5

| Depth (cm) | Profile 1 | Profile 2 | Profile 3 | Profile 4 | Profile 5 |
|------------|-----------|-----------|-----------|-----------|-----------|
| -1.00 | 14.44 | 28.31 | 49.93 | 34.51 | 34.01 |
| -0.97 | 14.10 | 23.55 | 37.23 | 26.67 | 47.75 |
| -0.86 | 12.54 | 24.23 | 49.40 | 23.11 | 23.60 |
| -0.72 | 14.06 | 20.05 | 31.67 | 21.38 | 19.04 |
| -0.58 | 9.68 | 21.80 | 32.78 | 19.53 | 22.38 |
| -0.45 | 9.54 | 15.97 | 38.13 | 20.04 | 18.22 |
| -0.31 | 8.43 | 16.62 | 21.58 | 20.00 | 14.52 |
| -0.17 | 17.82 | 16.67 | 33.75 | 24.52 | 14.68 |
| -0.04 | 13.41 | 15.86 | 24.42 | 35.41 | 24.24 |
| 0.10 | 9.76 | 21.30 | 21.07 | 48.92 | 18.25 |
| 0.23 | 14.43 | 20.48 | 27.95 | 66.10 | 22.53 |
| 0.37 | 7.18 | 28.41 | 24.21 | 117.18 | 18.43 |
| 0.51 | 15.54 | 42.73 | 29.21 | 103.65 | 40.39 |
| 0.64 | 14.35 | 60.67 | 34.10 | 105.63 | 60.88 |
| 0.78 | 32.35 | 86.51 | 53.53 | 116.66 | 93.29 |
| 0.92 | 37.82 | 111.80 | 53.21 | 124.67 | 104.17 |
| 1.05 | 70.79 | 129.14 | 71.59 | 122.64 | 116.43 |
| 1.19 | 195.91 | 144.51 | 85.03 | 125.60 | 122.14 |
| 1.32 | 109.34 | 160.12 | 97.74 | 130.28 | 127.93 |
| 1.46 | 131.71 | 218.70 | 102.59 | 120.27 | 112.35 |
| 1.60 | 145.42 | 196.54 | 142.09 | 118.63 | 152.00 |
| 1.73 | 186.37 | 206.51 | 146.59 | 122.25 | 161.90 |
| 1.87 | 179.07 | 245.71 | 216.36 | 144.45 | 150.23 |

Table A1. 14: Concentrations (>LoQ) of Sb ($\mu\text{g/L}$) in the samples of profile 1 – profile 5

| Depth (cm) | Profile 1 | Profile 2 | Profile 3 | Profile 4 | Profile 5 |
|------------|-----------|-----------|-----------|-----------|-----------|
| -1.00 | 4.96 | 5.29 | 5.54 | 5.20 | 5.73 |
| -0.97 | 5.00 | 5.25 | 4.90 | 5.30 | 5.82 |
| -0.86 | 4.95 | 5.36 | 5.34 | 5.19 | 5.66 |
| -0.72 | 4.81 | 5.20 | 5.04 | 5.32 | 5.59 |
| -0.58 | 4.88 | 5.52 | 4.99 | 5.16 | 5.24 |
| -0.45 | 4.96 | 5.44 | 5.02 | 5.29 | 5.37 |
| -0.31 | 4.91 | 5.30 | 5.41 | 5.49 | 5.67 |
| -0.17 | 5.18 | 5.41 | 4.95 | 5.17 | 6.84 |
| -0.04 | 4.98 | 5.26 | 5.01 | 5.38 | 5.59 |
| 0.10 | 4.89 | 5.29 | 4.89 | 5.06 | 5.84 |
| 0.23 | 4.96 | 5.10 | 5.05 | 4.94 | 5.46 |
| 0.37 | 5.20 | 5.11 | 4.60 | 4.84 | 5.44 |
| 0.51 | 5.12 | 5.02 | 4.73 | 4.75 | 5.39 |
| 0.64 | 4.94 | 5.02 | 4.38 | 4.68 | 4.66 |
| 0.78 | 5.08 | 4.99 | 4.41 | 4.63 | 4.47 |
| 0.92 | 5.13 | 5.01 | 4.34 | 4.35 | 3.75 |
| 1.05 | 4.71 | 4.82 | 4.13 | 3.88 | 3.11 |
| 1.19 | 4.43 | 4.61 | 3.78 | 3.40 | 2.55 |
| 1.32 | 3.16 | 3.83 | 0.00 | 2.98 | 0.00 |
| 1.46 | 3.23 | 0.00 | 0.00 | 0.00 | 0.00 |
| 1.60 | 2.98 | 0.00 | 0.00 | 0.00 | 0.00 |
| 1.73 | 0.00 | 0.00 | 0.00 | 0.00 | 0.00 |
| 1.87 | 0.00 | 0.00 | 0.00 | 0.00 | 0.00 |

A1.II.II Single profiles of oxygen, redox potential and pH value

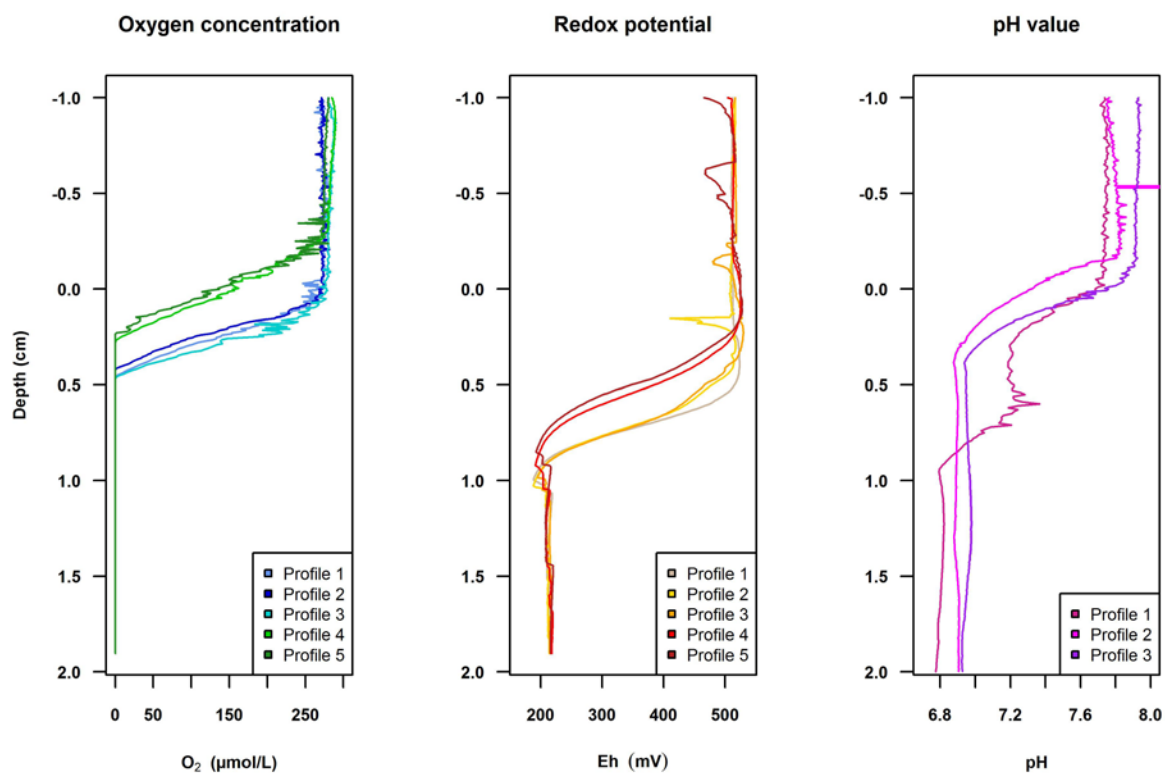


Figure A1. 1: Profiles of oxygen concentration, redox potential and pH value displayed as single profile plots (2D plots are presented in Figure 2.3). O₂ and redox potentials were measured in parallel; measurements of pH values were conducted subsequently. The sediment surface (0 cm) refers to the first profile and was kept static since the measurement settings (absolute sampling depth) were not changed. The differences of the profiles indicate the micro relief at the sediment surface also visible in the 2D-plots presented in the manuscript (refer to Figure 2.3).

A1.II.III Result of the micro annular gear pump

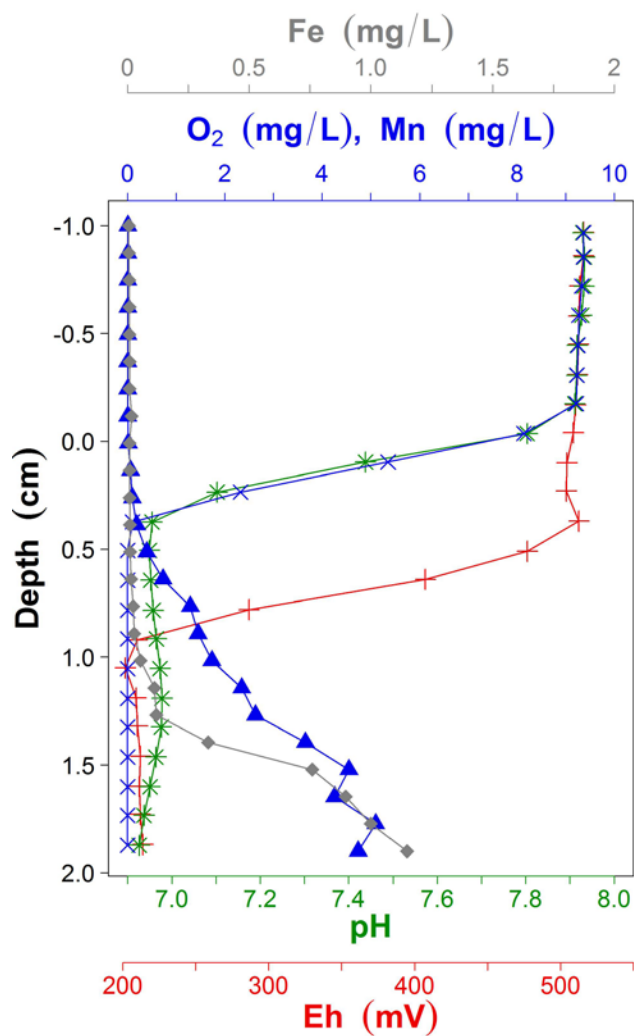


Figure A1. 2: Exemplary depth profile of Mn (▲) and Fe (◆) in pore water samples obtained by application of the micro annular gear pump related to profiles of O₂ (×), redox potential (+) and pH value (*) measured (for the latter refer to Figure 2.4). Sampling and measurements were performed as described in the manuscript.

AI.II.IV Carryover

To quantify the carryover of elements from one profile to the next, seven samples of the overlaying water were taken without a previous rinsing of the tubing and membrane. Samples were measured by means of ICP-MS as described in the experimental section.

Table A1. 15: Quantification of carryover from a previous experiment ($\mu\text{g/L}$).

| Sample | Mn | Fe | Co | Zn | Sb |
|-----------------------------------|-----------|-----------|-----------|-----------|-----------|
| Last sample from previous profile | 4879 | 647.0 | 12.96 | 142.0 | 2.08 |
| 1 | 1377 | 59.04 | 3.799 | 63.55 | 5.872 |
| 2 | 475.5 | 15.30 | 1.840 | 34.18 | 6.339 |
| 3 | 197.5 | 11.64 | 1.077 | 22.00 | 6.414 |
| 4 | 95.97 | 9.750 | 0.721 | 19.62 | 6.469 |
| 5 | 51.72 | 8.410 | 0.506 | 14.06 | 6.508 |
| 6 | 32.35 | 8.386 | 0.394 | 14.38 | 6.537 |
| 7 | 22.83 | 9.766 | 0.349 | 19.36 | 6.513 |

A significant carry over effect for Mn, Fe, Co and Zn is visible. Since the Sb concentration in the sediment pore water is lower than in the overlaying water a wash up for Sb was not detected.

AI.III References

1. Krivan, V.; Janickova, P., A direct solid sampling electrothermal atomic absorption spectrometric method for determination of trace elements in zirconium dioxide. *Analytical and Bioanalytical Chemistry* 2005, 382, (8), 1949-1957.
2. Bufflap, S. E.; Allen, H. E., Sediment pore-water collection methods for trace-metal analysis - a review. *Water Research* 1995, 29, (1), 165-177.
3. Mudroch, A. A., Jose M. , Manual of Aquatic Sediment Sampling. CRC Press, Inc. : 1995.
4. Filella, M.; Belzile, N.; Chen, Y. W., Antimony in the environment: a review focused on natural waters II. Relevant solution chemistry. *Earth-Science Reviews* 2002, 59, (1-4), 265-285.
5. S. Muhammad, S. T. H., M. Waseem, A. Naeem, J. Hussain and M. Tariq Jan, Surface charge properties of zirconium dioxide. *Iranian Journal of Science and Technology* 2013, 4, 481-486.
6. Nancolla.Gh; Paterson, R., Thermodynamics of ion exchange on hydrous zirconia. *Journal of Inorganic & Nuclear Chemistry* 1967, 29, (2), 565-&.

**Appendix II:
Supporting Information Chapter 3:**

**ICP-MS based characterization of inorganic
nanoparticles – Sample preparation and off-line
fractionation strategies**

Anne-Lena Fabricius, Lars Duester, Björn Meermann, and Thomas Ternes

AII.I Experimental

AII.I.I ENP suspensions

Table A2. 1: Information about the nanoparticle suspensions used given by the manufacturer.

| | AgPURE-W | TiO₂ | CeO₂ | Au 10 nm | Au 200 nm | ZnO |
|----------------------------|-----------------------------|------------------------|------------------------------------|---|-------------------------------|----------------------------------|
| | ras materials GmbH, Germany | Laboratory synthesized | NYACOL; Nanotechnologies, Inc, USA | Sigma-Aldrich, Germany | | Particular GmbH, Germany |
| Concentration | 10.0 ± 0.50 % | 5.9 g/L | 20 wt.% | 5.9 · 10 ¹² part/mL | 1.9 · 10 ⁹ part/mL | 100 mg/L |
| Additives | Ammonium nitrate (3-15%) | None | Nitrate (0.2 mol/mol) | Sodium citrate buffer (100 mg/L) + proprietary stabilizing surfactant | | Sodium citrate buffer (100 mg/L) |
| Core size; (diameter) [nm] | 15 (99% < 20) | 100 | 10-20 | 8-12 | 180-220 | - |
| Hydrodynamic diameter [nm] | - | - | - | 18-30 | 175-235 | 136.1 ± 4.2 |

All.I.II Microwave assisted digestion

Table A2. 2: Details about microwave assisted digestion procedures.

| | Silver | Titanium dioxide | Cerium dioxide | Zinc oxide | Gold |
|--------------------------------------|--------------------------------|---------------------------------|-------------------------------|------------------------------|-------------------------------|
| HNO ₃ (65%) | 1.4 mL | - | 1.2 mL | 0.35 mL | 0.35 mL |
| H ₂ SO ₄ (96%) | - | 1.4 mL | - | - | - |
| HCl (30%) | - | - | - | 1.05 mL | 1.05 mL |
| H ₂ O ₂ (30%) | - | - | 0.2 mL | - | - |
| Vessel material | Teflon | Teflon | Teflon | Teflon | Glass |
| Internal Standard | | | Ru (1 mg/l) 0.1 mL | | |
| Sample | | | 0.5 mL | | |
| Dilution | 1:100.000 | 1:1.000 | 1:100.000 | 1:100 | 1:100 |
| Assumed concentration | ~1 mg/L | ~5.9 mg/L | ~2 mg/L | ~1 mg/L | 99.4 µg/L* 253 µg/L* |
| pH value | 5.8 | 5.8 | 4.5 | 5.9 | 6.2 6.3 |
| Reference material | TMDA52.3**: 20.6 ± 1.8 µg/L | TMDA52.3**: 120.0 ± 7.6 µg/L | SPS-SW2*** 2.5 ± 0.02 µg/L | TMDA**: 263.0 ± 25.3 µg/L | Noble metals****: 100 µg/L |
| ICP-element std | Ag (1 mg/L) | Ti (1 mg/L) | Ce (1 mg/L) | Zn (1 mg/L) | Au (1 mg/L) |

* Conversion from concentrations given in particles/mL (information of the customer) to the concentration of Au in µg/L were conducted in accordance to.¹

** Certified Reference Waters for Trace Elements, Environment Canada.

*** Surface water – trace metals, Spectrapure Standards, Norway.

**** VHG certified NIST-traceable multi-element aqueous standard, VHG Labs, Inc (LGC standards), USA.

In case of Ag, TiO₂ and CeO₂ ENP suspensions the digestion procedure was carried out in Teflon vessels. For the Au ENP suspensions glass vials were used to avoid possible interaction with the Teflon surfaces. In case of ZnO, after testing both materials, also Teflon vials were chosen due to lower blank values and better recoveries. For ICP-MS measurements digested samples were transferred to polypropylene centrifuge tubes (VWR, Germany) or, in case of Au, to Rotilabo®-screw neck ND24 glass vials (Carl Roth, Germany).

AII.I.IIIICP-QMS analyses

Table A2. 3: Parameters of ICP-QMS analysis. Isotopes of the elements analyzed and the respective limits of detection (LoD; blank + 3 sigma) and limits of quantification (LoQ; blank + 10 sigma) for acidic and aqueous matrices analyzed. Collision cell modus, [He], was conducted at a helium gas flow of 3 ml/min. Certified concentrations of the reference materials (CRM) used for method validation are given for each element.

| Isotope | Silver [$\mu\text{g/L}$] | | Titanium [$\mu\text{g/L}$] | | Cerium [$\mu\text{g/L}$] | | Zinc [$\mu\text{g/L}$] | | Gold [$\mu\text{g/L}$] | |
|---------------|----------------------------|-------|---|-------|----------------------------|-------|--|-------|--------------------------|-------|
| | ^{107}Ag | | ^{47}Ti [He] | | ^{140}Ce | | ^{66}Zn [He] | | ^{197}Au | |
| Matrix | acid | Water | acid | water | acid | water | acid | water | acid | water |
| LoD | 0.26 | 0.21 | 0.71 | 0.18 | 0.21 | 0.21 | 1.0 | 0.1 | 0.35 | - |
| LoQ | 0.67 | 0.61 | 1.73 | 0.49 | 0.64 | 0.64 | 2.29 | 0.18 | 0.93 | - |
| CRM | TMDA 52.3 | | TMDA 52.3 | | SPS-SW2 | | TMDA 52.3 | | Noble metals | |
| | | | TM 27.3**: 2.01 \pm 0.26 $\mu\text{g/L}$ | | | | TM 27.3**: 16.2 \pm 2.6 $\mu\text{g/L}$ | | | |

** Certified Reference Waters for Trace Elements, Environment Canada (see ESM_2).

AII.II Results and Discussion

AII.II.I TEM-images of nanoparticle suspensions

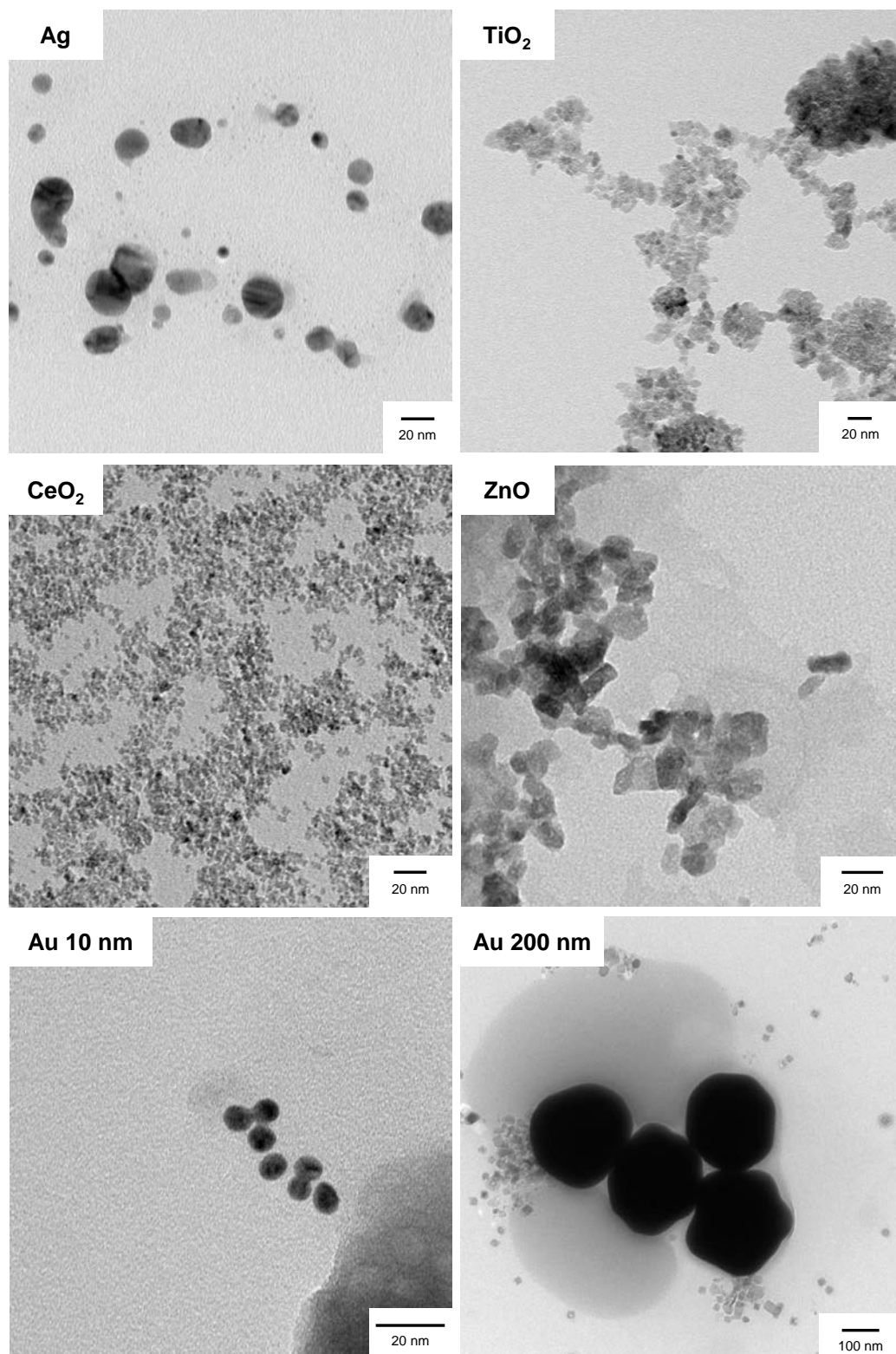


Figure A2. 1: TEM-images of the nanoparticle suspensions analyzed. Measurements and estimation of the particle size distribution were carried out as described in the manuscript.

All.II.II Centrifugation: calculation of the run time

The time needed for sedimentation of the silver nanoparticles was calculated in accordance to Griffith 2010¹ and the information given in the user manual of the rotor (TH-641, Thermo Scientific, Germany). The sedimentation time was estimated as follows:

The time (T) required for sedimentation of a particle to the bottom of the tube is defined by the ratio of the clearing factor of the rotor (K) and the sedimentation coefficient (S) of the particles (Eq.1):

$$T = \frac{K}{S} \quad \text{Eq.1}$$

The K-Factor describes the relative pelleting efficiency (sedimentation of particles to the bottom of the tube) of the rotor and can be calculated as followed (Eq.2):

$$K = (253000) \left[\ln \left(\frac{r_{\max}}{r_{\min}} \right) \right] \div \left(\frac{\text{rotor speed}}{1000} \right)^2 \quad \text{Eq.2}$$

The rotor speed was set to 41,000 rpm, the maximum and minimum distance between particle and the center of rotation (r_{\max} and r_{\min}) are determined by the rotor (TH-641, Thermo Scientific, Germany) and the length of the tubes:

$$r_{\max} = 7.19 \text{ cm}$$

$$r_{\min} = 15.32 \text{ cm}$$

The sedimentation coefficient was calculated in accordance to the following equations:

$$S = \frac{v}{\omega^2 \cdot r} \quad \text{Eq.3}$$

$$v = \text{sedimentation velocity of the particle [cm/s]}$$

$$\omega = \text{rotor speed in [rad/s]}$$

$$\omega = \frac{2rpm}{60}; rpm = 41000 \quad rpm = 41000$$

$$v = \frac{d^2(\rho_p - \rho_L)}{18 \cdot \mu} \cdot g \quad \text{Eq.4}$$

$$d = \text{diameter of the particle [cm/s]}$$

ρ_p = density of the particle

ρ_L = density of the liquid = 1 g/cm³

μ = viscosity of the liquid medium = 1.52 \times 10⁻³ Pa s

g = gravitational force; = 13.43 \times 10⁶ m/s²

$$g = \omega^2 \cdot r$$

The time required for the sedimentation of a 50 nm Ag particle in a tube of approximately 8 cm was ~1.52 days (36.5 hours, 41,000 rpm). Since particle size distribution of the Ag ENP suspension showed a certain polydispersity (refer to results and discussion). Hence, the centrifugation time was prolonged to 48 hours to ensure the sedimentation of smaller particles. Moreover, only the upper ~1 cm from the surface of the liquid within the centrifugation tube was sampled.

AII.II.III Time dependent dissolution during dialysis

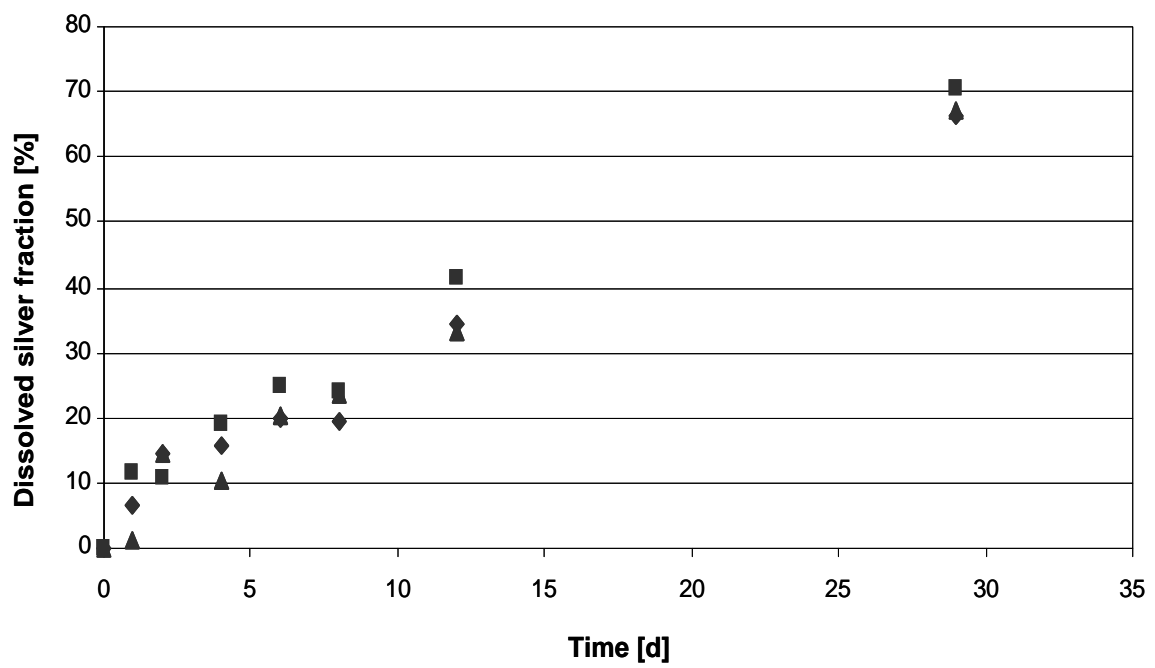


Figure A2. 2: Dissolution of Ag^+ from Ag ENP suspension of three samples (diamond, square and triangle) over a period of 29 days.

All.II.IV Calibration and results of the standard addition in ion selective electrode measurements

Calibration of the silver ion selective electrode (ISE) was conducted within a concentration range of 0.1 mg/L to 100 mg/L. The values measured as well as calibration curve are presented.

Table A2. 4: Concentrations and measured voltages of the calibration of the ISE.

| Concentration | log (Concentration) | Voltage [mV] |
|---------------|---------------------|--------------|
| Ag [mg/l] | log(Ag) | U [mV] |
| 0.1 | -1.00 | 261 |
| 0.2 | -0.70 | 266 |
| 0.5 | -0.30 | 278 |
| 1 | 0.00 | 301 |
| 2 | 0.30 | 317 |
| 5 | 0.70 | 341 |
| 10 | 1.00 | 359 |
| 20 | 1.30 | 376 |
| 50 | 1.70 | 398 |
| 100 | 2.00 | 413 |

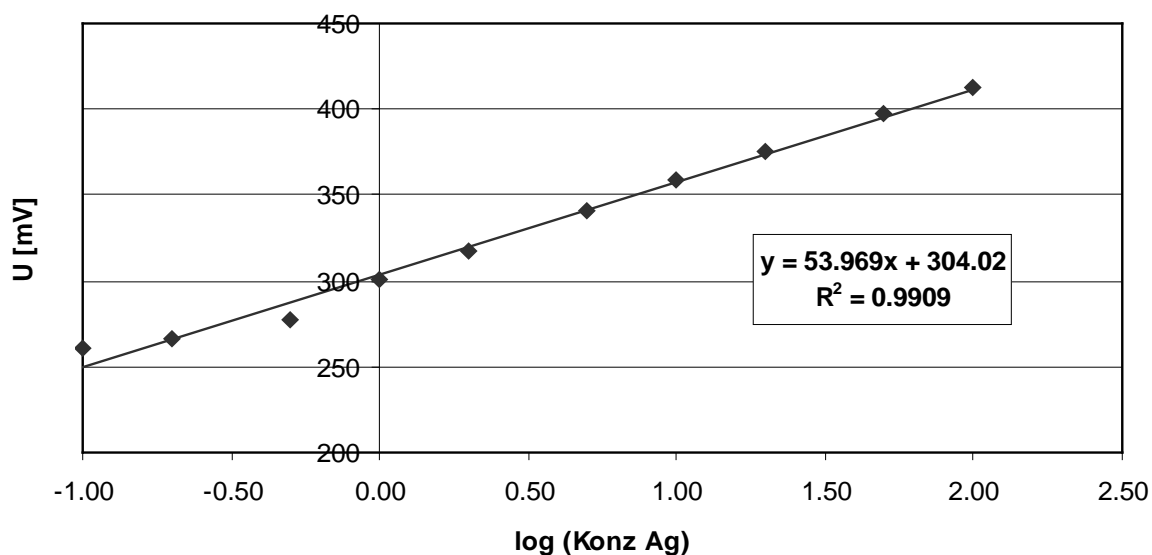


Figure A2. 3: Calibration curve of the silver ISE.

Prior to further measurements, the response of the electrode was tested by a standard addition procedure. A Ag ENP working suspension (WS 1:10,000 dilution of the stock suspension) was spiked with an ICP-element standard solution of different concentrations (see below). The concentration of

dissolved silver determined by ISE was calculated on the basis of the equation of the calibration curve. After blank correction, the recoveries were calculated on the basis of the concentrations of the Ag element standard added.

Table A2. 5: Results of a standard addition conducted to test the response of the ISE. Defined silver concentrations were added to an ENP working suspension (WS). The concentrations of ionic silver as well as the recoveries were calculated on the basis of the calibration equation determined (see above).

| | Voltage | Concentration | Blank correction | Recovery |
|------------------------|----------------|------------------------|-------------------------|-----------------|
| | U [mV] | Ag ⁺ [mg/L] | Ag ⁺ [mg/L] | [%] |
| WS + 0 mg/L Ag (blank) | 272 | 0.26 | | |
| WS + 1 mg/L Ag | 309 | 1.24 | 0.98 | 98.16% |
| WS + 2 mg/L Ag | 321 | 2.06 | 1.81 | 90.43% |
| WS + 5 mg/L Ag | 342 | 5.06 | 4.80 | 96.00% |
| WS + 10 mg/L Ag | 359 | 10.44 | 10.19 | 101.86% |
| WS + 20 mg/L Ag | 375 | 20.66 | 20.41 | 102.04% |
| WS + 50 mg/L Ag | 396 | 50.62 | 50.36 | 100.73% |

AII.III References

1. Lewis, D.J., et al., Luminescent nanobeads: attachment of surface reactive Eu(III) complexes to gold nanoparticles. *Chemical Communications*, 2006(13): p. 1433-1435.
2. Griffith, O.M., *Practical Techniques for Centrifugal Separations*. Thermo Fisher Scientific; Application guide, 2010.

Appendix III

Nanotechnology and Water Legislation

Published in German:

Nanotechnologie und Wasserrecht

Anne-Lena Fabricius & Tade Spanger

I+E - Zeitschrift für Immissionsschutzrecht und Emissionshandel, 2013, 3, pp 114-119

AIII.I Summary

Together with the increasing availability of numerous nanomaterials and the variety of different applications not only the need of analytical methods and techniques to characterize and detect nanomaterials in different matrices came into the focus of the public and political discussions, but also aspects concerning legislation and regulation. As a consequence, not only the safety of workers and consumers became important, but also aspects concerning the release into the environment, especially via the wastewater systems into surface waters. In this context, the question if the available, both analytical and regulatory standards originally developed for other substances are equally applicable to nanomaterials, became one of the main questions.

The article “Nanotechnology and Water Legislation” aims to outline the current situation and discussions with regard to both, the scientific as well as the regulatory issues. It describes on the one hand the current status of scientific research including the analytical challenges and uncertainties related to the detection and characterization of ENMs in complex, environmental matrices. On the other hand, the regulatory aspects are discussed with the main focus on the water legislation in Germany.

Even though the number and quality of analytical methods available to identify and characterize nanomaterials improved considerably during the last years, the methods are still far from implementation as validated routine-suitable protocols. The development of such standardized procedures is challenging due to the huge variety of different materials and the (potential) changes of their characteristics in dependence of the surrounding matrix. Moreover, only few certified reference nano materials are available, which are required for the validation of analytical methods. With regard to regulation, a methodological basis is compulsory that provides protocols also applicable by laboratories not specialized in nano analytics (e.g., administrative services or contract laboratories).

Concerning the regulatory aspects, the current German regulatory framework (namely the Water Resources Act; WHG) and the related legal acts can in general be considered as suitable for nanomaterials with regard to a potential discharge in ground and surface waters and potential water-endangering impacts: In case of adverse effects on the water quality caused by a substance, regardless if a nanomaterial or not, a discharge of the respective compound can be forbidden or restricted. Comparably, the installation and operation of a plant dealing with water-endangering substances can only be approved if the water quality is not negatively affected. However, both cases require the ascertainment of the harmfulness of the material which, in turn, necessitates the availability of suitable analytical methods to characterize the materials and investigate their

(potential) impacts. Even though on the European level a specific regulation of nanomaterials is advised under REACH, the problem of a missing or insufficient analytical basis remains.

In conclusion, the implementation of a nanospecific law is not necessary, because the current regulatory frameworks, on the national as well as on the international level, can equally be applied to nanomaterials. However, the assessment of the (eco)toxicological effects and potential risks for the environment or humans and the detection and characterization of nanomaterials in the environment are preconditions for the implementation of any legal regulation which in turn necessitate the availability of appropriate analytical methods. Besides, the interdisciplinary cooperation of experts of different scientific areas, representatives of political and public as well as industrial stakeholders is indispensable for the adaptation and implementation of regulations.

AIII.II Nanotechnologie und Wasserrecht (Deutsche Originalversion)

AIII.II.I Begriffliche Klärung

Die verschiedenen (Teil-)Disziplinen der Nanotechnologie befassen sich mit der Analyse und Bearbeitung von Materialien im Bereich von ein bis einhundert Nanometer; ein Nanometer (nm) entspricht dabei einem millionstel Millimeter. Dabei ist die Relation eines Nanopartikels zu einem Fußball in etwa der eines Fußballs zur Erde. Es ist bekannt, dass die mechanischen, optischen, magnetischen, elektrischen und chemischen Eigenschaften eines Materials sich im Nanobereich deutlich von denen makroskaliger Bestandteile unterscheiden können. Die große spezifische Oberfläche von Nanostrukturen und die hierdurch bedingte höhere Reaktivität ist dabei eine Schlüsseleigenschaft. Aufgrund dieser Eigenschaften finden Nanomaterialien bereits in einer Vielzahl von Produkten Anwendung: Nano-Silber wird aufgrund seiner antibakteriellen Wirkung in Kleidung sowie Wandfarben verarbeitet, Titan-, Cer- und Zink-Oxide werden als transparenter UV-Schutz in Sonnencremes verwendet, nanoskaliges Siliziumdioxid kommt in Solarzellen zum Einsatz und Kohlenstoffröhren verleihen Carbon-Fasern eine hohe Zugfestigkeit. Dabei kann sich die Funktionalität der eingesetzten Nanomaterialien sowohl durch deren geringe Größe als auch durch neu entstandene (optische, magnetische, elektrische, chemische) Eigenschaften des Stoffes ergeben: So wird beispielsweise Nano-Titandioxid (TiO_2) zur Beschichtung von Glasoberflächen eingesetzt, um ein Verschmutzen der Scheibe zu verhindern, wobei man sich zwei verschiedene Eigenschaften zunutze macht: eine besonders kleinskalige Oberflächenstruktur bewirkt, dass Wasser und Schmutz von der Scheibe abperlen (der sogenannte Lotus-Effekt), eine photokatalytische Wirkung des TiO_2 kann zudem zum Abbau organischer Verunreinigungen beitragen. Letzteres erfordert die katalytischen Eigenschaften des TiO_2 , wohingegen der physikalische Lotus-Effekt auch durch andere nanoskalige Materialien (wie z. B. Siliziumdioxid oder Polymere) erzielt werden kann.

In jüngster Zeit finden sich verschiedene Ansätze, den Begriff der Nanomaterialien spezifischer zu fassen. So definiert etwa die Internationale Organisation für Normung (International Organization for Standardization ISO) den Begriff „Nanomaterial“ als Material mit Außenmaßen im Nanobereich oder einer inneren Struktur oder Oberflächenstruktur im Nanobereich. Der Begriff „Nanobereich“ wird dabei definiert als Größenbereich zwischen etwa einem nm und 100 nm. Ferner hat die Europäische Kommission eine Empfehlung vorgelegt, die den Begriff des Nanomaterials wie folgt definiert: „Nanomaterial ist ein natürliches, bei Prozessen anfallendes oder hergestelltes Material, das Partikel in ungebundenem Zustand, als Aggregat oder als Agglomerat enthält, und bei dem mindestens 50 % der Partikel in der Anzahlgrößenverteilung ein oder mehrere Außenmaße im Bereich von ein nm bis 100 nm haben. In besonderen Fällen kann der Schwellenwert von 50 % für die Anzahlgrößenverteilung durch einen Schwellenwert zwischen ein und 50 % ersetzt werden, wenn

Umwelt-, Gesundheits-, Sicherheits- oder Wettbewerbserwägungen dies rechtfertigen. Abweichend von Nummer 2 sind Fullerene, Graphenflocken und einwandige Kohlenstoff-Nanoröhren mit einem oder mehreren Außenmaßen unter einem nm als Nanomaterialien zu betrachten.“¹ Die Begriffe Partikel, Agglomerat und Aggregat werden sodann für die Zwecke dieser Empfehlung weiter konkretisiert.

Diese wie andere Definitionsversuche sehen sich unterschiedlichster Kritik ausgesetzt, verdeutlichen aber ungeachtet dessen den erheblichen Harmonisierungsbedarf im regulatorischen Umgang mit Nanomaterialien ebenso wie die Unschärfen, die sich aus einer bisweilen noch unzureichenden wissenschaftlichen und technischen Basis ergeben. Im Rahmen des vorliegenden Beitrags sollen unter Nanomaterialien alle Materialien im Sinne des ISO-Vorschlags gefasst werden.

Im Bereich der Wasserwirtschaft etabliert sich die Nanotechnologie zunehmend als Schlüsseltechnologie, da sie von der Trinkwasseraufbereitung über die Abwasserreinigung bis hin zur Grundwassersanierung zum Einsatz kommen kann.

Allerdings können Nanomaterialien ihrerseits eine Herausforderung für die Wasserwirtschaft sowie den Gewässerschutz darstellen, weil davon ausgegangen werden muss, dass sie bereits heute über Abwassersysteme und verschiedene diffuse Quellen in die Umwelt gelangen. Potenzielle Punktquellen sind kommunale und industrielle Kläranlagen. Diffuse Quellen können Mischwasserentlastungssysteme (Regenüberläufe und Notüberläufe) sein (z. B. Fassadenfarben). Mögliche Folgen sind derzeit jedoch kaum abschätzbar. Um eine sichere Nutzung der Nanotechnologie zu ermöglichen, bedarf es nicht nur weiterer Forschung, sondern ebenso einer kritischen Risikoabschätzung sowie der Entwicklung differenzierter Regelwerke und Instrumente (wie standardisierte analytische Verfahren), um deren Vollzug gewährleisten zu können. An dieser Stelle soll zunächst eine Darstellung der aktuellen wissenschaftlichen Grundlage erfolgen, wobei ein Schwerpunkt auf die Gewässerkunde gelegt wird. Vor diesem Hintergrund soll sodann die Frage gestellt werden, inwieweit die möglicherweise resultierenden Gefahren durch das aktuelle Rechtsregime berücksichtigt werden bzw. welche Rechtslücken sich identifizieren lassen.

AIII.II.II Stand der (umwelt)wissenschaftlichen Forschung

Wie bereits angesprochen, werden Nanotechnologie-basierte Produkte schon heute in vielen sehr unterschiedlichen Bereichen eingesetzt. Am häufigsten werden Silber, Titandioxid und Kohlenstoff-basierte Materialien (wie Fullerene oder Nanotubes) genutzt, aber auch Cer-, Zink- oder Silizium-Oxide sowie Gold finden zunehmend Verwendung.² Da Nanomaterialien bereits in zahlreichen Produkten des alltäglichen Lebens (wie Kleidung, Personal Care Produkten oder

Gegenständen des alltäglichen Lebens) zu finden sind, steigt die Wahrscheinlichkeit, dass diese über die Abwassersysteme auch in die Umwelt gelangen. Potenzielle Punktquellen sind kommunale und industrielle Klär- anlagen³ sowie Mischwasserentlastungssysteme (Regenüberläufe und Notüberläufe) und verschiedene diffuse Quellen wie z. B. Fassadenfarben⁴. Unabhängig davon, wofür, in welchen Formen oder Produkten Nanomaterialien eingesetzt werden, kann derzeit kaum abgeschätzt werden, in welchen Mengen sie in die Umwelt gelangen und welches Risiko sie für Mensch und Umwelt darstellen, da verlässliche Produktions- und Applikationszahlen aus der Industrie in den USA und Europa (sowie für den Rest der Welt) kaum verfügbar sind.⁵

Da es sich bei Nanomaterialien um eine große Anzahl verschiedenster Stoffe mit zum Teil völlig neuen Eigenschaften handelt, stellt schon deren Charakterisierung in Reinstform und unter Laborbedingungen eine methodische Herausforderung dar. Zum einen, weil es zumeist eines multidisziplinären Ansatzes bedarf, um Eigenschaften wie Partikelgrößenverteilung, Oberflächenbeschaffenheit, Form, Agglomerationsstatus oder Gesamtgehalte in verlässlichem Maße beschreiben zu können. Zum anderen, weil viele der etablierten Methoden im analytisch chemischen oder auch toxikologischen Bereich nicht oder nur nach Anpassung für Nanomaterialien und deren Suspensionen genutzt werden können. Hinzu kommt, dass viele Techniken (wie Lichtstreuendetektoren, Feldfluss-Fraktionierung oder Systeme zur Bestimmung der Oberflächenladung) erst seit kurzem verfügbar sind und derzeit lediglich von einem kleinen Anwenderkreis mit entsprechendem Know-how genutzt werden können. Neben dem Mangel an standardisierten Methoden sind nur sehr wenige zertifizierte Nano-Referenzmaterialien verfügbar, die für die Entwicklung verlässlicher und validierter analytischer Verfahren erforderlich sind.

Bei der Analyse von Umweltproben muss überdies bedacht werden, dass sich die Eigenschaften der Nanomaterialien in Abhängigkeit von der jeweiligen Matrix stark verändern können.⁶ Eine Verschiebung von pH-Wert, Salzgehalt, Temperatur, dem Gehalt an gelöstem Sauerstoff oder des Anteils an gelöster organischer Substanz kann zu Veränderungsprozessen wie Agglomeration, Aggregation, Auflösung oder Stabilisierung der (suspendierten) Nanomaterialien führen, so dass sich gänzlich andere Formen und Funktionen ergeben können. Als Beispiel ist von Silber-Nanopartikeln (Ag₀) bekannt, dass Silber-Ionen (Ag⁺) in Lösung gehen.⁷ Demgegenüber trägt das Vorhandensein schwefelhaltiger Substanzen zur Bildung schwer löslicher Silbersulfide bei (Ag₂S, teilweise in nano/kolloidaler Form).⁸ Im Vergleich zu Silber-Nanopartikeln und den von der Oberfläche freigesetzten Ionen kommt es dadurch zu einer Herabsetzung der Bioverfügbarkeit und damit auch der Toxizität.⁹ Dementsprechend müssen bei der Beurteilung möglicher Risiken, neben dem Nanomaterial selbst, auch mögliche Transformationsprodukte berücksichtigt werden, was sowohl aus naturwissenschaftlicher (Charakterisierung, Nachweis, Toxikologie) als auch juristischer Sicht eine

enorme Herausforderung darstellt. Zusätzlich wird die Identifikation künstlicher Nanomaterialien in Umweltmedien dadurch erschwert, dass auch natürliche Kolloide (wie z. B. Tonminerale, Eisen- und Mangan-Oxide oder organische Bestandteile wie Huminstoffe oder Proteine) in dem Größenbereich zwischen einem und 100 nm vorkommen¹⁰ und diese in deutlich höheren Konzentrationen als die künstlichen Nanomaterialien vorliegen. Da zusätzlich, wie beispielsweise im Fall von Titan, der natürliche geochemische Hintergrund so hoch ist, dass eine Unterscheidung von natürlichen und anthropogenen Verbindungen kaum möglich ist, ist die Umweltanalytik künstlicher Nanomaterialien mit der Suche nach der Nadel im Heuhaufen vergleichbar. Bewältigt werden könnte diese Aufgabe allenfalls durch den Einsatz geeigneter Tracerpartikeln sowie sehr nachweisstarken Methoden in aufwändigen und kostspieligen Multimethodenansätzen.

Auf der Grundlage dieser noch unzureichenden wissenschaftlichen Basis erscheint die Erarbeitung geeigneter regulatorischer Instrumente derzeit schwierig, insbesondere weil die Entwicklung standardisierter Mess- und Testverfahren voraussichtlich noch mehrere Jahre oder gar Jahrzehnte in Anspruch nehmen kann.

AIII.II.III Die Einleitung nanoskaliger Stoffe in Grund- und Oberflächenwasser

Gemäß § 48 I Wasserhaushaltsgesetz (WHG) darf eine Erlaubnis für das Einleiten von Stoffen in das Grundwasser nur erteilt werden, wenn eine nachteilige Veränderung der Wasserbeschaffenheit nicht zu besorgen ist. Vorgaben dazu, welche Stoffe als wassergefährdend einzustufen sind, finden sich in Anlage 7 der Grundwasserverordnung (GrwV). Der Eintrag von Stoffen aus Anlage 8 GrwV ist derart zu beschränken, dass die Besorgnis einer negativen Veränderung des Grundwassers ausgeschlossen werden kann. Allerdings werden sowohl in Anlage 7 als auch in Anlage 8 der GrwV keine Angaben zur Berücksichtigung der Spezifität von Nanomaterialien gemacht. Fraglich bleibt damit, ob die aufgelisteten Stoffe konkludent auch in ihrer nanoskaligen Variante erfasst werden oder ob bisher nicht erfasste Stoffe (wie z.B. Titandioxid) nun in ihrer Nanoform erfasst werden müssen. Als problematisch erweist sich in diesem Zusammenhang auch, dass die Beweislast für potenzielle schädliche Auswirkungen von Nanomaterialien auf das Grundwasser bei den zuständigen Wasserbehörden liegt, denen eine derartige Beurteilung mittels der derzeit dort zur Verfügung stehenden Methoden kaum möglich ist.

Erhebliche Schwierigkeiten zeigen sich auch bei der Einleitung in Gewässer. Die Einleitung erfolgt nach den Vorgaben des WHG entweder durch eine Direkteinleitung (§ 57 WHG) oder durch eine Indirekteinleitung in öffentliche oder private Abwasseranlagen (§§ 58, 59 WHG). Gemäß § 57 I Nr. 1 WHG darf eine entsprechende Erlaubnis nur erteilt werden, wenn die Schadstofffracht nach Prüfung der Verhältnisse im Einzelfall so gering gehalten wird, wie dies bei Einhaltung der jeweils in Betracht

kommenden Verfahren nach dem Stand der Technik möglich ist. Nähere Ausführungen zum Stand der Technik finden sich in den Anhängen der Abwasserverordnung. Auch in diesem Zusammenhang fehlt es jedoch an spezifischen Festlegungen zum Umgang mit nanoskaligen Materialien.

AIII.II.IV Umgang mit wassergefährdenden Stoffen

Vorgaben hinsichtlich des Umgangs mit wassergefährdenden Stoffen finden sich in den §§ 62 ff WHG, die durch entsprechende landesrechtliche Verordnungen über Anlagen zum Umgang mit wassergefährdenden Stoffen und über Fachbetriebe sowie durch die Grundwasserverordnung konkretisiert werden. Gemäß § 63 WHG bedarf es für die Errichtung und den Betrieb von Anlagen zum Lagern, Abfüllen oder Umschlagen wassergefährdender Stoffe einer Eignungsfeststellung. Die materiell-rechtlichen Vorgaben finden sich hingegen in § 62 WHG, nach dem Anlagen zum Lagern, Abfüllen, Herstellen, Behandeln und Verwenden sowie zum Umschlagen wassergefährdender Stoffe derart beschaffen sein müssen, dass eine nachteilige Veränderung der Eigenschaften von Gewässern nicht zu besorgen ist. Hinsichtlich der Ausstattung der Anlagen sind dabei die allgemeinen anerkannten Regeln der Technik einzuhalten. Entsprechend den Verordnungen über Anlagen zum Umgang mit wassergefährdenden Stoffen und über Fachbetriebe können hinsichtlich der Anforderungen an die Beschaffenheit und den Betrieb von Anlagen zwei Kriterien maßgebend sein. Dies ist entweder das Gefährdungspotenzial, das aus den in der Anlage vorhandenen wassergefährdenden Stoffen resultiert oder die Gefährdungsstufe der Anlage, die sich nach den Wassergefährdungsklassen (WGK) richtet.¹¹ Zu beachten ist jedoch, dass der Stoff in die höchste Gefährdungsstufe einzuordnen ist, sofern die WGK nicht mit Sicherheit festgestellt werden kann.

Die Einordnung in die entsprechenden WGK ergibt sich aus der Verwaltungsvorschrift wassergefährdende Stoffe (VwVwS).¹² Für Stoffe, die nicht in den Anhängen 1 (nicht-wassergefährdende Stoffe) und 2 (wassergefährdende Stoffe) aufgeführt sind, ist von den Anlagenbetreibern entsprechend den Vorgaben des Anhangs 3 der VwVwS selbstständig¹³ ein Einstufungsverfahren durchzuführen, dessen Ergebnisse dem Umweltbundesamt zu melden sind. Nanomaterialien könnten zwar anhand ihres makroskaligen Ebenbildes einer WGK zugeordnet werden,¹⁴ finden jedoch weder in der VwVwS noch in ihren Anhängen ausdrücklich Erwähnung. Vor dem Hintergrund, dass sich Stoffe je nach Partikelgröße unterschiedlichst verhalten können, erscheint die unreflektierte Übernahme der makroskaligen Kategorisierung als problematisch. Zur Veranschaulichung sei hier auf Titandioxid hingewiesen, das in Anlage 1 der VwVwS als nicht wassergefährdender Stoff geführt wird, weshalb die Vorgaben der §§ 62 ff WHG sowie die Einstufung in die WGK nach dem Anhang 3 der VwVwS nicht einschlägig sind. Aktuell wird jedoch eine – wenn auch geringe – Toxizität von Titandioxid in seiner nanoskaligen Form für aquatische Organismen zumindest diskutiert.¹⁵ Die Überlegung, Nanomaterialien wegen ihrer unbekanntem Risiken

umgekehrt in die höchste Gefährdungsklasse einzuordnen,¹⁶ könnte hingegen einen Verstoß gegen den Gleichbehandlungsgrundsatz nach Art. 3 Abs. 1 GG darstellen¹⁷ und wäre darüber hinaus aus Sicht betroffener Unternehmen anhand von Art. 12 Abs. 1 GG (Berufsfreiheit) zu bemessen.

AIII.II.V Der Rückgriff auf die REACH-Verordnung

Der Umstand, dass sich derzeit in keinem Teilrechtsgebiet nanospezifische Ausführungen finden, führt zur Suche nach Regularien, die im Rahmen der rechtlichen Prüfung hilfsweise hinzugezogen werden könnten. In diesem Kontext wird regelmäßig die Europäische REACH-Verordnung (Registration, Evaluation, Authorization and Restriction of Chemicals) genannt. Diese schreibt die Registrierung von Chemikalien (ab einer Menge >1 t/Jahr) durch Hersteller, Importeure und Anwender vor, wobei diese zugleich deren sichere Verwendung gewährleisten müssen.¹⁸ Die Identität der Stoffe wird dabei über die Molekülstruktur und die chemische Zusammensetzung definiert, so dass nanoskalige Materialien derzeit als eine Erscheinungsform des jeweiligen Bulkmaterials erfasst werden. Darüber hinausgehende Angaben über Eigenschaften, die das Verhalten von Nanomaterialien bestimmen können (wie Partikelgrößenverteilung oder Oberflächeneigenschaften) sind jedoch nicht verpflichtend. Die durch die Europäische Kommission vorgelegte „zweite Überprüfung der Rechtsvorschriften zu Nanomaterialien“ lässt die Implementierung in REACH allerdings als wahrscheinlich erscheinen, wobei die dazu erforderlichen Anpassungen (u. a. Vereinheitlichung der Definitionen, Anpassung von Tonnagen- Grenzen und für die Stoffsicherheitsbeurteilung zu erbringende Informationen) auf europäischer Ebene kontrovers diskutiert werden.¹⁹

Ungeachtet dessen, welche Daten für die Registrierung von Nanomaterialien erforderlich sein werden, bleibt unklar, wie eine umfassende Sicherheitsbeurteilung sowie die (behördliche) Durchsetzung der Bestimmungen erfolgen kann, solange standardisierte analytische Verfahren zur Identifizierung, Charakterisierung und Quantifizierung von Nanomaterialien nicht verfügbar bzw. sehr aufwändig sind. Vor diesem Hintergrund bleibt zudem fraglich, wie eine sichere Verwendung der Materialien (durch den Registrant) gewährleistet werden könnte und inwieweit dies im Zweifelsfall überprüfbar wäre.

In Anbetracht der zunehmenden Nutzung von Nanomaterialien erscheint die Einführung nanospezifischer Registrierungspflichten sowie einzelfallbezogener Risikobewertungen als erstrebenswert, nicht zuletzt um Rechtsklarheit und Gleichbehandlung zu gewährleisten. Dabei impliziert die Festschreibung der zu erbringenden Daten im Rahmen von REACH, dass eine Registrierung, und die damit einhergehende Genehmigung zum Inverkehrbringen von Stoffen, nur auf der Grundlage vollständiger Informationen erteilt wird.

AIII.II.VI Ausblick

Nanospezifische Herausforderungen werden im geltenden Wasserrecht – wie in allen anderen Teilrechtsgebieten auch – derzeit nicht abgebildet. Die zur Verfügung stehenden wasserrechtlichen Instrumentarien können zudem aufgrund der bestehenden Wissenslücken nicht voll ausgeschöpft werden. Eine Kompensation dieses Zustandes durch einen Rückgriff auf die REACH-Verordnung erscheint nur unter Voraussetzung der erforderlichen Anpassungen als erfolgsversprechend, wobei ein durch die zuständigen deutschen Behörden vorgelegtes Konzept zur Implementierung von Nanomaterialien ein dahingehendes Interesse dokumentiert.²⁰ Im Wasserrecht dürfte hingegen die Betonung des einzelfallbezogenen behördlichen Ermessensspielraums zielführender sein, den jüngst etwa das VG Düsseldorf in Bezug auf eine Gewässerverunreinigung durch perfluorierte Tenside (PFT) hervorgehoben hat. Das Urteil betrifft zwar keine Substanzen im nanoskaligen Bereich, ist aber aufgrund der dort angestellten grundsätzlichen Erwägungen zum behördlichen Ermessen im Falle wissenschaftlichen Klärungsbedarfes auf die vorliegend interessierende Fragestellung unmittelbar übertragbar: „Die Belastung des im Betrieb der Klägerin entstehenden Abwassers mit PFT lässt eine Beeinträchtigung des Wohls der Allgemeinheit befürchten, wenn dieses Abwasser über die öffentliche Kanalisation und die Kläranlage I-B in ein Gewässer, nämlich in den S.Bach und über diesen in die Ruhr, gelangt. Diese Befürchtung wird nicht dadurch ausgeschlossen, dass die Indirekteinleitung des Abwassers der Klägerin den für den maßgeblichen Herkunftsbereich festgelegten Anforderungen des Anhangs 40 zu der auf der Grundlage des § 7 a Abs. 1 S. 3 WHG a.F. erlassenen Abwasserverordnung entspricht (§ 59 Abs. 3 S. 1 Nr. 1 LWG a.F.). Daraus, dass dort keine Grenzwerte für PFT festgesetzt werden und auch die Chemikalienverbotsverordnung hinsichtlich PFOS (Perfluorooctansulfonat) eine Ausnahmeregelung für galvanische Betriebe enthält [...], kann nicht abgeleitet werden, dass die Klägerin Abwasser mit hoher PFT-Konzentration in die öffentliche Abwasseranlage einleiten darf und der Beklagte gehindert wäre, Maßnahmen zur Reduzierung dieser Schadstoffbelastung zu ergreifen. Denn Perfluorierte Tenside sind grundsätzlich geeignet, im Wasserkreislauf Gefahren oder erhebliche Nachteile zu bewirken.

Eine solche Eignung besteht, wenn im Hinblick auf den Wasserhaushalt nachteilige Auswirkungen einer gewissen Mindestintensität hinreichend wahrscheinlich sind. Der erforderliche Grad an Wahrscheinlichkeit bestimmt sich nach Art und Ausmaß des drohenden Schadens einerseits und des hohen Schutzes, den die Gewässer genießen, andererseits. Substanzen, die das Wasser verunreinigen oder eine sonstige nachteilige Veränderung seiner Eigenschaften hervorrufen [...], gehören nicht in Gewässer, insbesondere nicht in Wasservorkommen, die – wie hier die Ruhr – konkret für die öffentliche Trinkwasserversorgung genutzt werden. Eine zum behördlichen Tätigwerden ermächtigende Beeinträchtigung der Wassergüte liegt insofern nicht erst dann vor, wenn feststeht,

dass die bewirkten Veränderungen allgemein und/oder im Besonderen hinsichtlich der Trinkwasserversorgung den Ge- oder Verbrauchswert des Wassers aufheben oder wesentlich herabsetzen. Angesichts der zentralen Bedeutung, der dem Erhalt und dem Schutz naturgegebenen Wasservorkommen zukommt reicht es in diesem Zusammenhang bereits aus, wenn eine nachteilige Beeinflussung als gering wahrscheinlich eingestuft wird, insbesondere wenn es sich dabei um einen zur Trinkwasserversorgung genutzten Wasserkörper handelt. Nichts anderes gilt im Hinblick auf den Schutz der ökologischen Funktionen der Gewässer (§ 1 a Abs. 1 S. 1 WHG a.F.). Unabhängig von dem allgemein beim Schutz von Gewässern geltenden Maßstab, vor allem dem Besorgnisgrundsatz, liegt dieser hohe Schutzstandard auch § 6 TrinkwV 2001 zu Grunde. Danach dürfen im Trinkwasser chemische Stoffe nicht in Konzentrationen enthalten sein, die eine Schädigung der menschlichen Gesundheit besorgen lassen (§ 6 Abs. 1 TrinkwV 2001); Konzentrationen von chemischen Stoffen, die die Beschaffenheit des Trinkwassers nachteilig beeinflussen können, sollen so niedrig gehalten werden, wie dies nach den allgemein anerkannten Regeln der Technik mit vertretbarem Aufwand unter Berücksichtigung der Umstände des Einzelfalles möglich ist (§ 6 Abs. 3 TrinkwV 2001).

Bei den im geschilderten Fall angesprochenen [...] Per- fluorierten Tensiden handelt es sich um Stoffe, die sich nach den Maßstäben des Wasserrechts und den Vorgaben der Trinkwasserverordnung potenziell nachteilig auf den Ge- oder Verbrauchswert der Gewässer auswirken. Die Folgen von PFT und der zur Gruppe dieser chemischen Verbindungen gehörenden Einzelsubstanzen – vor allem von PFOS und PFOA (Perfluorooctansäure) – für die menschliche Gesundheit sind zwar noch nicht abschließend geklärt. Hinlänglich gesichert ist jedoch, dass PFT – und/oder bestimmte Einzelsubstanzen dieser Gruppe – wissenschaftlich einhellig als Stoffe mit erheblichem gesundheitlichem Risikopotential eingestuft werden. [...] Das Fehlen eines Grenzwerts für diese Stoffe ist mithin kein Umstand, der gegen die Schädlichkeit ihrer Einleitung in Gewässer angeführt werden könnte.“²¹

Bei adäquater Nutzung der umrissenen Ermessens- und Handlungsspielräume sind die wasserrechtlichen Herausforderungen der Nanotechnologie, trotz großer wissenschaftlicher Unsicherheiten, (aus juristischer Sicht) grundsätzlich zu meistern, sofern (für den Umweltbereich) geeignete Definitionen und Identifikationsmöglichkeiten entwickelt werden können, was auch die erfolgreiche Identifikation von Kontaminationsquellen einschließt. Ungeachtet dessen bedarf es zudem unter Vorsorgegesichts- punkten des Versuchs, eine wasserwirtschaftliche Gesamtbilanz nanotechnologischer Implikationen zu erstellen (potenzielle Einsatzbereiche vs. Gefährdungen) sowie der Durchführung „wasserspezifischer“ Forschungsarbeiten, etwa zur Toxizität oder des Verhaltens der Stoffe in der Umwelt. Der mitunter geforderte Erlass eines gesonderten Nanogesetzes lässt hingegen keinen regulatorischen Vor- teil erwarten. Zum einen würde eine Spezialmaterie wie das

Wasserrecht in einem solchen Gesetz kaum detailliert behandelt werden. Zum anderen würde das Ziel einer Stärkung der Rechtssicherheit durch explizite und v. a. einheitliche Normierung der Nanomaterialien durch eine Fundamentierung rasch überholter Standards sowie die Probleme technikbezogener Regulierungen²² wohl überkompensiert.

Abgesehen von der Notwendigkeit, der Schaffung regulatorischer Instrumente und der Erarbeitung einer belastbaren wissenschaftlichen Basis sowie standardisierter Verfahren zum Nachweis von Nanomaterialien in komplexen Umweltmedien sowie der Beurteilung von deren Toxizität unter den herrschenden Umweltbedingungen, bedarf es zudem der verstärkten transdisziplinären Zusammenarbeit beteiligter Experten. Die Voraussetzung für die Entwicklung geeigneter und durchsetzbarer Regelwerke ist dabei einerseits die allgemein verständliche Darstellung des aktuellen Wissensstandes unter Benennung der bestehenden Unsicherheiten und Wissenslücken durch Vertreter der naturwissenschaftlichen Disziplinen. Andererseits bedarf es der Formulierung der aus juristischer Sicht erforderlichen Informationen sowie der Möglichkeiten und Grenzen gesetzlicher Beschränkungen. Eine zentrale Frage wird dabei sein, inwiefern Industrievertreter Daten zu Produktions- und Applikationsmengen liefern können oder wollen, um so eine Abschätzung der in die Umwelt gelangenden Mengen an Nanomaterialien sowie eine realistische Risikobewertung zu ermöglichen. Nicht zuletzt gilt es, die allgemeine Öffentlichkeit (Verbraucher, Betroffene) in nicht Eigeninteressen getriebener Form zu informieren und in die Diskussionen und Entscheidungsprozesse soweit wie möglich mit einzubeziehen.

AIII.II.VII Literatur

- 1 Nr. 2 und 3 der Empfehlung der Kommission vom 18. Oktober 2011 zur Definition von Nanomaterialien (2011/696/EU).
- 2 Musee, „Nanowastes and the environment: Potential new waste management paradigm.“, *Environment international* 37(1), 112–128; Hendren, Mesnard et al. (2012), „Estimating Production Data for Five Engineered Nanomaterials As a Basis for Exposure Assessment“, *Environmental Science & Technology* 45(7), 2562–2569; Gottschalk et al. (2011), „The release of engineered nanomaterials to the environment“, *Journal of Environmental Monitoring* 13(5), 1145–1155.
- 3 Gottschalk et al. (2011), „The release of engineered nanomaterials to the environment“, *Journal of Environmental Monitoring* 13(5), 1145–1155.
- 4 Kaegi / Ulrich et al. (2008), „Synthetic TiO₂ nanoparticle emission from exterior facades into the aquatic environment“, *Environmental Pollution* 156(2), 233–239.
- 5 Hendren, Mesnard et al. (2012), „Estimating Production Data for Five Engineered Nanomaterials As a Basis for Exposure Assessment“, *Environmental Science & Technology* 45(7), 2562–2569.
- 6 Lowry, Gregory et al. (2012), „Transformations of Nanomaterials in the Environment.“, *Environmental Science & Technology* 46(13), 6893–6899.
- 7 Liu/Hurt (2010), „Ion Release Kinetics and Particle Persistence in Aqueous Nano-Silver Colloids“, *Environmental Science & Technology* 44(6), 2169–2175; Glover, Miller et al. (2011), „Generation of Metal Nanoparticles from Silver and Copper Objects: Nanoparticle Dynamics on Surfaces and Potential Sources of Nanoparticles in the Environment.“, *Acs Nano* 5(11), 8950–8957.
- 8 Kaegi, Voeglin et al. (2011), „Behavior of Metallic Silver Nanoparticles in a Pilot Wastewater Treatment Plan.“, *Environmental Science & Technology* 45(9), 3902–3908.
- 9 Levard, Hotze et al. (2012), „Environmental Transformations of Silver Nanoparticles: Impact on Stability and Toxicity.“, *Environmental Science & Technology* 46(13), 6900–6914
- 10 Wigginton, Haus et al., „Aquatic Environmental Nanoparticles.“, *Journal of Environmental Monitoring* 9(12), 1306–1316; Klaine, Alvarez et al. (2008), „Nanomaterials in the environment: Behavior, fate, bioavailability, and effects.“, *Environmental Toxicology and Chemistry* 27(9), 1825–1851.
- 11 SRU-Gutachten 2011, S. 422, Rn. 601.
- 12 Allgemeine Verwaltungsvorschrift zum Wasserhaushaltsgesetz über die Einstufung wassergefährdender Stoffe in Wassergefährdungsklassen vom 17.5.1999.
- 13 Vgl. hierzu Nr. 3a der VwVwS.
- 14 Führ et.al., in: ReNaTe (2007), Abschlussbericht, S.76.
- 15 Dabrunz, Duester et al., „Biological Surface Coating and Molting Inhibition as Mechanisms of TiO₂ Nanoparticle Toxicity in *Daphnia Magna*.“, *PLoS ONE* 6 (5); Cardinale, Bier et al. (2012), „Effects of TiO₂ nanoparticles on the growth and metabolism of three species of freshwater algae.“, *Journal of Nanoparticle Research* 14 (8); Clemente, Castro et al. (2012), „Ecotoxicology of Nano-TiO₂ An Evaluation of its Toxicity to Organisms of Aquatic Ecosystems.“, *Journal of Environmental Research* 6 (1), 33–50.
- 16 So ist z.B. das Land NRW durch den Erlass einer ordnungsbehördlichen Verordnung über die Genehmigungspflicht für die Einleitung von Abwasser mit gefährlichen Stoffen in Abwasseranlagen des Landes NRW i.V.m. § 62 IV Nr.1 WHG verfahren.
- 17 Vgl. zu der Diskussion den Bericht von Karrenstein, *Nanotechnologie und Wasserrecht*, NuR 2012, 402.
- 18 UBA, „REACH Informationsportal“, abgerufen am 5.3.2013 unter <http://www.reach-info.de>.
- 19 EC 2012, Communication from the Commission to the European Parliament, the Council and the European Economies and Social Committee; Second Regulatory Review on Nanomaterials, COM(2012) 572 final, abgerufen am 5.3.2012 unter: [http://ec.europa.eu/nanotechnology/pdf/second_regulatory_review_on_nanomaterials_-_com\(2012\)_572.pdf](http://ec.europa.eu/nanotechnology/pdf/second_regulatory_review_on_nanomaterials_-_com(2012)_572.pdf) ; EC 2013, Workshop on the Second Regulatory Review on Nanomaterials,

abgerufen am 13.1.2013 unter
http://ec.europa.eu/enterprise/sectors/chemicals/reach/events/index_en.htm#h2-1.

20 UBA, „REACH Informationsportal“, abgerufen am 5.3.2013 unter <http://www.reach-info.de>.

21 VG Düsseldorf, Urteil vom 3.8.2011 – 10 K 2228/09

Appendix IV
Supporting Information Chapter 4:
Metal and Metalloid Size Fractionation Strategies
in Spatial High Resolution Sediment Pore Water
Profiles

Anne-Lena Fabricius, Lars Duester, Dennis Ecker and Thomas A. Ternes

AIV.I Sediment Characteristics

The sediment used within the experiments was sampled at stream kilometer 136 at the water gate Lahnstein (Germany, 50°18'29.47"N 7°36'46.24"O). Freeze drying was conducted by means of a GAMMA 1-16 LSC (Christ Gefriertrocknungsanlagen GmbH, Germany). To determine the element contents of the sediment, a microwave assisted digestion was carried out using a MLS μ Prep-A (Ethos plus, MLS, Germany). Therefore, 1 g of the sediment was mixed with 10 mL of HNO₃ (65%) and digested applying the program listed below (Table A3. 1). After dilution with ultrapure water to a volume of 100 mL, the element concentrations were determined by means of ICP-QMS (setup 1) as described in the experimental section of the manuscript. The element contents are given in Table A3. 2

Table A3. 1: Microwave program.

| Time (min) | Energy (W) | Temperature (°C) |
|------------|------------|------------------|
| 9:30 | 500 | 100.0 |
| 2:41 | 750 | 125.0 |
| 7:32 | 1,000 | 210.0 |
| 5:00 | 1,000 | 205.0 |
| 15:00 | 500 | 205.0 |

Table A3. 2: Element content (measured by ICP-QMS) and standard deviations of the sediment used in the experiments.

| Element | Mn | Fe | Co | As | Sb |
|-----------------------|------------|---------------|--------------|-------------|---------------|
| Concentration (mg/kg) | 223 ± 0.03 | 5,949 ± 99.36 | 2.99 ± 0.058 | 3.66 ± 0.03 | 0.011 ± 0.001 |

The content of total carbon, nitrogen, sulfur (CNS) and total organic carbon (TOC, Table A3. 3) were determined using a Eltra Helios (Eltra GmbH, Germany). 1 ml 1M HCl was added to 150-200 mg of the freeze-dried sediment and incubated for 3-4 h at room temperature. Subsequently, the pre-digested samples were heated to 55°C for ~12 h. Calibration was undertaken by threefold analysis of calcium carbonate (12%, pro analysis, Merck, Germany) and graphite (100% C, Eltra, Germany) and validated measuring (for channel 1, low carbon content) 100 mg CaCO₃ (12%), 200 mg graphite (100%, covered with sea sand) and ~150 mg of certified standard reference materials (1941a and 1941b; organics in marine sediment, TC 4.8% and 3.3% respectively). In the case of high carbon

contents (channel 2), validation was performed by measurements of 130 mg EDTA (42.1%, pro analysi, AppliChem, Germany) and 200 mg graphite (100%, covered with sea sand). Samples were analyzed in triplicates.

Table A3. 3: Results of CNS and TOC analyses of the sediment used within the experiments.

| TC (%) | TOC (%) | N (%) | S (%) | TC/N | TC/S |
|---------------|----------------|--------------|--------------|-------------|-------------|
| 5.03 | 4.82 | 0.76 | 0.20 | 6.59 | 25.55 |

AIV.II Microprofiling and micro sampling

High-resolution profiling was carried out using a microprofiling and a micro sampling (filtration) system (missy) developed and established in the authors' laboratory. An extensive description of the development and validation of the system and the analytical methods as well as the manufacturing of the sample probes can be found in Fabricius et al. (2014).¹ The microprofiling system consists of a computer controlled motorized micromanipulator and two microsensors connected to a microsensor multimeter (all Unisense, Denmark). The micro sampling system is a combination of a sampling probe connected to a micro annular gear pump (mzr[®]-2542) controlled by a console drive module (mzr-S06, both HNP Microsystems, Germany) and a fraction collector (rotAXYS[®], Cetoni, Germany). The sampling probes, developed in the authors' laboratory¹ were made of a piece of porous polyethersulfone (PES) hollow fiber (0.45 μm) that was connected to a tube and stabilized by two pipette tips. In order to maintain the measurements of the sediment parameters (the O_2 concentration and the redox potential) and the sampling of the sediment pore water in parallel, the software settings of the programs of the microprofiling and micro sampling systems (SensorTrace PRO, Unisense, Denmark and QmixElements, Cetoni GmbH, Germany) were synchronized (refer to Table A3. 4). Per profile 26 samples were taken, each over a distance of 1.17 mm. In order to consider the shift of the sampling depth in relation to that of the measurements caused by the dead volume of the tubings, the first two samples were excluded from further analyses. The sampling parameters and distances of the 24 samples analyzed are given in Table A3. 4 and Table A3. 5. To obtain a sample volume sufficient for a fractionation and a direct analysis in parallel, two samples were pooled (as described in the manuscript).

Table A3. 4: Measurement settings of the microprofiling and the micro sampling system.

| Unisense (profiling) | | | Cetoni (sampling) | | |
|---|------------------------------|---------|-------------------------------|------------------------------|------|
| Unisense start | (μm) | -10,000 | Sampling velocity | ($\mu\text{l}/\text{min}$) | 3,33 |
| Unisense end | (μm) | 20,000 | Intended sample volume | (μL) | 500 |
| Length profile | (μm) | 30,000 | Samples per profile | | 26 |
| | | | Time per sample | (sec) | 9000 |
| Wait before measure | (sec) | 430.0 | | (h) | 2.5 |
| Measure period | (sec) | 10.0 | Time per profile | (h) | 60 |
| Step size μm | (μm) | 65 | | (d) | 2.5 |
| Measurement points | | 490 | | | |
| Averaged speed of the probe/electrodes | ($\mu\text{m}/\text{min}$) | 8.2 | | | |

Table A3. 5: Sampling distances and mean values for pore water samples. To correlate the microprofiling measurements (O_2 , redox potential) with the element concentrations, the mean (rounded) values of the sampling distance were determined for each single sample and the pooled ones. Negative values indicate samples from the water body above the sediment.

| Sample | Start (cm) | End (cm) | Mean (cm) | Pooled (cm) | Sample | Start (cm) | End (cm) | Mean (cm) | Pooled (cm) |
|--------|------------|----------|-----------|-------------|--------|------------|----------|-----------|-------------|
| 1 | -0.95 | -0.83 | -0.89 | | 13 | 0.53 | 0.65 | 0.59 | |
| 2 | -0.83 | -0.71 | -0.77 | -0.83 | 14 | 0.66 | 0.78 | 0.72 | 0.65 |
| 3 | -0.70 | -0.58 | -0.64 | | 15 | 0.78 | 0.90 | 0.84 | |
| 4 | -0.58 | -0.46 | -0.52 | -0.58 | 16 | 0.90 | 1.02 | 0.96 | 0.90 |
| 5 | -0.45 | -0.34 | -0.40 | | 17 | 1.03 | 1.15 | 1.09 | |
| 6 | -0.33 | -0.21 | -0.27 | -0.33 | 18 | 1.15 | 1.27 | 1.21 | 1.15 |
| 7 | -0.21 | -0.09 | -0.15 | | 19 | 1.28 | 1.39 | 1.33 | |
| 8 | -0.08 | 0.03 | -0.03 | -0.09 | 20 | 1.40 | 1.52 | 1.46 | 1.40 |
| 9 | 0.04 | 0.16 | 0.10 | | 21 | 1.52 | 1.64 | 1.58 | |
| 10 | 0.16 | 0.28 | 0.22 | 0.16 | 22 | 1.65 | 1.76 | 1.70 | 1.64 |
| 11 | 0.29 | 0.40 | 0.35 | | 23 | 1.77 | 1.89 | 1.83 | |
| 12 | 0.41 | 0.53 | 0.47 | 0.41 | 24 | 1.89 | 2.01 | 1.95 | 1.89 |

AIV.III ICP-QMS analyses

The information on the ICP-QMS measurements including the isotopes analyzed, the measurement modes (no gas = standard, He = collision cell; He gas flow of 5 mL/min) and the certified values of the certified reference materials (CRM) used are given in Table A3. 6. At least two of three CRMs included in each measurement differed <10% from the certified values at any time of a measurement series. Limits of detection (LoD, blank + 3 sigma) and limits of quantification (LoQ, blank + 10 sigma) of the measurements of the different experiments are given together with the results in the respective tables (see below). Measurements were performed at a RF power of 1450 W. Each sample was measured in 5 replicates. As described in the manuscript, measurements were carried out using two different setups: setup 1 was used for routine measurements of samples of volumes of ≥ 3 mL, setup 2 for sample volumes of 300 μ L. In the case of the latter, the nebulizer was directly connected to the Ar-gas line. The pressure for optimal signal intensity was manually tested and set to ~ 3.5 bar (~ 50 psi = ~ 1 L/min). The carrier gas line of the ICP-QMS was connected to the drainless spray chamber shear gas port and set to 0.75 L/min. Similar to setup 1, the integrated sample introduction system (ISIS) of the device was used for sample introduction, equipped with a sample loop of ~ 100 μ L. To avoid a time consuming switching between different measurement modes and thereby reducing the measuring time per sample, all elements were measured in the collision cell gas modus (He mode). Sample introduction was performed from a 96-deep well plate. Within the wells, 270 μ L of the sample was mixed with 30 μ L of internal standard (IS; Ge, Rh, Re, each 50 μ g/L). Matrix matched calibration standards as well as certified reference materials (CRMs) were equally treated and introduced from the well plates.

Table A3. 6: Information on ICP-QMS analyses.

| | Manganese | Iron | Cobalt | Arsenic | Antimony |
|---------------------------|--|------------------|------------------|------------------|-------------------|
| Isotope | ⁵⁵ Mn | ⁵⁶ Fe | ⁵⁹ Co | ⁷⁵ As | ¹²¹ Sb |
| Modus setup 1 | He | He | He | He | no gas |
| Modus setup 2 | He | He | He | He | He |
| Reference material | Concentration (μg/L) | | | | |
| SPS-SW 2 (1:10)* | 5.0 \pm 0.03 | 10.0 \pm 0.1 | 1.00 \pm 0.005 | 5 \pm 0.03 | - |
| TM 27.3 ** | 2.27 \pm 0.35 | 10.9 \pm 3.0 | 2.05 \pm 0.18 | 2.15 \pm 0.30 | 1.51 \pm 0.19 |
| SRM 1640a *** | 40.39 \pm 0.36 | 36.8 \pm 1.8 | 20.24 \pm 0.24 | 8.010 \pm 0.07 | 5.105 \pm 0.046 |

* Surface water – trace metals, LGC standards GmbH

** Certified Reference Waters for Trace Elements, Environment Canada

*** National Institute of Standards and Technology

AIV.IV Preliminary experiments for CPE method adjustment

In order to test the general applicability of the CPE method, originally developed to extract and pre-concentrate Ag nanoparticles, from samples of 40 mL to small volumes of 0.5 mL, preliminary experiments were carried out prior to the profiling experiments. Therefore, ~5 g of the sediment also used for the sediment core (refer to the manuscript) was mixed with ~40 mL of deionized water in a 50 mL polypropylene centrifuge-tube (VWR International, Darmstadt, Germany) and shaken overhead for several hours (Intelli-Mixer, ELMI Ltd., Latvia) to obtain samples comparable to the sediment pore water. To separate the water from the sediment, the samples were centrifuged for 10 min at 2000 g (Sigma Laboratory Centrifuge 3K30, Sigma Laborzentrifugen GmbH, Germany). Comparable to the size cut-off of the sample probes used in the profiling experiments, the supernatant was filtered to <0.45 µm (syringe filters Minisart NML, Celluloseacetate, Sartorius, Germany). CPE was conducted sixfold as described in the manuscript. Method blanks were determined in triplicates replacing the sample by ultrapure water. The 0.45 µm filtrate as well as the ultrapure water was acidified to 1.3% HNO₃ and analyzed together with the samples by means of ICP-QMS to determine the total element concentrations. After blank correction, the concentrations determined in the CPE fractions were related to the total concentrations of the 0.45 µm filtrates set as 100%. Recoveries were calculated by relating the sum of the two fractions to the 100% of the SPW. Results of the last preliminary experiment conducted are given in Table A3. 7. In contrast to the profiling experiments, CPE was carried out under normal laboratory conditions and not in the glove box probably causing biases of the Fe results due to contaminations by the laboratory background (refer also to the explanations in the manuscript).

Table A3. 7: Percentage of element concentrations of CPE fractions (aq = aqueous phase and TRX = Triton-X114 phase) in relation to the total concentration of the SPW 0.45 µm filtrate. Results crossed out were excluded from mean value calculation after testing for outliers (Grubb's and Dixon-Test^{2,3}, *p*-values Fe <0.05).

| Phase | Manganese | | | Cobalt | | | Iron | | | Arsenic | | | Antimony | | |
|-------|-----------|------|------|--------|-------|------|-----------------|-----------------|-----------------|---------|-------|-------|----------|-------|------|
| | aq | TRX | Σ | aq | TRX | Σ | aq | TRX | Σ | aq | TRX | Σ | aq | TRX | Σ |
| LoD: | 0.28 | | | 0.02 | | | 1.05 | | | 0.02 | | | 0.27 | | |
| LoQ: | 0.78 | | | 0.06 | | | 1.75 | | | 0.06 | | | 0.84 | | |
| | 107% | 3.8% | 111% | 103% | 2.7% | 106% | 49.4% | 58.6% | 108% | 103% | 1.4% | 104% | 103% | 2.9% | 106% |
| | 104% | 3.8% | 108% | 105% | 4.3% | 110% | 253% | 40.4% | 294% | 102% | 0.0% | 102% | 114% | 5.0% | 119% |
| | 106% | 3.9% | 110% | 103% | 3.7% | 107% | 41.1% | 33.3% | 82.3% | 80.1% | 0.0% | 80.1% | 102% | 2.3% | 105% |
| | 100% | 5.0% | 105% | 99.9% | 13.7% | 114% | 40.6% | 169% | 209% | 108% | 12.5% | 120% | 97.2% | 16.5% | 114% |
| | 101% | 5.5% | 107% | 96.9% | 7.5% | 104% | 40.2% | 92.5% | 133% | 98.8% | 1.7% | 100% | 96.4% | 4.7% | 101% |
| | 106% | 4.5% | 110% | 102% | 7.1% | 109% | 46.8% | 270% | 317% | 117% | 18.8% | 136% | 100% | 23.3% | 123% |
| Mean | 108% | | | 106% | | | 107% | | | 105% | | | 107% | | |
| | 2.3% | | | 3.3% | | | 25.2% | | | 19.1% | | | 8.8% | | |

AIV.V Calculation of the dead volume and shift of the sampling depth

The dead volume of the *missy* was calculated on the basis of the dead volumes of the single components including the tubings and the fittings used for connection of the probe with the tubings and the pump, the PES membrane and the useable volume of the micro annular gear pump, given by the manufacturer. The volumes of the tubing as well as of the PES membrane were calculated on the basis of equation 1 (Eq. 1).

$$V = r^2 \cdot \pi \cdot l \quad \text{Eq.1}$$

In the case of the connectors, the volume was measured by filling the adapter with water using a 250 μL syringe (Hamilton, Switzerland, Gastight #1725) and reading the difference from the scale. Since 1 mm^3 equals $1 \mu\text{L}$, the results were not further corrected.

Table A3. 8: Calculation of the dead volume of the sampling systems.

| Component | Symbol | Setup 2 |
|------------------------------------|---------------------|---------------------|
| Inner radius tubing | r_{tube} | = 0.13 mm |
| Length tubing | l_{tubing} | = 800 mm |
| Inner radius PES membrane | r_{PES} | = 1.59 mm |
| Length PES membrane | l_{PES} | = 2.00 mm |
| Volume tubing | V_{tubing} | = 40 μL |
| Volume PES membrane | V_{PES} | = 16 μL |
| Fittings | V_{Luer} | = ~5 μL |
| Useable volume annular gear pump | V_{AGP} | = 17 μL |
| Dead volume sampling system | V_{dead} | = ~77 μL |

Table A3. 9: Calculation of the shift of the sampling depth caused by the dead volume of the sampling system in relation to the measurements of the sediment parameters.

| Component | Symbol | Setup 1 |
|-----------------------------------|---|---------------------|
| Distance for one sample | d_s | = 1.17 mm |
| Sample volume | V_s | = 500 μL |
| Dead volume | V_{dead} | = 77 μL |
| Distance shift due to dead volume | | |
| | $d_{\text{dead}} = \frac{d_s \cdot V_{\text{dead}}}{V_s}$ | = 0.19 mm |

Table A3. 10: Mean values of the oxygen concentration, the temperature and the redox potential of the water phase and the deep sediment layers (mean of the deepest 0.5 cm). * = sensor broken

| Start of the experiment | O ₂ concentration [mg O ₂ /L] | Temperature [°C] | Redox potential [mV] | |
|-------------------------|---|------------------|----------------------|----------|
| | Water phase | Water phase | Water | Sediment |
| Reference | | | | |
| 23.09.2014 | 6.9 | 18.1 | 470 | -30 |
| 26.09.2014 | 5.8 | 19.1 | 310 | -50 |
| 02.10.2014 | 7.3 | 19.8 | 490 | -50 |
| UF | | | | |
| 19.10.2014 | 7.3 | 18.8 | -* | -* |
| 22.10.2014 | 7.1 | 17.6 | 510 | -20 |
| 25.10.2014 | 7.3 | 18.0 | 390 | -40 |
| 28.10.2014 | -* | 17.4 | 360 | -20 |
| CPE | | | | |
| 07.11.2014 | 7.8 | 17.7 | 500 | -60 |
| 13.11.2014 | 9.2 | 18.1 | 400 | 50 |
| 15.11.2014 | 8.6 | 18.2 | 440 | 50 |
| 21.11.2014 | 10.3 | 17.7 | 370 | 50 |
| 24.11.2014 | 8.4 | 17.7 | 370 | 60 |

AIV.VI Concentrations of As and Sb in pore water samples

Together with the Mn, Fe and Co, the As and Sb concentrations were analyzed in the sediment pore water samples. The results of the reference profiles and the fractionation experiments are presented in Figure A1. 1 and Figure A1. 2, concentrations of the individual profiles are given in Table A3. 11, Table A3. 16, Table A3. 17 and Table A3. 22, Table A3. 23). The discussion of the results of the oxygen concentration and the redox potential can be found in the manuscript.

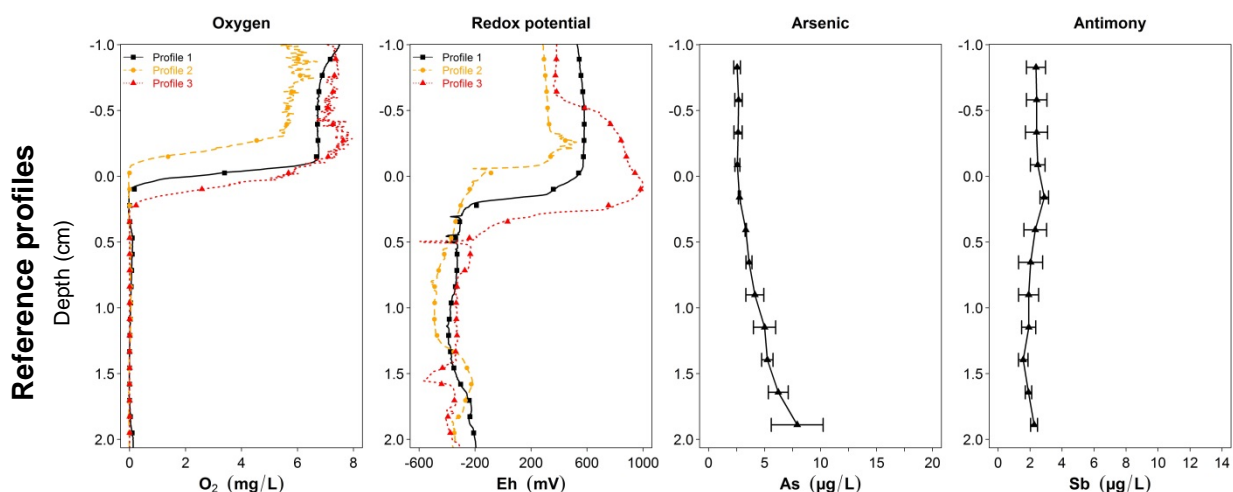


Figure A3. 1: Sediment depth profiles of the O_2 concentration, the redox potential as well as the As and Sb concentrations in sediment pore water samples of the three reference profiles, taken from 1 cm above to 2 cm in the sediment. Data points are plotted at the middle of the sampling distance of 2.4 mm representing in the case of the O_2 concentration and the redox potential the mean values of the sampling distance, in the case of the element concentrations the mean of the replicate profiles. Error bars represent the standard deviation of the replicate profiles including the uncertainty of the measurements as well as of the natural spatial heterogeneity

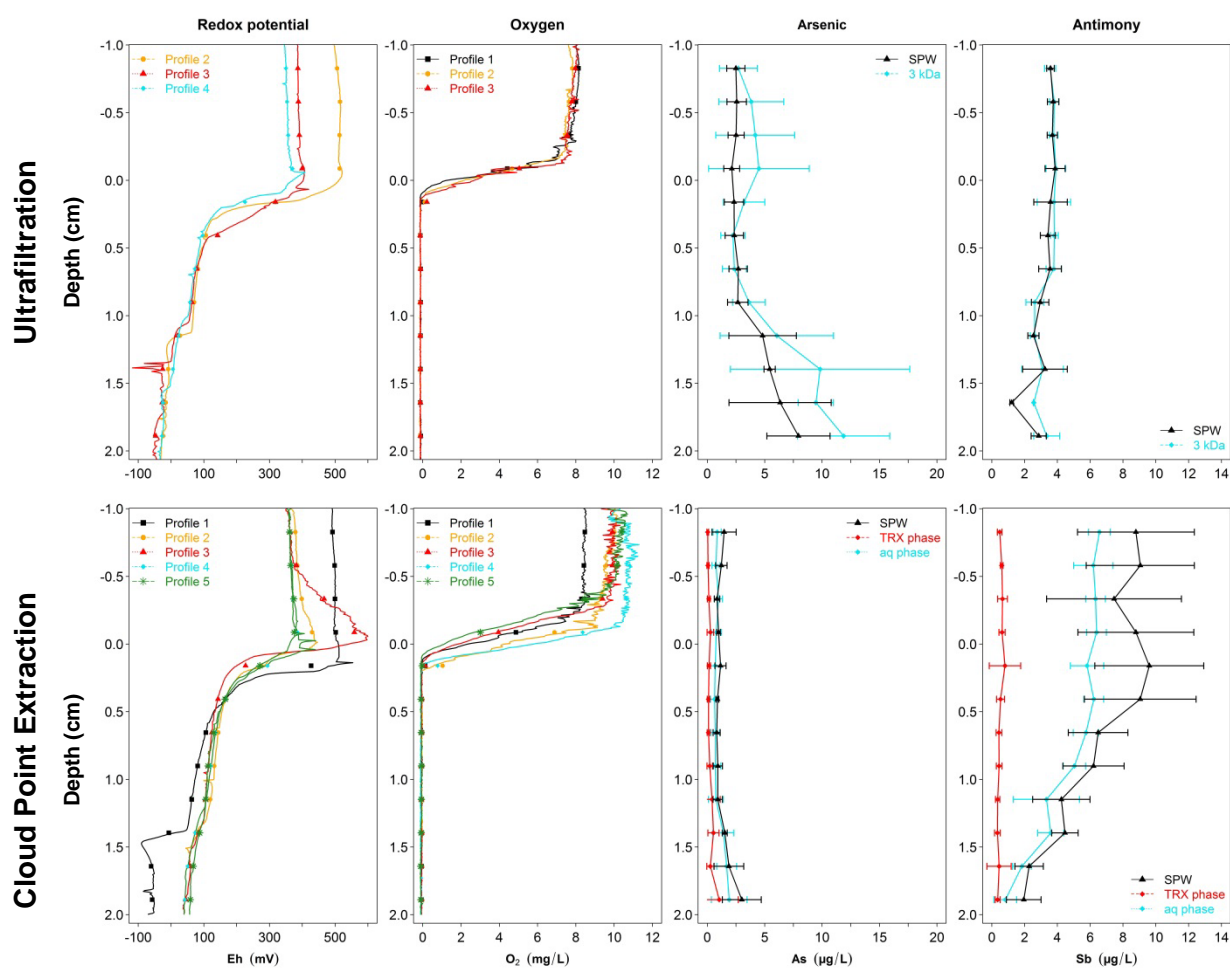


Figure A3. 2: Sediment depth profiles of the O_2 concentration, the redox potential as well as the As and Sb concentrations in different fractions of sediment pore water samples, taken from 1 cm above to 2 cm in the sediment (SPW = sediment pore water; 3 kDa = dissolved fraction UF; TRX = surfactant rich, colloid containing CPE phase; aq phase = aqueous CPE phase containing the dissolved fraction). Data points are plotted at the middle of the sampling distance of 2.4 mm representing in the case of the O_2 concentration and the redox potential the mean values of the sampling distance, in the case of the element concentrations the mean of the replicate profiles. Error bars represent the standard deviation of the replicate profiles including the analytical uncertainty as well as the natural spatial heterogeneity of the independent profiles. For UF only three profiles for the O_2 concentration and the redox potential are given due to a broken sensor.

Regarding the total concentrations of As in the SPW samples of the different experiments, the results of the reference experiments and the UF profiles were in good agreement to each other, showing an increase of the concentration from $\sim 2 \mu\text{g/L}$ in the overlaying water body to $8 \mu\text{g/L}$ in the SPW of the deeper sediment layers (Figure A1. 1 and Figure A1. 2 and Table A3. 11, Table A3. 17). This can be explained by the reduction of Mn and Fe (oxyhydr)oxides causing a release of associated trace elements.²⁻⁴ In contrast to that, only a slight increase to $\sim 3 \mu\text{g/L}$ of the total concentrations of the SPW was found in the samples of the CPE experiments (Figure A1. 1 and Figure A1. 2 and Table

A3. 22) potentially caused by less reducing conditions in the deeper areas of the sediment. However, this effect was not found for the other elements and may also be due to natural variations and/or to the low concentrations found in the SPW and related higher analytical uncertainties. Nevertheless, comparing the results of the two fractionation methods applied, As was, like Mn and Sb, nearly exclusively found in the dissolved fraction (<3 kDa of the UF and in the aqueous phase of the CPE). The concentrations determined in the surfactant rich phase of the CPE (TRX phase), containing the colloidal fraction, were below the respective quantification limit, in many cases below the detection limit (refer to Table A3. 22). This was equally found in other studies, even though As can be present up to ~20% in colloidal fractions of sediment pore waters.⁵⁻⁹

The results of Sb indicate a time-dependent process over the experimental period: concerning the total concentrations in the samples, the values determined in the overlaying water increased from 2 µg/L in the reference profiles (Figure A1. 1, Table A3. 11) to 3.5-4 µg/L and 8-9 µg/L in the UF and the CPE profiles, respectively (Figure A1. 2, SPW in Table A3. 17 and Table A3. 23). The concentrations in the deeper sediment layers remained constant at ~2 µg/L over the whole experimental period. This can be explained by an ongoing diffusional flux of anionic Sb (Sb(OH)_6^-) from the sediment into the water phase under oxidizing conditions and the presence of insoluble Sb(OH)_3 under reducing conditions,^{10, 11} leading to an inverse distribution compared to the other metal(loid)s. The finding that oxidizing conditions can cause a flux of Sb from the sediment into the water phase was already observed in previous experiments with comparable sediment contents¹ as well as at contaminated mining sites¹⁴⁻¹⁶. These results emphasize the relevance of time-depending processes for the release of Sb and the impact of changing environmental conditions, especially with regard to contaminated urban sediments, impacted by, e.g., traffic^{12, 13} or (former) mining activities.¹⁴⁻¹⁶ Comparable to Mn and As, Sb was found in the dissolved fractions of the UF and the CPE (Table A3. 17, Table A3. 23) this is in agreement to other studies showing that Sb is mainly present as dissolved anionic species in oxic surface waters and SPWs. Since for the digestion of the CPE phases a gentle procedure was applied using only HNO_3 (and no HCl which is recommended for Sb analyses), the discrepancies between the total concentration in the SPW (0.45 µm) and the two fractions might be related to certain losses of Sb due to an adsorption on vessel walls or organic material.¹⁷

AIV.VII Metal(loid) concentrations in SPW samples of the reference profiles

Table A3. 11: Element concentrations (>LoD) and standard deviations in the sediment pore water samples (SPW, 0.45 µm filtrates) of the reference experiments and the LoDs and LoQs of the respective ICP-QMS measurements. Samples marked in grey were below the LoQ due to a required sample dilution. Results crossed out were excluded from mean value calculation after testing for outliers (Grubb's and Dixon-Test^{2, 3}, p -values Fe <0.01, Co <0.02, testing the first 11 samples).

| Depth | Manganese | | | Cobalt | | | Iron | | | | | | | | | | | |
|-------|---------------------------|---------------------------|---------------------------|---------------------------|---------------------------|---------------------------|---------------------------|---------------------------|---------------------------|------|---------------------------------|------|-------|------|------|------|---------------------------------|------|
| | Profile 1 (10/19/2014) | Profile 2 (10/22/2014) | Profile 3 (10/22/2014) | Profile 1 (10/19/2014) | Profile 2 (10/22/2014) | Profile 3 (10/22/2014) | Profile 1 (10/19/2014) | Profile 2 (10/22/2014) | Profile 3 (10/22/2014) | | | | | | | | | |
| LoD: | | 0.15 | | | 0.01 | | | 0.29 | | | | | | | | | | |
| LoQ: | | 0.34 | | | 0.03 | | | 0.74 | | | | | | | | | | |
| cm | SPW | | SPW | | SPW | | SPW | | SPW | | | | | | | | | |
| | µg/L | σ | µg/L | σ | µg/L | σ | µg/L | σ | µg/L | σ | | | | | | | | |
| -0.83 | 4.8 | 0.23 | 34.0 | 0.92 | 2.4 | 0.12 | 0.30 | 0.02 | 0.27 | 0.03 | 0.35 | 0.02 | 8.35 | 0.49 | 11.8 | 0.36 | 20.6 | 1.0 |
| -0.58 | 1.9 | 0.09 | 19.3 | 0.73 | 2.3 | 0.09 | 0.19 | 0.02 | 0.18 | 0.01 | 0.29 | 0.02 | 5.94 | 0.22 | 14.8 | 0.59 | 14.4 | 0.9 |
| -0.33 | 1.3 | 0.10 | 21.2 | 0.12 | 2.0 | 0.08 | 0.20 | 0.01 | 0.23 | 0.01 | 0.28 | 0.01 | 6.68 | 0.40 | 15.1 | 0.40 | 89.0 | 5.5 |
| -0.09 | 22.4 | 1.35 | 34.8 | 1.13 | 2.9 | 0.09 | 0.21 | 0.02 | 0.29 | 0.00 | 0.29 | 0.02 | 7.47 | 0.70 | 23.7 | 0.94 | 8.9 | 0.5 |
| 0.16 | 296 | 8.22 | 199 | 3.55 | 16.0 | 0.52 | 0.56 | 0.56 | 0.45 | 0.03 | 0.32 | 0.01 | 8.22 | 0.72 | 50.4 | 1.03 | 12.7 | 0.3 |
| 0.41 | 839 | 28.0 | 764 | 26.2 | 212 | 6.5 | 0.61 | 0.03 | 0.66 | 0.01 | 9.83 0.20 | | 59.1 | 1.97 | 14.2 | 0.41 | 4106 99.7 | |
| 0.65 | 944 | 23.0 | 956 | 31.6 | 846 | 30.1 | 0.66 | 0.05 | 0.77 | 0.02 | 1.09 | 0.04 | 85.3 | 1.98 | 30.7 | 1.30 | 56.4 | 1.9 |
| 0.90 | 992 | 12.2 | 1937 | 58.2 | 2061 | 89.1 | 0.67 | 0.05 | 1.36 | 0.05 | 2.20 | 0.02 | 116.9 | 1.94 | 133 | 3.99 | 481 | 20.6 |
| 1.15 | 1293 | 52.8 | 2116 | 81.8 | 3108 | 93.2 | 0.90 | 0.05 | 1.53 | 0.05 | 2.77 | 0.17 | 119.8 | 5.46 | 272 | 10.9 | 503 | 15.0 |
| 1.40 | 1983 | 48.9 | 1741 | 91.8 | 4196 | 191.6 | 1.45 | 0.08 | 1.85 | 0.04 | 3.32 | 0.09 | 117.1 | 4.13 | 302 | 17.6 | 529 | 24.8 |
| 1.64 | 3278 | 76.8 | 1008 | 24.4 | 630 | 18.6 | 2.57 | 0.12 | 4.34 | 0.19 | 5.13 | 0.29 | 294.9 | 6.55 | 522 | 14.7 | 1001 | 31.8 |
| 1.89 | 5589 | 251 | 2485 | 119 | 289 | 12 | 5.36 | 0.23 | 4.69 | 0.21 | 6.82 | 0.31 | 534.5 | 25.6 | 750 | 29.7 | 499 | 10.7 |

Table A3.11 continued.

| Depth | Arsenic | | | | | | Antimony | | | | | |
|-------|---------------------------|----------|---------------------------|----------|---------------------------|----------|---------------------------|----------|---------------------------|----------|---------------------------|----------|
| | Profile 1 (09/23/2014) | | Profile 2 (09/26/2014) | | Profile 2 (09/29/2014) | | Profile 1 (09/23/2014) | | Profile 2 (09/26/2014) | | Profile 2 (09/29/2014) | |
| LoD: | 0.01 | | | | | | 0.04 | | | | | |
| LoQ: | 0.04 | | | | | | 0.11 | | | | | |
| cm | SPW | | SPW | | SPW | | SPW | | SPW | | SPW | |
| | $\mu\text{g/L}$ | σ | $\mu\text{g/L}$ | σ | $\mu\text{g/L}$ | σ | $\mu\text{g/L}$ | σ | $\mu\text{g/L}$ | σ | $\mu\text{g/L}$ | σ |
| -0.83 | 2.21 | 0.14 | 1.94 | 0.10 | 2.79 | 0.10 | 2.15 | 0.04 | 1.40 | 0.02 | 3.04 | 0.03 |
| -0.58 | 1.64 | 0.12 | 1.30 | 0.08 | 2.88 | 0.12 | 1.54 | 0.02 | 0.89 | 0.03 | 3.14 | 0.05 |
| -0.33 | 1.49 | 0.15 | 1.99 | 0.06 | 2.78 | 0.27 | 1.42 | 0.05 | 1.30 | 0.04 | 3.19 | 0.06 |
| -0.09 | 1.50 | 0.07 | 2.05 | 0.12 | 2.70 | 0.11 | 1.56 | 0.03 | 1.57 | 0.03 | 2.97 | 0.03 |
| 0.16 | 1.66 | 0.48 | 1.82 | 0.13 | 2.86 | 0.23 | 1.57 | 0.03 | 2.06 | 0.04 | 3.06 | 0.03 |
| 0.41 | 1.78 | 0.15 | 2.22 | 0.09 | 3.36 | 0.10 | 0.97 | 0.03 | 1.38 | 0.08 | 3.13 | 0.08 |
| 0.65 | 1.59 | 0.14 | 1.84 | 0.11 | 3.36 | 0.15 | 0.61 | 0.03 | 0.87 | 0.02 | 2.90 | 0.05 |
| 0.90 | 1.45 | 0.08 | 2.77 | 0.11 | 4.27 | 0.11 | 0.53 | 0.04 | 1.32 | 0.03 | 2.24 | 0.03 |
| 1.15 | 1.66 | 0.17 | 3.11 | 0.27 | 4.76 | 0.32 | 0.63 | 0.01 | 1.23 | 0.03 | 1.77 | 0.03 |
| 1.40 | 2.32 | 0.29 | 3.14 | 0.32 | 5.79 | 0.69 | 0.92 | 0.05 | 0.80 | 0.07 | 1.51 | 0.06 |
| 1.64 | 3.93 | 0.34 | 6.54 | 0.83 | 6.87 | 0.76 | 1.60 | 0.06 | 1.69 | 0.06 | 1.88 | 0.04 |
| 1.89 | 7.22 | 0.44 | 6.39 | 0.46 | 10.4 | 1.05 | 2.97 | 0.18 | 1.70 | 0.12 | 2.36 | 0.16 |

AIV.VIII Metal(loid) concentrations in fractions of pore water samples after UF

The sampling and fractionation procedure for the UF were conducted as described in the manuscript. Samples were analyzed without any further dilution by application of a newly established ICP-QMS method enabling for the measurement of sample volumes of 300 μL . The mean values of the UF graphics presented in the manuscript were calculated on the basis of the element concentrations determined in the 3 kDa fraction and the SPW for four subsequent profiles (Table A3. 12 – Table A3. 16). The method blank used for background corrections was determined tenfold by filtration of ultrapure water. Equally, blank samples were measured by application of the ICP-QMS method for small sample volumes.

Table A3. 12: Element concentrations (>LoD) and standard deviations of the method blanks of UF (3 kDa filtrates) determined 10-fold by analyzing ultrapure water as well as the LoDs and LoQs of the respective ICP-QMS measurements. Samples <LoQ are marked in grey.

| | Manganese | Iron | Cobalt | Arsenic | Antimony |
|--------|-----------------------------------|-----------------------------------|-----------------------------------|-----------------------------------|---------------------------------|
| LoD: | 0.46 | 0.60 | 0.10 | 0.13 | 0.22 |
| LoQ: | 1.28 | 1.18 | 0.25 | 0.49 | 0.61 |
| Sample | 3 kDa $\mu\text{g/L}$ σ | 3 kDa $\mu\text{g/L}$ σ | 3 kDa $\mu\text{g/L}$ σ | 3 kDa $\mu\text{g/L}$ σ | SPW $\mu\text{g/L}$ σ |
| 1 | 0.46 0.09 | 1.15 0.05 | 0.29 0.06 | 1.12 0.27 | 1.11 0.04 |
| 2 | <LoD | 1.96 0.15 | 0.25 0.03 | 1.74 0.26 | 0.90 0.04 |
| 3 | 0.82 0.14 | 2.04 0.10 | 0.24 0.02 | 2.17 0.26 | 0.87 0.05 |
| 4 | 0.47 0.08 | 1.37 0.12 | 0.16 0.03 | 1.28 0.28 | 0.63 0.05 |
| 5 | <LoD | 2.30 0.18 | 0.14 0.02 | 1.38 0.26 | 0.56 0.05 |
| 6 | <LoD | 3.08 0.21 | <LoD | 1.34 0.339 | 0.56 0.03 |
| 7 | 1.05 0.08 | 5.12 0.54 | <LoD | 0.95 0.09 | 0.51 0.02 |
| 8 | <LoD | 2.51 0.17 | <LoD | 1.05 0.23 | 0.48 0.04 |
| 9 | <LoD | 1.84 0.21 | <LoD | 1.03 0.13 | 0.43 0.03 |
| 10 | <LoD | 1.00 0.17 | <LoD | 0.82 0.20 | 0.39 0.03 |

Table A3. 13: Concentrations (>LoQ) of Mn ($\mu\text{g/L}$) and standard deviations in the 3 kDa filtrates and the sediment pore water samples (SPW, 0.45 μm filtrates) of the UF experiments as well as the LoDs and LoQs of the respective ICP-QMS measurements. (* = Sample lost due to errors during sampling of SPW, **= no results available due to errors during measurement).

| | Profile 1 (10/19/2014) | | | | Profile 2 (10/22/2014) | | | | Profile 3 (10/25/2014) | | | | Profile 4 (10/28/2014) | | | |
|-------------|------------------------|----------|-----------------|----------|------------------------|----------|-----------------|----------|------------------------|----------|-----------------|----------|------------------------|----------|-----------------|----------|
| LoD: | 0.44 | | | | 0.60 | | | | 0.37 | | | | 0.77 | | | |
| LoQ: | 0.23 | | | | 1.61 | | | | 1.01 | | | | 1.89 | | | |
| Depth cm | 3 kDa | | SPW | | 3 kDa | | SPW | | 3 kDa | | SPW | | 3 kDa | | SPW | |
| | $\mu\text{g/L}$ | σ | $\mu\text{g/L}$ | σ | $\mu\text{g/L}$ | σ | $\mu\text{g/L}$ | σ | $\mu\text{g/L}$ | σ | $\mu\text{g/L}$ | σ | $\mu\text{g/L}$ | σ | $\mu\text{g/L}$ | σ |
| -0.83 | 15.3 | 0.74 | 12.6 | 0.61 | 33.6 | 0.49 | 36.4 | 1.12 | 40.7 | 1.25 | 40.2 | 0.80 | 42.0 | 1.28 | 43.9 | 0.96 |
| -0.58 | 14.5 | 0.68 | 13.3 | 0.39 | 25.0 | 1.07 | 25.9 | 0.51 | 26.9 | 0.25 | 26.3 | 0.55 | 32.7 | 1.06 | 34.6 | 0.60 |
| -0.33 | 23.7 | 0.80 | 22.7 | 0.72 | 16.2 | 0.68 | 18.5 | 3.07 | 19.5 | 0.14 | 18.5 | 0.71 | 24.4 | 0.52 | 26.4 | 0.19 |
| -0.09 | 29.2 | 0.52 | 29.1 | 1.51 | 23.2 | 1.73 | 23.0 | 1.02 | 18.4 | 0.30 | 17.3 | 0.44 | 22.8 | 0.40 | 24.6 | 0.85 |
| 0.16 | 76.0 | 4.77 | 78.2 | 4.08 | 151 | 3.40 | 108 | 4.06 | 55.7 | 1.45 | 53.1 | 0.70 | 115 | 1.66 | 103 | 1.48 |
| 0.41 | ** | | 512 | 14.0 | 672 | 28.1 | 485 | 17.8 | 425 | 8.33 | 428 | 8.31 | 562 | 5.47 | 595 | 8.31 |
| 0.65 | 1210 | 52.4 | 1366 | 79.0 | 1114 | 41.3 | 968 | 54.7 | 1455 | 31.6 | 1389 | 24.3 | 1234 | 37.7 | 1539 | 39.8 |
| 0.90 | 2099 | 83.3 | 2083 | 69.8 | 2084 | 61.8 | 1800 | 62.4 | 2663 | 53.2 | 3174 | 42.2 | 1962 | 26.4 | 2718 | 89.5 |
| 1.15 | 2975 | 172 | 3061 | 149 | 1457 | 57.3 | 901 | 48.5 | 4278 | 112 | 3119 | 43.5 | 2673 | 45.3 | 3119 | 42.1 |
| 1.40 | 4163 | 164 | 4365 | 180 | 2410 | 80.4 | 4953 | 178 | 2469 | 79.2 | 3836 | 91.9 | 3032 | 72.3 | 3681 | 81.5 |
| 1.64 | 50.2 | 1.44 | 247 | 22.2 | 1003 | 35.0 | 1262 | 44.8 | 3920 | 86.4 | 455 | 17.1 | | * | | |
| 1.89 | 29.9 | 1.86 | ** | | 303 | 3.52 | 558 | 25.3 | 232 | 9.64 | 8221 | 165 | 1210 | 19.7 | 1269 | 41.3 |

Table A3. 14: Concentrations (>LoD) of Co ($\mu\text{g/L}$) and standard deviations in the 3 kDa filtrates and the sediment pore water samples (SPW, 0.45 μm filtrates) of the UF experiments as well as the LoDs and LoQs of the respective ICP-QMS measurements. Values <LoQ are marked in grey, samples below the respective LoD were excluded from calculations of the mean values. (* = Sample lost due to errors during sampling of SPW, **= no results available due to errors during measurement).

| | Profile 1 (10/19/2014) | | | | Profile 2 (10/22/2014) | | | | Profile 3 (10/25/2014) | | | | Profile 4 (10/28/2014) | | | |
|-------------|------------------------|----------|-----------------|----------|------------------------|----------|-----------------|----------|------------------------|----------|-----------------|----------|------------------------|----------|-----------------|----------|
| LoD: | 0.12 | | | | 0.10 | | | | 0.15 | | | | 0.17 | | | |
| LoQ: | 0.93 | | | | 0.26 | | | | 0.28 | | | | 0.45 | | | |
| Depth cm | 3 kDa | | SPW | | 3 kDa | | SPW | | 3 kDa | | SPW | | 3 kDa | | SPW | |
| | $\mu\text{g/L}$ | σ | $\mu\text{g/L}$ | σ | $\mu\text{g/L}$ | σ | $\mu\text{g/L}$ | σ | $\mu\text{g/L}$ | σ | $\mu\text{g/L}$ | σ | $\mu\text{g/L}$ | σ | $\mu\text{g/L}$ | σ |
| -0.83 | 0.39 | 0.07 | 0.17 | 0.01 | 0.34 | 0.06 | 0.38 | 0.02 | 0.47 | 0.05 | 0.29 | 0.02 | 0.21 | 0.02 | 0.26 | 0.02 |
| -0.58 | 0.35 | 0.02 | 0.17 | 0.02 | 0.32 | 0.04 | 0.29 | 0.01 | 0.66 | 0.16 | 0.31 | 0.01 | 0.17 | 0.01 | 0.27 | 0.01 |
| -0.33 | 0.38 | 0.04 | 0.19 | 0.01 | 0.16 | 0.01 | 0.84 | 0.62 | 0.40 | 0.02 | 0.29 | 0.01 | 0.22 | 0.02 | 0.24 | 0.01 |
| -0.09 | 0.21 | 0.02 | 0.18 | 0.02 | 0.12 | 0.01 | <LoD | | 0.21 | 0.01 | 0.28 | 0.01 | 0.19 | 0.01 | 0.27 | 0.03 |
| 0.16 | <LoD | | 0.19 | 0.02 | 0.17 | 0.02 | <LoD | | 0.36 | 0.02 | 0.29 | 0.02 | 0.36 | 0.02 | 0.32 | 0.02 |
| 0.41 | ** | | 0.58 | 0.02 | 0.49 | 0.03 | <LoD | | 0.47 | 0.02 | 0.60 | 0.03 | 0.74 | 0.02 | 0.90 | 0.05 |
| 0.65 | ** | | 1.89 | 0.02 | 1.38 | 0.03 | 1.69 | 0.05 | 1.59 | 0.03 | 2.43 | 0.13 | 1.91 | 0.12 | 2.45 | 0.14 |
| 0.90 | 2.58 | 0.12 | <LoD | | 1.90 | 0.09 | 3.01 | 0.19 | 2.62 | 0.03 | 3.68 | 0.12 | 2.61 | 0.05 | 2.47 | 0.09 |
| 1.15 | 1.65 | 0.05 | 3.67 | 0.08 | 3.34 | 0.12 | 4.34 | 0.28 | 2.79 | 0.06 | 4.81 | 0.20 | 2.96 | 0.08 | 4.46 | 0.09 |
| 1.40 | 1.98 | 0.14 | <LoD | | 4.37 | 0.19 | 6.17 | 0.25 | 3.64 | 0.26 | 9.57 | 0.13 | 2.08 | 0.12 | <LoD | |
| 1.64 | <LoD | | <LoD | | 5.85 | 0.32 | 5.87 | 0.45 | 3.65 | 0.05 | 3.52 | 0.10 | | | * | |
| 1.89 | <LoD | | ** | | 3.51 | 0.18 | 6.43 | 0.58 | 4.36 | 0.25 | 10.10 | 0.42 | 3.13 | 0.23 | 6.16 | 0.14 |

Table A3. 15: Concentrations (>LoQ) of Fe ($\mu\text{g/L}$) and standard deviations in the 3 kDa filtrates and the sediment pore water samples (SPW, 0.45 μm filtrates) of the UF experiments as well as the LoDs and LoQs of the respective ICP-QMS measurements. (* = Sample lost due to errors during sampling of SPW, **= no results available due to errors during measurement).

| | Profile 1 (10/19/2014) | | | | Profile 2 (10/22/2014) | | | | Profile 3 (10/25/2014) | | | | Profile 4 (10/28/2014) | | | |
|-------------|------------------------|----------|-----------------|----------|------------------------|----------|-----------------|----------|------------------------|----------|-----------------|----------|------------------------|----------|-----------------|----------|
| LoD: | 0.35 | | | | 0.47 | | | | 1.00 | | | | 0.88 | | | |
| LoQ: | 0.90 | | | | 1.03 | | | | 2.37 | | | | 2.25 | | | |
| Depth cm | 3 kDa | | SPW | | 3 kDa | | SPW | | 3 kDa | | SPW | | 3 kDa | | SPW | |
| | $\mu\text{g/L}$ | σ | $\mu\text{g/L}$ | σ | $\mu\text{g/L}$ | σ | $\mu\text{g/L}$ | σ | $\mu\text{g/L}$ | σ | $\mu\text{g/L}$ | σ | $\mu\text{g/L}$ | σ | $\mu\text{g/L}$ | σ |
| -0.83 | 34.0 | 0.47 | 28.5 | 0.77 | 20.7 | 0.69 | 38.5 | 1.11 | 27.9 | 0.59 | 32.1 | 0.94 | 12.5 | 0.64 | 19.3 | 0.78 |
| -0.58 | 22.2 | 0.31 | 16.5 | 0.50 | 12.5 | 0.58 | 28.9 | 0.67 | 30.6 | 0.35 | 32.7 | 0.47 | 10.8 | 0.34 | 17.0 | 0.59 |
| -0.33 | 24.6 | 0.36 | 20.5 | 0.38 | 21.0 | 1.21 | 33.0 | 6.21 | 39.3 | 0.65 | 24.1 | 0.39 | 10.6 | 0.25 | 15.6 | 0.52 |
| -0.09 | 37.1 | 0.72 | 19.9 | 0.37 | 15.5 | 0.75 | 18.0 | 0.68 | 22.8 | 0.57 | 16.0 | 0.56 | 10.4 | 0.11 | 17.4 | 0.86 |
| 0.16 | 25.1 | 0.57 | 32.8 | 0.85 | 49.8 | 1.14 | 24.6 | 1.19 | 59.3 | 0.36 | 27.3 | 0.47 | 39.3 | 1.91 | 22.0 | 0.90 |
| 0.41 | ** | | 45.7 | 0.34 | 35.2 | 1.36 | 39.6 | 2.55 | 14.2 | 0.20 | 11.0 | 0.32 | 15.9 | 0.54 | 26.7 | 0.98 |
| 0.65 | 101 | 5.61 | 90.1 | 0.65 | 72.1 | 3.81 | 76.0 | 2.42 | 43.9 | 1.14 | 34.9 | 1.59 | 76.8 | 1.58 | 240 | 12.5 |
| 0.90 | 378 | 8.03 | 403 | 14.9 | 29.1 | 0.90 | 214 | 18.1 | 122 | 1.10 | 628 | 26.9 | 166 | 6.34 | 1663 | 25.9 |
| 1.15 | 180 | 33.6 | 583 | 10.8 | 128 | 4.70 | 569 | 35.1 | 82.9 | 1.36 | 1417 | 46.9 | 395 | 19.1 | 2614 | 112 |
| 1.40 | 471 | 5.71 | 546 | 11.6 | 90.5 | 3.52 | 793 | 28.8 | 151 | 3.17 | 3285 | 63.8 | 504 | 23.9 | 4293 | 145 |
| 1.64 | 101 | 3.28 | 880 | 30.6 | 165 | 6.88 | 660 | 49.4 | 160 | 4.15 | 1915 | 72.0 | | * | | |
| 1.89 | 150 | 1.82 | ** | | 376 | 10.1 | 863 | 35.7 | 175 | 4.07 | 5105 | 102 | 133 | 5.11 | 4643 | 65.5 |

Table A3. 16: Concentrations (>LoQ) of As ($\mu\text{g/L}$) and standard deviation in the 3 kDa filtrates and the sediment pore water samples (SPW, 0.45 μm filtrates) of the UF experiments as well as the LoDs and LoQs of the respective ICP-QMS measurements. Values <LoQ are marked in grey, samples below the respective LoD were excluded from calculations of the mean values. (* = Sample lost due to errors during sampling of SPW, **= no results available due to errors during measurement).

| | Profile 1 (10/19/2014) | | | | Profile 2 (10/22/2014) | | | | Profile 3 (10/25/2014) | | | | Profile 4 (10/28/2014) | | | |
|-------------|------------------------|----------|-----------------|----------|------------------------|----------|-----------------|----------|------------------------|----------|-----------------|----------|------------------------|----------|-----------------|----------|
| LoD: | 0.89 | | | | 0.48 | | | | 0.22 | | | | 0.20 | | | |
| LoQ: | 2.29 | | | | 1.29 | | | | 0.57 | | | | 0.49 | | | |
| Depth cm | 3 kDa | | SPW | | 3 kDa | | SPW | | 3 kDa | | SPW | | 3 kDa | | SPW | |
| | $\mu\text{g/L}$ | σ | $\mu\text{g/L}$ | σ | $\mu\text{g/L}$ | σ | $\mu\text{g/L}$ | σ | $\mu\text{g/L}$ | σ | $\mu\text{g/L}$ | σ | $\mu\text{g/L}$ | σ | $\mu\text{g/L}$ | σ |
| -0.83 | 5.06 | 0.52 | 3.5 | 0.19 | 2.48 | 0.25 | 2.39 | 0.10 | 2.01 | 0.12 | 2.55 | 0.08 | 1.29 | 0.09 | 1.55 | 0.14 |
| -0.58 | 8.02 | 0.67 | 3.8 | 0.29 | 2.22 | 0.25 | 2.43 | 0.14 | 3.06 | 0.27 | 2.24 | 0.16 | 2.01 | 0.12 | 1.80 | 0.16 |
| -0.33 | 9.21 | 0.65 | 3.1 | 0.19 | 3.46 | 0.25 | 3.07 | 0.79 | 2.47 | 0.15 | 2.09 | 0.08 | 1.58 | 0.08 | 1.74 | 0.14 |
| -0.09 | 11.0 | 0.43 | 3.1 | 0.12 | 3.30 | 0.09 | 1.82 | 0.27 | 2.26 | 0.18 | 2.13 | 0.21 | 1.47 | 0.15 | 1.48 | 0.10 |
| 0.16 | 5.78 | 0.74 | 3.3 | 0.27 | 3.12 | 0.11 | <0.48 | | 2.15 | 0.17 | 0.17 | 1.91 | 1.79 | 0.26 | 1.77 | 1.77 |
| 0.41 | ** | | 3.4 | 0.17 | 3.25 | 0.23 | <0.48 | | 2.30 | 0.20 | 0.20 | 2.04 | 1.15 | 0.10 | 1.54 | 1.54 |
| 0.65 | ** | | 3.7 | 0.17 | 3.31 | 0.25 | 2.89 | 0.28 | 2.53 | 0.18 | 2.42 | 0.20 | 1.24 | 0.10 | 1.79 | 0.15 |
| 0.90 | 5.15 | 0.47 | <LoD | | 4.02 | 0.25 | 3.57 | 3.57 | 3.64 | 0.45 | 0.45 | 2.61 | 1.72 | 0.22 | 1.80 | 0.2 |
| 1.15 | 13.1 | 1.71 | 9.0 | 0.72 | 5.36 | 0.33 | 4.48 | 0.33 | 4.32 | 0.33 | 3.48 | 0.19 | 1.50 | 0.13 | 2.31 | 0.24 |
| 1.40 | 21.3 | 2.36 | <0.89 | | 7.20 | 0.42 | 5.09 | 5.09 | 7.33 | 0.89 | 0.89 | 5.78 | 3.56 | 0.13 | <0.20 | |
| 1.64 | 11.2 | 1.37 | 155 | 35.2 | 9.01 | 0.74 | 9.48 | 1.32 | 8.21 | 0.64 | 3.19 | 0.58 | | | * | |
| 1.89 | 14.3 | 2.41 | ** | | 13.2 | 1.88 | 10.9 | 2.57 | 14.1 | 2.17 | 7.50 | 1.23 | 5.88 | 0.98 | 5.44 | 1.01 |

Table A3. 17: Concentrations (>LoQ) of Sb ($\mu\text{g/L}$) and standard deviation in the 3 kDa filtrates and the sediment pore water samples (SPW, 0.45 μm filtrates) of the UF experiments as well as the LoDs and LoQs of the respective ICP-QMS measurements. Values <LoQ are marked in grey, samples below the respective LoD were excluded from calculations of the mean values. (* = Sample lost due to errors during sampling of SPW, **= no results available due to errors during measurement).

| | Profile 1 (10/19/2014) | | | | Profile 2 (10/22/2014) | | | | Profile 3 (10/25/2014) | | | | Profile 4 (10/28/2014) | | | |
|-------------|------------------------|----------|-----------------|----------|------------------------|----------|-----------------|----------|------------------------|----------|-----------------|----------|------------------------|----------|-----------------|----------|
| LoD: | 0.09 | | | | 0.14 | | | | 0.26 | | | | 0.13 | | | |
| LoQ: | 0.22 | | | | 0.37 | | | | 0.52 | | | | 0.29 | | | |
| Depth cm | 3 kDa | | SPW | | 3 kDa | | SPW | | 3 kDa | | SPW | | 3 kDa | | SPW | |
| | $\mu\text{g/L}$ | σ | $\mu\text{g/L}$ | σ | $\mu\text{g/L}$ | σ | $\mu\text{g/L}$ | σ | $\mu\text{g/L}$ | σ | $\mu\text{g/L}$ | σ | $\mu\text{g/L}$ | σ | $\mu\text{g/L}$ | σ |
| -0.83 | 3.32 | 0.19 | 3.6 | 0.11 | 3.50 | 0.04 | 3.27 | 0.09 | 4.05 | 0.12 | 3.83 | 0.12 | 3.37 | 0.13 | 3.63 | 0.09 |
| -0.58 | 3.71 | 0.07 | 3.7 | 0.20 | 3.48 | 0.13 | 3.28 | 0.09 | 4.04 | 0.12 | 3.86 | 0.07 | 4.00 | 0.06 | 4.10 | 0.15 |
| -0.33 | 3.69 | 0.12 | 3.3 | 0.06 | 3.43 | 0.07 | 3.54 | 0.31 | 4.01 | 0.03 | 3.83 | 0.17 | 3.93 | 0.05 | 4.04 | 0.07 |
| -0.09 | 3.63 | 0.08 | 3.4 | 0.13 | 3.35 | 0.07 | 3.54 | 0.10 | 3.93 | 0.10 | 3.72 | 0.09 | 4.74 | 0.21 | 4.76 | 0.08 |
| 0.16 | 2.90 | 0.10 | 3.3 | 0.07 | 3.24 | 0.12 | 2.41 | 0.11 | 3.80 | 0.10 | 3.74 | 0.08 | 5.21 | 0.10 | 4.87 | 0.10 |
| 0.41 | ** | | 3.2 | 0.13 | 4.02 | 0.06 | 2.9 | 0.19 | 3.85 | 0.11 | 3.76 | 0.11 | 3.55 | 0.12 | 3.84 | 0.06 |
| 0.65 | ** | | 2.8 | 0.11 | 3.24 | 0.10 | 3.33 | 0.18 | 4.13 | 0.30 | 4.44 | 0.18 | 3.96 | 0.11 | 3.63 | 0.07 |
| 0.90 | 1.82 | 0.15 | <LoD | | 2.85 | 0.07 | 3.08 | 0.08 | 2.91 | 0.13 | 3.07 | 0.20 | 2.96 | 0.08 | 2.20 | 0.08 |
| 1.15 | 2.62 | 0.17 | 2.1 | 0.83 | 2.98 | 0.11 | 2.77 | 0.13 | 2.39 | 0.15 | 2.84 | 0.20 | 2.46 | 0.12 | 2.44 | 0.18 |
| 1.40 | 4.90 | 0.48 | <LoD | | 2.59 | 0.11 | 2.29 | 0.19 | 2.91 | 0.18 | 4.20 | 0.30 | 1.98 | 0.10 | <LoD | |
| 1.64 | 2.59 | 0.16 | <LoD | | 2.53 | 0.30 | <LoD | | 2.57 | 0.28 | 1.21 | 0.11 | | | * | |
| 1.89 | 2.53 | 0.23 | ** | | 3.22 | 0.22 | <LoD | | 4.33 | 0.15 | 3.19 | 0.36 | 3.21 | 0.27 | 2.53 | 0.04 |

AIV.IX Metal(loid) concentrations in fractions of pore water samples after CPE

Sampling and sample preparation were carried out as described in the manuscript. After fractionation (conducted under inert argon atmosphere in a glove box) CPE phases were digested under normal laboratory conditions. Recoveries of the internal standard (100 μ L Ru, 100 mg/L) added to control the digestion procedure were in a range between 90% and 110%, with the exception of 5 samples (3 x 84%-89%, 2 x 111% - 113%). Digested samples were measured by means of ICP-QMS setup 1. SPW samples were acidified and measured directly without any further sample preparation by means of the ICP-QMS setup 2. Element concentrations of the SPW samples as well as the aqueous and the TRX phases and the blank values determined for five profiles (Table A3. 18 – Table A3. 23) were used to calculate the mean value of the fractions and the SPW presented in the manuscript (Figure 4.2). For background correction the mean value of 10 method blanks was used, determined similarly to the samples by using ultrapure water instead of pore water samples. In cases of extremely high concentrations suggesting contaminations (Fe and Co), the results were tested for outliers (Dixon and Grubb's-test^{2,3}) and, if identified as one, excluded from mean value calculation.

Table A3. 18: Method blanks of CPE determined 10-fold by analyses of ultrapure water. Concentrations determined in the TRX and the aqueous phase after fractionation and microwave assisted digestion. Values <LoQ are marked in grey. Digestion-vessel specific blanks were used for background correction, resulting in negative values (<0) for some samples.

| | Manganese | | Iron | | Cobalt | | Arsenic | | Antimony | |
|------|-----------|------|---------|------|---------|------|---------|------|----------|------|
| LoD: | 0.03 | | 0.14 | | 0.03 | | 0.04 | | 0.04 | |
| LoQ: | 0.09 | | 0.40 | | 0.09 | | 0.11 | | 0.11 | |
| | aqueous | TRX | aqueous | TRX | aqueous | TRX | aqueous | TRX | aqueous | TRX |
| | µg/L | σ | µg/L | σ | µg/L | σ | µg/L | σ | µg/L | σ |
| | 0.62 | 0.00 | 0.46 | 0.01 | <0 | <0 | <LoD | <LoD | <LoD | <LoD |
| | <0 | | 1.29 | 0.11 | <0 | 85.9 | 2.09 | <LoD | <LoD | <LoD |
| | 0.18 | 0.02 | 1.14 | 0.03 | <0 | 96.2 | 2.05 | <LoD | <LoD | <LoD |
| | <0 | | 0.15 | 0.01 | <0 | 18.6 | 0.37 | <LoD | <LoD | <LoD |
| | <0 | | <0 | | <0 | <0 | <LoD | <LoD | <LoD | <LoD |
| | <0 | | <0 | | <0 | <0 | <LoD | <LoD | <LoD | <LoD |
| | <0 | | <0 | | <0 | <0 | <LoD | <LoD | <LoD | <LoD |
| | <0 | | <0 | | <0 | <0 | <LoD | <LoD | <LoD | <LoD |
| | <0 | | <0 | | <0 | <0 | <LoD | <LoD | <LoD | <LoD |
| | <0 | | 0.78 | 0.04 | <0 | 9.13 | 0.17 | <LoD | <LoD | <LoD |

Table A3. 19: Concentrations (>LoQ) of Mn ($\mu\text{g/L}$) and standard deviations in the aqueous and TRX phase after CPE and in the sediment pore water samples (SPW, 0.45 μm filtrates) as well as the LoDs and LoQs of the respective ICP-QMS measurements. Values <LoQ are marked in grey. Samples <LoD were excluded from calculation of the mean values. (* = Sample lost due to errors during sampling or sample preparation procedure).

| | Profile 1 (11/07/2014) | | | Profile 2 (11/13/2014) | | | Profile 3 (11/15/2014) | | | Profile 4 (11/21/2014) | | | Profile 5 (11/24/2014) | | | | | | | | | | | | | | | | | | |
|-------|------------------------|----------|-----------------|------------------------|-----------------|----------|------------------------|----------|-----------------|------------------------|-----------------|----------|------------------------|----------|-----------------|----------|------|------|------|------|-------|------|------|-------|------|------|------|------|------|------|------|
| LoD | 0.25 | | 0.46 | 0.04 | | 0.14 | 0.04 | | 0.22 | 0.03 | | 0.37 | 0.03 | | 0.37 | | | | | | | | | | | | | | | | |
| LoQ: | 0.51 | | 1.28 | 0.10 | | 0.28 | 0.10 | | 0.56 | 0.06 | | 1.01 | 0.06 | | 1.01 | | | | | | | | | | | | | | | | |
| Depth | aqueous | TRX | SPW | aqueous | TRX | SPW | aqueous | TRX | SPW | aqueous | TRX | SPW | aqueous | TRX | SPW | | | | | | | | | | | | | | | | |
| cm | $\mu\text{g/L}$ | σ | $\mu\text{g/L}$ | σ | $\mu\text{g/L}$ | σ | $\mu\text{g/L}$ | σ | $\mu\text{g/L}$ | σ | $\mu\text{g/L}$ | σ | $\mu\text{g/L}$ | σ | $\mu\text{g/L}$ | σ | | | | | | | | | | | | | | | |
| -0.83 | 6.35 | 0.64 | <LoD | | | 1.66 | 0.06 | | * | 81.0 | 2.63 | 7.91 | 2.60 | 85.0 | 2.01 | 230.0 | 5.53 | 22.3 | 0.77 | 214 | 10.9 | 100 | 2.85 | 7.22 | 1.30 | 96.5 | 2.86 | | | | |
| -0.58 | 9.18 | 0.20 | <LoD | | | 3.10 | 0.28 | | * | 41.0 | 0.97 | 20.1 | 0.48 | 43.6 | 1.23 | 44.4 | 2.58 | 3.90 | 0.11 | 39.9 | 1.26 | 84.9 | 2.43 | 6.79 | 0.25 | 76.7 | 2.58 | | | | |
| -0.33 | 5.94 | 0.55 | <LoD | | | 3.82 | 0.14 | 8.68 | 0.54 | 1.87 | 1.00 | 2.72 | 0.17 | 29.1 | 1.46 | 5.76 | 0.44 | 28.5 | 0.68 | 28.9 | 1.26 | 3.57 | 0.43 | 28.1 | 1.72 | 48.4 | 1.40 | 3.34 | 0.13 | 45.0 | 2.12 |
| -0.09 | 8.98 | 0.45 | 9.60 | 0.38 | 4.28 | 0.21 | 4.39 | 0.46 | 0.72 | 0.03 | 2.25 | 0.22 | 24.9 | 1.65 | 5.54 | 1.57 | 30.0 | 1.22 | 26.9 | 0.80 | 2.54 | 0.17 | 23.5 | 0.59 | 46.3 | 1.05 | 3.69 | 0.28 | 43.2 | 0.87 | |
| 0.16 | 42.1 | 2.39 | 1.63 | 0.08 | 36.3 | 2.03 | 4.70 | 0.23 | 1.54 | 0.06 | 9.90 | 0.88 | 69.8 | 1.07 | 5.32 | 0.23 | 73.9 | 2.50 | 51.7 | 1.86 | 7.22 | 0.39 | 46.7 | 1.52 | 71.8 | 1.07 | 5.21 | 0.20 | 67.4 | 3.06 | |
| 0.41 | 388 | 7.36 | 16.0 | 0.63 | 323.8 | 7.41 | 45.4 | 0.83 | 4.20 | 0.19 | 46.6 | 1.95 | 428 | 8.86 | 30.6 | 0.69 | 442 | 4.27 | 277 | 8.58 | 31.4 | 0.34 | 291 | 18.6 | 456 | 7.81 | 34.7 | 0.71 | 442 | 23.9 | |
| 0.65 | 1052 | 54.8 | 57.1 | 1.26 | 1267 | 43.0 | 317 | 10.5 | 19.0 | 0.23 | 279 | 9.07 | 1280 | 39.24 | 103 | 3.69 | 1551 | 20.6 | 740 | 13.7 | 93.1 | 2.22 | 614 | 41.3 | 838 | 16.7 | 57.5 | 1.43 | 906 | 72.3 | |
| 0.90 | 1734 | 89.1 | 93.7 | 2.97 | 1734 | 31.2 | 775 | 27.8 | 64.6 | 1.26 | 686 | 20.6 | 2128 | 54.23 | 173 | 1.64 | 2627 | 53.2 | 1232 | 35.0 | 178 | 6.19 | 1702 | 66.6 | 1719 | 39.2 | 122 | 2.37 | 2551 | 119 | |
| 1.15 | 2678 | 64.8 | 160 | 10.3 | 3445 | 147 | 1238 | 31.8 | 88.3 | 3.03 | 1298 | 50.0 | 2698 | 74.97 | 339 | 11.8 | 3056 | 44.9 | 1764 | 54.4 | 233 | 6.32 | 3070 | 95.3 | 0.11 | 0.01 | 215 | 6.96 | 2232 | 159 | |
| 1.40 | 3758 | 172 | 201 | 6.92 | 3903 | 54.7 | 1972 | 66.3 | 125 | 2.75 | 2321 | 284 | 3847 | 65.06 | 336 | 2.85 | 2740 | 63.1 | 2743 | 68.6 | 304 | 15.3 | 4536 | 227 | 4142 | 128 | 263 | 3.80 | 2562 | 111 | |
| 1.64 | 5278 | 128 | 223 | 14.9 | 5237 | 147 | 2187 | 97.7 | 130 | 4.57 | 2.72 | 0.17 | 4704 | 277 | 404 | 17.1 | 5871 | 116 | 3432 | 43.0 | 416 | 11.1 | 1713 | 56.63 | 4584 | 94.5 | 317 | 9.58 | 4129 | 226 | |
| 1.89 | 6105 | 233 | 315 | 19.1 | 5777 | 196 | | | * | 5710 | 309 | 1056 | 42.8 | 6773 | 107 | 3882 | 43.1 | 382 | 8.15 | 1891 | 34.84 | 4932 | 87.2 | 403 | 9.39 | 4305 | 130 | | | | |

Table A3. 20: Concentrations (>LoQ) of Co ($\mu\text{g/L}$) and standard deviations in the aqueous and TRX phase after CPE and in the sediment pore water samples (SPW, $0.45 \mu\text{m}$ filtrates) as well as the LoDs and LoQs of the respective ICP-QMS measurements. Values <LoQ are marked in grey. Samples <LoD and those crossed out were excluded from calculation of the mean values, the latter after testing for outliers (Dixon and Grubbs test p -value <0.01). (* = Sample lost due to errors during sampling or sample preparation procedure).

| | Profile 1 (11/07/2014) | | | Profile 2 (11/13/2014) | | | Profile 3 (11/15/2014) | | | Profile 4 (11/21/2014) | | | Profile 5 (11/24/2014) | | |
|-------|--------------------------|--------------------------|--------------------------|--------------------------|--------------------------|--------------------------|--------------------------|--------------------------|--------------------------|--------------------------|--------------------------|--------------------------|--------------------------|--------------------------|--------------------------|
| LoD: | 0.02 | | 0.10 | 0.01 | | 0.1 | 0.01 | | 0.17 | 0.02 | | 0.09 | 0.02 | | 0.09 |
| LoQ: | 0.05 | | 0.25 | 0.03 | | 0.21 | 0.03 | | 0.37 | 0.07 | | 0.17 | 0.07 | | 0.17 |
| Depth | aqueous | TRX | SPW | aqueous | TRX | SPW | aqueous | TRX | SPW | aqueous | TRX | SPW | aqueous | TRX | SPW |
| cm | $\mu\text{g/L}$ σ | $\mu\text{g/L}$ σ | $\mu\text{g/L}$ σ | $\mu\text{g/L}$ σ | $\mu\text{g/L}$ σ | $\mu\text{g/L}$ σ | $\mu\text{g/L}$ σ | $\mu\text{g/L}$ σ | $\mu\text{g/L}$ σ | $\mu\text{g/L}$ σ | $\mu\text{g/L}$ σ | $\mu\text{g/L}$ σ | $\mu\text{g/L}$ σ | $\mu\text{g/L}$ σ | $\mu\text{g/L}$ σ |
| -0.83 | 0.64 0.03 | <LoD | 0.26 0.02 | | * | | 0.41 0.03 | <LoD | <LoD | 1.28 0.07 | <LoD | 1.03 0.07 | 0.10 0.04 | <LoD | 0.16 0.02 |
| -0.58 | 0.99 0.09 | <LoD | 0.41 0.05 | | * | | 0.29 0.08 | <LoD | <LoD | 0.41 0.04 | <LoD | 0.19 0.02 | 0.16 0.08 | <LoD | 0.16 0.01 |
| -0.33 | 0.47 0.07 | <LoD | 0.29 0.02 | 0.21 0.04 | <LoD | <LoD | 0.63 0.27 | <LoD | <LoD | 0.23 0.02 | <LoD | 0.19 0.01 | 0.25 0.01 | <LoD | 0.16 0.03 |
| -0.09 | 0.38 0.01 | <LoD | 0.36 0.04 | 0.26 0.13 | <LoD | <LoD | 0.56 0.03 | 0.21 0.03 | <LoD | 0.44 0.02 | <LoD | 0.20 0.00 | 0.93 0.03 | 0.11 0.01 | 0.15 0.01 |
| 0.16 | 0.90 0.89 | <LoD | 0.34 0.03 | 0.19 0.02 | <LoD | <LoD | 0.74 0.04 | <LoD | <LoD | 0.42 0.03 | 0.33 0.01 | 0.25 0.02 | 0.47 0.03 | 0.18 0.01 | 0.18 0.01 |
| 0.41 | 0.71 0.04 | <LoD | 0.67 0.02 | 0.20 0.02 | <LoD | 0.16 0.01 | 0.90 0.05 | <LoD | 0.50 0.03 | 0.69 0.03 | <LoD | 0.49 0.02 | 2.87 0.08 | 0.05 0.00 | 2.91 0.17 |
| 0.65 | 1.88 0.12 | <LoD | 1.88 0.03 | 0.61 0.03 | <LoD | 0.54 0.07 | 1.85 0.06 | 0.19 0.02 | 1.77 0.29 | 1.31 0.04 | 0.20 0.02 | 0.60 0.02 | 2.02 0.10 | <LoD | 1.71 0.05 |
| 0.90 | 2.88 0.18 | <LoD | 2.84 0.15 | 1.61 0.05 | <LoD | 1.53 0.38 | 3.77 0.10 | 0.57 0.39 | 2.91 0.11 | 2.12 0.11 | 0.55 0.03 | 1.12 0.04 | 2.38 0.14 | <LoD | 2.81 0.13 |
| 1.15 | 4.35 0.21 | 0.26 0.03 | 3.92 0.08 | 2.59 0.06 | 0.17 0.03 | 2.59 0.07 | 3.64 0.12 | 0.94 0.04 | 1.37 0.02 | 2.84 0.10 | 0.43 0.02 | 1.50 0.04 | | <LoD | 5.00 0.26 |
| 1.40 | 5.29 0.32 | 0.40 0.02 | 5.46 0.10 | 3.91 0.09 | 0.22 0.03 | 4.54 0.61 | 4.72 0.11 | 0.64 0.04 | 4.44 0.09 | 4.34 0.17 | 1.06 0.08 | 3.49 0.18 | 5.71 0.24 | <LoD | 7.22 0.29 |
| 1.64 | 7.69 0.21 | 1.19 0.29 | 6.70 0.31 | 3.79 0.12 | <LoD | 0.03 0.01 | 5.02 0.30 | 0.55 0.06 | 5.61 0.16 | 4.80 0.23 | 0.69 0.05 | 1.92 0.07 | 5.21 0.13 | <LoD | 5.18 0.06 |
| 1.89 | 10.6 0.39 | 0.38 0.06 | 7.69 0.26 | | * | | 5.52 0.25 | 52.20 0.62 | 6.02 0.28 | 4.20 0.15 | 0.87 0.15 | 1.89 0.06 | 4.95 0.18 | <LoD | 5.87 0.17 |

Table A3. 21: Concentrations (>LoQ) of Fe ($\mu\text{g/L}$) and standard deviations in the aqueous and TRX phase after CPE and in the sediment pore water samples (SPW, 0.45 μm filtrates) as well as the LoDs and LoQs of the respective ICP-QMS measurements. Values crossed out were excluded from calculation of the mean values after testing for outliers (Dixon and Grubbs test p-value <0.01). (* = Sample lost due to errors during sampling or sample preparation procedure, *** = Negative values after method background correction).

| | Profile 1 (11/07/2014) | | | | | | Profile 2 (11/13/2014) | | | | | | Profile 3 (11/15/2014) | | | | | | Profile 4 (11/21/2014) | | | | | | Profile 5 (11/24/2014) | | | | | | |
|-------|------------------------|----------|-----------------|----------|-----------------|----------|------------------------|----------|-----------------|----------|-----------------|----------|------------------------|----------|-----------------|----------|-----------------|----------|------------------------|----------|-----------------|----------|-----------------|----------|------------------------|----------|-----------------|----------|------|------|------|
| LoD | 0.48 | | 0.44 | | | | 0.26 | | 0.88 | | | | 0.26 | | 1.06 | | | | 0.18 | | 0.75 | | | | 0.18 | | 0.75 | | | | |
| LoQ: | 1.49 | | 1.18 | | | | 0.45 | | 1.62 | | | | 0.45 | | 1.71 | | | | 0.26 | | 1.07 | | | | 0.26 | | 1.07 | | | | |
| Depth | aqueous | | TRX | | SPW | | aqueous | | TRX | | SPW | | aqueous | | TRX | | SPW | | aqueous | | TRX | | SPW | | aqueous | | TRX | | SPW | | |
| cm | $\mu\text{g/L}$ | σ | $\mu\text{g/L}$ | σ | $\mu\text{g/L}$ | σ | $\mu\text{g/L}$ | σ | $\mu\text{g/L}$ | σ | $\mu\text{g/L}$ | σ | $\mu\text{g/L}$ | σ | $\mu\text{g/L}$ | σ | $\mu\text{g/L}$ | σ | $\mu\text{g/L}$ | σ | $\mu\text{g/L}$ | σ | $\mu\text{g/L}$ | σ | $\mu\text{g/L}$ | σ | $\mu\text{g/L}$ | σ | | | |
| -0.83 | 99.9 | 7.75 | 24.2 | 1.73 | 24.6 | 1.85 | | | * | | | | 18.5 | 0.25 | | *** | | 24.8 | 1.45 | 32.2 | 0.75 | 21.2 | 0.54 | 12.5 | 0.11 | 81.6 | 3.13 | 22.9 | 0.55 | 43.7 | 0.93 |
| -0.58 | 122 | 7.15 | 43.4 | 3.89 | 70.3 | 3.15 | | | * | | | | 16.3 | 0.21 | 30.65 | 0.66 | 11.0 | 0.05 | 42.2 | 1.16 | 33.2 | 1.34 | 13.0 | 0.26 | 38.5 | 2.07 | 31.3 | 0.73 | 29.5 | 0.38 | |
| -0.33 | 66.6 | 3.58 | 11.7 | 0.92 | 12.9 | 0.77 | 33.0 | 0.48 | 118 | 0.53 | 14.6 | 0.81 | 15.3 | 0.37 | 79.43 | 0.97 | 6.18 | 0.41 | 4.62 | 0.17 | 0.0 | 0.00 | 10.1 | 0.52 | 22.2 | 0.62 | 17.5 | 0.34 | 11.2 | 0.26 | |
| -0.09 | 79.6 | 3.58 | 80.3 | 2.26 | 40.4 | 1.21 | 33.0 | 0.59 | 14.4 | 0.07 | 6.84 | 0.59 | 23.2 | 0.43 | 25.95 | 0.52 | 7.03 | 0.14 | 956 | 20.23 | 10.6 | 0.31 | 14.4 | 0.57 | 107 | 2.35 | 26.0 | 0.85 | 39.3 | 0.92 | |
| 0.16 | 51.6 | 1.52 | 8.79 | 0.74 | 31.3 | 2.18 | 22.5 | 0.52 | 1.56 | 0.02 | 27.1 | 1.78 | 79.9 | 0.83 | | *** | | 7.15 | 0.14 | 10.8 | 0.39 | 221 | 8.52 | 8.84 | 0.14 | 24.0 | 0.31 | 45.0 | 0.77 | 39.0 | 0.73 |
| 0.41 | 132 | 2.29 | 5.57 | 0.42 | 34.2 | 1.18 | 25.2 | 0.54 | 22.8 | 0.07 | 8.55 | 0.35 | 0.00 | 0.00 | 53.10 | 0.69 | 6.73 | 0.38 | 26.1 | 0.83 | 22.8 | 0.55 | 8.29 | 0.10 | 238 | 3.99 | 49.6 | 1.07 | 14.4 | 0.35 | |
| 0.65 | 70.9 | 4.85 | 276 | 7.40 | 48.2 | 2.34 | 141 | 0.76 | 0.00 | 0.00 | 5.86 | 0.44 | 37.9 | 0.50 | | *** | | 14.8 | 0.62 | 50.5 | 1.11 | 30.0 | 0.81 | 10.8 | 0.17 | 105 | 2.15 | 43.5 | 0.73 | 65.0 | 0.88 |
| 0.90 | 217 | 12.5 | 45.6 | 1.26 | 192 | 3.70 | 244 | 2.81 | 0.00 | 0.00 | 17.7 | 1.02 | 64.6 | 0.57 | 91.68 | 1.55 | 76.7 | 4.18 | 197 | 5.62 | 165 | 4.98 | 114 | 1.40 | 26.5 | 0.93 | 0.00 | 0.00 | 29.6 | 0.88 | |
| 1.15 | 334 | 7.44 | 104 | 8.62 | 256 | 14.3 | 178 | 3.50 | 31.1 | 0.69 | 169 | 6.27 | 237 | 2.37 | 1285 | 12.7 | 130 | 3.43 | 639 | 18.89 | 137 | 3.17 | 319 | 5.35 | 30.0 | 1.00 | 69.4 | 3.18 | 455 | 10.4 | |
| 1.40 | 377 | 17.8 | 52.3 | 2.74 | 398 | 9.16 | 496 | 9.57 | 34.1 | 0.57 | 553 | 30.5 | 1232 | 16.8 | 41.45 | 0.93 | 710 | 48.6 | 1810 | 46.82 | 805 | 35.6 | 1135 | 30.6 | 2161 | 63.2 | 137 | 1.20 | 2675 | 45.3 | |
| 1.64 | 671 | 17.7 | 33.2 | 2.68 | 576 | 21.2 | 585 | 6.98 | 36.8 | 0.62 | 14.6 | 0.81 | 1830 | 20.7 | 80.66 | 0.63 | 1412 | 32.9 | 1742 | 27.68 | 289 | 9.50 | 831 | 12.0 | 3299 | 62.3 | 213 | 5.74 | 3100 | 62.0 | |
| 1.89 | 588 | 24.8 | 443 | 30.9 | 507 | 14.2 | | | * | | | | 1298 | 16.9 | 1726 | 141.6 | 1834 | 83.1 | 2295 | 27.41 | 4133 | 81.4 | 917 | 12.0 | 4399 | 78.5 | 464 | 10.7 | 4295 | 117 | |

Table A3. 22: Concentrations (>LoQ) of As ($\mu\text{g/L}$) and standard deviations in the aqueous and TRX phase after CPE and in the sediment pore water samples (SPW, 0.45 μm filtrates) as well as the LoDs and LoQs of the respective ICP-QMS measurements. Values <LoQ are marked in grey. Samples <LoD were excluded from calculation of the mean values. (* = Sample lost due to errors during sampling or sample preparation procedure).

| | Profile 1 (11/07/2014) | | | Profile 2 (11/13/2014) | | | Profile 3 (11/15/2014) | | | Profile 4 (11/21/2014) | | | Profile 5 (11/24/2014) | | |
|-------|--------------------------|--------------------------|--------------------------|--------------------------|--------------------------|--------------------------|--------------------------|--------------------------|--------------------------|--------------------------|--------------------------|--------------------------|--------------------------|--------------------------|--------------------------|
| LoD: | 0.01 | 0.13 | | 0.03 | 0.18 | | 0.03 | 0.16 | | 0.03 | 0.14 | | 0.03 | 0.14 | |
| LoQ: | 0.03 | 0.49 | | 0.10 | 0.43 | | 0.10 | 0.30 | | 0.09 | 0.28 | | 0.09 | 0.28 | |
| Depth | aqueous | TRX | SPW | aqueous | TRX | SPW | aqueous | TRX | SPW | aqueous | TRX | SPW | aqueous | TRX | SPW |
| cm | $\mu\text{g/L}$ σ | $\mu\text{g/L}$ σ | $\mu\text{g/L}$ σ | $\mu\text{g/L}$ σ | $\mu\text{g/L}$ σ | $\mu\text{g/L}$ σ | $\mu\text{g/L}$ σ | $\mu\text{g/L}$ σ | $\mu\text{g/L}$ σ | $\mu\text{g/L}$ σ | $\mu\text{g/L}$ σ | $\mu\text{g/L}$ σ | $\mu\text{g/L}$ σ | $\mu\text{g/L}$ σ | $\mu\text{g/L}$ σ |
| -0.83 | 1.32 0.17 | <LoD | 3.04 0.29 | | * | | 0.50 0.19 | <LoD | 1.00 0.09 | 0.94 0.14 | <LoD | 0.96 0.08 | 0.67 0.09 | <LoD | 0.87 0.15 |
| -0.58 | 1.19 0.21 | <LoD | 1.96 0.53 | | * | | <LoD | <LoD | 1.09 0.04 | 0.76 0.06 | <LoD | 0.83 0.12 | 0.77 0.13 | <LoD | 1.04 0.06 |
| -0.33 | 1.44 0.09 | <LoD | 1.09 0.13 | 1.05 0.27 | <LoD | 0.45 0.03 | 0.64 0.26 | <LoD | 0.90 0.09 | 1.13 0.24 | <LoD | 0.89 0.11 | 0.60 0.03 | <LoD | 0.92 0.20 |
| -0.09 | 1.42 0.18 | 0.24 0.10 | 1.17 0.18 | 0.87 0.23 | <LoD | 1.05 0.05 | <LoD | 0.75 0.05 | 1.05 0.07 | 0.90 0.10 | <LoD | 0.88 0.09 | 0.51 0.03 | <LoD | 0.76 0.18 |
| 0.16 | 1.49 0.78 | <LoD | 1.03 0.16 | 0.41 0.03 | <LoD | 2.00 0.25 | <LoD | <LoD | 0.98 0.04 | 0.84 0.12 | <LoD | 0.89 0.08 | 0.52 0.08 | <LoD | 0.85 0.06 |
| 0.41 | 1.11 0.20 | 0.10 0.04 | 0.92 0.06 | 0.41 0.16 | <LoD | 1.07 0.06 | <LoD | <LoD | 0.88 0.06 | 0.88 0.07 | <LoD | 0.81 0.07 | 0.55 0.04 | <LoD | 0.73 0.09 |
| 0.65 | 1.20 0.23 | 0.02 0.01 | 0.78 0.15 | 0.25 0.18 | <LoD | 0.88 0.08 | 0.45 0.15 | <LoD | 0.99 0.16 | 0.68 0.11 | <LoD | 0.32 0.05 | 0.92 0.05 | <LoD | 1.13 0.25 |
| 0.90 | 1.34 0.21 | 0.24 0.08 | 1.03 0.21 | 0.24 0.13 | <LoD | 0.95 0.10 | <LoD | 0.61 0.71 | 1.47 0.09 | 0.76 0.13 | <LoD | 0.35 0.03 | 0.93 0.08 | <LoD | 0.80 0.12 |
| 1.15 | 1.76 0.25 | <LoD | 1.16 0.10 | 0.58 0.12 | <LoD | 1.38 0.07 | <LoD | 1.67 0.22 | 0.55 0.02 | 0.91 0.11 | <LoD | 0.43 0.04 | <LoD | <LoD | 1.03 0.12 |
| 1.40 | 2.78 0.45 | 0.80 0.03 | 1.39 0.37 | 0.91 0.28 | <LoD | 1.67 0.14 | <LoD | 1.21 0.12 | 1.49 0.24 | 1.89 0.25 | <LoD | 1.27 0.09 | 0.79 0.16 | <LoD | 1.81 0.09 |
| 1.64 | 2.49 0.64 | 0.23 0.10 | 2.11 0.48 | 1.25 0.23 | <LoD | 0.45 0.03 | 2.22 0.53 | <LoD | 3.54 0.24 | 1.48 0.32 | <LoD | <LoD | 0.55 0.05 | <LoD | 1.41 0.19 |
| 1.89 | 3.96 0.63 | 0.12 0.03 | 4.45 0.49 | | * | | <LoD | 3.50 0.31 | 4.29 0.52 | 2.13 0.20 | <LoD | 0.89 0.11 | 1.21 0.28 | <LoD | 2.39 0.32 |

Table A3. 23: Concentrations (>LoQ) of Sb ($\mu\text{g/L}$) and standard deviations in the aqueous and TRX phase after CPE and in the sediment pore water samples (SPW, 0.45 μm filtrates) as well as the LoDs and LoQs of the respective ICP-QMS measurements. Values <LoQ are marked in grey. Samples <LoD were excluded from calculation of the mean values. (* = Sample lost due to errors during sampling or sample preparation procedure).

| | Profile 1 (11/07/2014) | | | | | | Profile 2 (11/13/2014) | | | | | | Profile 3 (11/15/2014) | | | | | | Profile 4 (11/21/2014) | | | | | | Profile 5 (11/24/2014) | | | | | |
|-------|------------------------|----------|-----------------|----------|-----------------|----------|------------------------|----------|-----------------|----------|-----------------|----------|------------------------|----------|-----------------|----------|-----------------|----------|------------------------|----------|-----------------|----------|-----------------|----------|------------------------|----------|-----------------|----------|------|------|
| LoD: | 0.01 | | 0.22 | | | | 0.01 | | 0.13 | | | | 0.01 | | 0.11 | | | | 0.01 | | 0.09 | | | | 0.01 | | 0.09 | | | |
| LoQ: | 0.02 | | 0.61 | | | | 0.02 | | 0.34 | | | | 0.02 | | 0.26 | | | | 0.03 | | 0.26 | | | | 0.03 | | 0.26 | | | |
| Depth | aqueous | | TRX | | SPW | | aqueous | | TRX | | SPW | | aqueous | | TRX | | SPW | | aqueous | | TRX | | SPW | | aqueous | | TRX | | SPW | |
| cm | $\mu\text{g/L}$ | σ | $\mu\text{g/L}$ | σ | $\mu\text{g/L}$ | σ | $\mu\text{g/L}$ | σ | $\mu\text{g/L}$ | σ | $\mu\text{g/L}$ | σ | $\mu\text{g/L}$ | σ | $\mu\text{g/L}$ | σ | $\mu\text{g/L}$ | σ | $\mu\text{g/L}$ | σ | $\mu\text{g/L}$ | σ | $\mu\text{g/L}$ | σ | $\mu\text{g/L}$ | σ | $\mu\text{g/L}$ | σ | | |
| -0.83 | 5.91 | 0.16 | 0.38 | 0.01 | 5.19 | 0.12 | | | * | | | | 6.09 | 0.20 | 0.44 | 0.04 | 7.29 | 0.04 | 7.22 | 0.52 | 0.69 | 0.05 | 13.6 | 0.58 | 7.03 | 0.58 | 0.42 | 0.03 | 9.10 | 0.21 |
| -0.58 | 4.62 | 0.07 | 0.72 | 0.49 | 5.08 | 0.41 | | | * | | | | 5.99 | 0.05 | 0.54 | 0.02 | 7.75 | 0.16 | 6.72 | 0.60 | 0.63 | 0.04 | 12.5 | 0.47 | 7.44 | 0.61 | 0.54 | 0.04 | 10.9 | 0.18 |
| -0.33 | 5.75 | 0.32 | 0.50 | 0.01 | 4.80 | 0.12 | 5.88 | 0.33 | 0.44 | 0.02 | 1.89 | 0.09 | 6.28 | 0.07 | 1.16 | 0.11 | 8.20 | 0.15 | 6.44 | 0.55 | 0.68 | 0.06 | 11.9 | 0.25 | 7.27 | 0.55 | 0.48 | 0.04 | 10.4 | 0.18 |
| -0.09 | 5.93 | 0.11 | 0.44 | 0.03 | 4.65 | 0.07 | 6.61 | 0.09 | 0.51 | 0.03 | 5.86 | 0.36 | 5.59 | 0.25 | 0.91 | 0.02 | 9.53 | 0.16 | 6.85 | 0.54 | 0.71 | 0.05 | 13.3 | 0.55 | 6.96 | 0.50 | 0.56 | 0.05 | 10.6 | 0.26 |
| 0.16 | 5.20 | 0.14 | 0.23 | 0.01 | 4.44 | 0.16 | 4.42 | 0.06 | 0.49 | 0.02 | 12.55 | 0.73 | 5.90 | 0.13 | 0.36 | 0.02 | 8.26 | 0.30 | 6.88 | 0.46 | 2.51 | 0.20 | 11.9 | 0.34 | 6.64 | 0.48 | 0.44 | 0.04 | 10.8 | 0.27 |
| 0.41 | 5.28 | 0.18 | 0.26 | 0.01 | 4.32 | 0.14 | 6.01 | 0.05 | 0.38 | 0.01 | 7.60 | 0.24 | 6.76 | 0.25 | 0.44 | 0.03 | 8.93 | 0.19 | 6.36 | 0.54 | 0.76 | 0.06 | 13.2 | 0.22 | 6.67 | 0.50 | 0.83 | 0.55 | 11.2 | 0.38 |
| 0.65 | 4.79 | 0.27 | 0.27 | 0.04 | 4.51 | 0.14 | 5.77 | 0.10 | 0.36 | 0.01 | 6.52 | 0.30 | 5.24 | 0.10 | 0.36 | 0.02 | 6.44 | 0.09 | 6.11 | 0.46 | 0.72 | 0.06 | 5.55 | 0.23 | 6.81 | 0.56 | 0.47 | 0.05 | 9.38 | 0.43 |
| 0.90 | 3.94 | 0.23 | 0.31 | 0.02 | 3.86 | 0.20 | 5.51 | 0.14 | 0.50 | 0.05 | 6.34 | 0.26 | 4.82 | 0.06 | 0.31 | 0.01 | 8.33 | 0.14 | 5.33 | 0.42 | 0.72 | 0.06 | 4.84 | 0.10 | 5.58 | 0.49 | 0.39 | 0.02 | 7.64 | 0.22 |
| 1.15 | 3.12 | 0.21 | 0.30 | 0.05 | 3.64 | 0.10 | 5.03 | 0.21 | 0.35 | 0.05 | 6.04 | 0.25 | 3.75 | 0.12 | 0.24 | 0.00 | 2.0 | 0.04 | 4.76 | 0.37 | 0.58 | 0.04 | 3.53 | 0.07 | <LoD | 0.31 | 0.02 | 6.01 | 0.26 | |
| 1.40 | 2.50 | 0.11 | 0.47 | 0.02 | 3.58 | 0.14 | 4.29 | 0.12 | 0.29 | 0.03 | 5.36 | 0.46 | 3.14 | 0.02 | 0.18 | 0.00 | 3.84 | 0.14 | 4.41 | 0.46 | 0.58 | 0.03 | 4.29 | 0.14 | 3.65 | 0.32 | 0.20 | 0.02 | 5.22 | 0.20 |
| 1.64 | 1.76 | 0.02 | <LoD | | 3.36 | 0.09 | 2.37 | 0.13 | 0.05 | 0.01 | 1.89 | 0.09 | 1.07 | 0.06 | 0.25 | 0.23 | 1.94 | 0.11 | 2.38 | 0.14 | 1.54 | 0.12 | 1.32 | 0.06 | 2.13 | 0.17 | <LoD | | 2.49 | 0.18 |
| 1.89 | <LoD | | 0.49 | 0.06 | 3.28 | 0.16 | | | * | | | | 0.61 | 0.03 | 0.36 | 0.02 | 1.80 | 0.14 | 1.10 | 0.08 | 0.44 | 0.03 | 0.69 | 0.04 | 1.61 | 0.15 | 0.15 | 0.01 | 2.02 | 0.23 |

AIV.X References

1. Fabricius, A. L.; Duester, L.; Ecker, D.; Ternes, T. A., New Microprofiling and Micro Sampling System for Water Saturated Environmental Boundary Layers. *Environmental Science & Technology* 2014, *48*, (14), 8053-8061.
2. Balistrieri, L. S.; Murray, J. W.; Paul, B., The geochemical cycling of trace-elements in a biogenic meromictic lake. *Geochimica Et Cosmochimica Acta* 1994, *58*, (19), 3993-4008.
3. Rigaud, S.; Radakovitch, O.; Couture, R. M.; Deflandre, B.; Cossa, D.; Garnier, C.; Garnier, J. M., Mobility and fluxes of trace elements and nutrients at the sediment-water interface of a lagoon under contrasting water column oxygenation conditions. *Applied Geochemistry* 2013, *31*, 35-51.
4. Giblin, A. E., Iron and Manganese. In *Encyclopedia of Inland Waters*, Likens, G. E., Ed. Academic Press: Oxford, 2009; pp 35-44.
5. Huerta-Diaz, M. A.; Rivera-Duarte, I.; Sanudo-Wilhelmy, S. A.; Flegal, A. R., Comparative distributions of size fractionated metals in pore waters sampled by in situ dialysis and whole-core sediment squeezing: Implications for diffusive flux calculations. *Applied Geochemistry* 2007, *22*, (11), 2509-2525.
6. Itoh, A.; Nagasawa, T.; Zhu, Y. B.; Lee, K. H.; Fujimori, E.; Haraguchi, H., Distributions of major-to-ultratrace elements among the particulate and dissolved fractions in natural water as studied by ICP-AES and ICP-MS after sequential fractionation. *Anal. Sci.* 2004, *20*, (1), 29-36.
7. Dabrin, A.; Roulier, J. L.; Coquery, M., Colloidal and truly dissolved metal(oid) fractionation in sediment pore waters using tangential flow filtration. *Applied Geochemistry* 2013, *31*, 25-34.
8. Kottelat, R.; Vignati, D. A. L.; Chanudet, V.; Dominik, J., Comparison of small- and large-scale ultrafiltration systems for organic carbon and metals in freshwater at low concentration factor. *Water Air and Soil Pollution* 2008, *187*, (1-4), 343-351.
9. Durin, B.; Bechet, B.; Legret, M.; Le Cloirec, P., Role of colloids in heavy metal transfer through a retention-infiltration basin. *Water Sci. Technol.* 2007, *56*, (11), 91-99.
10. Filella, M.; Belzile, N.; Chen, Y. W., Antimony in the environment: a review focused on natural waters II. Relevant solution chemistry. *Earth-Science Reviews* 2002, *59*, (1-4), 265-285.
11. Takayanagi, K.; Cossa, D., Vertical distributions of Sb(III) and Sb(V) in Pavin Lake, France. *Water Research* 1997, *31*, (3), 671-674.
12. Hjortenkrans, D. S. T.; Bergback, B. G.; Haggerud, A. V., Metal emissions from brake linings and tires: Case studies of Stockholm, Sweden 1995/1998 and 2005. *Environmental Science & Technology* 2007, *41*, (15), 5224-5230.
13. Dietl, C.; Reifenhauer, W.; Peichl, L., Association of antimony with traffic - occurrence in airborne dust, deposition and accumulation in standardized grass cultures. *Science of the Total Environment* 1997, *205*, (2-3), 235-244.
14. Okkenhaug, G.; Yong-Guan, Z.; Junwen, H.; Xi, L.; Lei, L.; Mulder, J., Antimony (Sb) and Arsenic (As) in Sb Mining Impacted Paddy Soil from Xikuangshan, China: Differences in Mechanisms Controlling Soil Sequestration and Uptake in Rice. *Environmental Science & Technology* 2012, *46*, (6), 3155-3162.
15. Ashley, P. M.; Craw, D.; Graham, B. P.; Chappell, D. A., Environmental mobility of antimony around mesothermal stibnite deposits, New South Wales, Australia and southern New Zealand. *Journal of Geochemical Exploration* 2003, *77*, (1), 1-14.
16. Casiot, C.; Ujevic, M.; Munoz, M.; Seidel, J. L.; Elbaz-Poulichet, F., Antimony and arsenic mobility in a creek draining an antimony mine abandoned 85 years ago (upper Orb basin, France). *Applied Geochemistry* 2007, *22*, (4), 788-798.
17. Kingston, H. M.; Haswell, S. J., *Microwave-enhanced chemistry : fundamentals, sample preparation, and applications*. Washington, DC : American Chemical Society, c1997.: 1997.